ResearchGate

See discussions, stats, and author profiles for this publication at: https://www.researchgate.net/publication/265205819

DYNAMIC MODELLING OF SOIL ORGANIC MATTER USING PHYSICALLY DEFINED FRACTIONS

Article

CITATIONS
6

READS
58

1 author:

Saran Sohi
The University of Edinburgh

107 PUBLICATIONS 5,487 CITATIONS

SEE PROFILE

Some of the authors of this publication are also working on these related projects:

Project SUCCESS (Sustainable Urban Carbon Capture: Engineering Soils for Climate Change) View project

Project Standard biochar View project

All content following this page was uploaded by Saran Sohi on 17 March 2016.

The user has requested enhancement of the downloaded file.

DYNAMIC MODELLING OF SOIL ORGANIC MATTER USING PHYSICALLY DEFINED FRACTIONS

SARAN P. SOHI

Thesis submitted for the degree of Doctor of Philosophy

© 2001

IMPERIAL COLLEGE

UNIVERSITY OF LONDON

2001

To Susanna

ACKNOWLEDGEMENTS

I would like to thank Dr. John Gaunt for his support of my research at IACR; Dr. Georg Cadisch for his willing advice and comment, especially on drafts of this thesis, and Susanna for proof reading. I thank Dr. Jon Arah for his guidance in the development of the model, Helen Yates for her role in the fractionation work, and Dr. Nathalie Mahieu and her colleagues at the University of London for the NMR analyses. I also acknowledge the contribution of Andy Macdonald to the field incubation experiment (including calculations of gross N mineralisation), the Analytical Section at IACR for mass spectrometry, Alan Todd for statistical advice, and Paul Hargreaves for supplying meteorological data. I would also like to thank our external collaborators for supplying samples from long-term experiments, and Dr. Beata Madari and Rienk Smittenberg for their contribution. I wish to express my appreciation of the many colleagues, past and present, who have participated in related research areas during my time at IACR.

ABSTRACT

The objective of this thesis was to develop and parameterise a model of soil organic matter dynamics based on measurable variables, and able to simulate C and N dynamics on a time scale relevant to crop nutrient supply. The model is mechanistic, simulating organic matter decomposition through successive changes in physical location within the soil matrix. It includes a greater number of flows and types of flow than most existing models, and accounts for the affects of N availability on C turnover. Parameterisation of the model required simultaneous, time-dependent measurements of C, N and their respective isotope tracers in each measurable compartment. Data used to parameterise the model was gathered during the decomposition of ^{15}N-labelled maize straw in a sandy loam soil, under field conditions. Simulation of rate processes was assessed by independent measurements of gross N mineralisation and CO_2 production. Although the separation method developed in this thesis identified fractions which consistently contrast in their chemical composition, heterogeneity in FREE organic matter (organic particles between stable aggregates), and the assumption of first order kinetics were the main obstacles to parameterisation. Heterogeneity was most problematic in the simulation of the tracer data, since these were associated mainly with active (maize-derived) FREE organic matter, and not with an apparent, almost stable sub-fraction. The best achievable r^2 for simulation of C, N, C-to-N, $\delta^{13}C$ and ^{15}N and derived variables was 0.40. The optimised model parameters suggest turnover times of 250 days for FREE organic matter, and 435 days for INTRA-AGGREGATE (organic particles within aggregates). Since these fractions are dynamic on a seasonal time scale, a validated model is likely to be relevant to the prediction of crop nutrient supply.

TABLE OF CONTENTS

LIST OF TABLES **9**

LIST OF FIGURES **12**

CHAPTER 1: INTRODUCTION AND LITERATURE REVIEW .. **20**

1.1. Introduction **20**

1.2. Soil N supply **21**

1.2.1. Mineralisation 21
1.2.2. Crop requirement 22
1.2.3. The fate of crop residues 23

1.3. Soil organic matter models **24**

1.3.1. Modelling soil N supply 24
1.3.2. Definition of model compartments 26
1.3.3. Parameterisation and validation 29
1.3.4. Measurable model compartments 30

1.4. Modelling measurable fractions **33**

1.4.1. Operationally-defined fractions for modelling 34
1.4.2. Physical fractionation 35

1.5. Isotopic tracers for soil organic matter **37**

1.5.1. Stable isotope studies 37
1.5.2. Natural abundance 38
1.5.3. Radioisotopes 40

1.6. Chemical characterisation **41**

1.6.1. Nuclear magnetic resonance spectroscopy 42
1.6.2. Infrared spectroscopy 43

1.7. Thesis outline **47**

CHAPTER 2: A STANDARD FRACTIONATION PROCEDURE 49

2.1. Introduction 49

2.1.1. Essential fraction characteristics 49

2.1.2. Aggregation and soil dispersion 51

2.1.3. Alternate physical fractionation approaches 52

2.2. Materials and methods 53

2.2.1. Soils 55

2.2.2. Density fractionation 55

2.2.3. Particle-size fractionation 59

2.3. Chemical characterisation 60

2.4. Results and discussion 62

2.4.1. Optimisation of density fractionation 62

2.4.2. Chemical properties 64

2.4.3. A conceptual model 74

2.5. Conclusion 76

CHAPTER 3: CHEMICAL CHARACTERISATION 78

3.1. Introduction 78

3.2. Materials and methods 80

3.2.1. Soils 80

3.2.2. Density fractionation 82

3.2.3. ^{13}C NMR analysis 84

3.2.4. Statistical analysis 84

3.3. Results and discussion 85

3.3.1. Sensitivity of fraction composition to fertilisation on the UK site 85

3.3.2. Differences between fractions across locations 90

3.4. Conclusion 95

CHAPTER 4: A MATHEMATICAL MODEL 96

4.1. Introduction 96

4.1.1. Compartment reactivity 96
4.1.2. Representation of microbial biomass 97
4.1.3. Reconciling C and N dynamics 98
4.1.4. Isotope tracers 99

4.2. Model definition 100

4.2.1. Compartments 103
4.2.2. Tracer flows 104
4.2.3. C and N flows 105
4.2.4. Flow limitation 112
4.2.5. Simulation of gross processes 113
4.2.6. Modifiers 115
4.2.7. Numeric parameter values 116
4.2.8. Scenario simulations 116
4.2.9. Sensitivity analysis 123

4.3. Results and discussion 124

4.3.1. Dynamics of C and N under non-limiting N 124
4.3.2. Dynamics of tracers under non-limiting N 130
4.3.3. Processes under non-limiting N 132
4.3.4. Processes under N limitation 134
4.3.5. Sensitivity of the model to parameter values 141

4.4. Conclusion 143

CHAPTER 5: A PARAMETERISATION DATASET 145

5.1. Introduction 145

5.1.1. Obtaining a minimum dataset for model parameterisation 146

5.2. Materials and methods 147

5.2.1. Decomposition experiment 149
5.2.2. Measurement of modelled SOM fractions 152

5.2.3. Independent measurement of other pools and processes 161
5.2.4. Statistical analysis 163

5.3. Results and discussion 163

5.3.1. Recovery of mass 164
5.3.2. Dynamics of C and N 164
5.3.3. Dynamics of isotope tracers 171

5.4. Conclusion 180

CHAPTER 6: MODEL PARAMETERISATION 181

6.1. Introduction 181

6.2. Method 181

6.2.1. Temperature rate modifier 183
6.2.2. Soil moisture rate modifier 183
6.2.3. Initial values 185
6.2.4. Organic inputs 188
6.2.5. Parameter optimisation of model constants 188
6.2.6. Sensitivity analysis 189

6.3. Results and discussion 189

6.3.1. Optimisation of initial values and model parameters 189
6.3.2. Considerations in interpretation of optimised model 194
6.3.3. Simulation of C, N and tracer dynamics in measured fractions 196
6.3.4. Simulation of *Sol* and *Bug* 201
6.3.5. Simulation of measured processes 203
6.3.6. Sensitivity analysis of model parameters 205

6.4. Conclusions 214

CHAPTER 7: GENERAL DISCUSSION AND FUTURE WORK .. 215

REFERENCES 228

LIST OF TABLES

Table 1.1. Detailed peak assignments for ^{13}C nuclear magnetic resonance spectra 45

Table 1.2. Peak assignments for diffuse reflectance Fourier transform infrared spectroscopy 46

Table 2.1. The basic properties of the soils used in the optimisation and comparison of fractionation methods 56

Table 2.3. C-to-Fe ratios and the distribution of carbon amongst functional groups in FREE and INTRA-AGGREGATE organic matter fractions from the three soils as estimated from peak area analysis of ^{13}C nuclear magnetic resonance spectra .. 72

Table 3.1 List of the long-term experiments sampled for characterisation of soil organic matter fractions under contrasting fertilisation including the categories of treatment sampled at each site 81

Table 3.2. The significance of the variance components in determining the differences in the composition of organic matter fractions obtained from 26 long-term plots in eight long-term experiments under contrasting management, assessed from ^{13}C nuclear magnetic resonance peak areas using residual maximum likelihood ……94

Table 4.1. List of optimisable parameters invoked in the model and the values assigned to them in the decomposition scenarios 117

Table 4.2. List of variables representing initial values for which numeric values are required in order to run the model 117

Table 4.3. The nature of the four straw additions used in the scenarios, encompassing high (H) and atypically high addition rates (XH) and residues of high (HQ) and low (LQ) quality 119

Table 4.4. The distribution and isotopic composition of C and N between and within measured SOM fractions assumed for the scenarios (before the straw addition) ……...119

Table 4.5. The calculated distribution and isotopic composition of C and N between and within the modelled SOM compartments in the scenarios (before the straw addition) 119

Table 4.6. Colour and format coding used in model outputs 122

Table 4.7. Threshold parameter values for preventing limitation of C incorporation in the otherwise N-limited scenario of an atypical addition of low quality straw (LQ/XH scenario) 142

Table 5.1. Variables measured during soil incubation for the purpose of model parameterisation 148

Table 5.2. Chemical and isotopic composition of the ^{15}N labelled maize straw incorporated into soil for the incubation experiment 151

Table 5.3. The calculated effect of maize straw incorporation on the C and N content and isotopic composition of the pre-incubation soil 153

Table 5.4. Analysis of the standard SOM fractions and organomineral sub-fractions isolated from maize- and non-amended soils during incubation: (i) C content (ii) mass and (iii) C enrichment factor 166

Table 5.5. The comparative ^{15}N enrichments of organomineral sub-fractions during the incubation with ^{15}N labelled maize straw relative to the corresponding fractions from non-amended soil 179

Table 6.1. The optimised values for the key model parameters evaluated against experimental data using Marquadt algorithms and starting values obtained from trial and error optimisation of the values used for the scenarios run in Chapter 4 ……...182

Table 6.2. Optimisation of initial value parameters in the model using Marquadt algorithms, with the starting values obtained by prior trial and error optimisation against the experimental data 191

Table 6.3. The optimised values for the key model parameters evaluated against experimental data using Marquadt algorithms and starting values obtained from trial and error optimisation of the values used for the scenarios run in Chapter 4 ……...193

LIST OF FIGURES

Figure 1.1. The main functional groups identified by a solid-state 13C nuclear magnetic resonance spectrum with associated chemical shift limits 44

Figure 2.1. An experiment to simultaneously optimise density fractionation and compare an approach based on particle-size using chemical characterisation techniques 54

Figure 2.2. Organic matter recovered in (a) free and (b) intra-aggregate fractions at different separation densities and / or ultrasonic energy input 63

Figure 2.3. The effect of sodium iodide density on the yield of the organomineral clay sub-fraction from heavy clay soil with different levels of energy input 65

Figure 2.4. A standard procedure for the isolation of soil organic matter fractions suitable for modelling 66

Figure 2.5. The contrasting appearance of free and intra-aggregate fractions isolated on glass fibre filters 68

Figure 2.6. ^{13}C nuclear magnetic resonance spectra for fractions obtained by density–size versus size-only fractionation from (a) sandy loam (b) silty clay loam and (c) heavy clay soils 69–71

Figure 2.7. Diffuse reflectance infrared Fourier transform spectra for FREE and INTRA-AGGREGATE organic matter fractions from (a) sandy loam (b) silty clay loam and (c) heavy clay soils 75

Figure 3.1. ^{13}C nuclear magnetic resonance spectra for contrasting organic inputs received by plots of the Broadbalk continuous wheat experiment in the UK..... 86

Figure 3.2. ^{13}C nuclear magnetic resonance spectra for FREE organic matter from four Broadbalk plots under contrasting nutrient management.....87

Figure 3.3. ^{13}C nuclear magnetic resonance spectra for INTRA-AGGREGATE organic matter from four Broadbalk plots under contrasting nutrient management.....89

Figure 3.4. The mean distribution of C between functional groups in FREE organic matter from long-term plots receiving inorganic or no fertiliser, based on ^{13}C nuclear magnetic resonance peak areas.....91

Figure 3.5. The mean distribution of C between functional groups in INTRA-AGGREGATE organic matter obtained from long-term plots receiving inorganic or no fertiliser, based on ^{13}C nuclear magnetic resonance peak areas.....91

Figure 3.6. The mean distribution of C between functional groups in free organic matter obtained from long-term plots receiving inorganic or no fertiliser versus those receiving farmyard manure, based on ^{13}C nuclear magnetic resonance peak areas 92

Figure 3.7. The mean distribution of C between functional groups of free and intra-aggregate fractions obtained from 26 long-term plots under contrasting management estimated from ^{13}C nuclear magnetic resonance peak areas using residual maximum likelihood (bars indicate the standard error of difference)...92

Figure 3.8. The mean distribution of C between functional groups of free and intra-aggregate fractions obtained from 26 long-term plots under contrasting management, estimated from ^{13}C nuclear magnetic resonance peak areas and residual maximum likelihood.....94

Figure 4.1. Sschematic showing the structure of the model with respect to C, with an indication of the corresponding N flows.....101

Figure 4.2. Schematic illustrating the pattern in modelled **r**elocation flows resulting from the utilisation of the various primary substrate compartments.....108

Figure 4.3 Schematic illustrating the influence of C-to-N ratio on the division of substrate C and N between incorporation and relocation flows in the model...109

Figure 4.4. Schematic of the microbial C cycle represented in the model.....111

Figure 4.5. Possible structure for an adapted model featuring three microbial compartments but which may not be adequately parameterised unless methods are available to measure microbial sub-fractions.....114

Figure 4.6. The general relationship between C and N flows from substrate compartments using the example of the ***LF1*** and parameter values used in the scenarios.....125

Figure 4.7. Simulated dynamics of (a) C and (b) N for the HQ / H scenario.....126

Figure 4.8. Simulated dynamics of (a) C and (b) N in the HQ / XH scenario 127

Figure 4.9. Simulated dynamics of (a) C and (b) N under LQ / H scenario.....128

Figure 4.10. Simulated dynamics of ^{15}N ratio in the HQ/H scenario.....131

Figure 4.11. Simulated dynamics of $\delta^{13}C$ in the HQ/H scenario 131

Figure 4.12. Gross N mineralisation (GNM) and immobilisation (GNI) in the contrasting LQ/H and HQ/H scenarios.....133

Figure 4.13. Balance between the supply and demand for supplementary N in the HQ/H and LQ/H scenarios.....133

Figure 4.14. Flows contributing to gross N mineralisation in the (a) LQ/H and (b) HQ/H scenarios 135

Figure 4.15. The simulated balance between supply of and demand for N over time in the N limiting LQ/XH scenario 136

Figure 4.16. The simulated status of the C flow limiter λ, calculated as the balance between N supply and N demand, for the LQ/XH scenario 136

Figure 4.17. The impact of N limitation on C incorporation from ***LF1*** 138

Figure 4.18. Gross N mineralisation and gross N immobilisation in the LQ/XH and LQ/XH scenarios 138

Figure 4.19. Simulated dynamics of (a) C and (b) N under N limitation (LQ/XH) 139

Figure 4.20. Alterations in compartment and fraction C-to-N ratio with N limitation . 140

Figure 4.21. The simulated ratio of C utilisation to gross N mineralisation in contrasting scenarios 140

Figure 5.1. Differential ^{15}N enrichment in components of the maize plants grown for incorporation during the incubation study 151

Figure 5.2. The weak correspondence between the mass and C content of light fractions recovered from soil during 64 weeks incubation with and without maize straw 165

Figure 5.3. Dynamics of C in the standard SOM fractions after addition of maize straw (solid lines) compared to those in non-amended soil (dashed lines). Data for the organomineral fraction are plotted on the secondary axis 173

Figure 5.4. Dynamics of $\delta^{13}C$ in the standard SOM fractions after addition of maize straw (solid lines) compared to those in non-amended soil (dashed lines). Data for the organomineral fraction are plotted on the secondary axis 173

Figure 5.5. Dynamics of N in the standard SOM fractions after addition of maize straw (solid lines) compared to that in non-amended soil (dashed lines). Data for the organomineral fraction are plotted on the secondary axis 174

Figure 5.6. Dynamics of the 15N content of the standard SOM fractions after addition of 15N-labelled maize straw (solid lines) compared to those in non-amended soil (dashed lines). The organomineral data are plotted on the secondary axis..... 174

Figure 5.7. Dynamics of 15N enrichment in standard fractions after addition of maize straw (solid lines) compared to those in non-amended soil (dashed lines)..... 175

Figure 5.8. Dynamics of C-to-N ratio in standard SOM fractions after addition of maize straw (solid lines) and relative to those in non-amended soil (dashed lines) ……...175

Figure 5.9. Rates of gross N mineralisation measured during incubation of soil with and without (control) maize straw as estimated by ^{15}N isotope dilution 176

Figure 5.10. Spot measurements of the temperature in the sand-bed during incubation of soil with and without maize straw..... 176

Figure 5.11. CO_2 production during incubation of soil with and without (control) maize straw measured by trapping in NaOH..... 177

Figure 5.12. Dynamics of microbial C and N during incubation of soil with and without maize straw, measured by the fumigation–extraction method..... 177

Figure 5.13. Dynamics of total soluble C during incubation of soil with and without (control) maize straw 178

Figure 5.14. Dynamics of mineral N as a surrogate for NaI-soluble N during incubation of soil with and without maize straw 178

Figure 6.1. The relationship between spot temperature measurements in the sand-bed and the mean temperature under soil recorded at the meteorological station ... 184

Figure 6.2. The daily mean temperature in the sand bed estimated using data from the meteorological station 184

Figure 6.3. The status of the temperature rate modifier during the incubation 186

Figure 6.4. Comparison of estimated and occasionally measured gravimetric soil moisture during the incubation 186

Figure 6.5. Status of soil moisture rate modifier during the incubation 187

Figure 6.6 The combined effect of temperature and soil moisture modifiers on substrate utilisation rate 187

Figure 6.7. The simulated limitation of C flows governed by the balance between N supply and N demand, and indicated by the flow limiter λ 195

Figure 6.8. The **s**imulated **v**ariation in the ratio of C utilised to N mineralised during the incubation 195

Figure 6.9. The simulated versus measured (a) C and (b) N content of fractions 197

Figure 6.10. The microbial contribution to (a) C and (b) N in *light1* and *light2* as indicated by the relative magnitude of the corresponding model compartments *LF1* and *LF2* 199

Figure 6.11. The simulated versus measured C-to-N ratios of the fractions 200

Figure 6.12. Simulated versus measured $\delta^{13}C$ in the fractions 200

Figure 6.13. Simulated versus measured ^{15}N in the fractions 202

Figure 6.14. Simulated versus measured ^{15}N enrichment in thefractionss 202

Figure 6.15. The simulated C and N contents of ***Sol*** and ***Bug*** plotted against analyses of K_2SO_4-extractable and microbial biomass fractions 204

Figure 6.16. Simulated rates of gross N mineralisation plotted against independent measurement by ^{15}N pool dilution 204

Figure 6.17. The simulated relative contribution of flows other than microbial mortality to gross N mineralisation 206

Figure 6.18. Simulated CO_2 production against independent measurement by NaOH trapping 207

Figure 6.19. Simulated cumulative CO_2 production plotted against those calculated form periodic measurements 207

Figure 6.20. The sensitivity of *light1C* and *light2C* to the value assigned to the microbial incorporation constant η 209

Figure 6.21. The sensitivity of *light1C* and *light2C* to the value of the respiration constant α 209

Figure 6.22. Sensitivity of *light1C* and *light2C* to the initial magnitude of ***SolN*** 210

Figure 6.23. Sensitivity of *light1C* and *light2C* to the value of the microbial mortality rate constant *kmort* 210

Figure 6.24. Sensitivity of *light1C* and *light2C* to the microbial C-to-N ratio ρ*bug* 211

Figure 6.25. Sensitivity of simulated gross N mineralisation under standardised conditions to (a) the initial value of and (b) the initial value of *light2* 212

Figure 6.26. The simulation of (a) C and (b) N in non-amended soil 213

CHAPTER 1: INTRODUCTION AND LITERATURE REVIEW

1.1. Introduction

In the UK, approximately 1.4 Mt of N is applied each year to agricultural soils as mineral fertiliser to optimise crop yield (FMA 1999). A roughly equal quantity is added in 200 Mt of animal manure and other organic material (Pain and Smith 1994). Despite the economic cost of applying supplemental N, around 13–42 % of the total added may be lost in drainage water (Burns and Greenwood 1982; Royal Society 1983). This leaching of N contributes to the eutrophication of watercourses, and contaminates drinking water (MAFF 1999).

However, ill-timed or superfluous application of mineral fertiliser accounts for a relatively minor proportion of the loss: the inability to manage the temporal disparity between crop demand for N and its release from soil organic matter (SOM) is more fundamental (Jansson and Persson 1982; Stockdale *et al.* 1997). Despite the key importance of soil N supply, the description of biological processes is the key weakness in simulation models designed to aid nutrient management (de Willigen 1991). The uncertainty associated with model output, coupled with the low marginal cost of fertiliser application, has limited the application of models to fertiliser recommendation (Stockdale *et al.* 1997). This thesis is based on the premise that model prediction can be improved by developing robust mineralisation sub-models based around measurable parameters. Integrated within an existing system framework, such models may lead to improved management of N, and thus lessen its impact on the environment and water quality.

1.2. Soil N supply

Most N in the soil is contained in the complex, diverse organic molecules that comprise SOM. The mineral (inorganic) N component accessed by plant roots is relatively small and transient (typically 1 % of total soil N; Shepherd *et al.* 1996) and is released mainly by heterotrophic protozoa, bacteria and fungi in the utilisation of C for energy and growth. Whilst the N made available to plants through fertiliser application is predictable (being in the mineral form), instantaneous rates of mineralisation are determined both by the chemical composition of SOM, and its physical location within the soil matrix. This may in turn be influenced by past returns of organic matter (e.g. crop remains and manure), as well as by agronomic, soil and climatic factors.

1.2.1. Mineralisation

In temperate arable systems SOM accounts for a few per cent of soil weight. In approximate order of abundance SOM comprises organic macromolecules bound to mineral surfaces (chemically recalcitrant), decomposing plant debris and manure, dead microbial cells (fungal and bacterial), root exudates and deposits, and the remains of soil fauna (Christensen 1992). Although synthesis of the requisite enzymes limits mineralisation of a particular SOM component, the requirement for N in formation of new biomass (i.e. microbial growth) presents a more general limitation. If the microbial requirement for N cannot be met through utilisation of the substrate alone, microbes must draw on mineral N or low molecular weight compounds already present in the soil (Barraclough 1997). Thus in the short term, N-poor substrates can provide a sink rather

than a source of mineral N. The incorporation of mineral N into microbial biomass (re-conversion of mineral N into organic forms) is termed immobilisation, and counteracts mineralisation. The balance between mineralisation and immobilisation is strongly influenced by the C-to-N ratio of accessible C substrates.

The conversion of organic N into the mineral form and back into SOM (as microbial biomass) is described as mineralisation–immobilisation turnover (MIT). New measurement techniques have shown that MIT is extremely rapid, and measuring net changes in mineral N concentrations may not reflect mineralisation activity. Over a cropping season the gross rate of N mineralisation may exceed the net accumulation of mineral N by a factor of four (Gaunt *et al.* 1998). In addition, mineralisation estimates would be greater if direct assimilation of low molecular weight compounds (such as amino acids) could be captured in these measurements (Barraclough, 1997).

1.2.2. Crop requirement

The availability of nitrogen is a key influence on the primary productivity and species composition of natural ecosystems (Sutton *et al.* 1993). The response of crop yield to supplemental N is non-linear however, and application rates are determined by economic and legislative (i.e. environmental) considerations: economically optimal or environmentally acceptable yields are lower than the maximum achievable yield. The EU Nitrates Directive requires controls to ensure drinking water does not contain > 50 mg NO_3^- L^{-1} i.e. 11.3 mg NO_3^-–N L^{-1} (CEC 1991). Strict limits have been placed on N application in nitrate vulnerable zones and nitrate sensitive areas designated (MAFF 1999).

Temporally, crop demand for N is neither constant nor continuous: it peaks in spring (during crop development), and declines as the plant matures prior to harvest. Autumn sown cereals demand little N over winter. The application of supplemental N reflects these patterns but takes little account of variation in soil N supply (Myers 1996).

1.2.3. The fate of crop residues

A large proportion of N taken up and incorporated into crop plants is recycled to the soil, mainly through exudation of organic compounds by roots during expansion, and their rhizo-deposition. Roots have a high turnover and dead roots are also a major source of SOM (Cheshire and Mundie 1990). Further, although a significant proportion of plant biomass is removed at harvest (approx. half of the above ground biomass as grain), at least 20 % of the total remains (as chaff and stubble) in the soil–plant system. This figure increases to 60 % if straw is incorporated (Powlson *et al.* 1986). With root death and the incorporation of the above ground remains by ploughing, these residues can instantaneously provide a large C substrate. The consequence is substantial N mineralisation (possibly preceded by a period of immobilisation), generally enhanced by increasing soil moisture. The result is that the mineral N accumulated during crop-senescence (when the crop ceases to provide a major sink) increases further. The post-harvest period – particularly with increasing rainfall – is thus characterised leaching loses. Cover crops may provide a temporary sink for surplus N, being returned to the soil before sowing of a spring-sown cereal when crop demand is higher and the rainfall lower. However, the pattern and duration of N release from cover crops is neither ideal nor entirely predictable (Harrison 1996).

1.3. Soil organic matter models

Although SOM decomposition at the microbial scale is a complex process involving a multitude of biological (enzyme mediated) interactions, it is simple to conceptualise fractions which differ in their decomposability (quality). Stubble for example degrades within weeks of incorporation (ploughing) and soil humus (conferring an inherent level of soil fertility) decomposes slowly. It may be assumed that other fractions – characterised by intermediate levels of reactivity – are also present, and that exchanges occur between them (Molina *et al.* 1994). The abundance and reactivity of a particular fraction will determine its contribution to the overall mineralisation rate, with large but relatively stable (low reactivity) fractions accounting for substantial background mineralisation and the addition of small but active substrates accounting for transient peaks. If the distribution of SOM between the various fractions can be estimated or – ideally – measured, instantaneous rates of mineralisation can be predicted for the soil as a whole. This substrate-orientated view of decomposition provides the basis for the majority of SOM models, although examples of models based on the disparate abundance and activity of decomposer organisms also exist (de Ruiter and van Faassen 1994; Paustian 1994).

1.3.1. Modelling soil N supply

Simulation of N supply requires an accurate understanding of C turnover (the utilisation of C effectively driving N mineralisation), and particularly the substrates or conditions that favour net N release over immobilisation. Models aimed at predicting

long-term change in SOM tend to operate on a monthly timestep e.g. CENTURY (Parton 1996) and RothC (Coleman and Jenkinson 1996). However, models that predict soil N supply require a shorter timestep in order to resolve the dynamics of the small and transient mineral N pool, ideally hours or days rather than weeks or months (Molina 1996). It follows that such models will emphasise compartments with higher turnover than those required for long-term simulations, the precise pattern of crop residue decomposition becoming critical whilst on an inter-annual basis only the net outcome would be relevant. Typically these models use detailed information on recent cropping history rather than measurements to estimate the initial magnitude of the key SOM fractions.

With a shorter simulation horizon and timestep, climatic variation – that affects the flows between model compartments – will become more important. At best, predictions can only be based on the assumption that weather in the current season will follow the pattern observed in previous years (Smith and Glendining 1996). Also, whilst SOM turnover is a key (albeit weak) element within models predicting nutrient supply (and potentially making fertiliser recommendations), such models usually comprise a system of that includes interacting plant and water sub-models. These provide sinks for mineralised N through crop uptake and leaching, as well as accounting for additional N sources, such as the atmosphere. Existing soil–plant–water models that have been applied in the field include ANIMO (Rijetma and Kroes 1991), DAISY (Mueller *et al.* 1996) and SUNDIAL (Smith *et al.* 1996a).

1.3.2. Definition of model compartments

The conceptualisation of the decomposition process underpinning mineralisation models is, as suggested at the beginning of Section 1.3., that the utilisation of C from qualitatively and quantitatively distinct SOM fractions occurs at discrete rates according to an assumed difference in chemical composition (i.e. degradability). In addition, more accessible substrates are progressively transformed – with repeated utilisation by soil organisms – into the more stable fractions (with an increasing proportion of microbial products).

As well as assuming it is realistic to divide SOM into discrete fractions that have a specific (and constant) level of reactivity, models tend to assume each fraction mineralises according to first-order kinetics (McGill 1996). Hence mathematically SOM fraction *i* obeys:

$$v_i = k_i Y_i$$

– where ν_i is its instantaneous mineralisation rate, k_i its first-order reactivity, and Y_i its magnitude.

The key parameter k_i is the first-order reactivity constant that characterises the SOM fraction *i*, such that v_i is dependent only on its magnitude. That the mineralisation rate in the soil as a whole in whole soil does not decrease exponentially over time reflects the sequential transfer of transformed SOM to fractions of progressively lower *k*. Since these transfers are an assumed consequence of microbial activity there will be

concomitant release of CO_2 by respiration, and an immobilisation of C into microbial cells. This usually requires one or more microbial biomass compartments, defined by *k* values that reflect microbial mortality.

The instantaneous rate of mineralisation in the soil, *V*, is given by:

$$V = \sum v_i$$

Cohort models such as that of Bosatta and Ågren (1985) and Bosatta and Ågren (1996) are conceptually distinct in that the reactivity of SOM fractions is governed by age rather than assumed differences in chemical composition *per se* (although age may reflect a declining quality of substrate). Mathematically, however, such models are similar, effectively functioning as models with compartments that encompass an infinite range of *k*. Some models have used alternative (although still fixed) kinetics to describe mineralisation processes, notably double exponential or second-order (Whitmore 1996a,b; Alvarez and Alvarez 2000).

Models using one or two compartments (representing conceptual SOM fractions) were insufficient to predict turnover of SOM, but the general approach has ultimately led to relatively simple models that successfully describe long-term changes (Jenkinson 1990). Typically three or four SOM compartments are defined – at least one of which comprises microbial biomass. Usually a dichotomy in the reactivity of primary substrates is assumed, with partitioning of plant inputs between two or more compartments of different *k* (for example decomposable- and resistant pant material in RothC; Coleman and Jenkinson 1996).

In these schemes no explicit account is made of soil structural influences i.e. physical factors. These effects tend to be accounted for implicitly through empirically derived relationships, which modify the partitioning of SOM flows between compartments. In reality, however, physical structure determines the micro-sites available to decomposer organisms and the physical protection of organic particles in stable aggregates, as well as the prevailing environmental conditions. The concept that these factors are the primary factors governing decomposition (Golchin *et al.* 1994a; Balesdent 1996; Skjemstad *et al.* 1996a) has not been incorporated into most models. One exception is the model described by Verberne *et al.* (1990), which contains physically protected compartments for both active organic matter and microbial biomass These compartments are characterised by lower *k* than the corresponding unprotected fractions, but behave functionally as slower turnover compartments defined in other models.

Models simulating both C and N feature two compartments for each SOM component. Although corresponding C and N compartments are characterised by the same *k* (reactivity), their relative magnitude may limit flows of C and / or N to microbial biomass in the absence of supplementary (i.e. mineral) N in the system. These C–N models, reflecting their likely application, also tend operate on a timestep of days to weeks rather than months to years (see Section 1.3.1 above). They also take account of short-term variation in temperature and soil moisture on microbial activity in modification of compartment *k* values on the basis of average or measured variation in climatic conditions.

Within a given layer, soil is assumed to be homogenous with respect to nutrients and water flow as well as distribution of SOM fractions including microbial biomass. However, depth resolution (i.e. the number and size of soil layers) varies according to application. Models simulating forest or grassland soils, or unploughed agricultural systems, demand fine depth resolution. In models concerned with topsoil of tilled arable land, the soil may be considered as a single layer e.g. Molina *et al.* (1983).

1.3.3. Parameterisation and validation

In order to develop a model that simulates real processes it is necessary to develop a conceptual framework, establish relationships within the framework, and validate model behaviour using measurements of the system. Relationships to be established include the reactivity (k) of the compartments, and the division of flows between sources and destinations. In models with several compartments and many connecting flows, but only one or two measurable variables (e.g. CO_2 production and total SOM), there are likely to be many combinations of parameter values that provide equal, simultaneous agreement with the limited measurements that are possible (Molina *et al.* 1994). Such models are often described as black box, since the measured variables tend to be at the system level (i.e. inputs, outputs and total stocks), and the largely conceptual compartments and exchanges between them yielding limited verifiable information on real processes. Further, without model compartments that can be measured, empirical relationships – similar to those relating numeric parameter values to site-specific soil properties – are required to initialise the model and make predictions. In short, the inability to measure sufficient model compartments and flows weakens parameterisation and imposes a fundamental limitation on application and

future development of current SOM models (Christensen 1996b; Elliott *et al.* 1996; Molina and Smith 1997).

Model validation tests the relationships developed during parameterisation against independent datasets – ideally relating to contrasting agronomic, soil or climatic circumstances. A range of statistical methods is available to assess agreement between model prediction and measured data (Smith *et al.* 1996b). The numeric value of model parameters for a specific validation dataset may be unique, but derived only through pre-established relationships encompassed in the model. If further adjustment is necessary the validation fails, and the data will be subsumed into the parameterisation process (relationships being re-defined to accommodate the new observation). In this sense parameterisation and validation are not entirely distinct.

1.3.4. Measurable model compartments

The number of ways in which model components can interact in order for the output to match experimental measurements is reduced if the number of measured variables is high (Molina *et al.* 1994). This is particularly the case where a number of these variables are dynamic over the short-term. In a model with many measurable variables, the combination of parameter values that provide correct simulation of processes can more easily be distinguished from those giving the right system level output for the wrong reason. Models that accurately simulate processes will be more robust, and hence operate with greater reliability in a wider range of situations.

Most existing SOM models feature at least one compartment that can be estimated experimentally i.e. microbial biomass (measured by the fumigation–extraction method; Brookes *et al.* 1985). Biomass is a relatively active SOM fraction and the microbial *k* can be determined from relatively short-term experiments (Gregorich *et al.* 1991; Ladd *et al.* 1995). Introducing other measurable variables progressively increases the likelihood of parameterisation resulting in a model that simulates real soil processes. (Alternatively, an additional measurement can permit the complexity of a model to be increased without compromising the certainty attached to its output.)

That existing models, despite their limitations, can describe long-term trends in SOM suggests their conceptual compartments should have equivalents in the soil. This is supported by the observation that the reactivity (*k*) of equivalent compartments in different models fall within a narrow range (Molina *et al.* 1994). Recognising the effort invested in development and parameterisation of current models, establishing methods to measure SOM fractions corresponding to existing model compartments (i.e. of equal size and reactivity) is an attractive approach to overcoming their limitations (Elliott *et al.* 1996). However, model compartments are effectively defined by *k*, and methods that reliably isolate SOM by their specific reactivity are difficult to envisage. Realistically, any measured fraction (and the model compartments themselves) will encompass a range of reactivity. However, this may be acceptable if the range is narrow and the mean reactivity is precisely matched. Where a measured fraction has an appropriate mean reactivity, but the magnitude is incorrect, sequential measurement of multiple compartments is ruled out, and only correlation is possible.

Due to the lack of success in identifying chemical fractions of biological relevance (Oades 1995), most attempts to link specific model compartments to experimental SOM fractions have – despite their conceptual basis in chemical composition – tended to rely on physical fractionation methods. In particular, particulate organic matter separated by sieving (POM) has been correlated to the Slow compartment in the CENTURY model (Cambardella 1997). In dynamic experiments, a redefined (sub-divided) Slow compartment has also been matched to density-defined size fractions (Sitompul *et al.* 2000), and similar fractions to the added organic matter (AOM1) compartment of the DAISY model (Magid *et al.* 1996b). Organic N fractions obtained by electro-ultrafiltration and simple extractions with $CaCl_2$ have, however, been correlated with Pool II and Pool III in NCSOIL (Appel and Mengel 1998). The inert organic matter compartment of RothC has been measured (but not isolated) using ^{14}C carbon dating (Jenkinson and Coleman 1994).

A major problem with these approaches is that they generally enable only one compartment to be estimated, else separate measurements of each compartment are required. Independent measurements are not desirable since they are associated with compounded measurement errors, and a risk of double counting. Where a correlation measurement provides a correlation rather than a precise match, sequential separation is impossible due to mixing of the residual fractions. (This applies to the main measurable compartment in existing models: fumigation–extraction method only recovers 45 % of the C and N in microbial biomass; Brookes *et al.* 1985).

Thus a more flexible approach is to model the measurable, that is to construct a model around SOM fractions defined by a new fractionation method which maintains

mutual exclusivity of SOM fractions through a sequential separation. Such a framework has been proposed by Christensen (1996).

1.4. Modelling measurable fractions

Models that contain several measurable compartments should be simpler to parameterise and verify, particularly if the dynamics of the fractions they simulate can be measured on a realistic time scale. Furthermore, model parameterisation will be more robust and straightforward, agreement having to be reached between the dynamic, simultaneous measurement of several variables. The predictions of the parameterised model could also be verified by monitoring the concentration of the various SOM fractions, and initialisation could be confirmed by measurement. A reliance on empirically derived rules (which require detailed site-specific information) should be reduced.

A simple experimental situation used to parameterise such a model would involve the incorporation of crop residues into soil, followed by incubation (possibly under controlled conditions), and fractionation to determine the size of model compartments over time. Once developed for use in complex systems, the model could be verified in the field. Long-term data would still be required to determine the turnover of the less reactive SOM fractions, but the dynamics of several key compartments would provide good indication of likely applicability, and rigorous parameterisation would be required only over the time period relevant to the application. Providing the model could simulate the fractions dynamic on the time scale relevant to the application, the background activity of stable (less reactive) fractions could be considered constant.

A model parameterised using relatively short-term data provide could provide adequate prediction of soil N supply.

1.4.1. Operationally-defined fractions for modelling

Since it is optimistic to expect an experimentally obtained SOM fraction to be perfectly defined with respect to a pre-determined reactivity (*k*), it is more realistic to consider them defined by a SOM fractionation procedure. These operationally- (rather than conceptually- defined SOM fractions are not only measurable, but may be isolated by physical rather than chemical fractionation, and thus reflect the influence of their location in the soil rather than their chemical reactivity *per se*.

Conceptually, current models (with exceptions e.g. Verberne *et al.* 1990) assume compartment reactivity is governed solely by chemical composition. Their reliance on texture modifiers (usually based on soil clay content) may reflect the lack of an explicit consideration of soil structure (e.g. physical protection of SOM in aggregates) as much as the functional characteristics of clay itself (McGill 1996). These modifiers are generally applied to the compartment rate constants (Molina and Smith 1997), but may also alter flow-partitioning parameters according to empirically derived equations e.g. CENTURY (Parton 1996). Evidence increasingly supports, however, the view that physical effects are of equal importance to SOM turnover as chemical composition, and should therefore be explicitly represented in models e.g. Balesdent (1996).

A conceptual model based on physical location is highly compatible with physical fractionation i.e. separation of SOM by particle-density and / or particle-size

(Christensen 1996b). Since physical fractionation is relatively non-destructive, they offer possibilities for the chemical characterisation of modelled fractions, and hence verification at a process-level.

A potential drawback in modelling the measurable, however, is that measured fractions may be seen to vary in composition, and potentially reactivity, over time. To accommodate these observations new, more radical mathematical frameworks may be required, possibly allowing time-dependent variation in *k*.

1.4.2. Physical fractionation

Physical fractionation is intended to emphasise the close relationship between the physical location of SOM and its decomposition. However, there is no presumption as to whether any observed differences in chemical composition are conferred by location, or *vice versa*. On the basis of the main separation properties available – particle-density and particle-size – conceptual categorisations can be made. On the basis of density SOM can be divided into light and heavy fractions, comprising organic particles and aggregated mineral particles respectively. Organic particles located within aggregates can be isolated as light material, if aggregates are first broken down into primary particles (Gregorich and Janzen 1996). Protected within aggregates, it seems such particles differ in decomposition rate (Gregorich *et al.* 1996), and this may be reflected in their chemical composition (Golchin *et al.* 1994b). The protected (or occluded / intra-aggregate) fraction may slowly form around residues of primary substrates, or around centres of microbial activity during substrate utilisation (Spycher *et al.* 1983). The surfaces of primary particles – mainly silt and clay-size – bind with

organic macromolecules to form organomineral complexes, products of the interaction between slowly decomposing organic material and microbial enzyme activity (Christensen 1996a).

Clay-size organomineral complexes may have a particular significance in the turnover of SOM (Christensen 1992), and can be isolated (after soil dispersion) using simple methods based on sedimentation. The settling velocity (*s*) of a spherical particle in suspension is determined by Stokes Law:

$$s = [\, G.\, D^2 (d_\rho - d_l\,) \,] \,/\, 18\, n$$

– where G is the acceleration induced by gravity, D the diameter of the particle, d_ρ its density, and d_1 and *n* the density and viscosity of the suspension (the latter being temperature dependent). The calculated settling rate is highly sensitive to particle diameter, although the assumption of spherical particles may be unrealistic for laminar clays.

Physical fractionation offers a new conceptual model for SOM decomposition, in which free light particles comprise the most reactive fraction, protected light particles a less reactive fraction, and organomineral material the least reactive (possibly varying with particle-size). It may be envisaged that plant inputs pass – with successive transformations through microbial biomass – from the free light to protected light fraction and / or organomineral material. If the distribution of microbial biomass were determined, it would likely be located within all three of these fractions.

The chemical composition of a SOM fraction is not likely to be greatly altered during separation, and non-invasive characterisation should reflect the composition of the material available to decomposer organisms in the soil. Physical protection may be measured by comparing the reactivity of a fraction *in situ* with that measured after isolation.

1.5. Isotopic tracers for soil organic matter

Isotopic methods have been widely used to aid parameterisation and validation of SOM models (Paul and van Veen 1978). Where isotopes are used dynamically (i.e. with multiple measurements), tracers are represented by separate model compartments operating in parallel to C or N equivalents, with tied flow rates e.g. Smith *et al.* (1996a). Using isotopes in this way enables a model to be constrained by a greater number or simultaneous measurements. However, isotopes may also be used to establish the current age of a fraction by a single ^{14}C measurement, or the average rate of turnover from the displacement of old C by distinct modern C using the $\delta^{13}C$ method e.g. Cadisch and Giller (1996) and Balesdent and Mariotti (1990).

1.5.1. Stable isotope studies

In soil the stable ^{13}C and ^{15}N isotopes useful for tracing SOM have a natural abundance of approximately 1·11 and 0·3663 atom% respectively (Wolf *et al.* 1994). Thus the dynamics of ^{13}C and ^{15}N in SOM resulting from addition of moderately enriched substrates will be more apparent than that of total C or N, and the activity of quite stable fractions can be inferred (providing they can be isolated for mass

spectrometry). This is particularly useful for fractions that are in steady or near-steady state (i.e. with balanced inputs and outputs), where there is no detectable change in magnitude of total C or N over the short term. The basic assumptions in isotope studies are that isotopic discrimination is not significant (i.e. that the tracers are utilised at the same rate as naturally abundant ^{12}C and ^{14}N) and that – within a fraction – the C and / or N derived from a labelled substrate has a typical rate of turnover. Gross rates of N mineralisation (which may correspond to certain flows between model compartments) have also been quantified using ^{15}N, either by observing the dilution of a ^{15}N-enriched mineral N pool (Murphy *et al.* 1997) or – for a specific added substrate – its increasing enrichment (Barraclough 1997).

1.5.2. Natural abundance

The natural abundance of the ^{13}C and ^{15}N isotopes in biological materials is not fixed (Boutton 1996; Hopkins *et al.* 1998). Relatively small differences occur as a consequence of isotopic fractionation during transformation from mineral and organic forms or phase change: it is typical for the proportion of the heavier isotopes to decline with successive biological transformations. The ^{13}C content of plant material is thus 0·4 to 2·0 % less than that of atmospheric CO_2 due to fractionation in photosynthesis. Soil organic matter is further and progressively depleted in ^{13}C with successive transformation by decomposer organisms. The small differences resulting from isotopic fractionation are expressed in ‰ (i.e. parts per thousand) deviation (δ) from the concentration in a standard. The standard material for ^{13}C was a carbonate formation of heavily transformed biological origin (Pee Dee Belemnite, PDB) so plant material and the atmosphere have negative $\delta^{13}C$ values. (The current standard material is

hypothetically identical to PDB.) Although $\delta^{13}C$ values for higher plants range between –6 and –34 ‰, they fall into two relatively well defined ranges according to their photosynthetic pathway i.e. whether they are C_3 or C_4 species: -34 to -24 ‰ and –9 to –6 ‰ respectively (Smith and Epstein 1971).

The isotopic difference between C_3- and C_4-derived organic matter is transferred into SOM. This enables the persistence of SOM from C_3 vegetation after conversion to C_4 crops to be measured (Gregorich *et al.* 1995), and the relative contributions of species in mixed C_3–C_4 systems to be quantified (Cadisch and Giller 1996). This approach has also been used to examine medium-term turnover of SOM in tropical agriculture where forest (exhibiting C_3 photosynthesis) have been replaced by C_4 crops including maize, sugarcane and many tropical grasses (Bonde *et al.* 1992; Arrouays *et al.* 1995). In temperate regions most agricultural soils have only received C_3 inputs, and the technique has been used to examine the dynamics of microbial biomass and physical SOM fractions following the introduction of C_4 species (Balesdent *et al.* 1987; Balesdent and Mariotti 1990; Ryan *et al.* 1995; Amelung *et al.* 1999). However, it has been established that for plants of a given category, the isotope ratio of contrasting chemical fractions can vary considerably (Benner *et al.* 1987; Schweizer *et al.* 1999).

The ^{15}N content of the atmosphere is highly constant (0·3663 atom% ^{15}N) and may be used as a standard in mass spectrometry (Mariotti 1983). Soils are generally slightly enriched in ^{15}N at natural abundance due to processes that involve phase change and also leaching (Hopkins *et al.* 1998; Cadisch *et al.* 2000). The natural abundance of ^{15}N in plant material generally reflects that of soil, but may be close to or less than that of the atmosphere where N_2 fixation is a significant or dominant source of nutrition

(Steele *et al.* 1983). However there are more caveats in the study of N turnover from plant residues using natural abundance than for ^{13}C: variation with soil depth and between SOM fractions tends to be large. However, it has been demonstrated as a workable method for the measurement of certain N flows, specifically N_2 fixation (Cadisch *et al.* 2000).

1.5.3. Radioisotopes

The ^{14}C isotope has a half-life of 5730 years, and has been used for tracing the fate of C from organic or inorganic substrates into microbial biomass (Amato and Ladd 1992; Ladd *et al.* 1995) and physical SOM fractions (Hassink and Dalenberg 1996; Ladd *et al.* 1996; Magid *et al.* 1996). This can be achieved without complex sample preparation or mass spectrometry, relying instead on scintillation counters..

The natural abundance of ^{14}C in the atmosphere is extremely low but well defined. Being radioactive, the decline in ^{14}C content can be used to determine the age of organic materials (i.e. years since photosynthetic fixation). Carbon dating is expensive since as the measurements are far below the sensitivity offered by mass spectrometers. However, the ^{14}C technique has been used to quantify the slowest turnover compartments such as inert organic matter in RothC (default average age is 50 000 y), and the passive compartment in CENTURY (average age 400 to 2000 y) (Jenkinson and Coleman 1994; Paul *et al.* 1997).

The near doubling of atmospheric ^{14}C resulting from above-ground weapons testing in the 1960s constituted a pulse labelling of the global C cycle, with C

incorporated into plants during this period significantly enriched compared with the past, and its current declining abundance (especially in the southern hemisphere). The fate of organic matter in SOM fractions of intermediate turnover formed during this period has been traced using their elevated concentration of ^{14}C e.g. Townsend *et al.* (1995), Richter *et al.* (1999).

1.6. Chemical characterisation

Techniques are required to measure the homogeneity of fractions represented in SOM models within and across soils, to establish their likely consistency and variation in reactivity (see Section 1.3.2). Suitable methods should be non-invasive, quantitative and provide more detailed biologically relevant information than C-to-N (or lignin-to-N) ratio, whilst not precluding summarisation (Christensen 1992). If neither fractionation nor the characterisation significantly alter the composition of SOM, the characterisation should be relevant to the analysed fractions *in situ*.

Nuclear magnetic resonance (NMR) and Fourier transform infra-red (FTIR) are spectroscopic techniques that broadly meet these criteria. Although there are caveats to quantitative interpretation, the position and magnitude of spectral peaks broadly reflect the relative abundance of key functional groups (ubiquitous molecular building blocks of organic macromolecules) or key atomic bonds. This information may indicate the chemical recalcitrance of a sample, and hence its susceptibility to microbial decomposition (Oades *et al.* 1987; Baldock *et al.* 1992; Niemeyer *et al.* 1992; Skjemstad *et al.* 1998; Leifield and Kogel-Knabner 2000).

1.6.1. Nuclear magnetic resonance spectroscopy

The NMR technique is isotope specific and has been used in SOM studies to determine the abundance of C, N and P in functional groups from the distribution of ^{13}C, ^{15}N and ^{31}P. The spectra reflect the contrasting patterns of energy release following resonance in an intense magnetic field. The technique is ideally suited to liquid samples and this, combined with low concentrations of the element, low natural abundance of the relevant isotope, and interference from paramagnetic materials (particularly Fe and Mn), limits application of NMR to samples of whole soil (Kinchesh *et al.* 1995). Since repeated resonance–relaxation–observation sequences are required to build an NMR spectrum, such samples are slow to analyse.

To obtain spectra from solids also requires rotation of the sample at a frequency comparable to that of the nucleus, and at a specific angle relative to the magnetic field (magic angle spinning, MAS). Sidebands to spectral peaks result, and since these may overlap and obscure others, correction sequences such as TOSS (total suppression of sidebands) are necessary (Dixon 1982). The low natural abundance of ^{13}C, and the low concentrations of C in soils, also necessitates cross-polarisation (CP) for ^{13}C NMR. However, the transfer of excitation energy by protons (H^+) is not entirely uniform i.e. different functional groups responding to CP to a greater or lesser extent depending on their proximity. The resultant loss of quantitative information can be minimised by optimising spectra acquisition parameters, but the presence of paramagnetic compounds can exacerbate it by differentially accelerating H^+ relaxation (Preston *et al.* 1994; Kogel-Knabner 1998).

The major functional groups and indicative peaks for ^{13}C NMR are indicated in Figure 1.1. Chemical shift regions (with the appropriate limits) which can be used to summarise a spectrum by integration of spectrum area are also shown. A more detailed analysis of ^{13}C NMR spectra is possible using the more definitive list of peak assignments in Table 1.1.

1.6.2. Infrared spectroscopy

Infrared spectroscopy is complimentary to NMR, deducing the relative abundance of C, O and H bonds from electromagnetic absorption peaks (stretching or bending of specific molecular bonds results in definable, wavelength-specific absorption in the infra-red region). Fourier transformation provides interpretable spectra, and the technique is generically referred to as FTIR. Diffuse reflectance FTIR (DRIFT) is a variant of the method, the wavelength of the absorbed radiation being determined from reflected rather than transmitted radiation (Skjemstad *et al.* 1998). The main limitations of DRIFT (and FTIR in general) lie in the required concentration of organic matter in a sample, overlapping peaks and matrix effects (peaks from mineral components). For these reasons the technique is most often applied to highly organic soils or SOM extracts (Niemeyer *et al.* 1992).

Absorption peaks are indicative of major molecular bonds, and are identified by their wavenumber or wavenumber range (Table 1.2.). Wavenumbers are calculated as $1/\lambda$, where λ is the absorbed wavelength (cm).

Figure 1.1. The main functional groups identified by a solid-state ^{13}C nuclear magnetic resonance spectrum with associated chemical shift limits

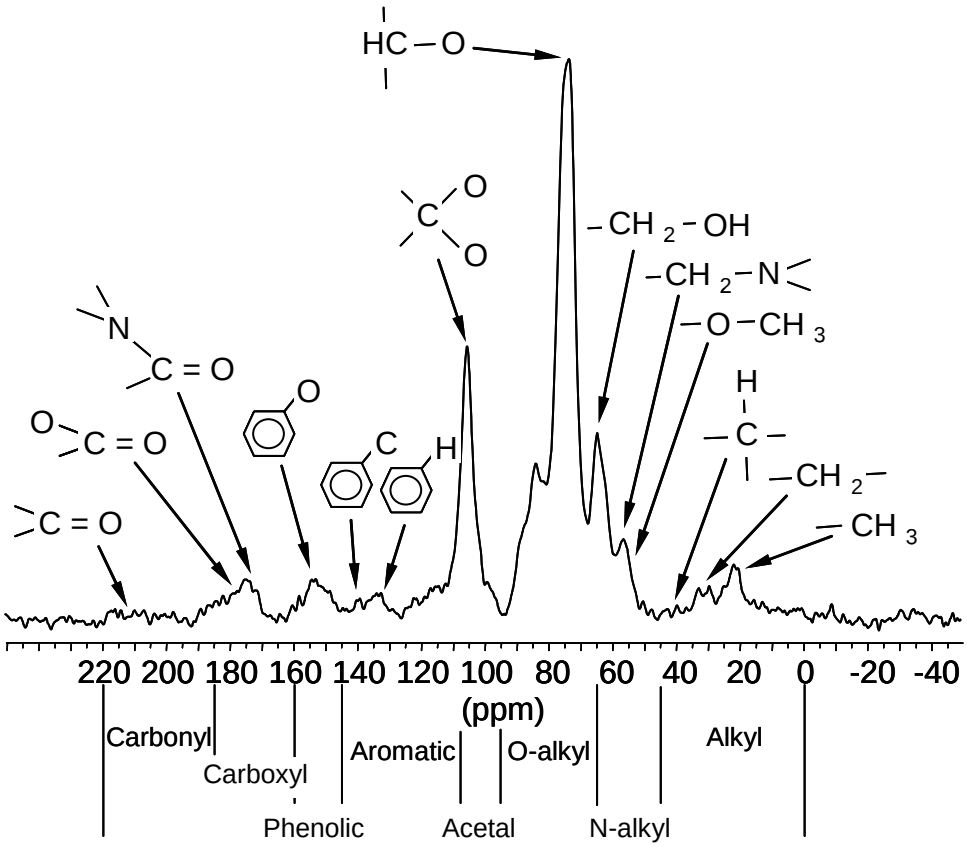

Source: Waite Solid-state NMR Facility, University of Adelaide, Australia (http://www.waite.adelaide.edu.au/NMR/) and Randall *et al*. (1995)

Table 1.1. Detailed peak assignments for ^{13}C nuclear magnetic resonance spectra

Functional group / sub-group	Typical shift assignment(s)	
Carbonyl 220-185		
C=C–C=O	~220	Quinoxyl
C=O	205	Ketone (aliphatic)
	190	Ketone & aldehyde
Carboxyl 185-160		
O–C=O	>175	Carboxylic acids (aliphatic)
N–C=O	<174	Amidic carboxylic esters (amino acids, aryl)
	174	Acetyl
	172	Alpha-hydroxyl esters
$(O)_2$–C=O	168–164	Carbonate
Phenolic (145-160)		
Aryl-O	158–135	Phenolic / aryl-ether
	155–150	Lignins / tannins
	153–148	Lignins / tannins
p-hydroxyphenyl	156–152	
Guaiacyl	150–140	
Syringyl	155–150	
Aromatic (145-108)		
Olefins	152–105	
Polycyclic aromatic hydrocarbons	+/-132	
	130	Fresh charcoal
	135	Coke
cyano, nitrile	120–104	
Acetal (108-95)		
O-CH_n-O	110	Anomeric C of saccharides
	105	Cellulose (I)
	107.9, 106.2	Cellulose (II)
	103.3	Cellulose (β form)
Hemicellulose	~103	
Polysaccharides	101.5–100	β-glucosyl
		α-xylopyranosyl
		galactouronan C1 carbons
O-alkyl (95-65)		
Acetylenic	90–60	
Cellulose (I)	89.5–88	C4
Xtalline	89.4	
Cellulose (II)	89	C1-C5
Cellulose (I)	87	C4
Hemicelluloses	83.9	Amorphous
Cellulose (II)	77	C1-C5
Cellulose (I)	74.17	C2, C3, C5
Cellulose (II)	73.5	C1-C5
Cellulose (I)	72	C2, C3, C5
Cellulose (I)	68.1	C6
N-alkyl (65-45)		
β-glucosyl	65–64.5	C6
β-galactosyl	65–64.5	C6
Cellulose (II)	64	C1-C5
Celluloses	61.5	Amorphous
CH_3–O–	62–60	Methoxyl aryl esters (e.g. syringyl)
	57–55	Methoxyl
Alkyl (45-0)		
>CH– (tertiary)	58–52	
Chitin	56	C2 (N-acetyl uronic acid)
β –C proteins	~55	
CR_4 (quaternary)	48–36	
CH, CH_2	42– -10	
CH_2	39	
	33	
	30	
	23	
CH_2 (cyclic)	23.5-18.5	
Acetyl–(CH_3)	21	
$(CH_3)_6C_6$ (Hexamethylbezene)	18.4	

Source: Waite Solid-state NMR Facility, University of Adelaide, Australia (http://www.waite.adelaide.edu.au/NMR/)

Table 1.2. Peak assignments for diffuse reflectance Fourier transform infrared spectroscopy

Wavenumber (cm^{-1})	Peak assignment
3400–3300	O–H stretching (H bonded OH groups)
	N–H stretching
3380	OH stretching of phenolic OH
3030	Aromatic C–H stretching
2940–2900	Aliphatic C–H stretching
2600	O–H stretching of H-bonded –COOH
1725–1720	C=O stretching of -COOH and ketones
1660–1630	C=O stretching of amide groups (amide I band)
	Stretching of quinone C=O
	C=O strectching of H-bonded conjugated ketones
	Asymmetric –COO stretching
1590–1517	COO– symmetric stretching
	N–H deformation
	C=N stretching (amide II band)
1525	Aromatic C=C stretching
1460–1450	Aliphatic C–H
1400–1390	OH deformation
	C–O stretching of phenolic OH
	C–H deformation of CH_2 and CH_3 groups
	COO– asymmetric stretching
1350	Symmetric COO– stretching
	–CH bending of aliphatics
1280–1200	C–O stretching and OH deformation of COOH
	C–O stretching of aryl ethers
1270	C–OH stretching of phenolic OH
1225	C–O stretching and OH deformation of COOH
1170–950	C–O stretching of polysaccharide-like substances
	Si–O stretching of silicate impurities
1170	C–OH stretching of aliphatic OH
1170	C-O stretching of polysaccharides
1070	C–C stretching of aliphatic groups
1050	C-O stretching of polysaccharides
830	Aromatic CH out of plane bending
775	Aromatic CH out of plane bending

Source: Baes and Bloom (1989), Bloom and Leenheer (1989) and Stevenson (1994)

1.7. Thesis outline

The objective of this research is to develop and parameterise a dynamic SOM model based around measurable fractions. Parameterisation will be limited to a relatively simple decomposition event: C and N mineralisation following a single addition of crop residues to unplanted soil. The model could ultimately substitute relatively weak descriptions of SOM processes in current system models (de Willigen 1991). However, a more comprehensive parameterisation would be required to address possible direct effects of plants on the dynamics of SOM fractions, not accounted for by the system framework.

In the first phase, the criteria required of modelable SOM fractions will be established, and a standard physical fractionation procedure defined to measure and isolate compatible fractions in soil (Chapter 2). Characterisation of chemical composition will be used to indicate whether the defined fractions are likely to meet these criteria (Chapter 3). In Chapter 4 a preliminary model structure will be defined. This will embody the conceptual understanding of the relationships between the measurable SOM fractions, and will be performed using a graphical modelling software package.

The second phase of the research is to parameterise the model using experimental data, to verify that the defined flows and compartments are able to describe mineralisation processes. This will involve measurement of model compartments and gross rates of C and N mineralisation during a mineralisation episode

in a test soil (Chapter 5). The optimisation of model parameters to fit the experimental data will be described in Chapter 6. The parameterisation will enable the model to describe a specific mineralisation event – that for which parameterisation data was obtained.

The third and continuing phase of the research is the development of the model for application to other situations, accounting for variables such as soil type, substrate quality and tillage. Within the scope of this thesis it is not possible to consider all these aspects. However, further decomposition experiments using two additional soil types are under way, and will establish the influence of soil texture.

The ultimate goal of this research is to develop a universally applicable model that not only describes measured mineralisation patterns, but can also predict them. Although this may require empirical relationships between model parameters and basic site-specific information, the model may be initialised at any location by experimental measurement. Key areas for development of the model will be identified in Chapter 7, along with other priorities for further research. In particular the measurement and modelling of variable reactivity (k) within SOM fractions will be discussed.

CHAPTER 2: A STANDARD FRACTIONATION PROCEDURE

2.1. Introduction

The first stage toward a model based around measurable SOM fractions is a standard experimental method, compatible with a conceptual model describing their mechanistic interaction. Physical fractionation isolates SOM according to location within the soil matrix, and thus offers a good basis for allocating SOM between compartments of discretely differing levels of reactivity (Molina *et al.* 1994; Balesdent 1996). This is important because a significant change in the reactivity of organic matter (k) is more likely to result from incorporation into aggregates (for example) than through a specific biochemical transformation. Physical fractionation also provides SOM fractions that are chemically and physically intact, permitting *ex-situ* characterisation of chemical composition (Christensen 1992). Whilst separated by their physical properties, such fractions are strictly defined by an experimental procedure i.e. operationally (see Section 1.4.1.). It is therefore essential that a fractionation method is both standardised, and applicable to the relevant range of soil types. In this chapter a standard protocol for the measurement of modelable SOM fractions will be defined.

2.1.1. Essential fraction characteristics

The mathematical framework used to model SOM dynamics places a fundamental limitation on suitable fractionation methods. The parameterisation data envisaged will encompass up to **4***n* measurements at each time interval (C, N, ^{13}C and ^{15}N in n compartments). The number of quantifiable flows (assuming bi-directional

exchange between compartments) will be $\mathbf{2}n.(n - \mathbf{1})$. This number can be halved if – as should be possible – a relationship between C and N flows can be established. Assuming $n.(n - \mathbf{1})$ unknown flows and $\mathbf{4}n$ measurements, it should be possible to infer the reactivity (k_i) of up to five measurable compartments. Although experimental evidence may justify the omission of specific flows, this relationship places a fundamental limit on the number of fractions that a useful procedure will identify. Schemes that define more than five fractions will be useful only if additional tracers are available. Parsimony should be a key requirement of a model and associated fractionation methods.

The chemical composition of SOM fractions may be assumed, as a first approximation, be assumed to reflect their *in-situ* reactivity. Consistency in the composition of each modelled fraction, and in the differences between fractions (across soils) should reflect the limits of model applicability. Although such consistency suggests suitability for modelling, greater differences may still be found between fractions defined using an alternative method.

By definition, models include compartments of contrasting reactivity to provide useful output. In addition, more than one compartment should be dynamic on a timescale relevant to the model application. The calculation timestep must also be compatible with the highest compartment *k* value. Current models fall into two groups in these respects – the long-term SOM models such as RothC (Coleman and Jenkinson 1996) and CENTURY (Parton 1996) featuring longer timesteps compared with those aimed at fertiliser recommendation e.g. SUNDIAL (Smith *et al.* 1996a) and DAISY (Mueller *et al.* 1996).

2.1.2. Aggregation and soil dispersion

The level of dispersion applied to a soil before or during physical fractionation will have a strong influence on the outcome. Although aggregation occurs at a range of spatial scales, aggregates can be broadly categorised according to their stability in water (Tisdall and Oades 1982; Oades and Waters 1991). This categorisation has relevance to the field environment where soils are subject to wetting and drying cycles, and most physical fractionation methods involve immersion of soil in water or an aqueous solution. Micro-aggregates are the most stable and generally defined as accretions of primary particles < 250 μm diam. (Christensen 1996a). Micro-aggregates have been shown to sequester particles of SOM, probably in their formation around dead microbial cells as well as primary substrates depleted of more chemically accessible components (Spycher *et al.* 1983; Golchin *et al.* 1994). The distinction between this fraction and intercalated material (which, located between clay plates, has near-total physical protection from decomposition irrespective of its composition) is unclear, although experimentally it is likely to reflect the energy used to disperse the soil (Christensen 1996a). The distinction between intra-aggregate and free organic particles is useful since they may be isolated sequentially in fractionation.

Conventional textural analysis achieves complete breakdown of micro-aggregates through chemical oxidation of SOM followed by extended shaking in water, usually with a chemical dispersant such as sodium hexametaphosphate (Gee and Bauder 1986). The potential for using shaking without prior oxidation in SOM fractionation are limited by the capacity of organic matter bound to mineral surfaces to withstand

abrasion: studies have shown that this fraction is rapidly released into suspension (Watson 1971; Hinds and Lowe 1980; Morra *et al.* 1991). Consequently ultrasonic dispersion is the most widely practised method for intact separation of primary particles and protected SOM from micro-aggregates. Ultrasonic generators produce high frequency (≈20 kHz), small amplitude (≈20 µm) oscillations in a titanium probe which, when immersed in solution, cause dissolution at the probe tip. The cavitation energy of resultant voids is transmitted rapidly through the suspension to the surface of micro-aggregates. The release of this energy is sufficient to break bonds between primary soil particles.

2.1.3. Alternate physical fractionation approaches

As suggested in Section 1.4.2., separating light fraction before and after dispersion increases the number of fractions identified by density fractionation (providing, with the residual heavy fraction, a total of three). Particle-size fractionation is based on the premise that diminution of substrates directly reflection stage of decomposition, or specifically a particular level of bio-physical fragmentation (Cambardella and Elliott 1992). Sand size fractions are assumed to contain relatively fresh organic matter (mainly as discrete particles distributed amongst mineral sand grains), with the silt and clay size particles encompassing the chemically protected fraction (i.e. bound to mineral surfaces). Sand-size fractions can be removed by wet sieving, with residual clay and silt separated by sedimentation. Complete dispersion is necessary to differentiate clay- and silt-size primary particles. However, some schemes do not require complete dispersion of stable aggregates before sieving (Balesdent *et al.* 1987), dividing SOM between a more reactive sand fraction (e.g. particles > 50 µm

diameter) and more fraction in micro-aggregates (comprising both protected organic particles and surface-protected components). Density- and size-based approaches can also be combined through size-separation of heavy fraction or density separation of sand-sized particles. This may be useful in comparing separation methods, but the total number of fractions may exceed the number that can be successfully modelled (see Section 2.1.1.).

In this chapter two-stage density separation will be compared with particle-size fractionation of dispersed soil. Since the fractions obtained by the density method are likely to be sensitive to separation density and aggregate dispersion, these parameters will be optimised as part of the comparison. The composition of the fractions will be compared using ^{13}C NMR and DRIFT (see Section 1.6.). These analyses will indicate which approach provides SOM fractions that are most likely to be suitable for modelling.

2.2. Materials and methods

In this experiment an integrated density–size fractionation method was used to simultaneously a) compare – by chemical characterisation – size fractions obtained before and after density separation and from whole soil, and b) optimise density fractionation (see scheme in Figure 2.1). The output will be a standard fractionation protocol, which defines SOM fractions that meet the necessary criteria (see Section 2.1.1.), and which is applicable to soils in a range of textural categories.

Figure 2.1. An experiment to simultaneously optimise density fractionation and compare an approach based on particle-size using chemical characterisation techniques

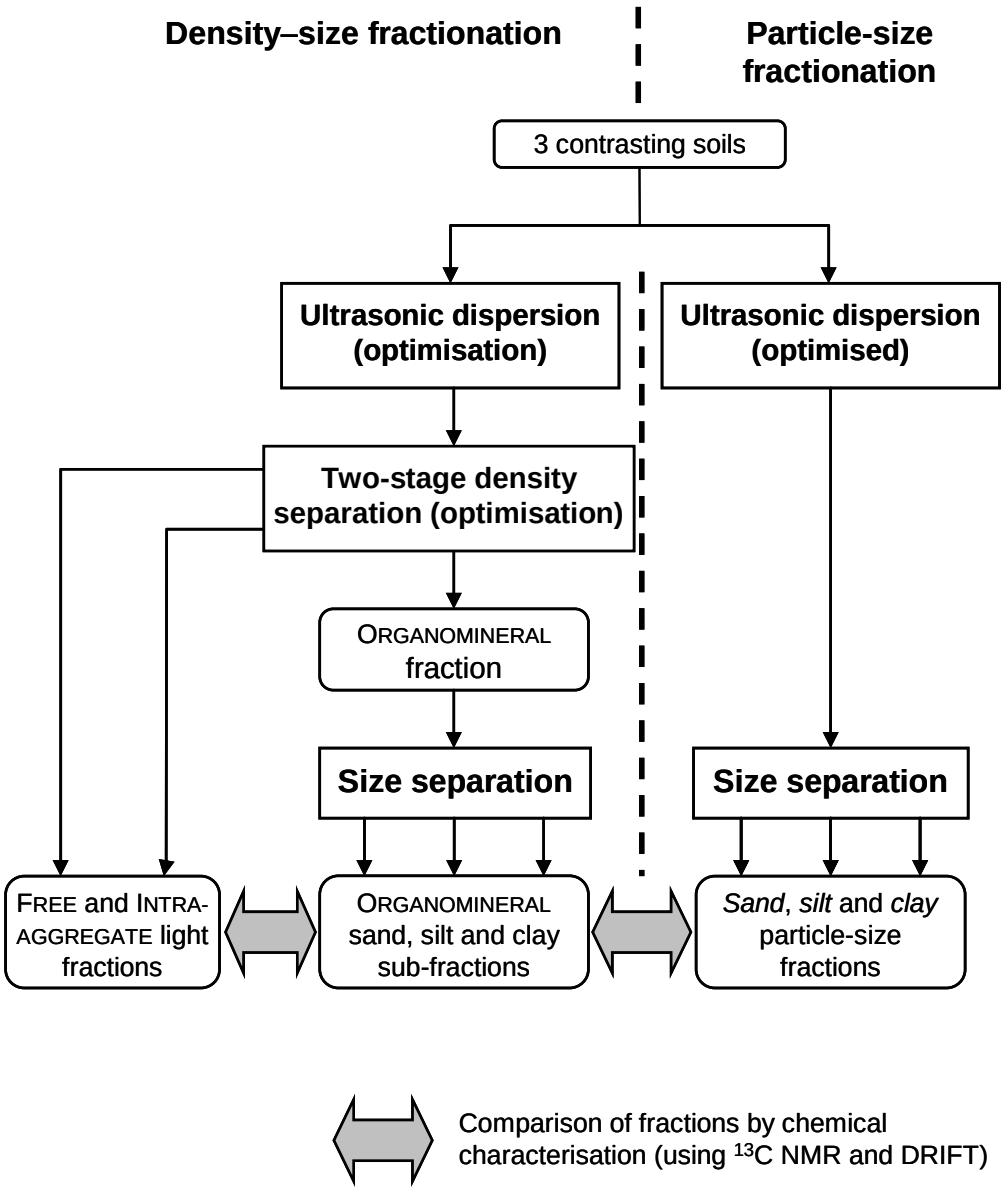

2.2.1. Soils

Three soils of contrasting texture were collected from two experimental farms at the Institute of Arable Crops Research (IACR) in south-east England: a silty clay loam from Rothamsted Experimental Station, Hertfordshire; a sandy loam and a heavy clay from the Woburn Experimental Farm, Bedfordshire. All the soils had been under continuous arable rotation for at least 10 y. Samples of topsoil (0 to 23 cm depth) were taken prior to crop establishment using a spade, and passed through a 6·25 mm sieve to remove large stones and coarse organic debris before fractionation. Although this material could not be included in the comparison of methods (due to its physical dimension and spatial variability) it would be independently measured in controlled experiments. The established properties for the three soils are shown in Table 2.1.

2.2.2. Density fractionation

Each soil was density fractionated (field-fresh) using nine combinations of separation density and ultrasonic dispersion (sonication). For each combination, 90 mL of NaI solution, prepared to a density of 1·60, 1·70 or 1·80 g cm^{-3} (determined by hydrometer) was added to six 250 mL polycarbonate centrifuge bottles, each containing 15 g of soil. The bottles were swirled by hand for 30 s to allow particles of SOM released by the breakdown of unstable aggregates to escape. The sedimentation of heavy particles was accelerated by centrifuging the bottles at 8000 × *g* for 30 min. The floating FREE light fraction was drawn from each bottle in turn, together with NaI solution, using a cut-down 25 mL plastic pipette (Bibby Sterilin Ltd., Staffordshire)

Table 2.1. The basic properties of the soils used in the optimisation and comparison of fractionation methods

Property	Quartzipsammettic Dystrudept	Rendollic Eutrudept	Vertic Endoaquept
Description	Sandy loam	Silty clay loam	Heavy clay
Physical			
Soil texture, %			
Clay (<2 µm)	14	39	50
Silt (2-60 µm)	18	47	27
Sand (60-2000 µm)	68	14	23
Chemical			
Total C, g kg^{-1}	6.5	23.0	26.3
pH_{H2O}	6.68	8.21	8.14

attached to a vacuum flask and pump via 6-mm diam. tubing. FREE light fraction from each sample was isolated by decanting the contents of the vacuum flask over a Whatman glass fibre filter (type GF/A, 47 mm diam., 1·6 µm retention; Whatman International ltd., Kent) in a Millipore vacuum filtration unit (Millipore U.K. Ltd., Hertfordshire). The NaI filtrate was returned to the relevant centrifuge bottle. The retained material was rinsed thoroughly with deionised water using a wash bottle and a separate collector. The receiver, filter platform and threads of the filtration unit were dried before re-attaching the alternate collector for the next sample. This prevented the separation density for the subsequent stage being lowered by dilution of the NaI with residual water.

INTRA-AGGREGATE light fraction, particles of SOM located within stable aggregates, were released by re-suspending the contents of the centrifuge bottles and sonicating for 5, 10 or 15 min. Treating the soil suspensions in the centrifuge bottles avoided transferral during fractionation, whilst permitting probe submersion comparable to sample depth, maintaining a low soil to suspension ratio, and providing a vessel of dimensions comparable with the probe diameter (i.e. optimal dispersion conditions). The ultrasonic generator used in this experiment was a MSE Soniprep 150 (Sanyo Gallenkamp PLC, Leicestershire), fitted with a 9·5-mm diam. probe submerged 15 mm into the soil suspension. The actual (calorimetric) energy transfer was 25·0 W (measured by temperature change in 100 mL cold water over 5 min; North 1976). This level of energy input was verified after each 300 min use. The sonication treatments thus equated to energy inputs of 500, 1000 and 1500 J g^{-1} soil. The sample temperature was maintained below 30 ºC during treatment by placing the centrifuge bottles in 500-mL ice-packed beakers.

INTRA-AGGREGATE light fraction was recovered after centrifugation, using the procedure described above for FREE light fraction. After re-adding NaI the bottles were centrifuged a third time (8000 × *g*, 15 min). The supernatant was decanted over a Whatman GF/A filter for re-use (Whatman International Ltd., Kent). The residual ORGANOMINERAL fraction was retained for particle-size separation (Section 2.2.3.).

The amount of organic matter contained in the FREE and INTRA-AGGREGATE light fractions (FREE and INTRA-AGGREGATE organic matter) was estimated by loss-on-ignition. The light fractions and their respective filters were placed inside porcelain crucibles (50 mm diam.), weighed after drying overnight at 105 ºC, and again after combustion at 500 ºC for 16 h. At this temperature residual NaI (melting point 650 ºC) and glass fibre filters (melting point 600 ºC) were stable. Weight loss therefore equated to the organic matter content of the samples. The results from loss-on-ignition were expressed on an oven dry soil basis i.e. mg organic matter g^{-1} dry soil, and the data analysed using Genstat 5 Version 4.1 (NAG Ltd., Oxford) and the ANOVA procedure (Payne *et al.* 1993).

For each density–sonication treatment, three replicates of the residual ORGANOMINERAL fraction were sub-divided by particle-size (see below). This enabled full comparison of the fractions obtained using the alternative density- and particle-size fractionation methods (see Section 2.2.3.). It also enabled the relationship between solution density and the level of aggregate dispersion to be assessed.

2.2.3. Particle-size fractionation

For each of the three soils, particle-size fractionation was applied to:

i) whole soil

ii) the ORGANOMINERAL fraction from density separation.

For the whole soil samples, three 15-g sub-samples were pre-dispersed using the same sonication equipment, dispersion medium (NaI), and containers as the optimised density-based method.

For both whole soil and ORGANOMINERAL fractions, *sand-size* particles (25 to 2000 μm diameter) were removed using a Fritsch Analysette 3E electro-magnetic wet sieving machine (Fritsch, Idar-Oberstein, Germany). The *silt*- (2 to 25 μm) and *clay-size* (< 2 μm) fractions in the residual suspensions were separated by sedimentation at constant temperature (25 ºC) in the dark. Each suspension was added to a plastic cylinder (of 35 cm height, 6 cm diam.) and the volume made up to 1200 mL. After settling for 17·25 h, the top 25 cm of each suspension contained – according to Stoke's law (Section 1.4.2.) – only *clay-size* particles. This portion was siphoned into a 1 L centrifuge bottle using a Perspex tube, hooked so as to draw suspension only from above the 25 cm mark. To flocculate fine clay particles (< 0·2 μm diam.) 2·5 mL of 1 *M* $CaCl_2$ was added to each bottle, and the contents centrifuged to sediment particles > 0·2 μm diam. (2500 × *g*, 35 min; Tanner and Jackson 1947). The supernatants were discarded, and the pellets retained in their respective centrifuge bottles and stored at 4 ºC. The cylinders were topped up to the original depth with deionised water,

thoroughly re-suspended using a plunger, and the sedimentation–centrifugation procedure repeated until no further *clay-size* particles were recovered. *Silt-size* particles remaining in the cylinder were isolated by centrifugation at 2500 × *g*, 15 min. Both the accumulated *clay-size* pellets and *silt size* fractions were washed into pre-weighed plastic Petri dishes, and evaporated to dryness at 50 ºC. The proportions of whole soil or ORGANOMINERAL fraction recovered as *sand-*, *silt-* and *clay-size* particles were calculated on a dry-weight basis (mg g^{-1} soil).

2.3. Chemical characterisation

Samples of the three whole soils, additional samples of FREE and INTRA-AGGREGATE fractions, sub-samples of the ORGANOMINERAL sub-fractions, and *sand-*, *silt-* and *clay-size* fractions were ground using a disc mill (3 min, 960 rpm). FREE and INTRA-AGGREGATE fractions were milled together with the glass fibre filters on which they were collected, since it was not possible to remove fine embedded particles (particularly of the INTRA-AGGREGATE fraction).

To acquire ^{13}C CPMAS NMR spectra, sub-samples of the milled materials were packed into cylindrical zirconia rotors (internal dimension 5·6 mm × 17·0 mm), sealed with Kel-F caps and analysed using a Bruker MSL 300 spectrometer (Bruker UK Ltd., Coventry). Experimental parameters were as follows: spectrometer frequency 75·5 MHz, contact time 1 ms, relaxation time 0·5 s, and spinning speed 4·0 to 4·6 kHz. Between 24 000 (3·3 h) and 113 000 (15·7 h) scans were accumulated for FREE and INTRA-AGGREGATE fractions, between 139 000 (19·3 h) and 305 000 (42·4 h) for whole soils, and between 109 000 (15·1 h) and 449 000 (62·1 h) for ORGANOMINERAL and

sand-, *silt-* and *clay-size* fractions. Spinning sidebands were fully suppressed using the TOSS sequence (Section 1.6.1.) for improved quantitative assessment (Dixon 1982).

As mentioned in Section 1.6.1., paramagnetic centres interfere with cross-polarisation and the proportion of ^{13}C detected in a sample is strongly influenced by Fe as well as C content. The Fe content of the samples was thus determined by inductively coupled plasma emission spectrometry (Accuris ICP-ES; Applied Research Laboratories, Vallaire, Switzerland) following Aqua Regia extraction. The corresponding C contents were determined by combustion analyser (Integra-CN; Europa Scientific Ltd., Cheshire). Magnetic susceptibility was also measured directly using a magnetic susceptibility balance housing a suspended magnet (Johnson Matthey Chemicals, Hertfordshire), and mercury tetrathiocyanatocobaltate as a calibration standard (Figgis and Nyholm, 1958).

Peak areas were calculated for spectra where (on a weight basis) sample C-to-Fe > 1 (Arshad *et al*. 1988). The distribution of C between functional groups was estimated according to the chemical shift limits identified in Figure 1.1.: 0 to 45 ppm (alkyl C), 45 to 65 ppm (N-alkyl C), 65 to 95 ppm (O-alkyl C), 95 to 108 ppm (acetal C), 108 to 145 ppm (aromatic C), 145 to 160 ppm (phenolic C), 160 to 185 ppm (carboxyl C), 185 to 220 ppm (carbonyl C) (Randall *et al.* 1995).

For DRIFT spectroscopy 2 to 4 mg of the milled sample was mixed with approximately 200 mg of KCl and ground to a fine powder in an agate mill. The samples were analysed using a Bio-Rad FTS 165 FT-IR Spectrometer fitted with a DTGS-KBr detector (Bio-Rad Laboratories Inc., Cambridge, USA). Resolution was set

to at 8 cm^{-1} and 64 scans made with a single single-sided beam and a spectral range of 400 to 4000 cm^{-1}. Win-IR Version 0.15 software was used to generate spectra (Bio-Rad Laboratories Inc., Cambridge, USA). Peak assignments (see Table 1.2.) were based on those established by Baes and Bloom (1989), Bloom and Leenheer (1989) and Stevenson (1994).

2.4. Results and discussion

2.4.1. Optimisation of density fractionation

Analysis of variance showed separation density was a significant factor ($P < 0.05$) in recovery of FREE organic matter only in the sandy loam soil, with a larger yield at a density of 1·80 g cm^{-3} than at 1·60 or 1·70 g cm^{-3} (Figure 2.2.a). In the other two soils the quantity of organic matter recovered in this fraction was not significantly different at the three densities. This relative insensitivity to separation density probably reflects a loose association between FREE organic matter and heavy ORGANOMINERAL particles. Since centrifugation expels entrapped air, buoyancy conferred by intra-cellular spaces in fresh plant debris is not a likely explanation (Magid *et al.* 1996).

For all three soils separation density had a highly significant effect on the recovery of INTRA-AGGREGATE organic matter ($P < 0.001$). For each sonication treatment, the maximum amount was obtained at 1·80 g cm^{-3} in the sandy loam and heavy clay soils. In the silty clay loam the amount was equal at 1·70 and 1·80 g cm^{-3} (Figure 2.2.b). The sensitivity of the INTRA-AGGREGATE fraction to separation density is probably due to its close association with ORGANOMINERAL particles: ORGANOMINERAL

Figure 2.2. Organic matter recovered in (a) FREE and (b) INTRA-AGGREGATE fractions at different separation densiti energy input (s.e.d. is the standard error in the difference of the means)

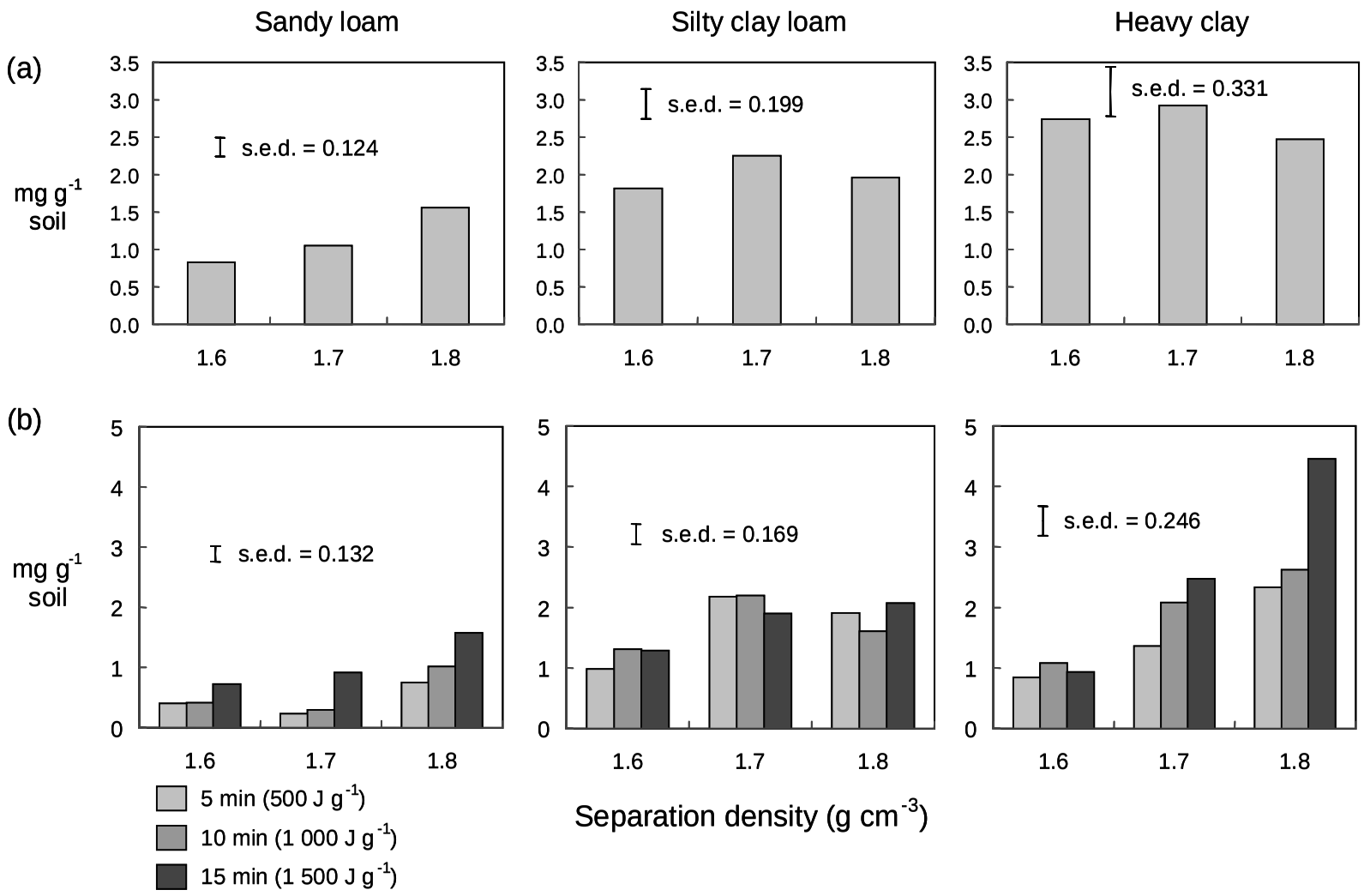

particles that remained attached after sonication and aggregate dispersion increasing the effective density of the fraction. The duration of sonication was also a significant factor for recovery of INTRA-AGGREGATE organic matter from sandy loam and heavy clay soils ($P<0.001$). At the highest separation density, the longest treatment time resulted in greatest recovery of INTRA-AGGREGATE organic matter.

In the heavy clay soil (but not the others) the density of the NaI in which the soil was dispersed affected the proportion of clay-size particles present in the ORGANOMINERAL clay-size fraction (Figure 2.3.). This could be due to a reduction in the zone around the sonicator probe tip in which particles are exposed to strong disruptive force. Although the yield of clay-size ORGANOMINERAL particles was lower after 5 and 10 min sonication in NaI solution of density 1·80 g cm^{-3} relative to 1·60 g cm^{-3}, the amount recovered after 15 min treatment (1500 J g^{-1} soil) was equal (Figure 2.3.).

The results show that to achieve efficient recovery of FREE and INTRA-AGGREGATE organic matter, separation at a density of 1·80 g cm^{-3} is required. The optimised procedure for dual-stage density fractionation shown in Figure 2.4. also specifies the greater duration of sonication (15 min, 1500 J g^{-1} soil) to maximise the breakdown of stable aggregates.

2.4.2. Chemical properties

The FREE and INTRA-AGGREGATE fractions obtained using the density fractionation procedure were visually l distinct. The FREE fraction comprised

Figure 2.3. The effect of sodium iodide density on the yield of the ORGANOMINERAL clay sub-fraction from the heavy clay soil with different levels of energy input (bars indicate standard error; n = 3)

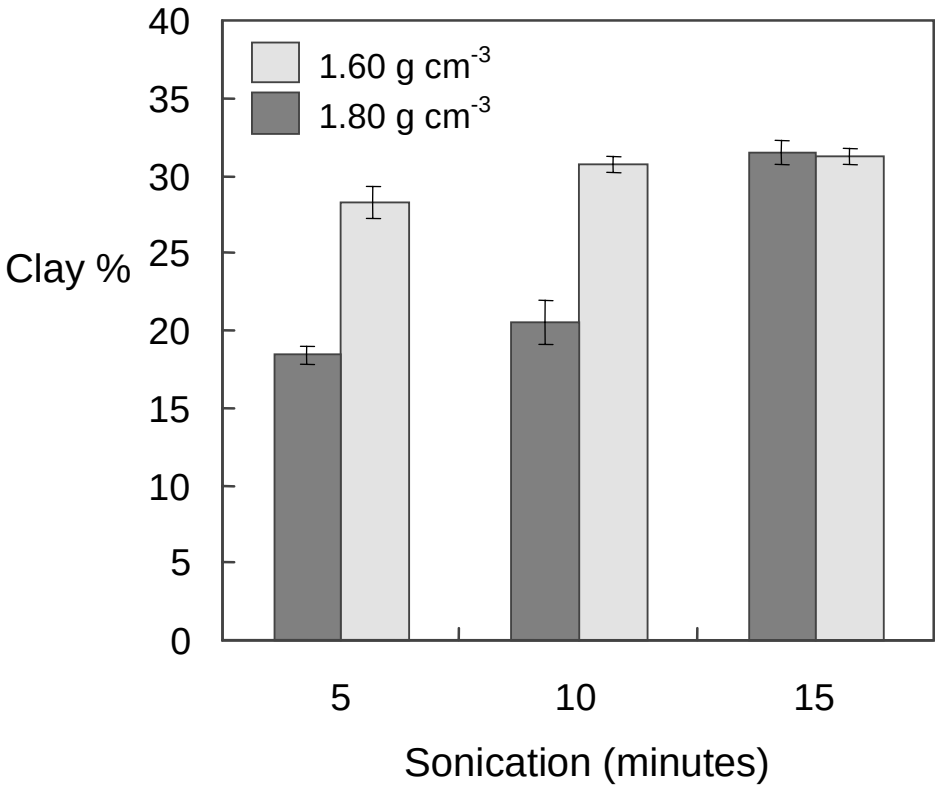

Figure 2.4. A standard procedure for the isolation of soil organic matter fractions suitable for modelling

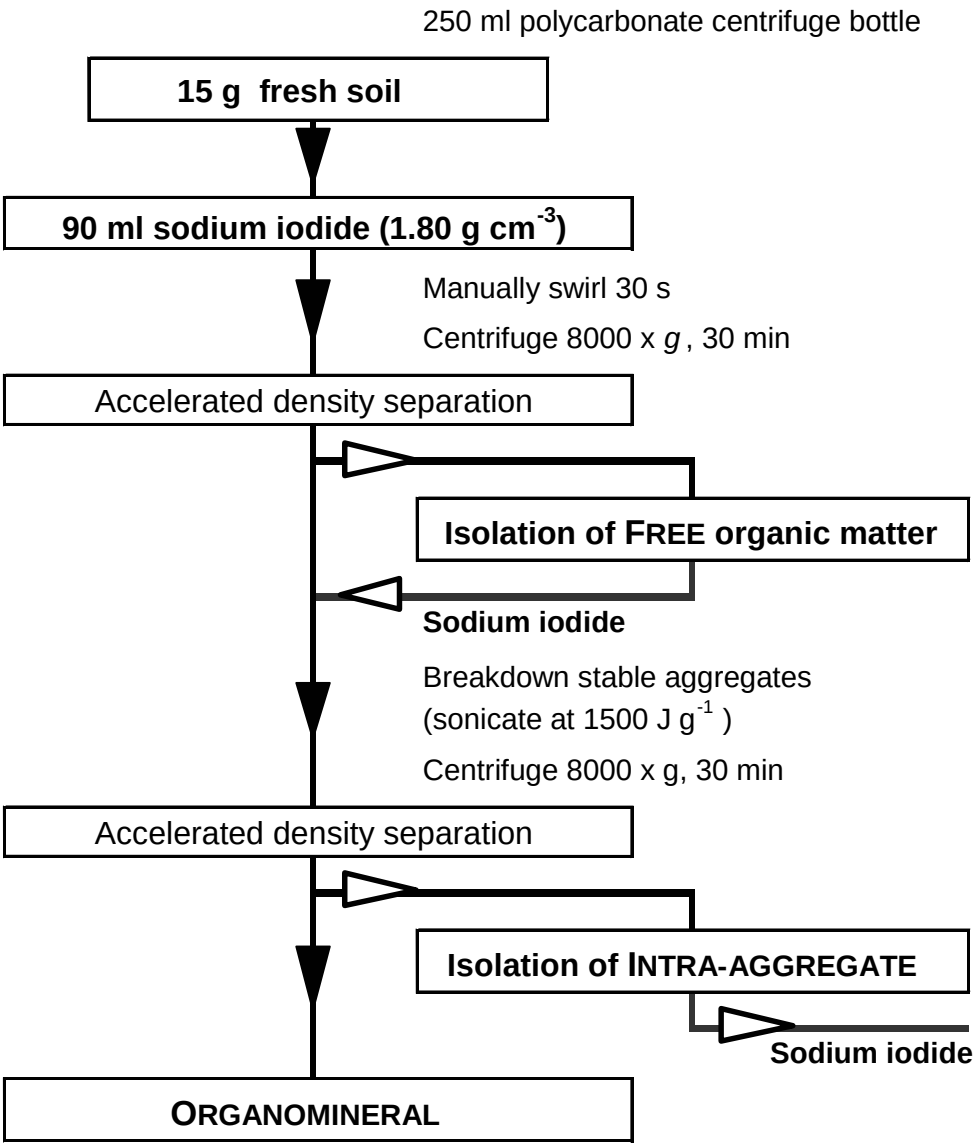

recognisable plant material, whereas the INTRA-AGGREGATE was finely divided and darker in colour (Figure 2.5.).

For the three soils, Figure 2.6. shows ^{13}C CPMAS NMR spectra for:

a) whole soil
b) fractions obtained using the optimised density fractionation procedure, including organomineral sub-fractions, and
c) particle-size fractions obtained without prior removal of FREE and INTRA-AGGREGATE organic matter

The whole soils had C-to-Fe ratios of 0·15 to 0·79 and generated little or no signal. In contrast the FREE and INTRA-AGGREGATE fractions were enriched in organic matter, displayed C-to-Fe ratios of 3.6 to 48.9 (Table 2.2.) and produced spectra with high signal-to-noise ratios, and readily identifiable peaks. The major peaks in FREE organic matter represented O-alkyl C or – in the case of the silty clay loam soil – O-alkyl and aromatic C. Although O-alkyl C was also prominent in the INTRA-AGGREGATE fraction from two of the soils (the sandy loam and heavy clay), peaks indicating alkyl and aromatic C were considerably enhanced in all three. From the analysis of peak areas, the ratio of O-alkyl to alkyl C in FREE organic matter was found to be 1·4 to 3·2 times greater than that of the INTRA-AGGREGATE fraction (from Table 2.2.). Since the decline of this ratio characterises SOM decomposition (Preston 1996) INTRA-AGGREGATE appeared to comprise a more altered fraction. The increasing content of aromatic C supports this view, although the aromatic peak may be enhanced by the

Figure 2.5. The contrasting appearance of free and intra-aggregate fractions isolated on glass fibre filters

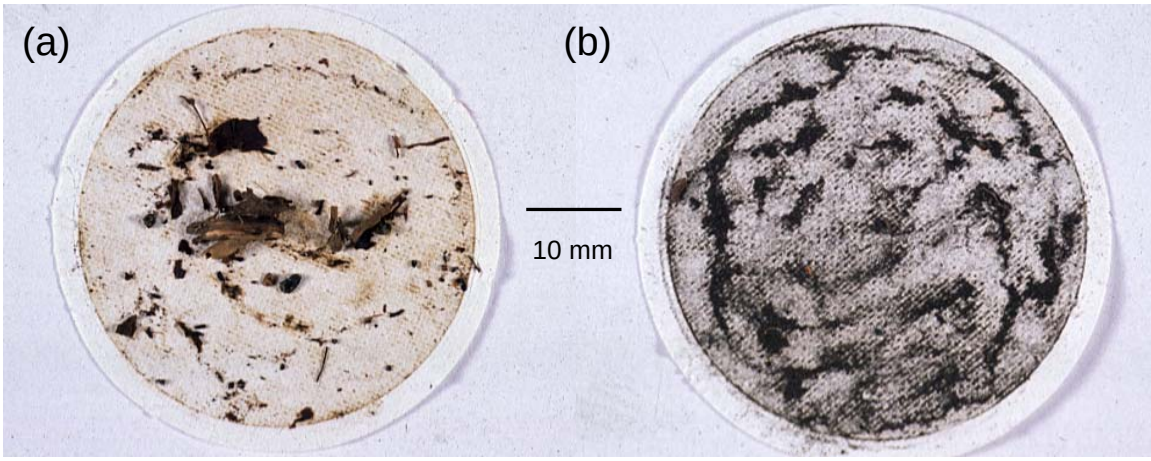

Figure 2.6. ^{13}C nuclear magnetic resonance spectra for fractions obtained by density-size versus size-only fractionation from (a) sandy loam (b) silty clay loam and (c) heavy clay soils

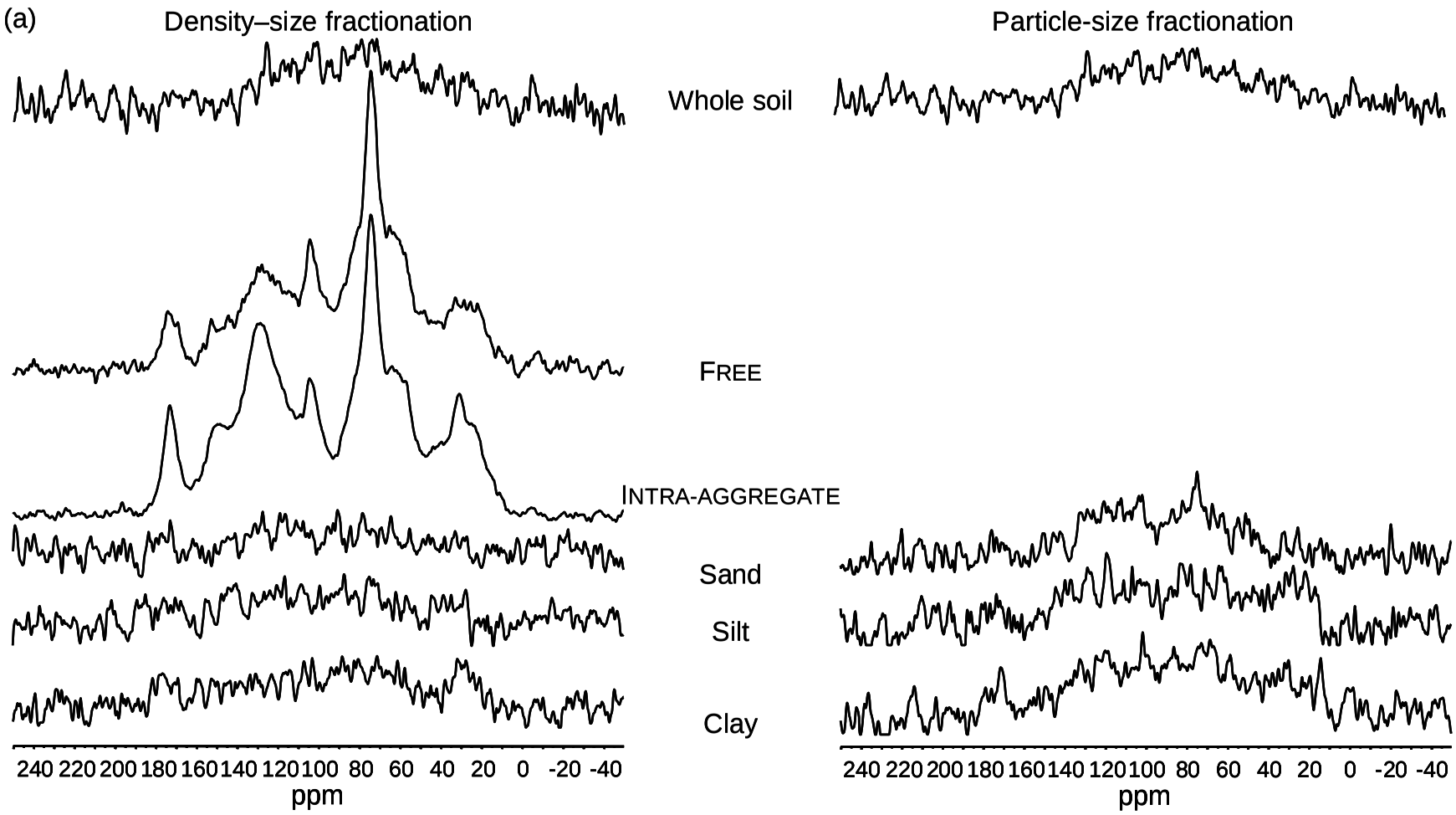

Figure 2.6. (continued)

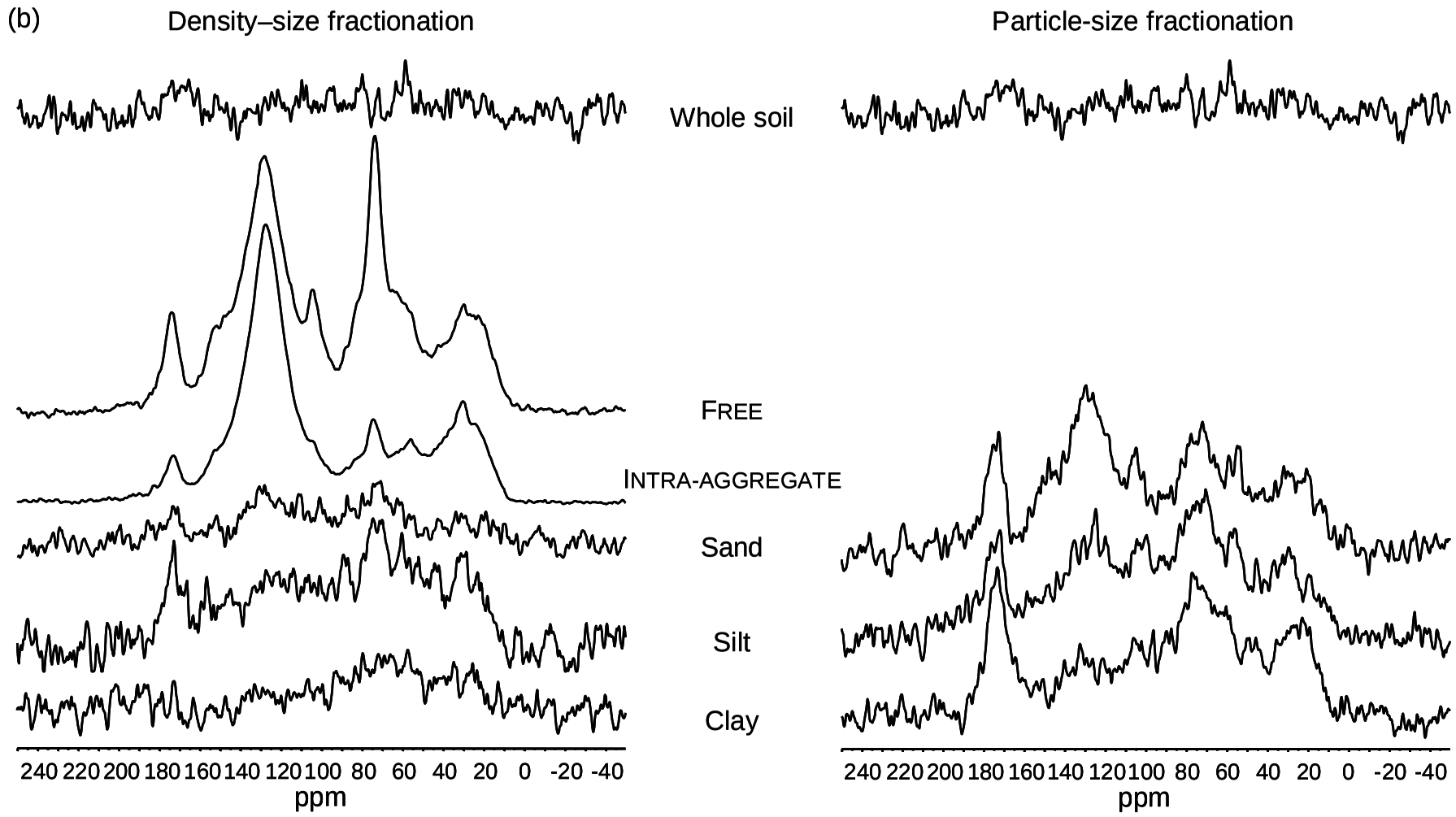

Figure 2.6. (continued)

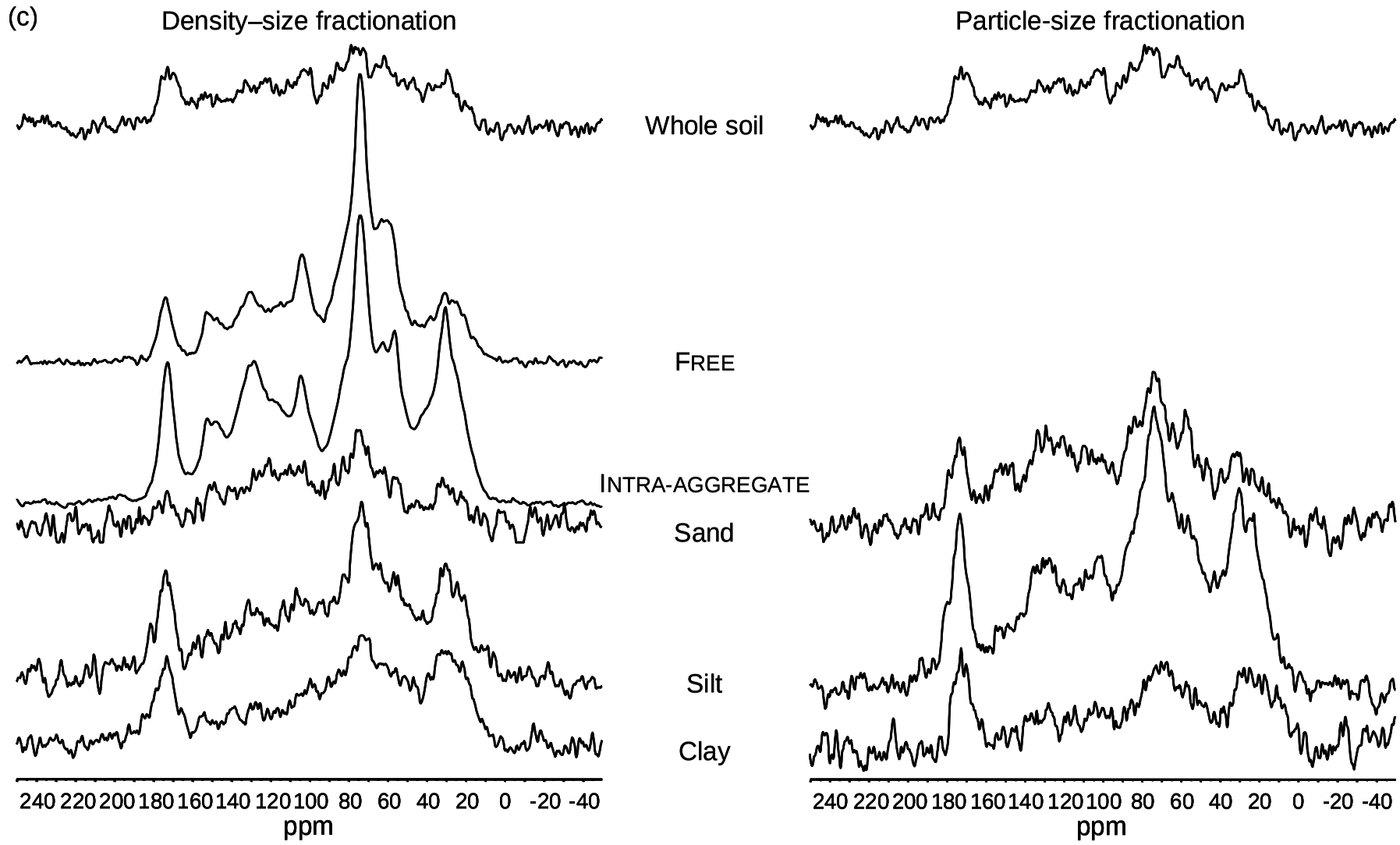

Table 2.2. C-to-Fe ratios and the distribution of carbon amongst functional groups in FREE and INTRA-AGGREGATE organic matter fractions from the three soils as estimated from peak area analysis of ^{13}C nuclear magnetic resonance spectra

Soil	Fraction	C-Fe	Alkyl	N-Alkyl	O-Alkyl	Acetal	Aromatic	Phenolic	Carboxyl	Carbonyl	O-Alkyl:Alkyl
			% peak area								
Sandy loam	Free	36	141	149	292	113	193	53	51	09	207
	Intra-aggregate	73	154	118	230	100	262	68	61	08	149
Silty clay loam	Free	193	154	101	199	79	322	74	62	09	129
	Intra-aggregate	746	178	78	99	47	493	53	42	10	056
Heavy clay	Free	77	129	174	329	119	135	54	53	08	256
	Intra-aggregate	251	203	136	237	83	185	70	76	10	117

presence of charcoal (possibly explaining the particularly high intensity of the aromatic peak in both FREE and INTRA-AGGREGATE fraction from the silty clay loam soil).

Spectra from ORGANOMINERAL and particle-size fractions were characterised by generally low signal-to-noise ratios, attributable to paramagnetic interference and / or low C concentration (only one sample displayed C-to-Fe > 1). However, particle-size fractions (Figure 2.6.; right hand side) generated consistently greater signal than the ORGANOMINERAL counterparts (Figure 2.6.; left hand side), presumably due to the presence of FREE and INTRA-AGGREGATE fraction not removed by prior density separation. It appears that this material is recovered with *clay*- and *silt*- as well as *sand-size* fractions, and – comprising relatively small amounts of SOM – contributes disproportionately to the NMR signal detected in these fractions. It seems the latter effect may result from the greater physical separation of the paramagnetic centres from cross-polarising protons in organic particles. If this can be proved it suggests that the NMR signal from fractions obtained without prior density separation will emanate from two sources: particulate SOM, and SOM attached to mineral surfaces.

The relatively well defined peaks apparent in *silt* and *clay* particle-size fractions from the silty clay loam and heavy clay soils, indicative of O-alkyl and alkyl C (Figures 2.6.b and 2.6.c; right hand side), may reflect particulate organic matter. The O-alkyl and aromatic C peaks were diminished in the *clay* fraction relative to *silt*, a trend previously described by Randall *et al* (1995). For the ORGANOMINERAL sub-fractions, discernible peaks were only present in the heavy clay soil. For this soil, ORGANOMINERAL silt and clay were enriched in carboxyl C when compared to FREE or INTRA-AGGREGATE fractions, and ORGANOMINERAL clay to a greater extent than silt.

The DRIFT spectra for FREE and INTRA-AGGREGATE fractions were interpretable in the wavenumber range 1430 to 4000 cm^{-1} (Si–O peaks emanating from the filter material in the milled sample overlapped at higher wavenumbers) (Figure 2.7.). All samples showed pronounced absorption between 1620 to 1600 cm^{-1}, indicating aromatic C (C=C stretching) and carboxylic anions (–COO asymmetric stretching). These peaks also confirmed the consistently greater aromatic C content of the INTRA-AGGREGATE fraction observed by NMR, and the generally higher proportion of aromatic C present in silty clay loam soil fractions. Less defined peaks at 1525 and 3030 cm^{-1} indicated further aromatic C, and C–H stretching on aromatic structures. Peaks between 1460 to 1450 cm^{-1} indicated aliphatic hydrocarbon (C–H stretching), and more pronounced peaks between 2940 to 2900 cm^{-1} the stretching of C–H on aliphatic chains. Their markedly greater intensity in INTRA-AGGREGATE organic matter (for the sandy loam and heavy clay soils) was further indication that this fraction has undergone greater microbial transformation than the FREE organic matter. The greater presence of alkyl C in INTRA-AGGREGATE was consistent with the NMR findings. The DRIFT spectra for ORGANOMINERAL and particle-size fractions could not be interpreted due to the predominance of peaks from mineral components.

2.4.3. A conceptual model

The comparison of fractionation approaches showed that dual-stage density identifies SOM fractions suitable for modelling: FREE, INTRA-AGGREGATE and ORGANOMINERAL fractions are small in number and display consistent differences in chemical composition. The results support the view that physical location and SOM

Figure 2.6. Diffuse reflectance infrared Fourier transform spectra for FREE and INTRA-AGGREGATE organic matter fractions from (a) sandy loam (b) silty clay loam and (c) heavy clay soils

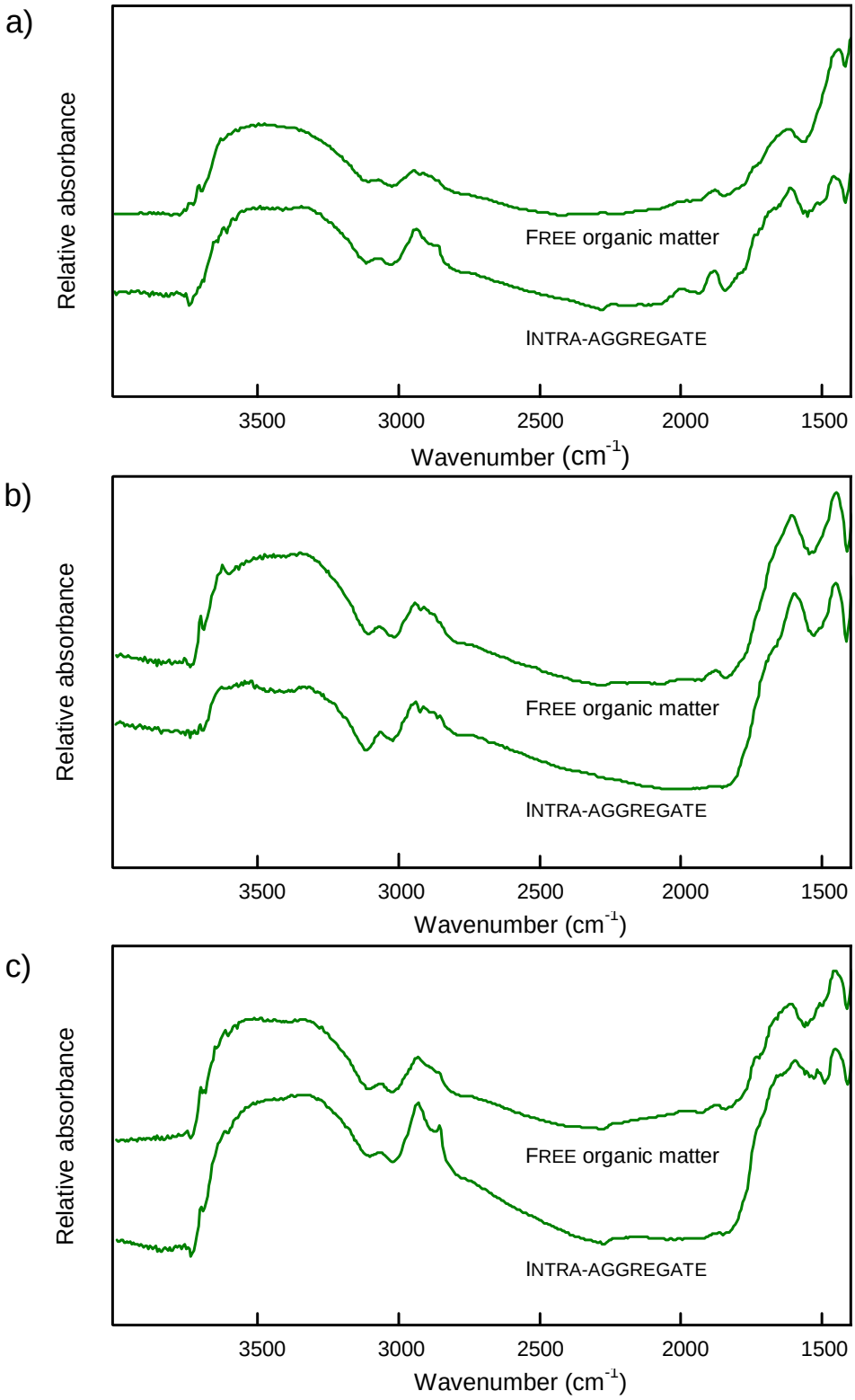

composition are interrelated, although it cannot be ascertained whether chemical composition determines physical location or *vice versa*.

Since the physical appearance and chemical composition of FREE organic matter resembles that of plant material, it is reasonable to believe it represents the more chemically accessible SOM substrate as compared to INTRA-AGGREGATE or ORGANOMINERAL. Comprising proportionally more stable organic matter, the INTRA-AGGREGATE fraction appears to be composed of residual substrate and / or transformed (microbial) SOM and will display a lower *in situ* reactivity. Formation of ORGANOMINERAL complexes requires close physical association between mineral surfaces and transformed organic matter (such as the INTRA-AGGREGATE fraction) in order for strong molecular bonds to form. The transfer of C and N to progressively more stable fractions through microbial transformation will result in the release of CO_2 and possibly a demand for mineral N.

2.5. Conclusion

The optimised density fractionation procedure (Figure 2.4.) identifies three measurable, mutually exclusive SOM fractions: FREE, INTRA-AGGREGATE and ORGANOMINERAL. Assuming the three soils tested are typical, these fractions are likely to display contrasting levels of reactivity reflecting their consistent differences in composition. These characteristics are a prerequisite for modelled SOM fractions (see Section 2.1.1.). The alternative fractionation method based on particle-size produced fractions that differed less in chemical composition, and contained a mixture of particulate organic matter and organic matter associated with mineral surfaces.

A conceptual model based around density fractions has been defined (Section 2.4.3.). Providing the general consistency in the composition of these fractions can be confirmed (see Chapter 3), a mathematical framework for a model will be developed around this conceptual understanding (Chapter 4). Parameterisation data will be obtained using the standard density fractionation procedure and instantaneous measurements of C, N, ^{13}C and ^{15}N (Chapter 5).

CHAPTER 3: CHEMICAL CHARACTERISATION

3.1. Introduction

To facilitate parameterisation, SOM fractions represented in models should be measurable, mutually exclusive and small in number (Section 2.1.1.). These requirements are mathematical. However, as an indication of their intrinsic reactivity (*k*), modelled fractions should also differ significantly in chemical composition, and display differences that are consistent across soils. In order to produce useful predictions, at least two fractions must be dynamic on a relevant time scale. These criteria were used in defining a procedure (Figure 2.4.) to measure model fractions (Chapter 2).

Existing SOM models generally feature compartments defined by a fixed value for *k*, implying that their intrinsic reactivity (whether they equate to conceptual or measurable SOM fractions) is site-independent (McGill 1996). The consistency with which a procedure separates fractions contrasting in composition should indicate the range of applicability expected for an associated model. Certain general differences between the composition of FREE and INTRA-AGGREGATE organic matter have been shown for three soils using ^{13}C NMR (Figure 2.6.) and DRIFT (Figure 2.7.). These soils were diverse in texture but small in number. The objective of this chapter is to explore the consistency and limits to these general differences across soils of different types, geographic location, crop cover and land management factors, including fertilisation and tillage. Whilst the quantitative impacts of these factors on physical SOM fractions have been established (Tiessen and Stewart 1983; Angers *et al.* 1993; Beare *et al.* 1994;

Bremer *et al.* 1994; Gregorich *et al.* 1996; Paustian *et al.* 1996; Gregorich *et al.* 1997; Larney *et al.* 1997) much less is known about qualitative effects (Randall *et al.* 1995; Madari *et al.* Submitted).

Complete equilibration of the soil–plant system following a change in management or land-use change may take decades or centuries. Long-term experiments offer near-equilibrium conditions, and plots that are free from short-term variations (Christensen and Johnston 1997). The abundance of modelled SOM fractions should differ with contrasting management strategies, reflecting differences in inputs. Corresponding effects on the composition of measurable fractions can be established by fractionation of soils from contrasting plots at long-term sites. The variation resulting from management can be compared with that due to climate, soil type, crop cover and other agronomic factors, by characterising samples from many long-term experiments (encompassing the most diverse range of geographical situations possible). This will simultaneously indicate the least difference between the different fractions, and hence the justification for their separate inclusion in models (Smith *et al.* Submitted).

In this chapter, the composition of FREE and INTRA-AGGREGATE organic matter is compared for soils of contrasting management and geographical location, using ^{13}C NMR. These fractions seem most likely, on the basis of the characterisation in Chapter 2, to be dynamic on an inter-seasonal time scale. The analysis will indicate the likely range of applicability for a model that includes these fractions, through the relative sensitivity of composition to management and location.

3.2. Materials and methods

3.2.1. Soils

Air-dry soil samples were collected from eight long-term experiments world-wide. Three were located in Europe, two in Asia, and one each in North America and the Middle East. A list of the sponsoring organisations is shown in Table 3.1. At each site plots under three basic categories of nutrient management were sampled: plots receiving no fertilisation, plots receiving one or more rates of inorganic N, and those receiving farmyard manure (FYM). In addition, plots receiving green manure were sampled from two of the experiments, and one plot receiving additional straw. At four sites, samples were taken from plots receiving two different rates of inorganic fertiliser. These were designated high N or low N relative to local practice. For the other experiments i.e. those with only one inorganic N treatment, plots receiving < 100 kg N $ha^{-1}y^{-1}$ were placed in the low N category. Inorganic fertiliser treatments included balanced inputs of other minerals, and the manure treatments occasionally supplementary mineral (inorganic) N. The crops grown at each site were all cereals, three sites cropped to rice under flooded conditions. For the UK site only, samples of FYM and wheat straw were also obtained, to establish the contrasting composition of inputs under the different treatments. The plots sampled at each site (with soil type and crop rotation) are listed in Table 3.1.

All plots were conventionally tilled, and in the case of rice soils puddled. At each site bulked samples representative of the plough layer were taken using a gouge auger. The depth of the plough layer varied between sites. All sample were imported

Table 3.1. List of the long-term experiments sampled for characterisation of soil organic matter fractions under contrasting fertilisation including the categories of treatment sampled at each site

Country	Site	Institute	Experiment	Age	Crop rotation *	Soil texture	Treatments				
							0N	LN	HN	GM	FYM
Bangladesh	Gazipur	BRRI	Organic matter incorporation	13	Rice-rice-rice	Silt-loam	✓	✓		✓✓	✓
England	Rothamsted	IACR	Broadbalk continuous wheat	155	Wheat	Silty-clay loam	✓	✓	✓		✓
Germany	Bad Lauchstadt	UFZ Halle	Static	95	Wheat	Silt-loam	✓	✓			✓
Hungary	Martonvasar	TAKI	Long term fertiity	42	Wheat	Loam	✓	✓			✓
Nepal	Bahairawa	NARC	Long term fertiity	20	Rice-rice-wheat	Silt-clay-loam	✓	✓		✓	✓
Philippines	Los Banos	IRRI	Long term triple crop	30	Rice-rice-rice	Clay	✓	✓	✓		
Syria	Tel Hadya	ICARDA	Wheat-wheat rotation	15	Wheat-wheat	Clay	✓	✓	✓		
USA	Pendleton	PARC	Residue Management	66	W.wheat / fallow	Silt-loam	✓	✓	✓		✓

* dashes (-) indicate within-year, and slashes (/) between-year, alternations of crops

0N - zero N application
LN - low N rate (< 100 kg ha^{-1})
HN - high N rate
GM - green manure
FYM - farmyard manure

air-dry, and pre-ground to pass a 2-mm mesh. Since the fractionation procedure was developed for application to fresh soil, the air-dry sub-samples were capillary wetted prior to fractionation. Sub-samples of 60 g were placed in 75-mm diam. plastic cores (lined with nylon mesh), and stood on a bed of saturated silica flour for 36 h, until an equilibrium weight was achieved.

3.2.2. Density fractionation

The soils were fractionated using the procedure proposed in Chapter 2 (see Figure 2.4.), with the following modifications.

Fractionation of re-wetted soil

The moisture content of the capillary wetted soil samples was greater than that of the field-fresh samples used in Chapter 2. The water in fractionated sub-samples was sufficient to significantly alter the density of the added separation medium (NaI solution). Since the experiments described in Chapter 2 showed the outcome of fractionation is highly sensitive to separation density, the NaI solution used in this experiment was prepared to a density of 1·82 g cm^{-3}. The density of the NaI solution recovered after fractionation was measured to verify that separation occurred at 1·80 ± 0·005 cm^{-3}. The standard method outlined in Figure 2.4. specifies a field-fresh weight for fractionated sub-samples. To maintain consistency in the amount of dry material processed, 16-g sub-samples were used for the re-wetted soils in this experiment.

Ultrasonic dispersion

The ultrasonic generator available for this and subsequent experiments differed from that used to define the standard procedure in Chapter 2 (see Figure 2.4.). The Soniprep 150 (Section 2.2.2.) was replaced with a Misonix XL 2020 generator, fitted with a dual horn and twin 19-mm diameter probes (Misonix Inc., Farmingdale, USA). The submergence of the probes was increased to 19 mm (compatible with their greater diameter). The energy transfer to the suspensions (from each probe) was 58·8 W (measured using the method described in Section 2.2.2.). On the basis of this calibration, the dispersion energy applied to samples in this and subsequent experiments was 750 J g^{-1} field-fresh soil (the duration of the treatment was 200 s). This was less than the 1500 J g^{-1} proposed in Figure 2.4., but was necessary to maintain compatibility with previous experiments where treatment time using the Soniprep 150 sonicator was reduced to the lower level to give the maximum practicable treatment time of 450 s.

Isolation of light fractions

To provide sufficient sample for ^{13}C NMR, the FREE and INTRA-AGGREGATE fractions collected from each sub-sample were aggregated during the filtration stage i.e. collected on a single filter. In this experiment smooth membrane filters (Millipore type SMTP, 5 μm retention) were used (Millipore UK Ltd., Hertfordshire). This enabled light fractions to be rinsed from the filter surface with deionised water, and thus avoid dilution of C by milling the combined sample. Water was evaporated from the samples by oven drying in Petri dishes at 50 ºC. The dried fractions were prepared for NMR by milling in a disc mill for three minutes (960 rpm).

.

3.2.3. ^{13}C NMR analysis

The experimental parameters for obtaining NMR spectra were essentially the same as those described in Section 2.3. However, the samples of FREE and INTRA-AGGREGATE organic matter were generally smaller than the rotor capacity (approx. 200 mg), and were therefore packed into the centre of the rotor using spacers at either end. The separation of light fraction from the collection filters resulted in a higher C concentration, and acquisition periods lower than those reported in Chapter 2. The average accumulation for the samples in this experiment was 76 000 scans (10.6 h). Peak areas were obtained according to Randall *et al*. (1995) (see Figure 1.1. and Section 2.3.). The FYM and straw samples were also analysed by ^{13}C NMR, using the same experimental parameters.

3.2.4. Statistical analysis

The NMR spectra were summarised by division of peak to provide data that – subject to the caveats mentioned in Section 1.6.1. – is suitable for statistical analysis. In this experiment, a variance components model was fitted to the dataset using Genstat 5 Version 4.1 (NAG Ltd., Oxford) and the residual maximum likelihood (REML) procedure (Payne *et al.* 1993). This procedure is designed for analysis of data obtained from experiments of unbalanced design i.e. those where not all treatments have been applied at each location.

3.3. Results and discussion

To gain a preliminary understanding of the relationship between fraction composition and fertiliser treatment a detailed qualitative comparison was made of spectra for fractions from the UK site (the Broadbalk continuous wheat experiment at Rothamsted; see Table 3.1.).

3.3.1. Sensitivity of fraction composition to fertilisation on the UK site

The ^{13}C NMR spectra for organic inputs to the Broadbalk plots (i.e. FYM and wheat straw) are shown in Figure 3.1. The NMR spectrum for the wheat straw was dominated by sharp O-alkyl and acetal C peaks, and also N-alkyl C (Figure 3.1.). This reflected the abundance of cellulose, hemicellulose and protein present in fresh plant debris (see Table 1.1.). The composition of FYM was closer to that of the SOM fractions (see below, and Figures 3.2. and 3.3.), a substantial proportion of peak area attributable to alkyl, N-alkyl, aromatic, phenolic and carboxyl groups.

Comparing equivalent spectra for FREE organic matter fractions obtained under contrasting fertilisation showed that composition was sensitive to the rate as well as nature of fertiliser application. Under the high N treatment the composition of FREE organic matter was similar to that of straw (comparison of spectra in Figures 3.1. and 3.2.). In this sample a large proportion of peak area was in the O-alkyl (34 %) and acetal (13 %) regions (with 19 % in alkyl groups). With lower rates of inorganic N application, stable (aromatic) C groups were increasingly prominent (Figure 3.2.). FREE organic matter from the zero N plot was distinct in showing a significant (10 %) proportion of C

Figure 3.1. ^{13}C nuclear magnetic resonance spectra for contrasting organic inputs received by plots of the Broadbalk continuous wheat experiment in the UK

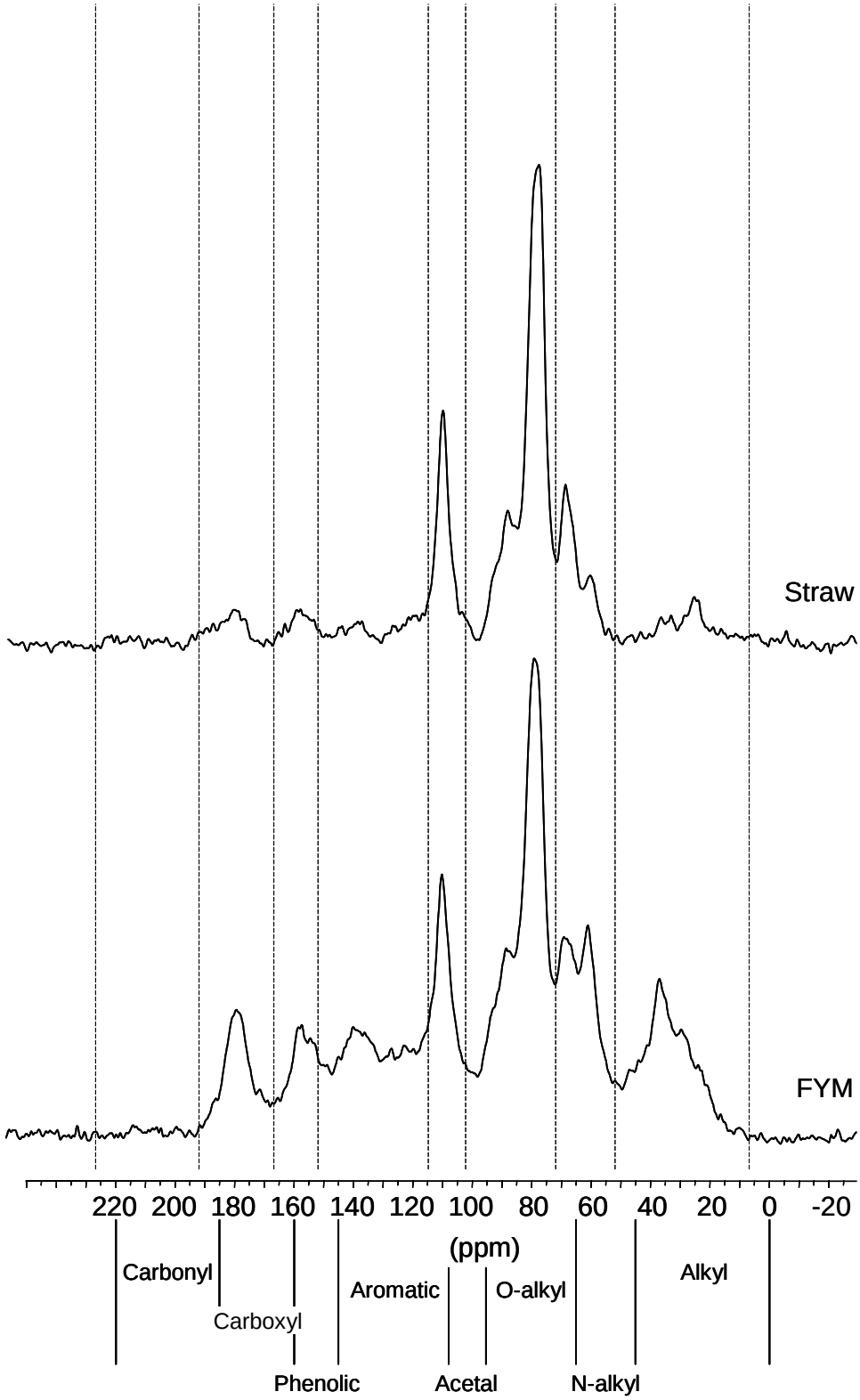

Figure 3.2. ^{13}C nuclear magnetic resonance spectra for FREE organic matter from four Broadbalk plots under contrasting nutrient management

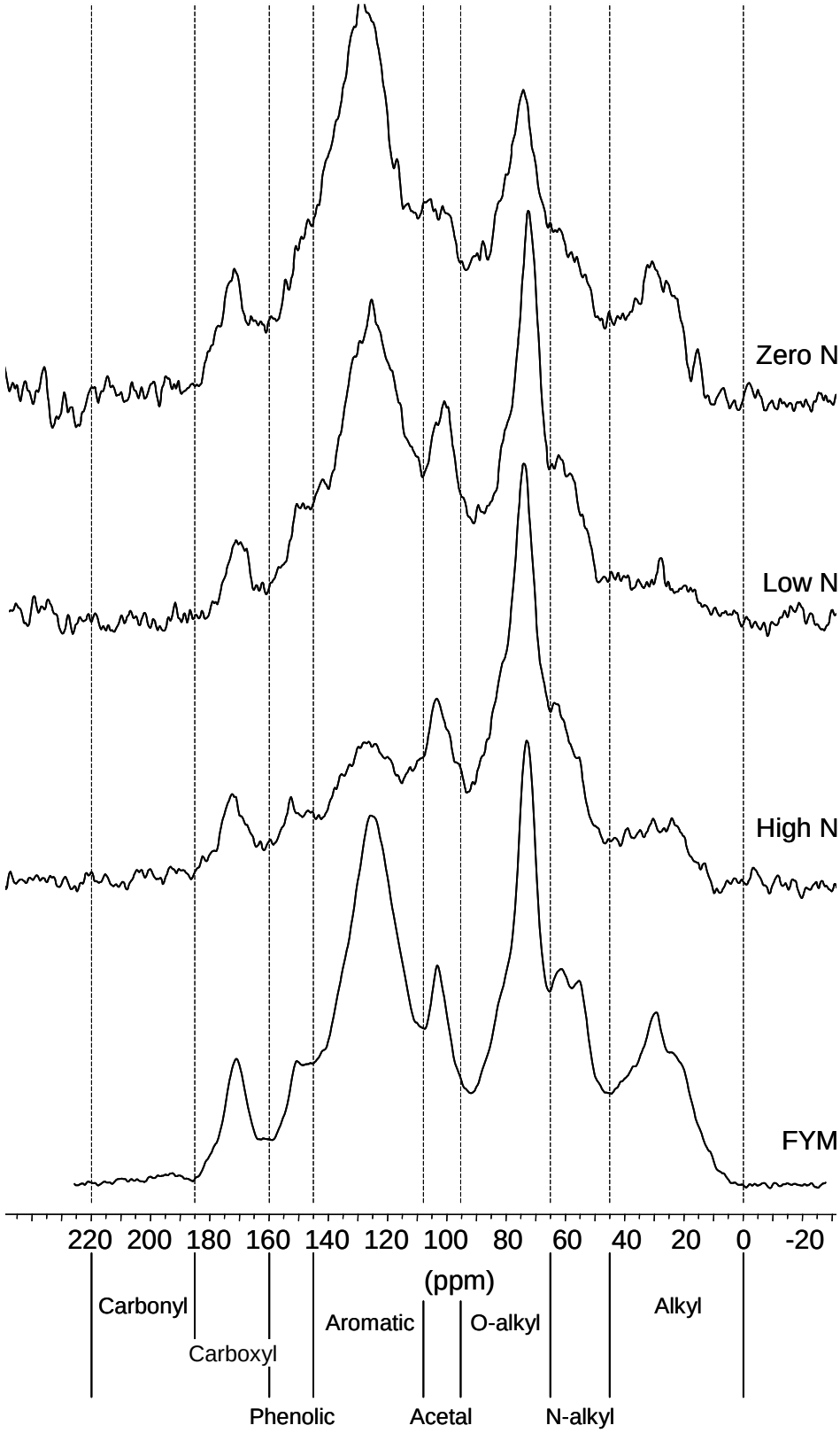

in the alkyl region, with a pronounced peak at 33 ppm indicating either plant derived waxes or microbial lipids (Table 1.1.). Aromatic C accounted for 36 % of total C, with only 21 % in O-alkyl groups, suggesting an accumulation of resistant (lignin derived) plant products. Previously Handayanto *et al* (1995) reported an accumulation of polyphenolics in plant residues in soils receiving low rates of N input. In terms of alkyl and aromatic C content, FREE organic matter from the FYM plot was closer to that of the zero N, despite receiving crop inputs similar in magnitude to those under the high N treatment (grain yield – which reflects residue inputs – was 5.6 times greater in the FYM plot than the zero N plot, and 63 % of that under high N – during the 1970s (Dyke *et al.* 1983)). FREE organic matter from the FYM plot also contained the highest proportion of N-alkyl C, with the sharp peak at 57 ppm that also distinguished FYM from wheat straw (Figure 3.1.). There was a correspondingly lower proportion of O-alkyl C in the sample from the FYM plot, and the lowest proportion of acetal C.

The INTRA-AGGREGATE fractions showed less variation in composition between the plots receiving inorganic or zero N application (Figure 3.3.). In each sample the aromatic groups accounted for more C than O-alkyl, and the difference increased with decreasing N (and hence plant debris) inputs, particularly between the high N and low N treatments and the zero N plot, which contained only 14 % of C in O-alkyl groups. The INTRA-AGGREGATE spectra for these plots also displayed marked alkyl peaks centred at 33 ppm. The spectrum for the FYM plot was distinct in that it not only displayed a prominent aromatic peak, and also the largest proportion of C attributed to N-alkyl groups and 15 % of peak area in the alkyl C region.

Figure 3.3. ^{13}C nuclear magnetic resonance spectra for INTRA-AGGREGATE organic matter from four Broadbalk plots under contrasting nutrient management

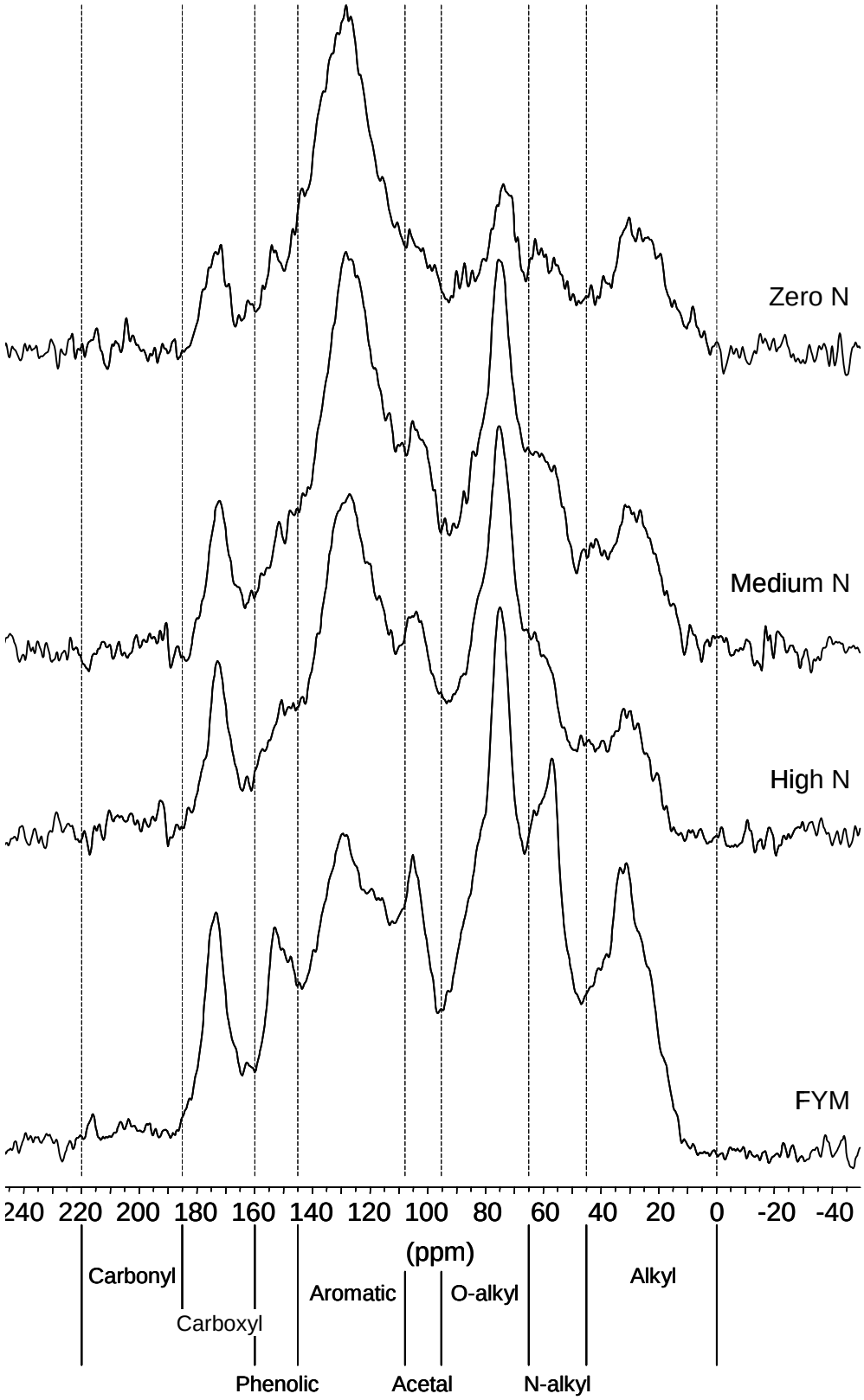

Marked differences were apparent between the composition of FREE and INTRA-AGGREGATE fraction from plots receiving inorganic (or zero) N application, notably a greater proportion of aromatic and alkyl C in the INTRA-AGGREGATE. These differences were consistent with those seen for the three soils used to test the fractionation method in Chapter 2 (see Figure 2.6.). Importantly, differences in the composition of corresponding whole soils were not found in an earlier study of the Broadbalk plots (Randall *et al*. 1995).

3.3.2. Differences between fractions across locations

Peak area data for the fractions from the other sites was grouped according to fertiliser treatment, with the purpose of establishing whether differences due to geographical origin (encompassing the effects of climate, soil and crop type) were greater or lesser than the general differences resulting from fertiliser treatment. Due to marked difference in composition between FREE and INTRA-AGGREGATE fractions in the FYM compared to inorganic and zero N plots for the UK site, the initial comparison was made only between plots receiving zero N, low N and high N. The distribution of C between functional groups between treatments was very similar, for both the FREE and INTRA-AGGREGATE fractions (Figures 3.4. and 3.5.). Since the differences were small, the data were combined for comparison against equivalent data for the FYM plots.

A considerable difference was found in the O-alkyl and aromatic C content of FREE organic matter from the inorganic N plots, and plots receiving FYM (Figure 3.6.). FREE organic matter from the FYM plots contained proportionally more aromatic and

Figure 3.6. The mean distribution of C between functional groups in FREE organic matter obtained from long-term plots receiving inorganic or no fertiliser versus those receiving farmyard manure, based on ^{13}C nuclear magnetic resonance peak areas

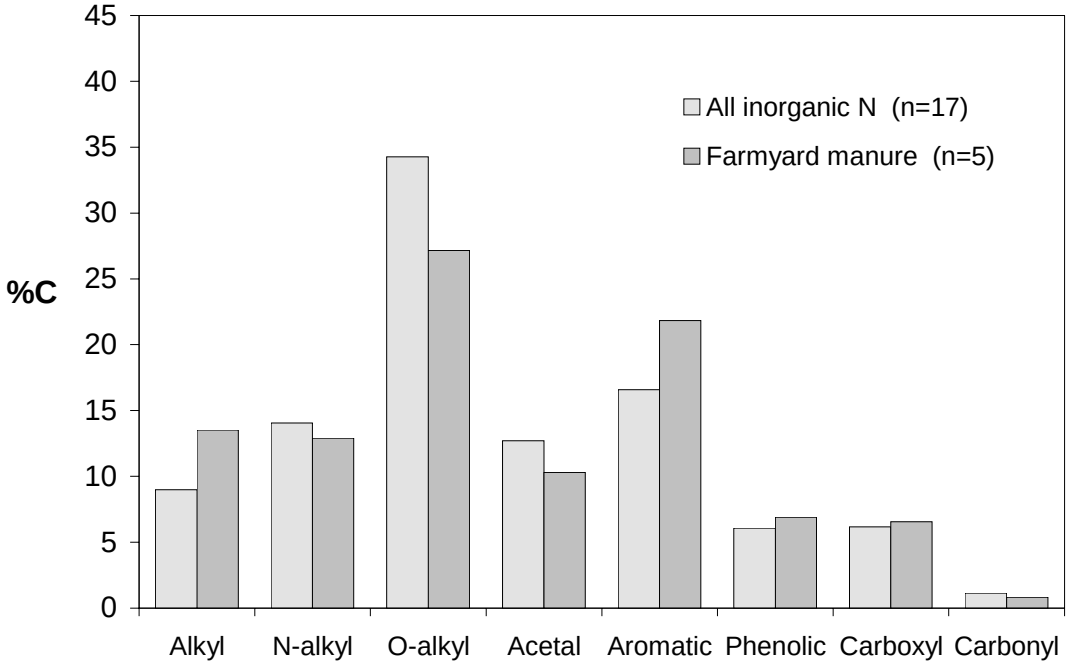

Figure 3.7. The mean distribution of C between functional groups in FREE organic matter obtained from long-term plots receiving inorganic or no fertiliser versus those receiving farmyard manure, based on ^{13}C nuclear magnetic resonance peak areas

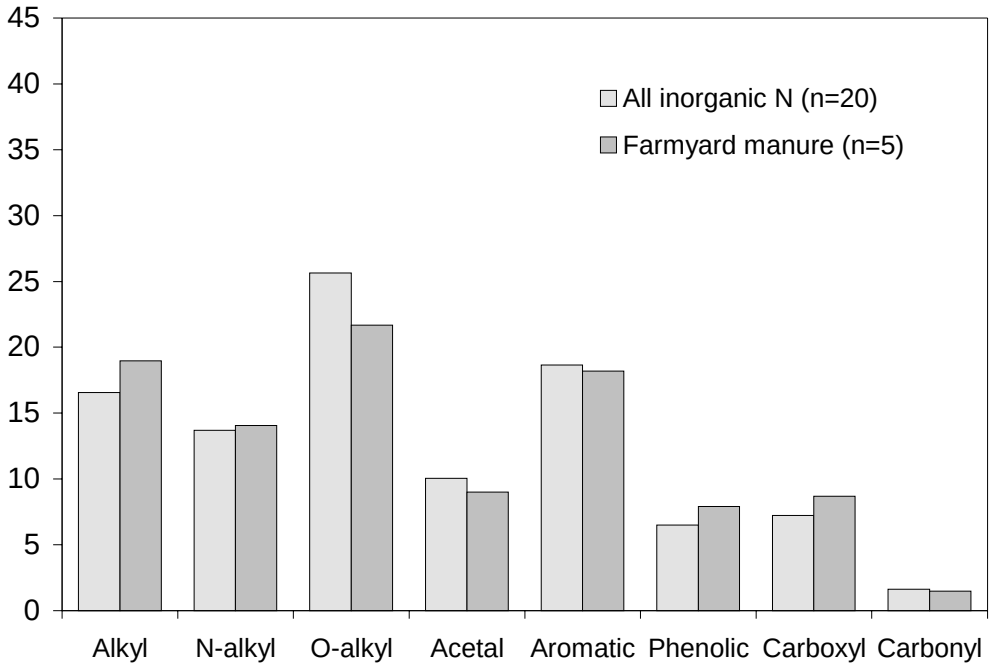

Figure 3.4. The mean distribution of C between functional groups in FREE organic matter obtained from long-term plots receiving inorganic or no fertiliser, based on ^{13}C nuclear magnetic resonance peak areas

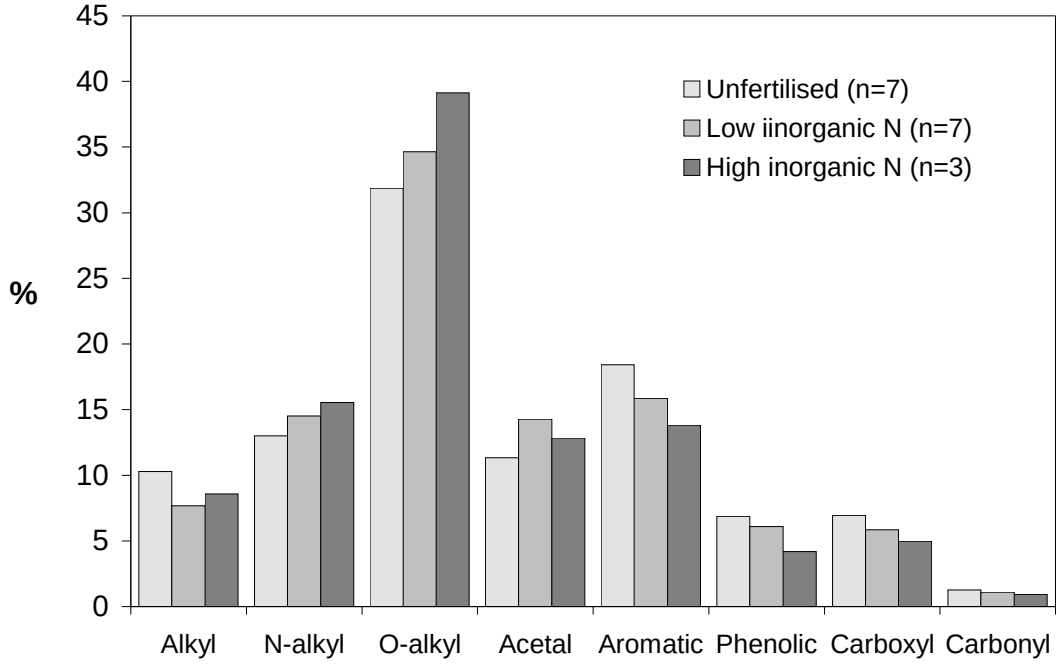

Figure 3.5. The mean distribution of C between functional groups in INTRA-AGGREGATE organic matter obtained from long-term plots receiving inorganic or no fertiliser, based on ^{13}C nuclear magnetic resonance peak areas

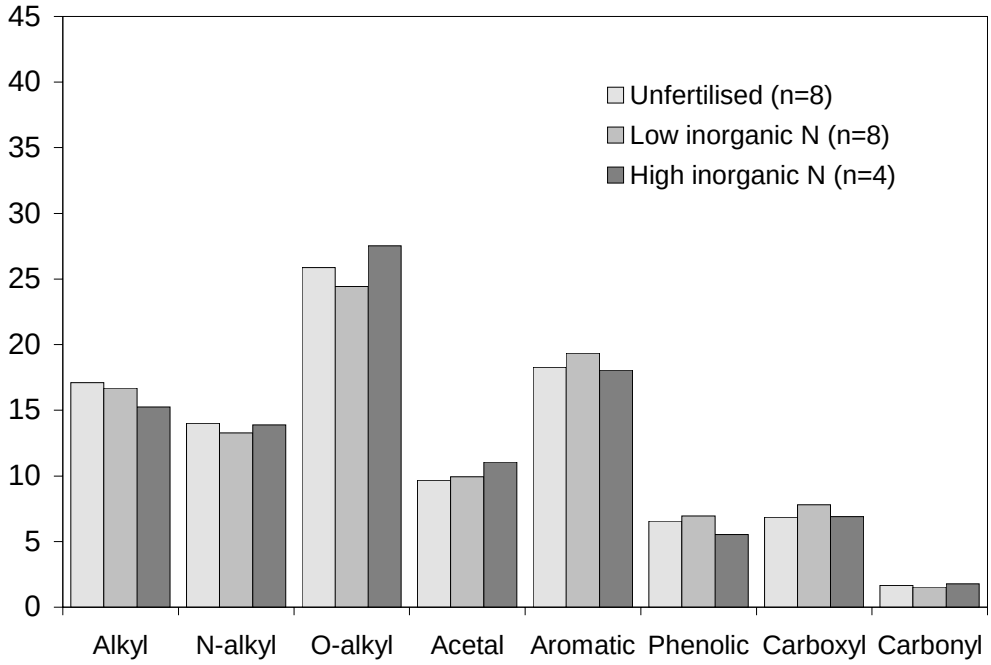

alkyl C, and less O-alkyl C. This was consistent with the analysis of spectra from the Broadbalk plots (Section 3.3.1.), and may result from digestion of carbohydrates in rumen (previously seen in FTIR studies; Russell and Fraser 1988). However, this difference was much diminished in the INTRA-AGGREGATE fraction (Figures 3.7.). The general convergence in composition between treatments in the INTRA-AGGREGATE fraction was less pronounced in the Broadbalk plots (Figure 3.3.).

For both FREE and INTRA-AGGREGATE organic matter, the distribution of C between functional groups showed general differences that apply across sites, and confirming that the Broadbalk example was broadly typical. The greatest proportion of C in FREE organic matter was in O-alkyl groups, this peak being much less dominant in INTRA-AGGREGATE organic matter. The alkyl peaks were also greater in the INTRA-AGGREGATE fraction, but the general trend in aromatic C was less pronounced than in the Broadbalk plots. The relative prominence of the alkyl region is centred on a peak representing lipids or waxes, suggesting a higher proportion of transformed organic matter (microbial debris, as well as highly recalcitrant plant components).

A statistical analysis of the peak area data was made using the REML procedure (see Section 3.2.4.), which was suited to the peak area dataset as data was not available for all treatments at all sites. However, since only two of the eight sites had plots receiving green manure, these were excluded. The analysis showed that the alkyl and O-alkyl C content of the FREE and INTRA-AGGREGATE fractions were significantly different ($P < 0.05$), irrespective of the site or treatment from which they were obtained (Table 3.2.). In addition there were corresponding, significant differences in the quantitatively smaller carboxyl and carbonyl groups, and also acetal C (representing

Figure 3.8. The mean distribution of C between functional groups of FREE a INTRA-AGGREGATE fractions obtained from 26 long-term plots under contrasting management, estimated from ^{13}C nuclear magnetic resonance peak areas using residual maximum likelihood (bars indicate the standard error of difference)

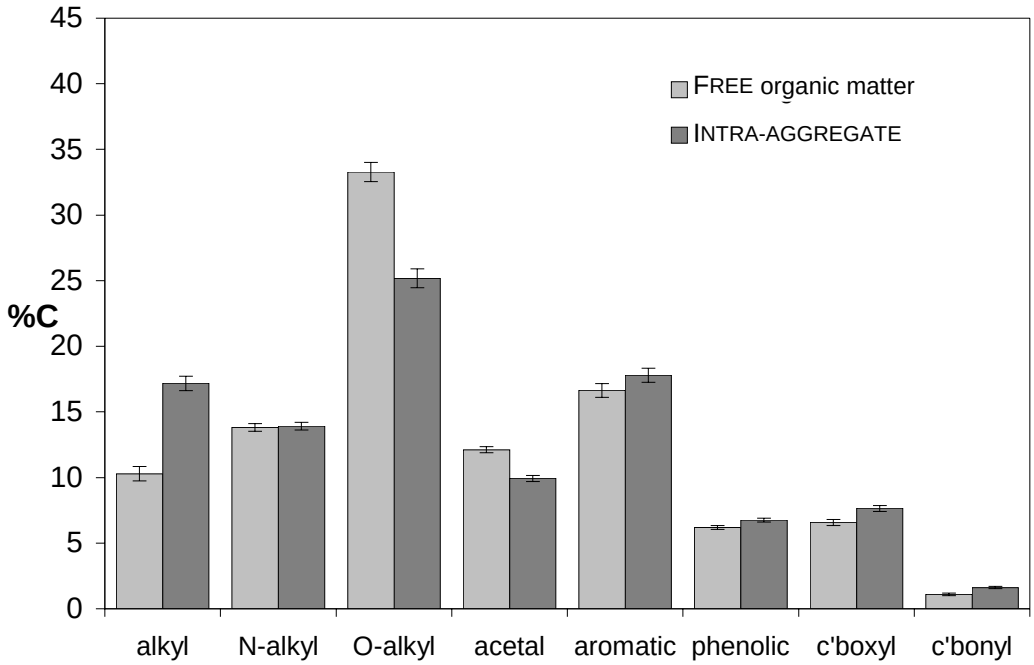

Table 3.2. Significance of the variance components leading to differences between FREE and INTRA-AGGREGATE organic matter compositon for 26 long-term plots in eight long-term experiments under contrasting management, assessed from ^{13} nuclear magnetic resonance peak areas using residual maximum likelihood

Factor	Functional C group							
	alkyl	N-alkyl	O-alkyl	acetal	aromatic	phenolic	c'boxyl	c'bonyl
	----------% peak area ----------							
Fertilisation	NS	NS	NS	NS	NS	NS	NS	NS
Fraction	*	NS	*	*	NS	NS	*	*
Fert x frac	NS	NS	NS	NS	*	NS	NS	NS

* = significant at 95 % NS = not significant

hemicellulose). Although the effect of fertilisation was not statistically significant, there was a significant interaction between fertilisation and fraction in the aromatic C content. This may be due to the particularly high aromatic C content of FYM. Mean values for the distribution of C between functional groups estimated by REML (across treatments) is shown for both fractions in Figure 3.8., together with the standard error of difference (s.e.d.) for each functional group.

3.4. Conclusion

In view of the diversity of soils fractionated in this experiment (in terms of soil type, climate, crop and land management), the differences in chemical composition and hence likely reactivity (*k*) between FREE and INTRA-AGGREGATE fractions were remarkably consistent. The statistical analysis showed that, with the exception of aromatic C derived from FYM, the differences between the fractions were greater than the combined effects of geographical origin or fertilisation strategy. Previously, Mahieu *et al*. (1998) have shown a surprising level of consistency in the composition of >300 whole soils characterised by ^{13}C NMR. A detailed examination of NMR spectra for the fractions isolated from a long-term site in the UK suggested that INTRA-AGGREGATE organic matter was more consistent between treatments than that of the FREE fraction, and comprised a greater proportion of more resistant C structures and / or microbial products. These findings support the view that FREE and INTRA-AGGREGATE organic matter occupy a contrasting position in the decomposition sequence, and that their reactivity may be sufficiently distinct and hence enhance model performance by their separate inclusion.

CHAPTER 4: A MATHEMATICAL MODEL

4.1. Introduction

The number of SOM fractions for which *in situ* reactivity can be inferred depends on the relative number of measured variables and interacting flows (Section 2.1.1.). The number of fractions identified by two-stage density separation is compatible, and the data presented in Chapters 2 and 3 suggest the fractions also differ consistently in their chemical composition. The current objective is to define a mathematical model based around these fractions and the concept described in Section 2.4.3. The parameters invoked in the model will be evaluated (by optimisation against experimental data) in Chapter 6.

Fundamentally, most substrate-oriented C–N models assume first-order kinetics (i.e. constant reactivity) within SOM fractions. Each fraction may be represented by separate C, N, ^{13}C and ^{15}N compartments of the same reactivity (k), but of contrasting magnitude, reflecting their C-to-N and isotope ratios. The actual flows between compartments may be limited when N is deficient in the substrate or the system as a whole. A model based around measurable fractions should be able to account for any observed variation in fraction composition (such as C-to-N ratio) with time.

4.1.1. Compartment reactivity

In models based on first order kinetics, a specific SOM component has a fixed reactivity that is defined by the compartment to which it is allocated. With transfer to

another compartment its reactivity instantaneously changes to reflect that of the recipient fraction. Such discrete changes in reactivity are more compatible conceptually with measurable SOM fractions, defined by their physical location (see Section 1.4.1.). However, measurement may also demonstrate time-dependent changes in reactivity, and mathematical frameworks that can accommodate this may be required.

4.1.2. Representation of microbial biomass

From a mechanistic perspective, soil microbial biomass is fundamental to the transfer of SOM between fractions (and hence 'stabilisation'). Jenkinson (1988) has described biomass as the "eye of the needle through which all organic matter must pass", reflecting the small proportion of SOM (1 to 3 %) for which it accounts (Theng *et al.* 1989). Most existing models define one or more compartments representing microbial biomass, which has the practical advantage of being measurable using the fumigation–extraction technique (Brookes *et al.* 1985). Such measurements have provided valuable (if limited) constraint for parameterisation of existing models, as well as possibilities for their verification (Magid *et al.* 1996) (see Section 1.3.4.). Soil microbial biomass also offers a conceptual link between corresponding C and N compartments, typically through a minimum requirement for N in substrate utilisation e.g. Molina *et al* (1983) (see Section 4.1.3. below). Many models appear to gain from the division of microbial biomass into two or more separate compartments e.g. CENTURY (Parton 1996), DAISY (Mueller *et al.* 1996) and that of Verberne *et al.* (1990). The benefits of this division are limited, however, in the absence of methods to distinguish them experimentally, leading to the consolidation of the zymogenous and

autochthonous biomass compartments in the current RothC model (Jenkinson and Rayner 1977; Coleman and Jenkinson 1996).

Since soil microbial biomass does not occupy a specific physical location in the soil matrix (Chotte *et al.* 1998) it will not be identified by physical fractionation schemes such as that proposed in Chapter 2. If microbial biomass and physical SOM fractions are not mutually exclusive (the former being associated with the latter), either a model based around such fractions must operate without a biomass compartment, or the measured and modelled compartments must be in only approximate correspondence. Although there are examples of models without explicit biomass compartments e.g SOMM (Chertov and Komarov 1996), their presence offers a stronger mechanistic basis for process-level simulation. In the model developed here, the measurable (physically defined) fractions differ from their equivalent model compartments by the amount of microbial biomass that they contain. The magnitude of the biomass compartment is thus the difference between the sum of the measured SOM fractions and the sum magnitude of the model compartments. The ability to verify rate processes offsets the need for additional parameters to define the distribution of biomass between different physical locations (between which reactivity may be assumed to be uniform).

4.1.3. Reconciling C and N dynamics

Respiration of C leads to a progressive decline of substrate C-to-N ratio over time. Some models feature fractions with defined C-to-N ratios that reflect the number of prior N-concentrating transformations e.g. NCSOIL (Molina *et al.* 1983). In models based on measurable fractions, mathematical models that accommodate the measured

variation in C-to-N ratio may be required. The turnover of C may also be linked to the availability of mineral N, the utilisation of substrates with high C-to-N limited in the absence of an additional mineral N source. This need reflects the generally lower C-to-N ratio maintained by microbial biomass relative to fresh plant material (tending toward 5:1 in bacteria and 15:1 in fungi; Theng *et al.* 1989), which also enables N immobilisation to be simulated. However, although C-to-N ratio is undoubtedly a major influence on the turnover of SOM (and thus the prediction of soil N supply), its use as the sole determinant in substrate utilisation may be simplistic. Microbial populations can, for example, respond to the substrates available by altering in composition (e.g. becoming more fungal; Cheshire *et al.* 1999).

4.1.4. Isotope tracers

Due to the low natural abundance of ^{15}N, relatively small additions of ^{15}N-enriched substrate can produce an observable effect at the whole soil level (Section 1.5). If the isotopic composition of measured SOM fractions can be determined following substrate addition, dynamic activity can be measured in relatively stable fractions that display very slow change in their total N content, or in which inputs and outputs are balanced. Since C_3 and C_4 plants display a discrete, natural difference in their ^{13}C content, natural abundance methodology provides an attractive alternative to the use of homogeneously enriched substrates for tracing C (Section 1.5.2.). In a mechanistic model structure with several compartments and many flows, tracer data are essential to provide adequate constraint for parameter optimisation (see Section 2.1.1.). The use of tracer models is mathematically straightforward, providing isotopic discrimination is not significant.

4.2. Model definition

The model contains 24 compartments, 12 of which approximate to the C, N, ^{13}C and ^{15}N contents of the FREE, INTRA-AGGREGATE and ORGANOMINERAL fractions identified by the standard procedure (Chapter 2). Four others comprise the C, N, ^{13}C and ^{15}N content of the fraction soluble in NaI, and potentially measurable through fractionation. These collectively comprise the substrate compartments. The remainder represents C, N, ^{13}C and ^{15}N in microbial biomass and gaseous release, which are independently measurable. The C and N models interact through a minimum requirement for N in the incorporation of C into microbial biomass. This requirement may be partly, completely, or more than satisfied by the release of N from the C substrate (depending on its C-to-N ratio). When the substrate contains insufficient N, the deficit may be obtained as soluble N (resulting in net N immobilisation). If insufficient soluble N is available, utilisation of C is limited until the demand for N matches its supply: both substrate- and system-based approaches were considered for this limitation. Flows of ^{13}C and ^{15}N are directly linked to the corresponding C and N flows by the isotope ratio of the relevant source compartment. The model was developed using *ModelMaker 3.0* (Adept Scientific, Oxford), which is a graphically interfaced software package. The model structure for the C flows is shown in Figure 4.1., with the corresponding N flows indicated.

Units and notation

The standard units for compartments and flows are mg and mg d^{-1} respectively. Since it is convenient to exclude the effects of soil density during model development,

Figure 4.1. Schematic showing the structure of the model with respect to C, with an indication of the corresponding N flows

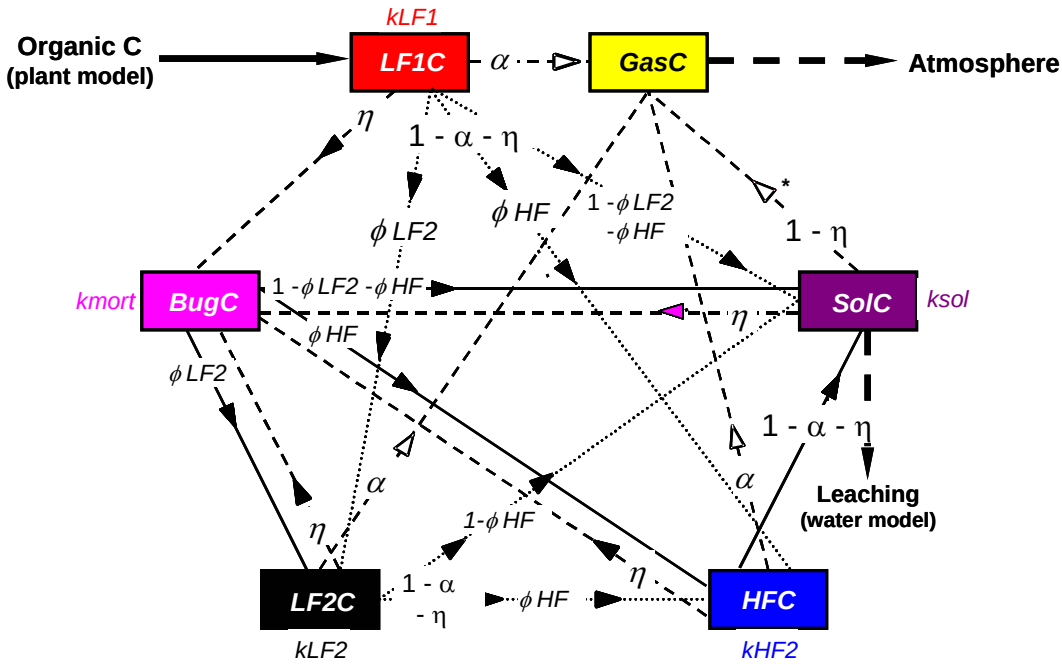

α respiration coefficient
η microbial efficiency
ϕ* universal flow partitioners

N flow occurs in the ratio of the microbial biomass
N flow occurs in the ratio of the source C and N compartment
N flow limited by ratio of source C and N compartments
N flow includes supplementary N to microbial biomass
No Corresponding N flow
Input and potential output flows to the SOM model

* A gaseous N flow (from ***SolN***) is present, but it is independent of the corresponding C flow

The total flow from a C compartment is:

temp . *moist* . *k** . *C * λ

- where *temp* and *moist* are are rate modifiers for temperature and moisture, and system-wide ratio of Ndemand in immobilisation, divided by mineralising and accessible-N)

values are expressed on a g^{-1} dry soil basis (field-based applications require data expressed on a volumetric and hence area basis). Output for the tracers will generally be expressed as isotope ratios however, calculated from the magnitude of corresponding C and ^{13}C or N and ^{15}N flows or compartments.

In the description of the mathematical framework and model outputs, compartments are italicised and emboldened. Variables and optimisable parameters are italicised, with zero subscripts denoting mandatory initial values ($LF1C_0$ for example, is the magnitude of ***LF1C*** at the beginning of the simulation). Asterisks are used to describe characteristics that apply equally to corresponding C, N, ^{13}C and ^{15}N compartments or variables: for example ***LF1**** refers equally to ***LF1C***, ***LF1N***, $\boldsymbol{LF1^{13}C}$ and $\boldsymbol{LF1^{15}N}$ (The composite of these compartments comprises the strictly conceptual SOM fraction, ***LF1***.) Asterisks are similarly used to describe characteristics that apply to all C, N, ^{13}C or ^{15}N compartments: ****C*** refers to ***LF1C***, ***LF2C*** and the four other C compartments. A similar notation may be used to describe characteristics applicable to both a C or N compartment and that of the corresponding tracer: ***LF1*C*** refers to both ***LF1C*** and $\boldsymbol{LF1^{13}C}$. The ratios of corresponding C and N compartments are indicated by ρ*: the C-to-N ratio of the model fraction ***LF1*** (approximating to FREE organic matter) is $\rho LF1$.

To aid interpretation, model outputs are colour-coded in Figures 4.7. to 4.21. In these figures the status of measurable variable are indicated by solid lines, conceptual variables by broken lines, and flows by dotted lines. The key to the coding is summarised in Table 4.6.

4.2.1. Compartments

The rate of change in each compartment (e.g. $\Delta \boldsymbol{LF1} / \Delta t$) is the sum of the associated flows. The magnitude of each interacting flow is determined by the first-order reactivity of the source compartment, and the relevant flow partitioning parameters (Section 4.2.4.). The magnitude of the C and N compartments at the start of a simulation are amongst the initial values required to run the model, together with the isotope ratios necessary to calculate their ^{15}N and ^{13}C equivalents (see Table 4.2.).

The measurable C, N, ^{13}C or ^{15}N contents of FREE, INTRA-AGGREGATE and ORGANOMINERAL fractions approximate to the model compartments ***LF1****, ***LF2**** and ***HF****. The variables *light1**, *light2**, and *heavy** are their direct equivalents, equating to the relevant measurable fraction plus a fraction of ***Bug****. The proportions of ***Bug**** in each fraction are defined by the optimisable parameters $\beta LF1$ and $\beta LF2$:

$$light1^* = \boldsymbol{LF1^*} + \beta LF1 \,.\, \boldsymbol{Bug^*}$$

$$light2^* = \boldsymbol{LF2^*} + \beta LF2 \,.\, \boldsymbol{Bug^*}$$

$$heavy^* = \boldsymbol{HF^*} + (1 - \beta LF1 - \beta LF2) \,.\, \boldsymbol{Bug^*}$$

– thus the initial size of each compartment ($LF1_0$, $LF2_0$, etc) is derived by fractionation, the fumigation–extraction technique (Brookes *et al.* 1985), and parameter optimisation.

Since the chemical characterisation in Chapter 3 suggested FREE organic matter is the least transformed fraction, ***LF1**** is the assumed recipient for organic matter

additions to the soil. Since recovery of ***LF1**** will be as *light1** (the measurable equivalent), it is assumed that microbial biomass associated with existing (native) *light1** is redistributed. Inputs to ***LF1**** are effected through a lookup table. Although a single input could be accounted for in the value of $LF1^*_0$ (the initial value of ***LF1****), a lookup table permits periodic inputs, possibly obtained from a static plant model. Methods for measuring ***Sol**** within the standard fractionation procedure (as the NaI-soluble fraction) are under development. The magnitude of ***Gas**** is likely to be calculated from a measured surface flux.

4.2.2. Tracer flows

The magnitude of the tracer (^{13}C and ^{15}N) flows are calculated simply from the corresponding C or N flows, and the ratio of source C or N and tracer compartments i.e. $*^{13}C / *C$ or $*^{15}N / *N$ i.e. assuming no isotopic fractionation These ratios are recalculated at each timestep for all compartments and their measurable equivalents as γ^* and α^* variables. Although driven by flows in C and N models, tracer flows produce a greater change in magnitude of the destination compartment when they emanate from an enriched source. Small differences in γ^* are also output as $\delta^{13}C$ values (defined as δ^* variables) which are more appropriate for tracing C in studies using the natural abundance technique.

$$\delta^* \ (‰) = (\gamma^* - 0{\cdot}0112372) / 0{\cdot}0112372 \ . \ 1000$$

– where 0·0112372 is the ^{13}C ratio in the PDB standard.

4.2.3. C and N flows

The modelled C flows represent microbial respiration, microbial incorporation, and physical relocation of substrate residues. All three types apply to ***LF1C***, ***LF2C***, ***HFC*** and ***SolC*** (the substrate C compartments), although relocation flows are conceptually restricted (and absent from ***SolC***). Flows from ***BugC*** represent the fate of active cells (physical disintegration and relocation of microbial products) and do not include a respiration or incorporation component. As the output compartment, ***Gas*C*** has no outgoing flows. Utilisation of C results in N release, but since N is conserved the there are no respiration flows for N. Also, N relocation occurs only when N release exceeds that required for maximum incorporation of C i.e. the magnitude of the corresponding C flow divided by the C-to-N ratio of the microbial biomass, ρBug. A supplementary flow from ***SolN*** allows maximum incorporation of C from N-deficient substrates into ***BugC***. The N model also features chemical stabilisation flows from ***SolN*** to ***LF1N*** and ***LF2N***.

Primary substrate flows

Ultimate control over flows from ***LF1C***, ***LF2C***, ***HFC*** and ***SolC*** is exerted by their respective first-order rate constants *kLF1*, *kLF2*, *kHF* and *kSol*, which reflect the inherent reactivity of their corresponding SOM fractions, and are assumed constant. The homogeneity and constancy in fraction reactivity is the major assumption of most SOM models. In this model, discrete levels of reactivity reflect the physical location from which the fractions are experimentally isolated.

The sum flow of C from a compartment under standard conditions is the first-order reactivity of the compartment, multiplied by its magnitude. Potential flow variables (j^*) encompass rate modifiers for temperature (*temp*) and moisture (*moist*), giving the maximum flow under the prevailing conditions. Thus the potential flow from ***LF1C*** is given by:

$$jLF1C = temp \,.\, moist \,.\, kLF1 \,.\, \mathbf{LF1C}$$

The actual flow may be less than the potential if it is limited by the availability of N (see Section 4.2.4.). The total flow is divided between incorporation (η), respiration (α) and relocation ($1-\alpha-\eta$), α and η being optimisable parameters.

It is assumed that N is required for formation of new biomass (incorporation) in a fixed proportion to incorporated C, and that this proportion reflects the microbial C-to-N ratio (defined by the optimisable parameter ρBug). Complete efficiency of N acquisition is assumed, with relocation occurring only when the release from the substrate exceeds microbial demand (i.e. $\rho^* = \rho Bug / \eta$). If N release is not sufficient, the balance is drawn from the part of ***SolN*** that is directly assimilable (independently of C), and mobile (physically accessible). The portion of ***SolN*** that is assimilable (comprising mineral N and some low molecular weight organic compounds) is defined by the optimisable parameter θ. The non-assimilable component comprises complex organic molecules of higher molecular weight. When demand for N exceeds its supply (including supplementary ***SolN***), the utilisation of substrates is progressively limited (see Section 4.2.5.).

Substrate residues are unlikely to maintain their physical location after microbial attack, becoming incorporated into aggregates or bound to mineral surfaces. The relocation component of substrate flows represent physical redistribution of residual C. As a consequence of the preferential flow of N to microbial biomass, these flows have a corresponding N component only when N release exceeds the demand resulting from C incorporation (Figure 4.2.). The C-to-N ratio of relocation flows is not therefore fixed, and may comprise only C. This may be important in moderating the ratio of recipient C and N compartments ($\rho^* = {}^*C / {}^*N$). On the basis of the measured composition of the standard fractions, certain relocation flows are excluded. Evidence from DRIFT (Chapter 2) and ^{13}C NMR (Chapters 2 and 3) suggests that the level of decomposition increases between the FREE and INTRA-AGGREGATE fractions, and between INTRA-AGGREGATE and ORGANOMINERAL. Since it is not likely that SOM will be transferred into ***LF1****, or from ***HF**** to ***LF2****, these flows are omitted. The optimisable parameters used to divide relocation flows (of both C and N) are $\phi LF2$ and ϕHF. The proportion of the relocation flow received by ***Sol**** depends on the range of alternative destinations available: $1-\phi LF2-\phi HF$, $1-\phi HF$ and 1 for ***LF1****, ***LF2**** and ***HF**** source compartments respectively. The division of relocation flows is summarised in Figure 4.1., and the conceptual mechanism illustrated in Figure 4.3.

Microbial flows

The total flow of C and N to ***Bug*** occur in the ratio ρBug. The reactivity of ***Bug*** reflects microbial mortality, and is defined by the first-order reactivity constant *kmort*. The lifetime of microbial cells is assumed to be governed by biological time, thus *kmort* is also modified by *temp* and *moist*. The return of ***Bug*** to non-living SOM fractions has

Figure 4.2. Schematic illustrating the pattern in modelled relocation flows resulting from the utilisation of the various primary substrate compartments

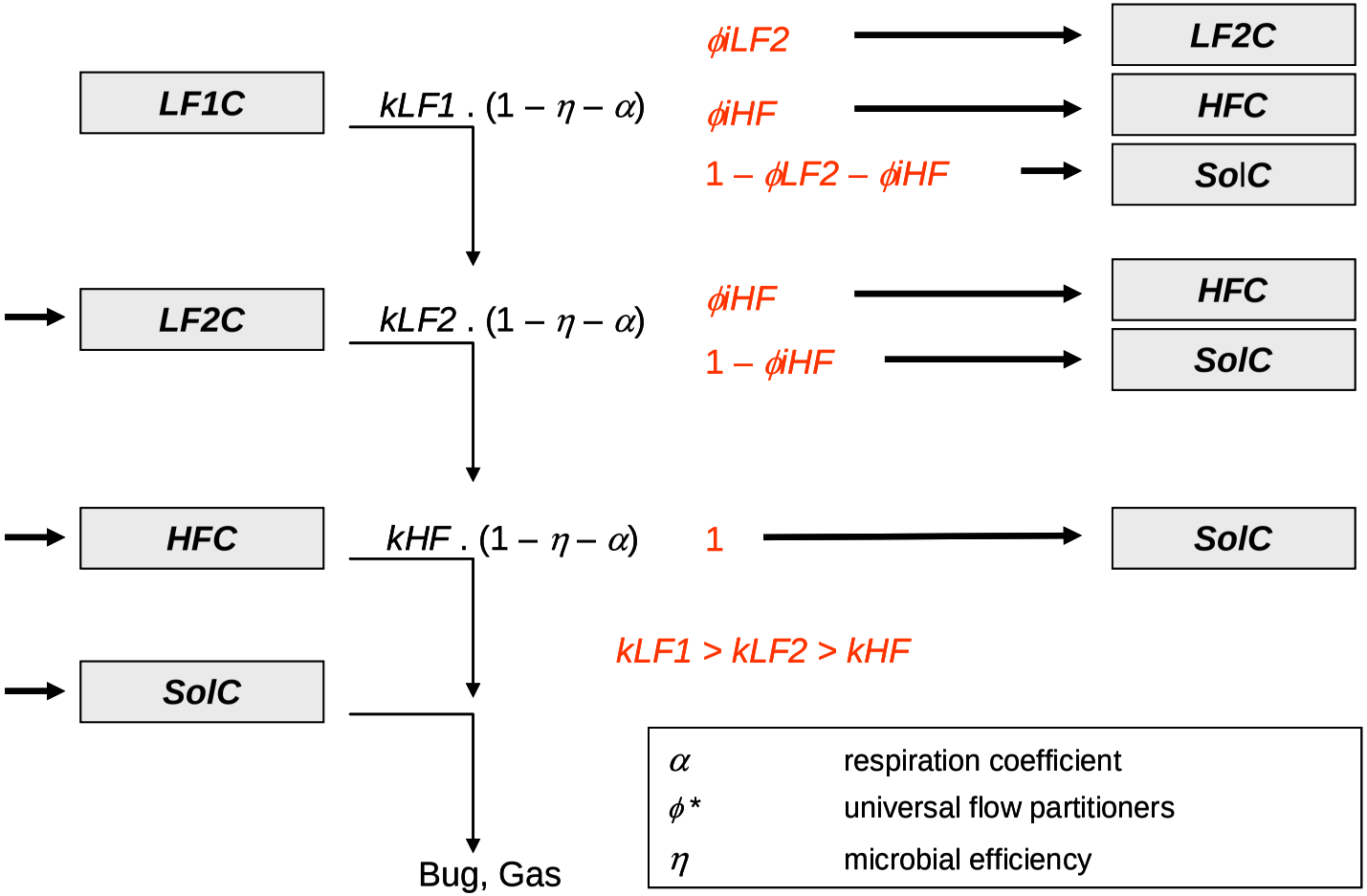

Figure 4.3. Schematic illustrating the influence of C-to-N ratio on the division of substrate C and N between incorporation and relocation flows in the model

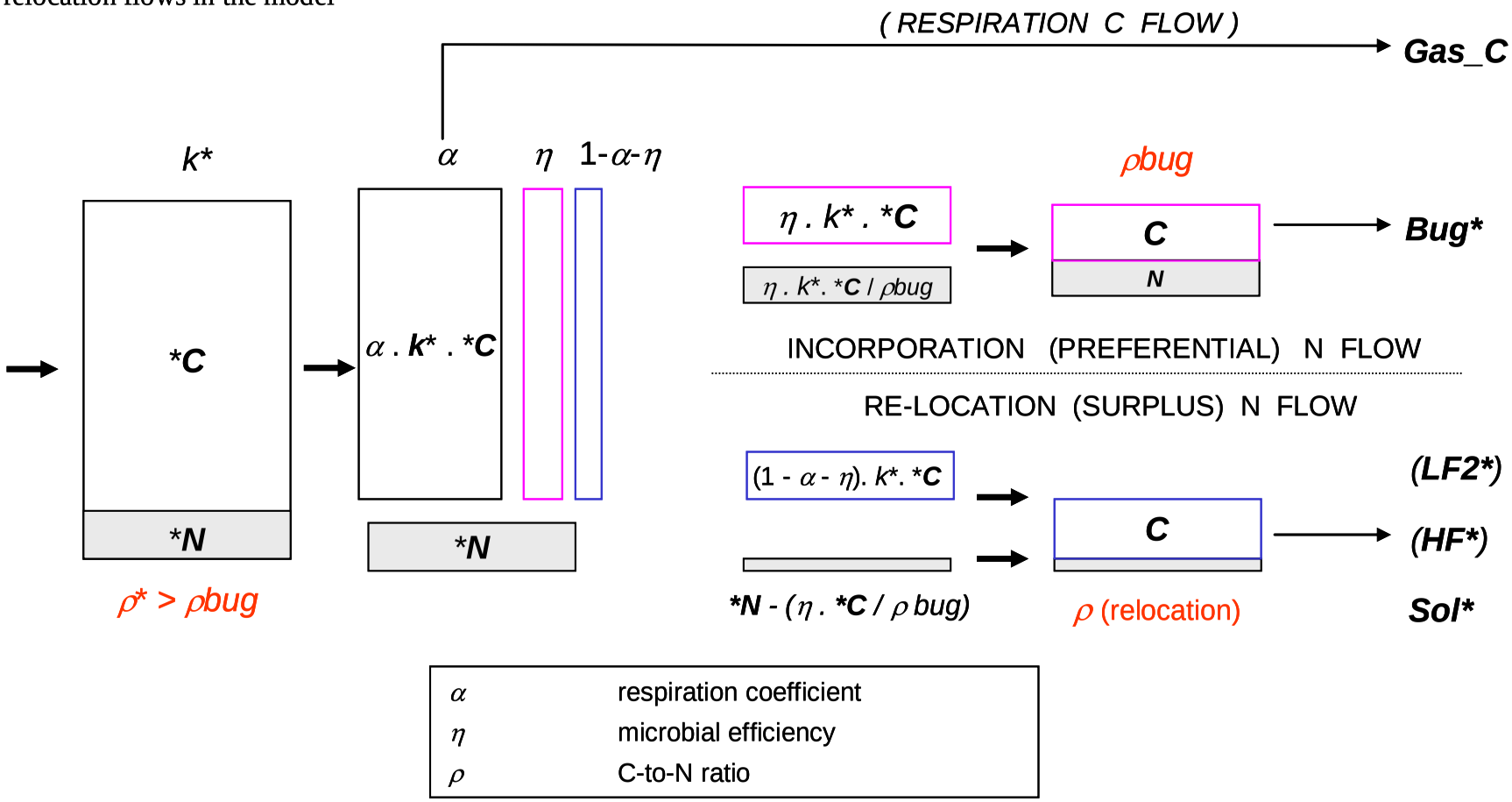

no respiration component (mineralisation proceeding after the detritus has been consolidated within the substrate compartments). The relocation of microbial products is also assumed to be governed by $\phi LF1$ and $\phi LF2$ i.e. the same parameters applied to relocation flows from the substrate compartments, with ***LF2***, ***HF*** and ***Sol*** the assumed recipients. However, as a purely physical process, the relocation of ***Bug***** occurs at the fixed C-to-N ratio of the microbial biomass (defined by ρBug). The cycling of C through microbial biomass is illustrated in Figure 4.4.

Other flows

The model includes additional flows to ***LF1N*** and ***LF2N*** from ***SolN***. These reflect the chemical modification of organic surfaces that occurs when N is in abundant supply (Fog, 1988), possibly by autopolymerisation of N with phenolic groups. The magnitude of these flows has not been established experimentally, but they have previously been used to explain unexpected enrichment of density fractions with N during straw decomposition (Magid *et al*. 1997). These flows could be functionally important if they are sufficient to modify the C-to-N ratio of substrate compartments independent of microbial activity. In this framework the magnitude of the fixation flows reflect the C content of the recipient fraction (i.e. ***LF1C*** or ***LF2C***), the magnitude of ***SolN***, and *kfix*, a first order reactivity constant. A simple first order equation (with rate constant *kvol*) is also used to represent gaseous N loss, primarily as a means for limiting the accumulation of ***SolN*** in the absence of the normal sinks (e.g. plant uptake or leaching).

Figure 4.4. Schematic of the microbial C cycle represented in the model

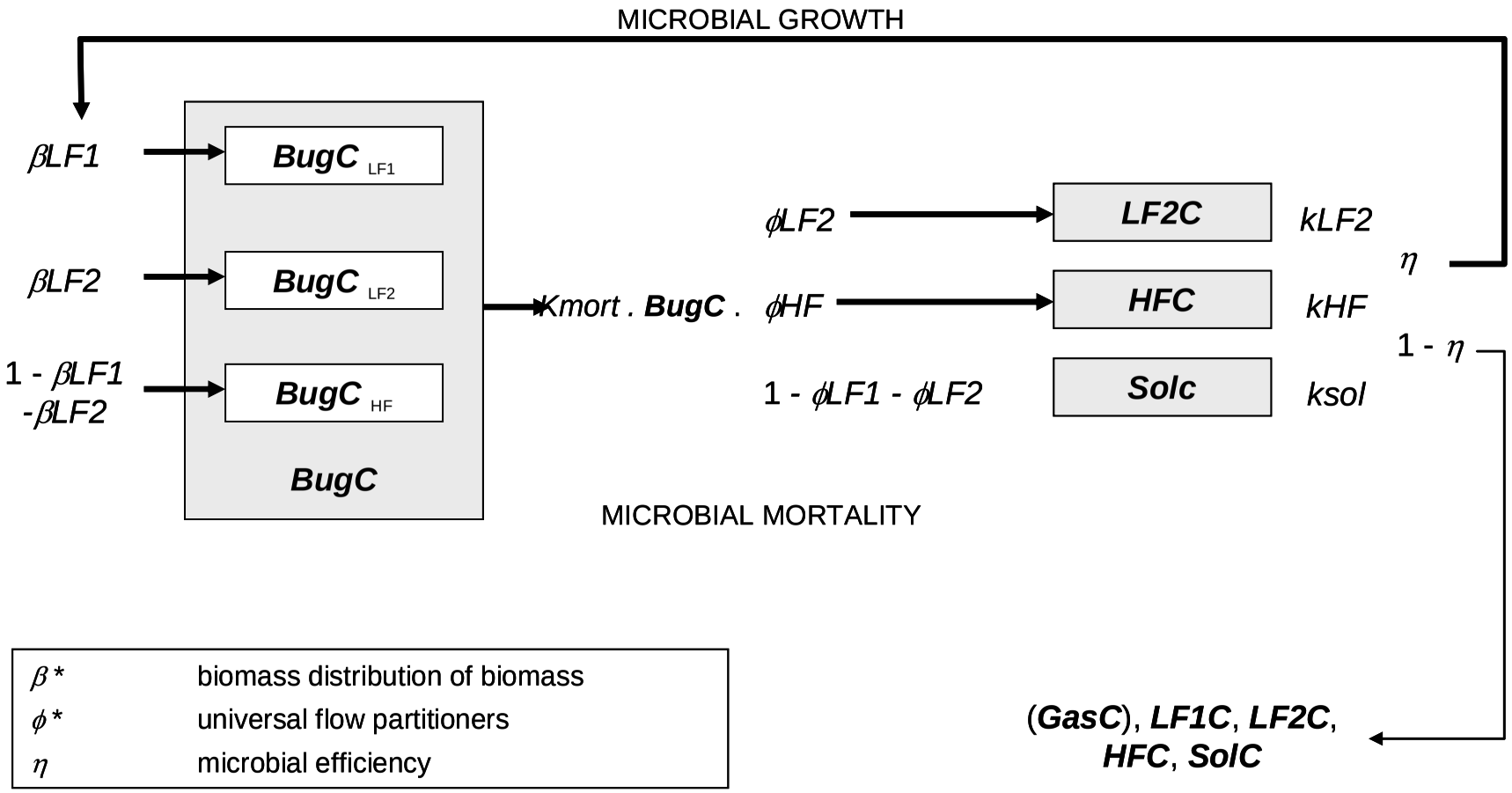

4.2.4. Flow limitation

The utilisation of N-deficient substrates depends on supplementary N from the ***SolN*** fraction. It is therefore essential that the model has a mechanism for limiting the demand for N (through the C model) when ***SolN*** becomes depleted, preventing it becoming negative. The mechanism implemented in the current framework scales down the utilisation of C substrates when both the system-wide requirement for N (*Ndemand*) exceeds its system-wide release (*Nsupply*), and ***SolN*** is exhausted. The limiter used to scale down C flows (λ) is the ratio of *Nsupply* to *Ndemand*, where $\lambda \leq 1$. Corresponding N flows remain at their potential maximum while C flows are limited, so decomposition effectively proceeds with enhanced efficiency of N acquisition. This results in N behaving – within limits – independently of C, allowing ρ^* for interacting compartments to fluctuate. This mechanism reflects changes in the microbial population (e.g. toward *r*-strategists) or a change in behaviour (increased efficiency of N acquisition at the expense of growth) arising from N stress. As the calculation of λ is made on a system-wide basis, the utilisation of substrate from all physical locations is affected. For substrates of lower C-to-N ratio (i.e. $\rho^* < \rho Bug / \eta$), relocation N flows are enhanced when $\lambda = 1$.

An alternative approach is to apply a similar mechanism on a substrate-specific rather than a system-wide basis, limitation affecting only C flows that cannot be sustained by the specific, release of N (i.e. where $\rho^* < \eta / \rho Bug$). This avoids limitation of C incorporation from substrates containing adequate or excess N, but requires proportionally large and extended increases in N acquisition efficiency to overcome limitation (resulting in a greater change of substrate C-to-N). This effect can be avoided

by applying the limitation factor to both C and N flows, but this effectively halts mineralisation when the main substrate is highly N-deficient.

Another alternative is to sub-divide ***Bug*** into three separate compartments, each associated with a specific substrate compartment, and subject to different limitation criteria e.g. governed by different ρBug. A possible framework for a model with three-***Bug*** compartments is shown in Figure 4.5. This has the conceptual advantage of discriminating between microbial populations of contrasting physical location, substrate preference or N response. However, it also yields additional flows and parameters without any additional variables that can be measured. For this reason it would be impossible to infer the reactivity of all compartments with the maximum available data.

4.2.5. Simulation of gross processes

Experimentally, gross N mineralisation can be estimated by enriching the soil NH_4^+ pool with $^{15}NH_4^+$, and observing the isotopic dilution that results from the release of $^{14}NH_4^+$ from decomposing substrates. Gross N immobilisation can be simultaneously estimated from the increasing enrichment of the microbial pool i.e. the incorporation of $^{15}NH_4$ (Barraclough 1995). In the model, gross N mineralisation is represented by incorporation N flows, and all flows to ***SolN*** (including those arising from microbial mortality). Only the NH_4^+ component of the ***SolN*** flows (approximating to the fraction θ) will be measured using isotopic dilution (assimilable N also includes some low molecular weight organic compounds). It is also an assumption that N incorporated into microbial biomass passes through the NH_4^+ phase. Gross N immobilisation is

Figure 4.5. Possible structure for an adapted model featuring three microbial compartments but which may not be adequately parameterised unless methods are available to measure microbial sub-fractions

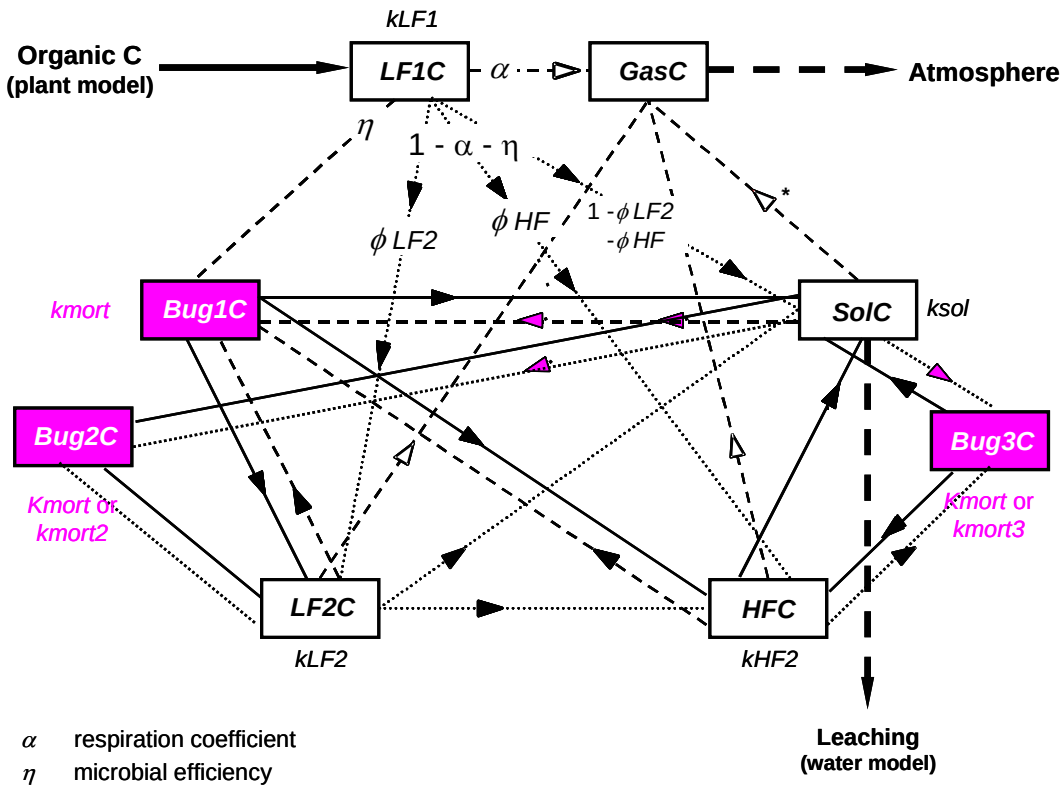

α respiration coefficient
η microbial efficiency
ϕ* universal flow partitioners

N flow occurs in the ratio of the microbial biomass
N flow occurs in the ratio of the source C and N compartment
N flow limited by ratio of source C and N compartments
N flow includes supplementary N to microbial biomass
No Corresponding N flow
Input and potential output flows to the SOM model

* A gaseous N flow (from ***SolN***) is present, but it is independent of the corresponding C flow

The total flow from a C compartment is:

temp . *moist* . *k** . *C * λ

- where *temp* and *moist* are are rate modifiers for temperature and moisture, and system-wide ratio of Ndemand in immobilisation, divided by mineralising and accessible-N)

represented by the incorporation N flows, and supplementary N flow from ***SolN*** to ***BugN***. In linking a plant model, incorporation N flows will not be available to plant roots if they access exclusively ***SolN***. Net N mineralisation is the calculated as the difference between gross rates of mineralisation and immobilisation.

4.2.6. Modifiers

Most SOM models use environmental conditions as driving variables, the notable exceptions are NCSOIL (Molina *et al.* 1983) and Q-SOIL. In this model, modifiers for soil temperature (*temp*) and soil moisture content (*moist*) are applied to all flows mediated by microbial activity including *kmort* (see Section 4.2.3.). The *temp* modifier is also applied to flows to ***GasN*** and the fixation flows from ***SolN***. Modifiers allow data acquired under ambient (but monitored) conditions to be used in parameterisation. The used are based on the empirical relationships established for the Roth-C model (Coleman and Jenkinson 1996):

$$temp = [\ 47\ /\ \{1 + \exp(106 / [T + 18{\cdot}3])\}\ ]$$

– where T is temperature in ºC (flow rates are unmodified at 9·25 ºC).

$$moist = 0.2 + 0{\cdot}8\ .\ (PSMD - SMD) / (0{\cdot}444\ .\ PSMD)$$

– where SMD is volumetric soil moisture deficit relative to field capacity (mm), and PSMD is its potential maximum (mm) i.e. when the soil is in its driest state. Flows

are unmodified whilst SMD is less than 0·444 of PSMD. The minimum value for *moist* is 0·2. In RothC PSMD (mm) of topsoil (0–23 cm) is estimated from % clay content:

$$\text{PSMD (mm)} = 20 + (1{\cdot}3 \,.\, \%\ \text{clay}) - (\%\ \text{clay})^2$$

4.2.7. Numeric parameter values

Numeric values must be assigned to parameters invoked by the model in order to perform simulations. These include values for the optimisable parameters introduced above and summarised in Table 4.1. and values for the initial magnitude of measurable variables and compartments (Table 4.2.). Model output is sensitive to the latter since these are used as starting points for simulations regardless of their associated error. Initial values may be optimised within the limits of the measurement uncertainty. Initial values for *light1**, *light2** and *heavy** are determined experimentally by measuring the C, N, ^{15}N and ^{13}C content of the FREE, INTRA-AGGREGATE and ORGANOMINERAL fractions. Strictly, the initial size of ***GasC*** should be expressed in terms of the soil atmosphere, but it is more convenient to assume that instantaneous production rates are reflected in surface flux. Although $BugN_0$ may be determined experimentally by fumigation–extraction (Brookes *et al.* 1985), it is calculated within the model from the measured (or otherwise specified) value for $BugC_0$, according to ρBug.

4.2.8. Scenario simulations

The sensitivity of simulations to substrate input and assigned parameter values was established by comparing the outcome of four scenarios representing the addition of two

Table 4.1. List of optimisable parameters invoked in the model and the values assigned to them in the decomposition scenarios

Parameter	Description	Model components directly influenced	Assigned value
Flow partitioners			
α	Respration coefficient	Primary flows to ***GasC***	0.55
η	Microbial incorporation coefficient	Primary flows to ***BugC***	0.30
$\beta LF1$	FREE microbial fraction	***Bug*** and ***LF1***	0.10
$\beta LF2$	INTRA-AGGREGATE microbieal fraction	***Bug*** and ***LF2***	0.10
$\phi LF2$	Universal flow partitioner	Relocation flows to ***LF2***	0.20
ϕiHF	Universal flow partitioner	Relocation flows to ***HF***	0.50
ρbug	Microbial C-to-N ratio	***BugN***	6.00
θ	Assimilable fraction	***SolN*** and N limitation	0.30
Reactivity constants			
kLF1	Reactivity constant	***LF1***	0.0100
kLF2	Reactivity constant	***LF2***	0.0020
kHF	Reactivity constant	***HF***	0.00005
ksol	Reactivity constant	***Sol***	0.0300
kmort	Mortality constant	***Bug***	0.0150
kfix	Chemical fixation rate constant	***SolN***	0.0005
kvol	Gaseous N loss rate constant	***SolN***	0.001

Table 4.2. List of variables representing initial values for which numeric values are required in order to run the model

Model	Parameter
C	$light1C_0$ $light2C_0$ $heavyC_0$ $solC_0$ + $gasC_0$ (+) $bugC_0$ +
N	$light1N_0$ $light2N_0$ $heavyN_0$ $solN_0$ + $gasN_0$ (+)
^{13}C	$light1\,^{13}C_0$ $light2\,^{13}C_0$ $heavy\,^{13}C_0$ γgas_0(+) γbug_0 + γsol_0 +
^{15}N	$light1\,^{15}N_0$ $light2\,^{15}N_0$ $heavy\,^{15}N_0$ αgas_0(+) αbug_0 + αsol_0 +

+	independent measurement required
(+)	nominal values or background estimates may be used
*light1**	relate to FREE organic matter
*light2**	relate to INTRA-AGGREGATE organic matter
*heavy**	relate to ORGANOMINERAL fraction
*sol**	strictly relate to NaI soluble organic matter
*bug**	relate to microbial biomass

contrasting straw residues (both C_4 and both enriched in ^{15}N), at two rates (Table 4.3.). Constant environmental conditions were assumed (*temp* = 1; *moist* = 1) and simulations run from 10 days before to 365 days after incorporation of straw. A control scenario (i.e. with no straw addition) was also run.

Initial values

Initial values defined the status of relevant variables and compartments at the beginning of the simulation i.e. 10 days prior to straw incorporation (Day –10). In the scenarios a total soil C content of 20 mg C g^{-1} was assumed, with its distribution between FREE, INTRA-AGGREGATE and ORGANOMINERAL fractions (represented by *light1C*, *light2C* and *heavyC*) based on that in the silty clay loam soil fractionated in Chapter 2 (Table 4.4.). The proportion allocated to ***SolC*** was based on the typical proportion measured as dissolved organic carbon (DOC) in arable soils (Gregorich *et al.* 2000). The equivalent $\delta^{13}C$ values (δ^*_0) reflected the differences in chemical composition of the measured fractions established in Chapter 2, the $\delta^{13}C$ of SOM increasing with repeated transformation (Boutton 1996). A value typical for C_3 plant material was specified for $\delta light1_0$ (–28 ‰) and a higher value (close to that of whole soil) for $\delta heavy_0$ (Table 4.4.). The value used for δSol_0 was closer to that of $\delta light2_0$, DOC being composed of predominantly active, less transformed SOM (Gregorich *et al.* 2000). Calculated from the sum of the fractions, the initial $\delta^{13}C$ of the whole soil was –26.61 ‰ (Table 4.4.). Values for $*^{13}C_0$ were calculated from δ^*_0 and $*C_0$ according to the equation in Section 5.2.2.2.

Table 4.3. The nature of the four straw additions used in the scenarios, encompassing high (H) and atypically high addition rates (XH) and residues of high (HQ) and low (LQ) quality

Scenario	HQ/H	HQ/XH	LQ/H	LQ/XH
Addition rate (g g^{-1})	2.0	6.0	2.0	6.0
C (mg g^{-1})	800	2400	800	2400
C:N ratio	15	15	60	60
$\delta^{13}C$ (‰)	-12.00	-12.00	-12.00	-12.00
^{15}N (atom%)	10.00	10.00	10.00	10.00

Table 4.4. The distribution and isotopic composition of C and N between and within measured SOM fractions assumed for the scenarios (before the straw addition)

Fraction	C			C-to-N	N		
	% total	mg g^{-1}	$\delta^{13}C$ (‰)	ratio	% total	mg g^{-1}	^{15}N atom%
*Light1**	5.0	1.0	-27.00	22.0	2.17	0.045	0.3663
*Light2**	5.0	1.0	-28.00	20.0	2.39	0.050	0.3664
*Heavy**	89.5	17.9	-26.50	9.0	94.96	1.989	0.3670
Sol*	0.5	0.1	-28.00	10.0	0.48	0.010	0.3663
Total	100	20.00	-26.61	9.55	100	2.09	0.3670

Table 4.5. The calculated distribution and isotopic composition of C and N between and within the modelled SOM compartments in the scenarios (before the straw addition)

Compartment	C			C-to-N	N		
	% total	mg g^{-1}	$\delta^{13}C$ (‰)	ratio	% total	mg g^{-1}	^{15}N atom%
LF1 *	4.80	0.96	-26.96	24.8	1.85	0.039	0.3663
LF2 *	4.80	0.96	-28.00	22.2	2.07	0.043	0.3664
HF *	87.90	17.58	-26.47	9.1	92.42	1.936	0.3670
Bug *	2.00	0.40	-28.00	6.0	3.18	0.067	0.3664
Sol *	0.50	0.10	-28.00	10.0	0.48	0.010	0.3663
Total	100	20.00	-26.61	9.55	100	2.09	0.3670

The initial distribution of N between the standard fractions ($*N_0$) was calculated from the distribution of C and their designated C-to-N ratios (Table 4.4.). The latter were chosen (as for $\delta*_0$) to reflect the contrasting levels of microbial transformation amongst the fractions, lower ratios assigned to the more transformed fractions. Due to the transient nature of mineral N, an arbitrary C-to-N ratio of 10 was used to determine $SolN_0$. On account of the higher C-to-N ratios expected in FREE and INTRA-AGGREGATE organic matter, the light fractions accounted for a smaller proportion of total soil N than total soil C (Table 4.4.). Although rather insignificant where enriched substrates are simulated, the small general increase in ^{15}N natural abundance with decomposition (Hopkins *et al.* 1998) was accounted for in calculation of $*^{15}N_0$ from $*N_0$ (Table 4.4).

To calculate the initial magnitude of model compartments from those assumed for the measured fractions, $BugC_0$ was taken as 2 % of total soil C, within the typical range of 1 to 3 % (Theng *et al.* 1989). The value for $BugN_0$ was determined from $BugC_0$ using ρBug. The isotopic composition of the microbial biomass was assumed equivalent to that of INTRA-AGGREGATE organic matter. Using the numeric values specified for $\beta*$ (see below), values for $LF1*_0$, $LF2*_0$ and $HF*_0$ were calculated from their measurable equivalents $light1*_0$, $light2*_0$ and $heavy*_0$ (Table 4.5.). Nominal values were used for $GasC_0$ and $GasN_0$,.

Optimisable parameters

Circumstantial evidence suggests that microbial biomass is a significant and possibly substantial component of light fraction (Gregorich and Janzen 1996). In the scenarios FREE and INTRA-AGGREGATE fractions were assumed to each contain 10 % of

the total soil microbial biomass (i.e. $\beta LF1$ = 0·1; $\beta LF2$ = 0·1). A value of 6·0 was used for ρBug, typical of a predominantly bacterial community (Theng *et al.* 1989).

A typical value of 0·45 was assumed for microbial efficiency, with the corresponding value for η (incorporation) set arbitrarily at 0·30; the balance between incorporation and relocation flows have not been explored experimentally. The values assigned to $\phi LF2$ and ϕHF (governing the sub-division of relocation flows) were intended to reflect the greater magnitude of *heavyC*, offset against the higher likely reactivity of light fractions (ϕHF = 0·5; $\phi LF2$ = 0·2). The utilisation of the C and N substrate compartments is broken down in Figure 4.6., using the example of ***LF1***.

The values assigned to *kLF1*, *kLF2* and *kHF* (Table 4.2.) were intended to reflect the contrasting reactivity expected of fractions differing in their physical association and chemical composition. The assigned values gave mean residence times of 100, 500 and 20 000 days for ***LF1***, ***LF2*** and ***HF*** respectively, compatible with the concept that FREE organic matter is dynamic on a seasonal timescale, INTRA-AGGREGATE over years, and ORGANOMINERAL over decades. The value assigned to *kmort* reflects the high rate of microbial turnover established experimentally and through parameterisation of existing models (50 % greater than that of ***LF1*** in this scenario). The mobile ***Sol*** compartment was assumed to be twice as active as the microbial biomass (giving a mean residence time of 33 days).

The value assigned to θ suggests one-third of soluble N is available for direct assimilation by microbial cells as NH_4^+ or low molecular weight compounds to balance their demand for N. This is based on the typical difference between mineral N and total

Figure 4.6. The general relationship between C and N flows from substrate compartments using the example of the ***LF1*** and parameter values used in the scenarios. Equivalent flows from ***Bug*** represent physical relocation with microbial mortality and occur at the C-to-N ratio of ***Bug*** (ρbug) with no ***Gas*** component

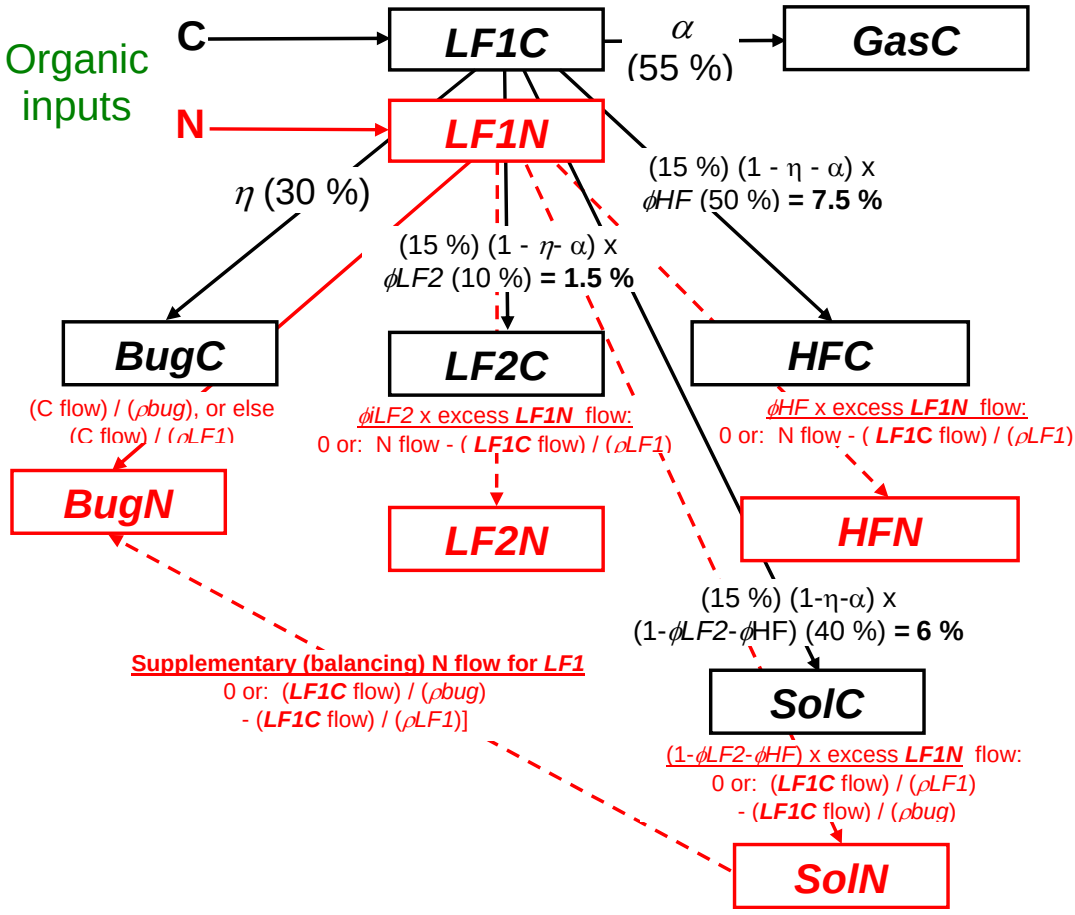

soluble N (TSN) measured in the field. In the scenarios, nominal values were assigned to *kvol* (governing gaseous N loss) purely to provide a sink for ***SolN***. Since there is little existing data to qualify or quantify chemical fixation flows (from ***SolN*** to substrate compartments), *kfix* was assigned a value of 0.

Substrates

The C-to-N ratio of active substrate compartments strongly influences immobilisation activity, and largely determines the demand for supplementary N. The scenarios encompass two types of straw of contrasting C-to-N ratio. The low quality (LQ) straw had a higher C-to-N than wheat straw (close to that of maize), that of the high quality (HQ) straw a C-to-N similar to that of rye grass (Table 4.3). A $\delta^{13}C$ value characteristic of C_4 plants (Smith and Epstein 1971) was used for both straw types to simulate the tracing of C using the natural abundance method (Section 1.5.2.). The lower incorporation rate (H) equated to a high field-rate of approx. 6 t dry matter ha^{-1} (assuming a soil bulk density of 1.30 kg L^{-1} and a topsoil depth of 23 cm). The alternate rate (XH) was more extreme, corresponding to a field rate of approx. 18 t dry matter ha^{-1}. The additions were made to ***LF1**** rather than *light1**, since the latter has a microbial component (Section 4.2.2.).

4.2.9. Sensitivity analysis

The sensitivity of the model to values assigned to the key parameters was investigated. Although parameterisation requires experimental data, it is useful to establish the sensitive parameters before attempting optimisation. The sensitivity of the

N limitation mechanism was considered by progressively increasing or decreasing the value of key parameters – including initial values– whilst leaving other parameters unchanged.

4.3. Results and discussion

The most extreme scenario (LQ/XH) resulted in the limitation of C flows through an imbalance in the system-wide demand for N relative to its supply. The outcome of the LQ/XH scenario and the performance of the mechanism used to model limitation of C flows are discussed in Section 4.3.4. The sensitive parameters in the model are identified in Section 4.3.5. A key to the coding of model outputs can be found in Table 4.7.

4.3.1. Dynamics of C and N under non-limiting N

The simulated dynamics of the C and N compartments and their ratio are shown in Figures 4.7. to 4.9., for the three scenarios that did not result in flow limitation (HQ/H, HQ/XH and LQ/H). The magnitude of ***LF1C*** declined rapidly in the 10 days prior to straw addition due to the values specified for $LF1C_0$ and *kLF1*. The initial magnitude of the microbial biomass could not be maintained with the available substrate, and the values specified for η (incorporation) and *kmort* (microbial mortality).

In the HQ/H scenario, straw addition doubled the magnitude of ***LF1N*** and lowered $\rho LF1$; the HQ/XH scenario had a proportionally greater effect (evident at the whole soil level). The LQ residue delivered a similar quantity of C as HQ but had a

Table 4.6. Colour and format coding used in model outputs

Fraction or compartment		
FREE organic matter	measured fraction	
LF1	modelled compartment	
INTRA-AGGREGATE	measured fraction	
LF2	modelled compartment	
ORGANOMINERAL	measured fraction	
HF	modelled compartment	
Soluble fraction	potentially measurable fraction	
Extractable SOM	measured analogue	
Sol	modelled compartment	
Gas	estimated fraction	
Gas	modelled compartment	
Microbial biomass	measured fraction	
Microbial biomass	modelled compartment	
Total soil C or N	calculated sum of fractions	
Flow to / from model compartment		

Figure 4.7. Simulated dynamics of (a) C and (b) N for the HQ / H scenario

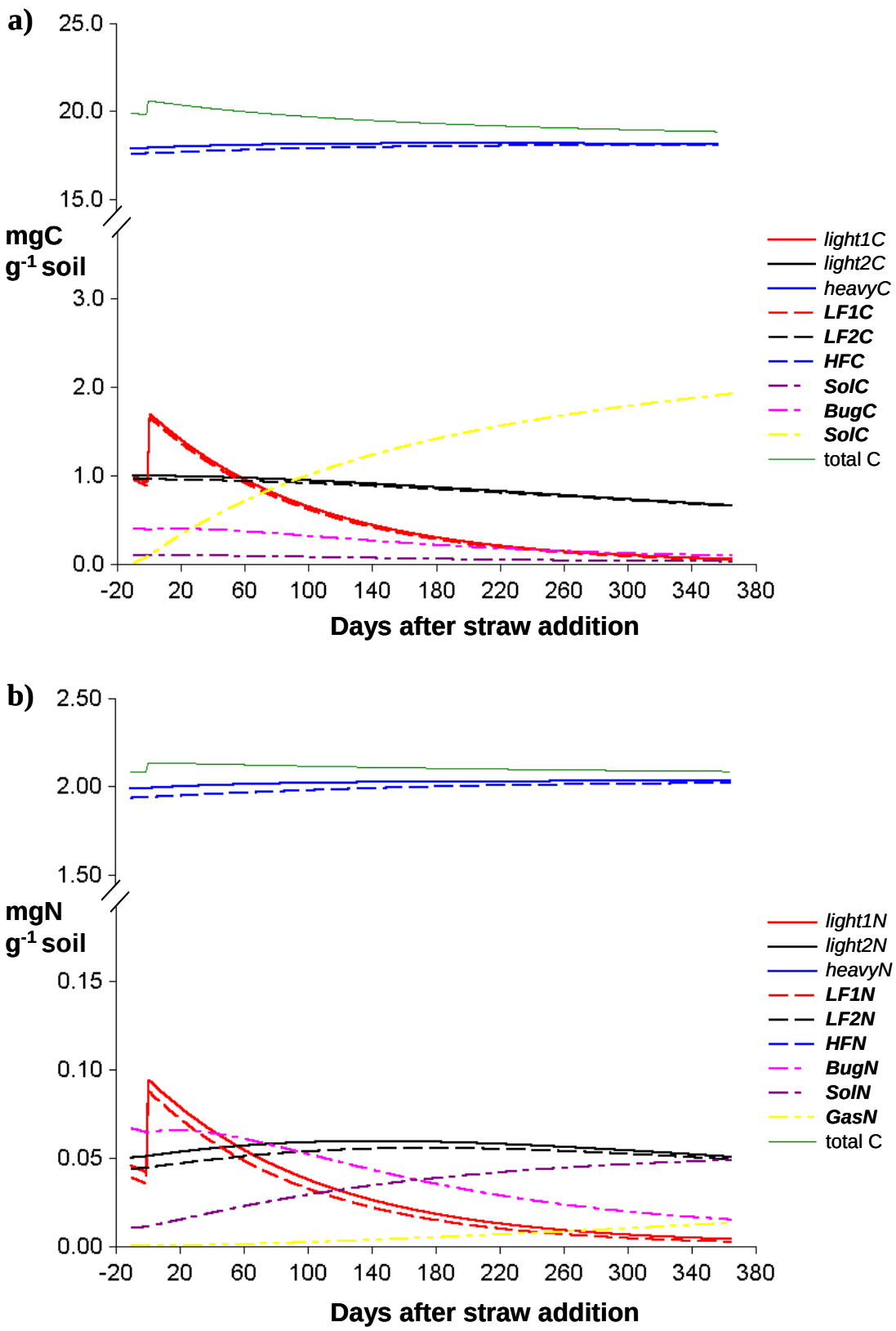

Figure 4.8. Simulated dynamics of (a) C and (b) N for the HQ / XH scenario

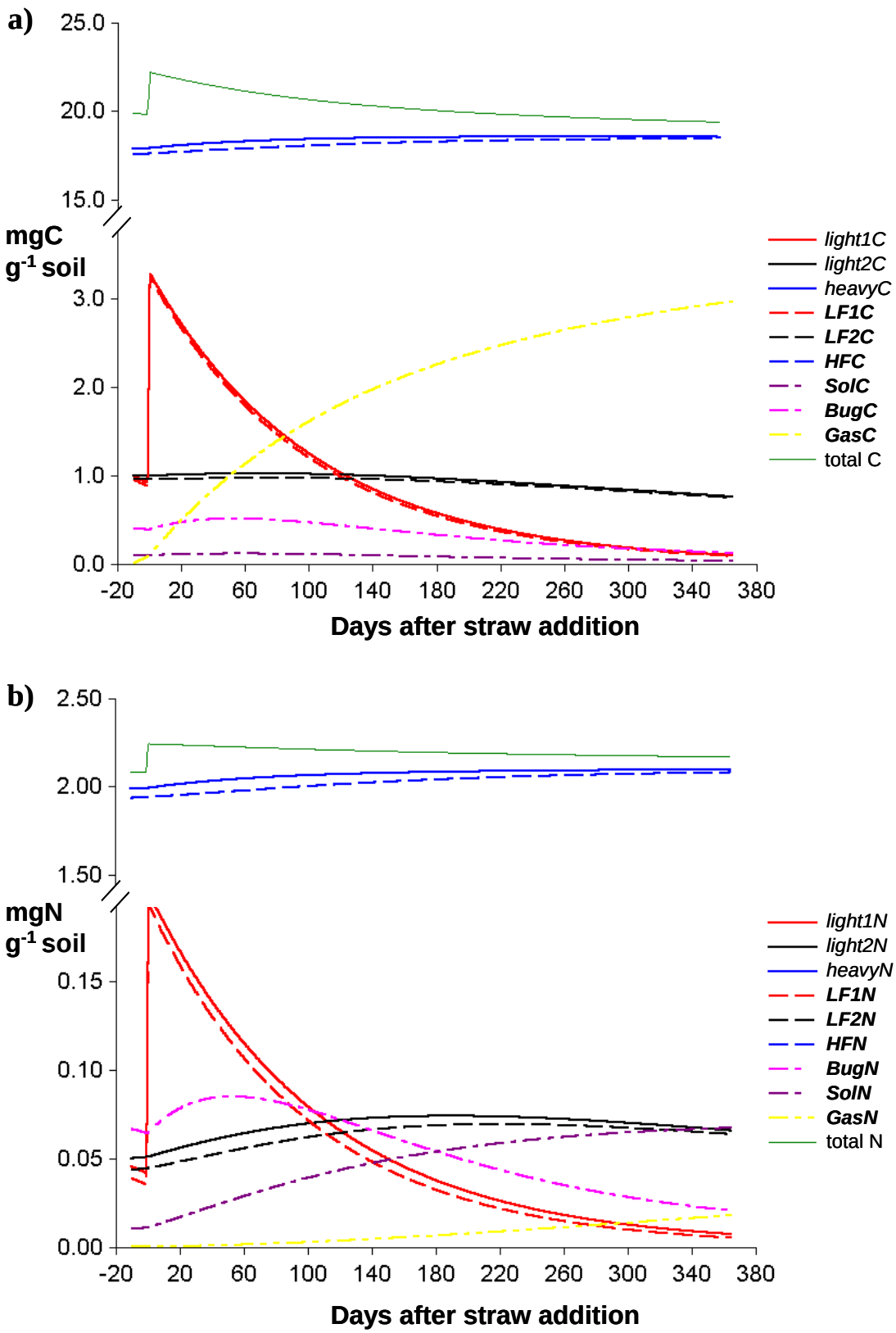

Figure 4.9. Simulated dynamics of (a) C and (b) N for the LQ / H scenario

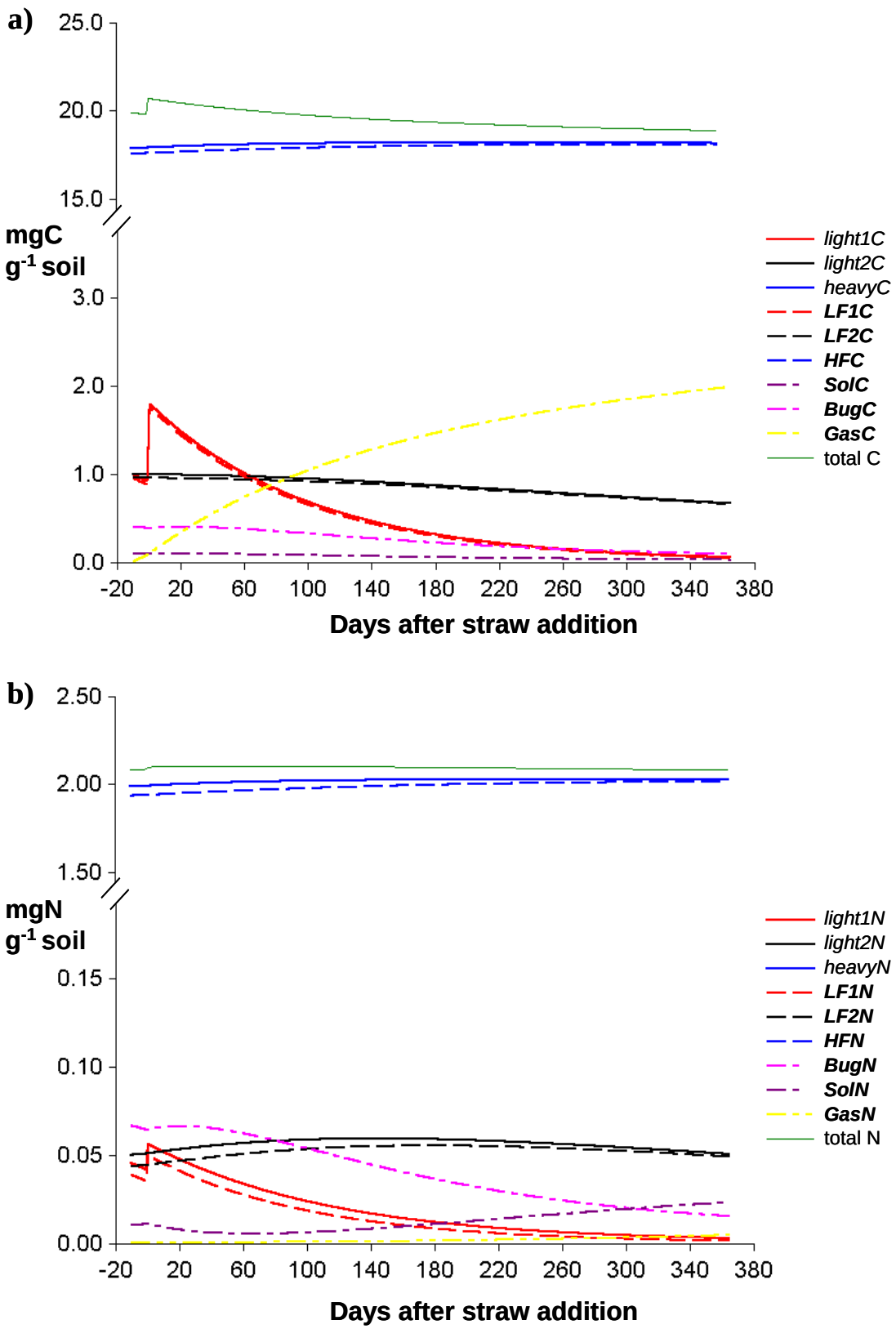

minor impact on ***LF1N*** due to its higher C-to-N ratio (Table 4.3.). With the assigned value of *kLF1*, the magnitude of ***LF1C*** returned to its initial value 55 and 120 days after straw incorporation in the HQ/H and HQ/XH scenarios respectively (Figures 4.7. and 4.8.). The C inputs in both LQ/H and HQ/H maintained $BugC_0$, HQ/XH resulted in an increase. Without further inputs of organic matter $\rho LF1$ was fixed. However, as a diminishing substrate compartment supporting a constant proportion of N-rich biomass, $\rho light1$ decreased over time. The magnitude of ***SolN*** increased rapidly in the HQ scenarios mainly due to relocation of microbial products and an N-enriched relocation flow from ***HF***.

The magnitude of ***LF2N*** was maintained under the control scenario, and increased progressively for LQ/H, HQ/H and HQ/XH. The dominant source of N was ***BugN***, although a significant proportion of the increase in the HQ scenario was through relocation of excess N from the input compartment i.e. ***LF1N***. The fate of ***LF2N*** was primarily to ***BugN*** and, whilst generally satisfying microbial requirement with respect to the corresponding C flow, excess N was small. The value of $\rho LF2$ decreased in all the scenarios, mainly because C-dominated relocation flows did not completely offset the effect of N-rich flows from ***Bug***. With respect to ***HF***, the three scenarios (including LQ/H) resulted in small (but unbalanced) inputs of N, mainly via ***BugN***. Over the duration of the simulation, there was little net gain in ***HFC***, flows from ***BugC*** counteracted by incorporation and respiration flows (to ***BugC*** and ***GasC***). These small net changes in magnitude would be difficult to measure experimentally without isotopic tracers.

It was clear that ρBug and the assumption of complete N acquisition are of key importance in the model. Because relocation flows comprise a fixed proportion of substrate C but only N in excess of the microbial requirement (i.e. that required to satisfy C incorporation and occurring when $\rho^* < \rho\ Bug / \eta$), the C-to-N ratio of relocation flows was dynamic. Relocation flows can thus enrich or deplete recipient compartments of N. The only source of consistently N-enriched relocation flows was ***HF****, on account of the low value of ρHF (Table 4.5.).

4.3.2. Dynamics of tracers under non-limiting N

The isotopic composition of model components is calculated from the relative magnitude of the corresponding C and ^{13}C or N and ^{15}N compartments or variables. These ratios are reflected in α^* and γ^* variables respectively (e.g. $\alpha light1$ and $\alpha LF1$). The dynamics of these variables in the HQ/XH scenario are shown in Figure 4.10. The effect of the enriched straw addition on $\alpha LF1$ depends on $LF1N_0$, and is consequently greater for this scenario than LQ/XH. After straw addition, the enrichment of the input compartment cannot change without a new addition of a different enrichment. However, as the magnitude of ***LF1N*** and ***LF1C*** declines, a change occurs in $\alpha light1$: the proportion comprising (less ^{13}C and ^{15}N enriched) microbial biomass increases. The value of $\alpha light2$ slightly exceeded $\alpha LF2$ until the end of the simulation since its enrichment is derived via the microbial biomass. The response depends on compartment size as well as the enrichment of the input flows: the amount of ^{15}N incorporated was more indicative of dynamics within ***HFN*** than αHF. The dynamics of ^{15}N in HQ/H and LQ/H were similar, the magnitude determined by the amount of N added in straw (Table 4.3.).

Figure 4.10. Simulated dynamics of ^{15}N ratio for the HQ / H scenario

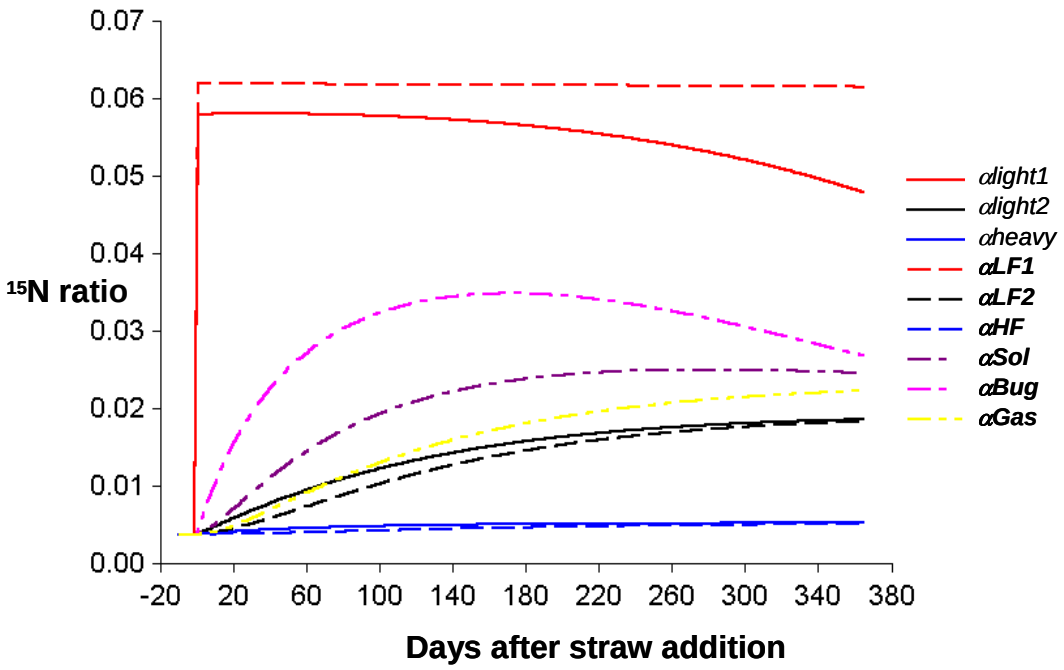

Figure 4.11. Simulated dynamics of $\delta^{13}C$ for the HQ / H scenario

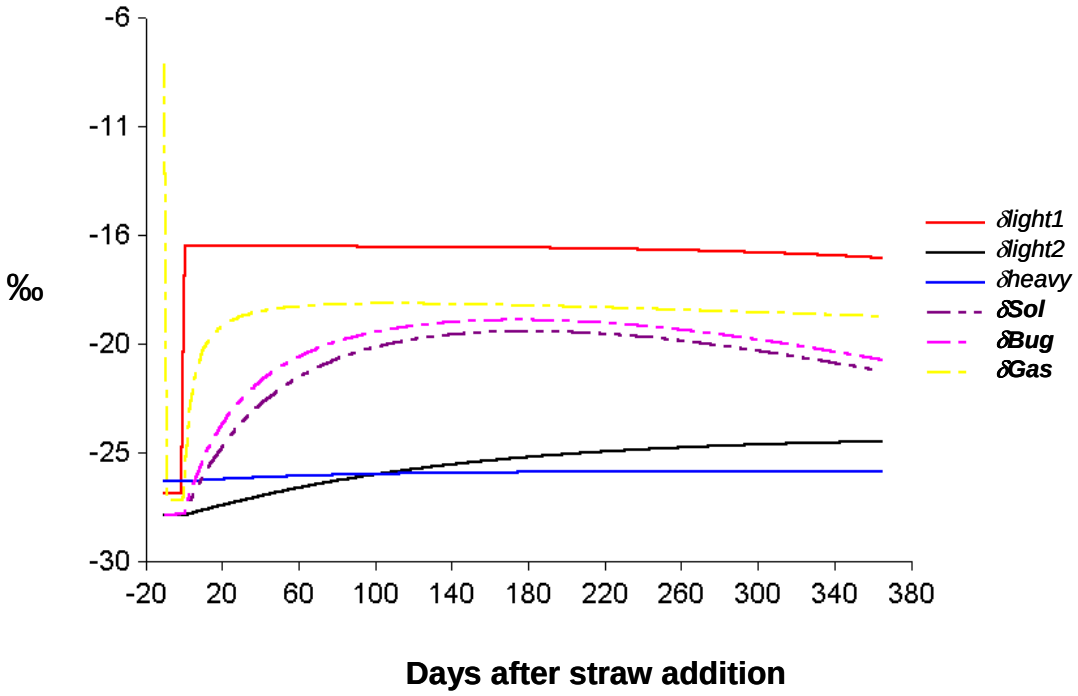

Using natural abundance discrimination (i.e. small but distinct levels of enrichment), trends in $\delta^{13}C$ (calculated from the γ^* variables) reflected the close relationship between C and N turnover – they resembled those of ^{15}N (Figure 4.11 illustrates the dynamics of $\delta^{13}C$ for the HQ/XH scenario). However, γ***Sol*** and γ*Bug* were more similar than α*Sol* and α*Bug*. This was partly due to the depletion of ***SolN*** through N immobilisation (i.e. supplementary N flow to ***BugN***). The value of γ*LF2C* increased more slowly than α*LF2* because the proportion of N received directly from the enriched substrate (rather than via ***Bug***) was greater than for C.

4.3.3. Processes under non-limiting N

As expected, the addition of the low N straw initially produced net immobilisation of N i.e. a supplementary N flow from ***SolN*** to ***BugN*** to enable maximum incorporation C (Figure 4.12.). However, the overall supply of N exceeded demand even for the LQ/H scenario (Figure 4.13). Equivalent additions of the N-rich straw (scenario HQ/H) resulted in net N mineralisation (Figure 4.12.). Rates of gross N immobilisation were slightly lower for LQ/H than HQ/H, since the low N straw had a slightly lower C content (Table 4.3.). The ratio of C respired to gross N mineralised differs from ρ*Bug* due to N mineralised or transferred in relocation flows. The ratio was therefore higher in HQ/H, where there was a general surplus of N in the system (Figure 4.21.). In LQ/H the efficiency of N capture increased, as expected of a situation where the quality (i.e. C-to-N) of the main substrates is poor (Figure 4.21.). This is contrary to the assumption that the measured ratio of CO_2–C production to gross N mineralisation reflects the C-to-N ratio of mineralising substrates (large relocation N flows from high quality substrates diminish gross N mineralisation, whilst the C

Figure 4.12. Simulated rates of gross and net N mineralisation (GNM and NNM), and gross N immobilisation (GNI) for the LQ / H and HQ / H scenarios

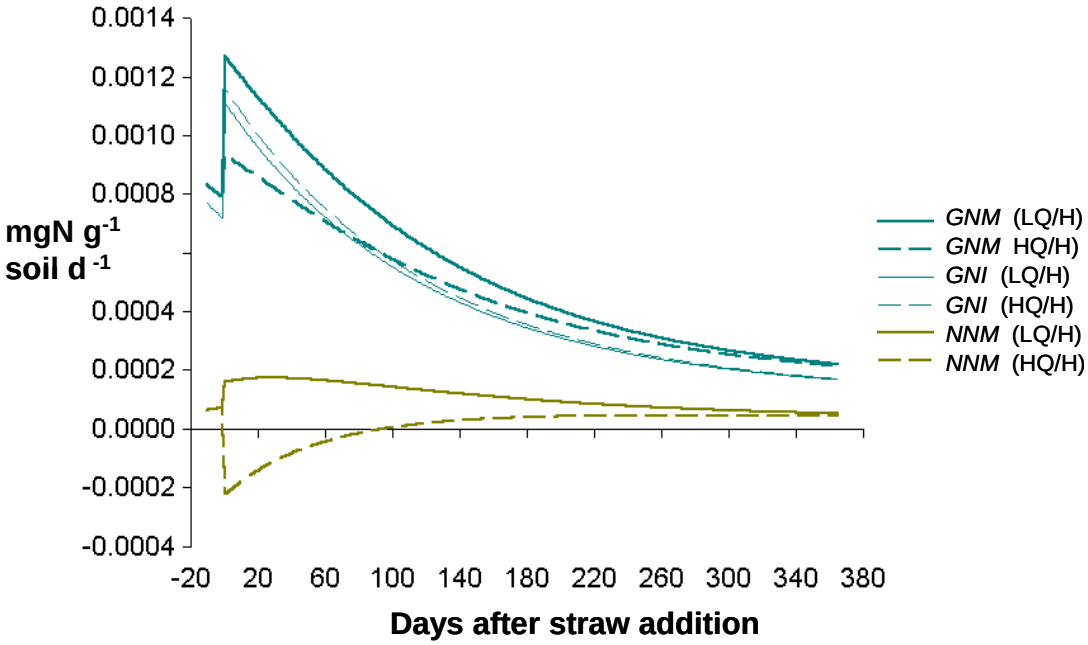

Figure 4.13. Simulated balance between the supply and demand for supplementary N for the HQ / H and LQ / H scenarios

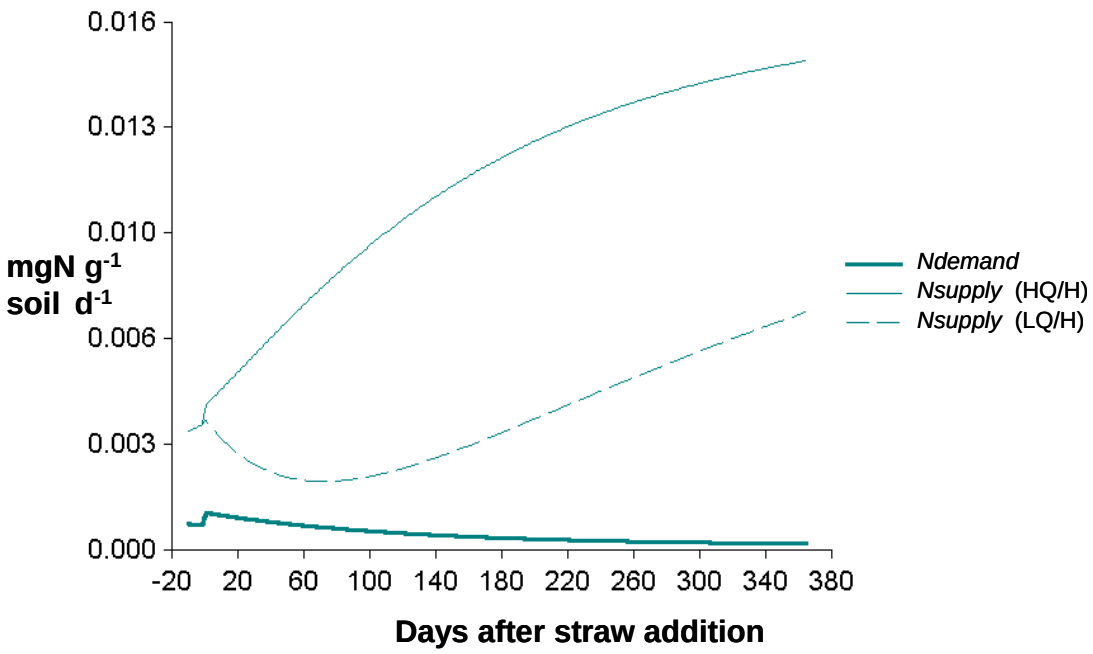

utilisation rate is maintained). It is not explicit that energy is expended in the immobilisation of N (i.e. there are no flows to ***GasC***), but implicitly the energy expended in utilisation of N-deficient substrate enables supplementary N flow from ***Sol***.

Components of gross N mineralisation are shown for contrasting straw additions (i.e. LQ/H and HQ/H scenarios) in Figure 4.14. The relocation flows from ***HFN*** and ***LF2N*** to ***BugN*** and – through microbial mortality – to ***SolN*** from ***BugN*** are proportionally more important in the LQ/H scenario. These flows contribute to a relatively constant background mineralisation rate.

4.3.4. Processes under N limitation

The LQ/XH scenario is described separately since – uniquely amongst the four scenarios – primary substrate C flows became limited through the exhaustion of supplementary N (i.e. ***SolN***). The addition of a large C substrate to the high reactivity ***LF1C*** compartment resulted in an immediate, high demand for supplementary N that could, initially, be met (Figure 4.15.). However, with the rapid depletion of ***SolN*** with no significant diminution of ***LF1C***, the supply of supplementary N became exhausted. However, the value of λ (the limiter) decreased sharply, restoring a balance between the demand for and supply of N through limitation of the substrate C flows (Figure 4.16.). Balance was restored only toward the end of the simulation period ($\lambda = 1$). The impact of limitation on the dominant C-incorporation flow (from ***LF1C*** to ***BugC***) is illustrated in Figure 4.17, and general dynamics of C and N fractions and compartments (for LQ/XH) in Figure 4.19. The balance between *Nsupply* and *Ndemand* is shown for the LQ/H and HQ/H scenarios in Figure 4.13.

Figure 4.14. The relative magnitude of flows contributing to gross N mineralisation in the (a) LQ / H and (b) HQ / H scenarios

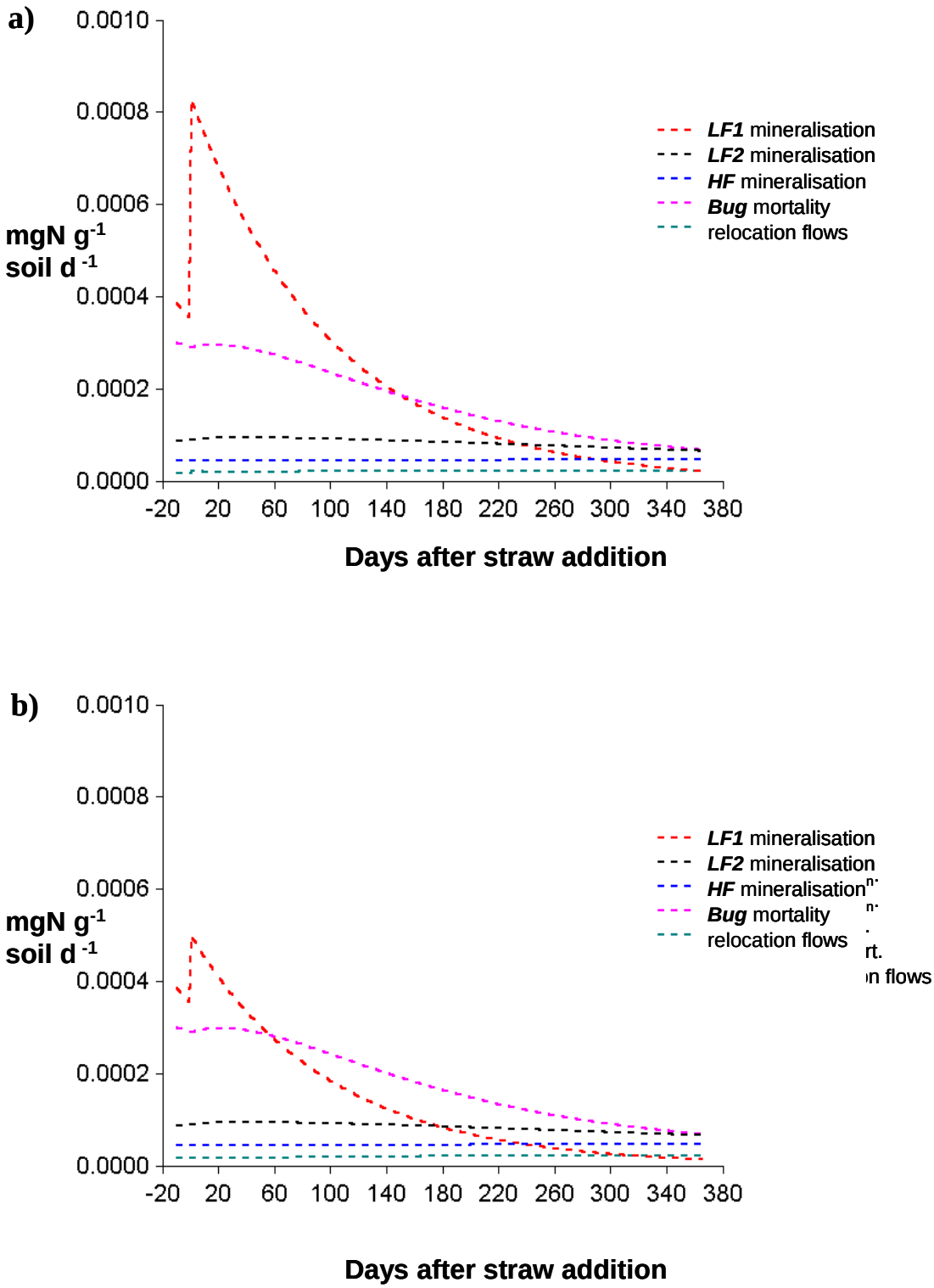

Figure 4.15. The simulated balance between N supply and N demand in the N limiting LQ / XH scenario

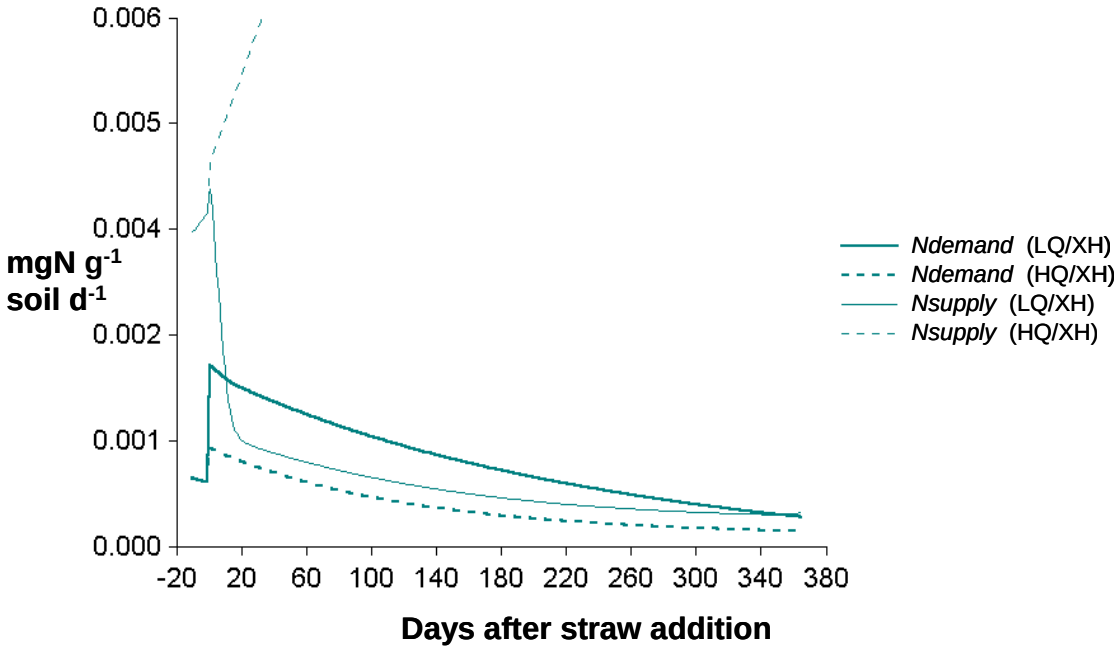

Figure 4.16. The simulated status of the C flow limiter λ for the LQ / XH scenario, calculated as the balance between N supply and N demand

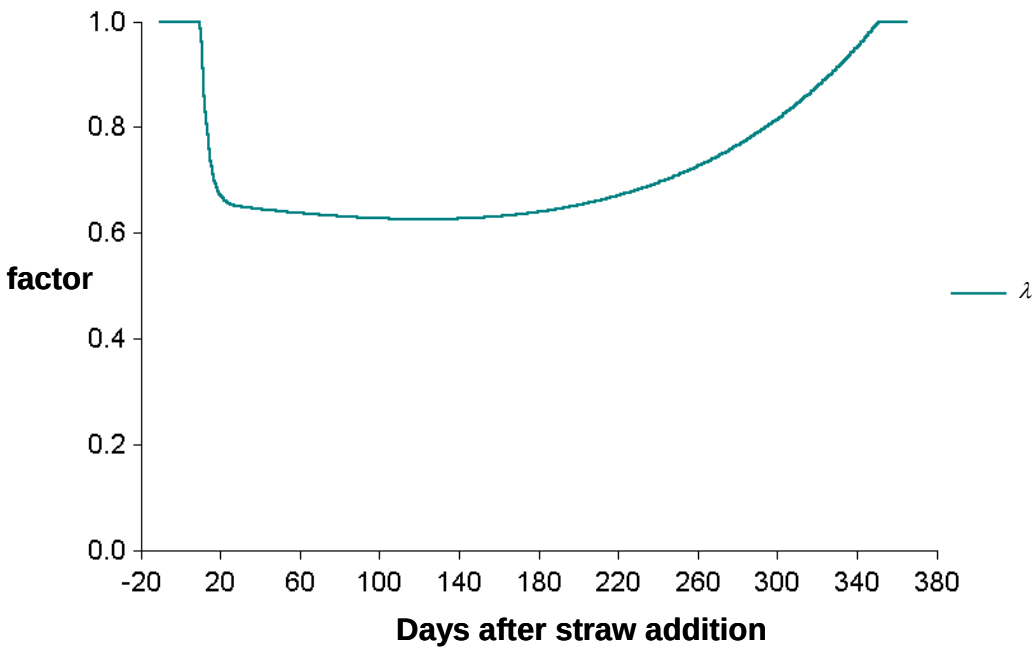

There were three main effects of flow limitation at the system level. Firstly, net N immobilisation occurred for the duration of the simulation (LQ/XH compared against LQ/H in Figure 4.18.). Secondly, a large increase in the C-to-N ratio of the diminishing source compartment resulted from an increase in N acquisition efficiency (Figure 4.20.). This also reflected a general increase in the ratio of CO_2–C production and N mineralisation rates (Figure 4.21.). The initial peak in this ratio reflected the predominance of primary substrate utilisation over the microbial source, and the higher C-to-N ratio of the former. The third main effect of flow limitation was an increase in relocation N flows from substrates with a higher N content.

The decomposition LQ/XH scenario that induced flow limitation was extreme, both in terms of the magnitude and composition of the straw addition. The outcome was also sensitive to the status of model constants and initial values, and thus its true significance cannot be quantified until the model has been parameterised. In the scenarios used in this chapter, the interaction of soil and plants was not accounted for. Representing roots only as a source of ***LF1**** and a sink for ***SolN*** would have been simplistic, since their role in the formation of the INTRA-AGGREGATE fraction (and their contribution to ***Sol****) has not been established. However, the more continuous supply of substrate expected in the field would likely have a strong influence on the outcome.

Although a mechanism for limiting C utilisation when supply of N is short is essential, the mechanism used in the current framework makes certain assumptions about the behaviour of microbial populations. In particular, it is assumed that key

Figure 4.17. The simulated effect of N limitation on C incorporation from ***LF1*** in the LQ / XH scenario

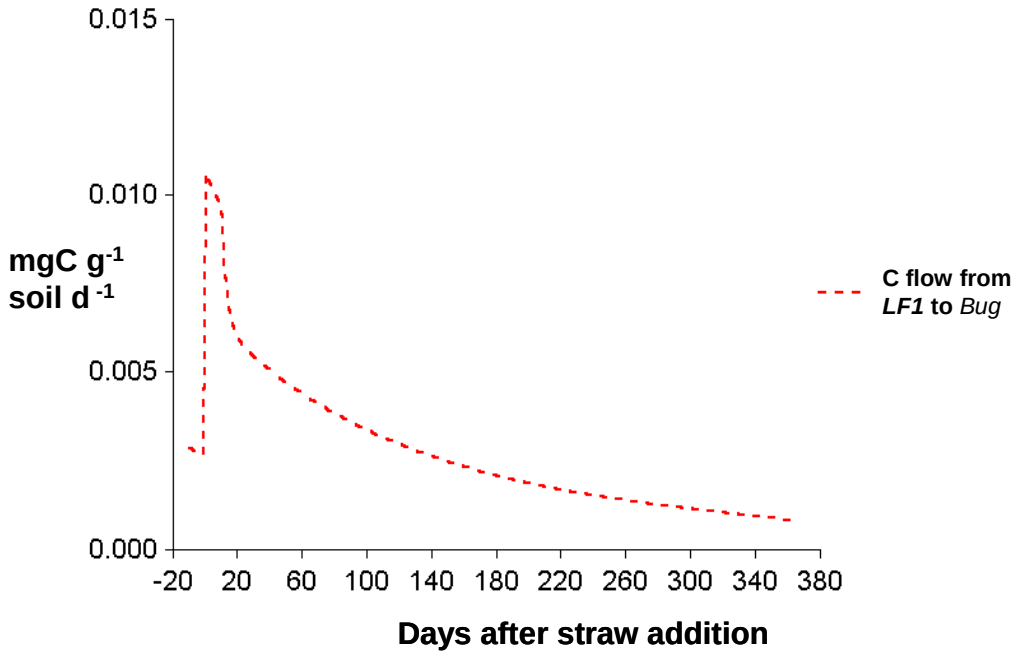

Figure 4.18. Simulated rates of gross N mineralisation and gross N immobilisation in the LQ / XH and LQ / XH scenarios

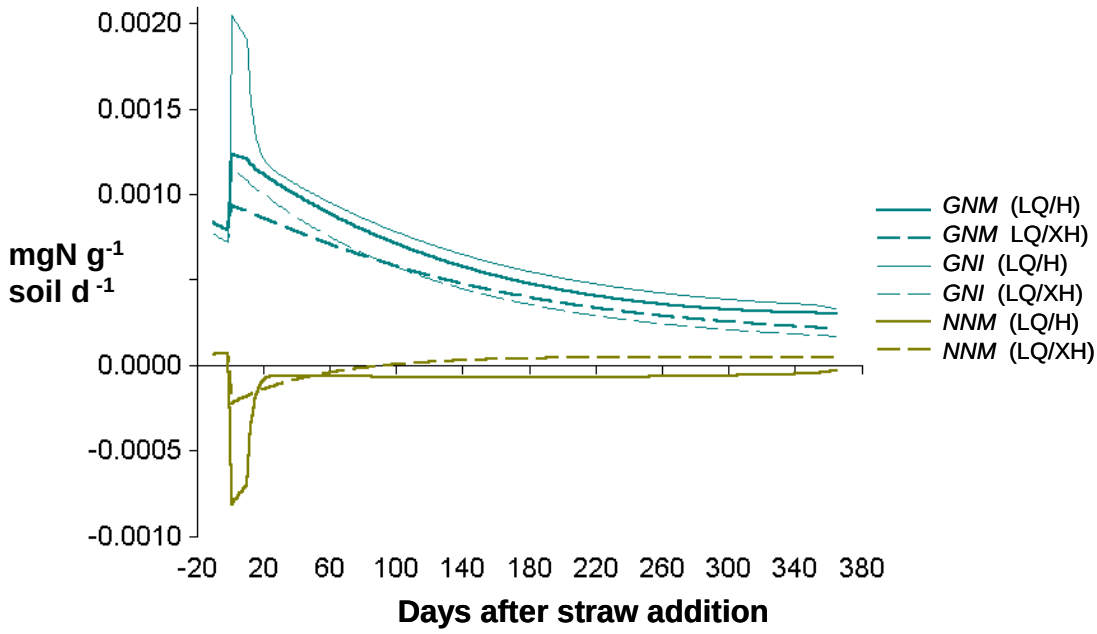

Figure 4.19. Simulated dynamics of (a) C and (b) N under N limitation (LQ / XH)

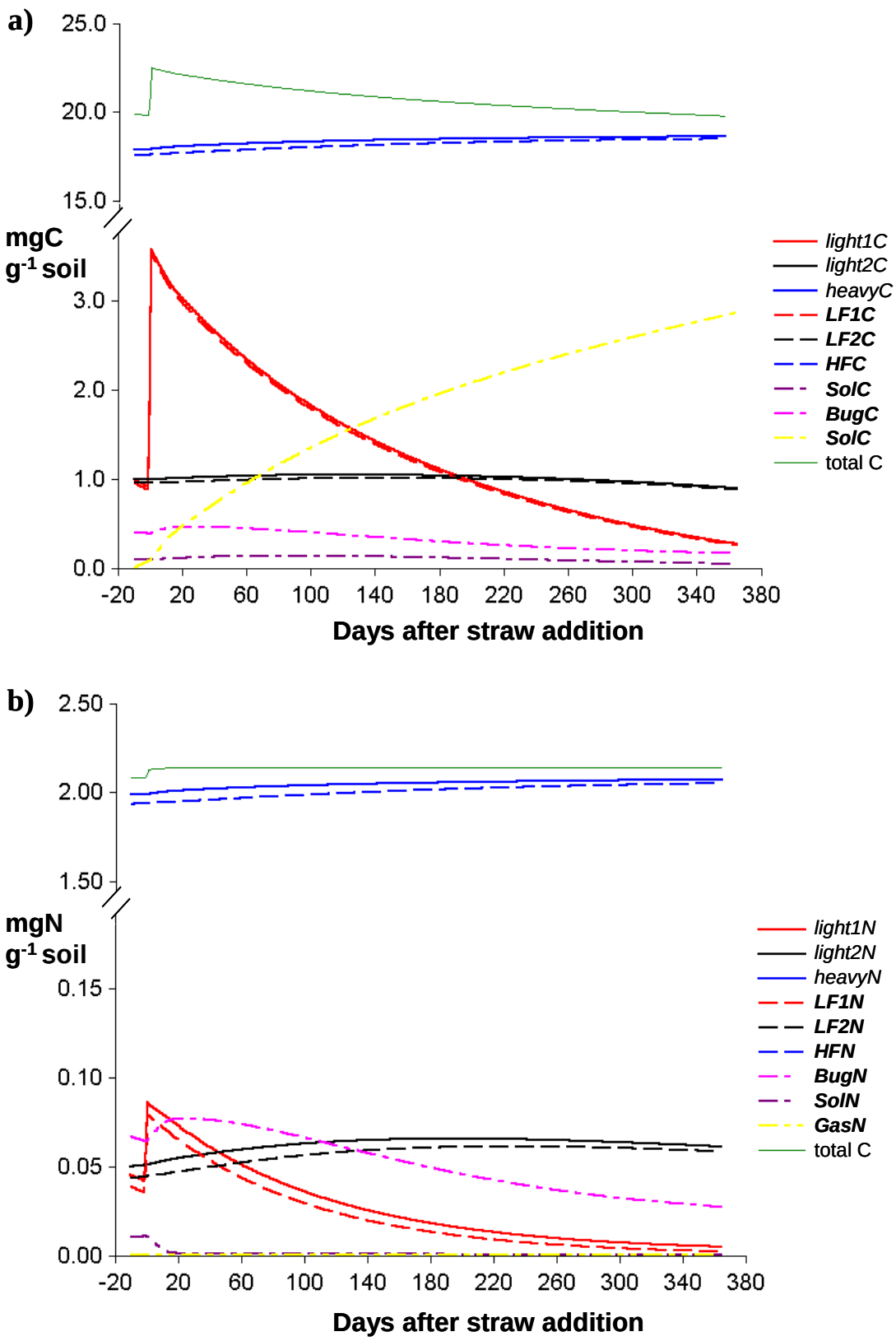

Figure 4.20. Alterations in compartment and fraction C-to-N ratio with N limitation in the LQ / XH scenario

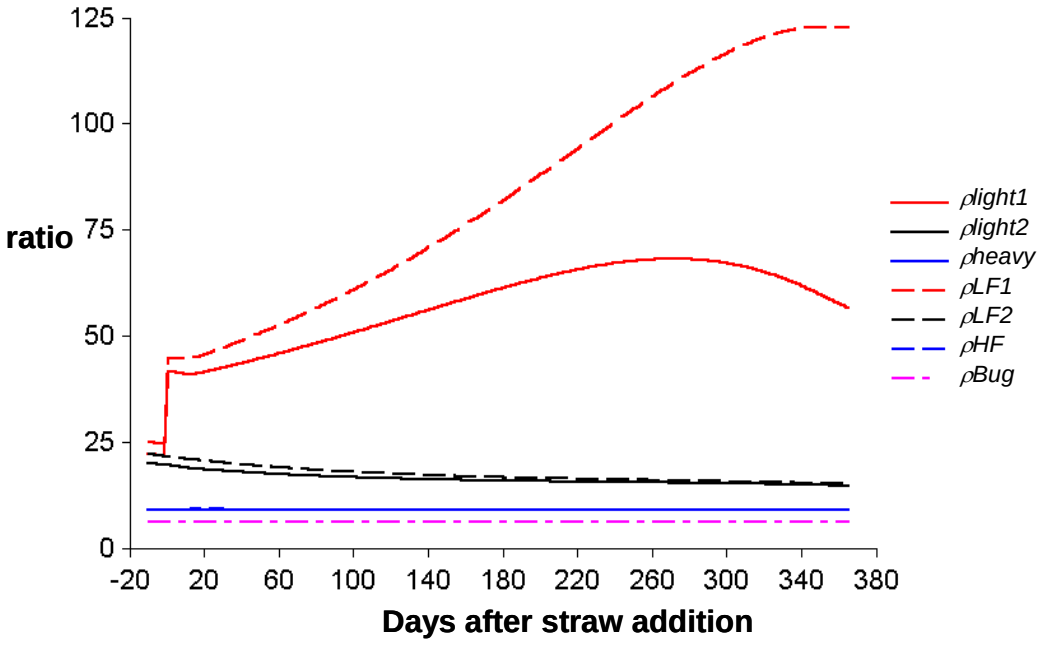

Figure 4.21. The simulated ratio of C utilisation to gross N mineralisation in three contrasting scenarios

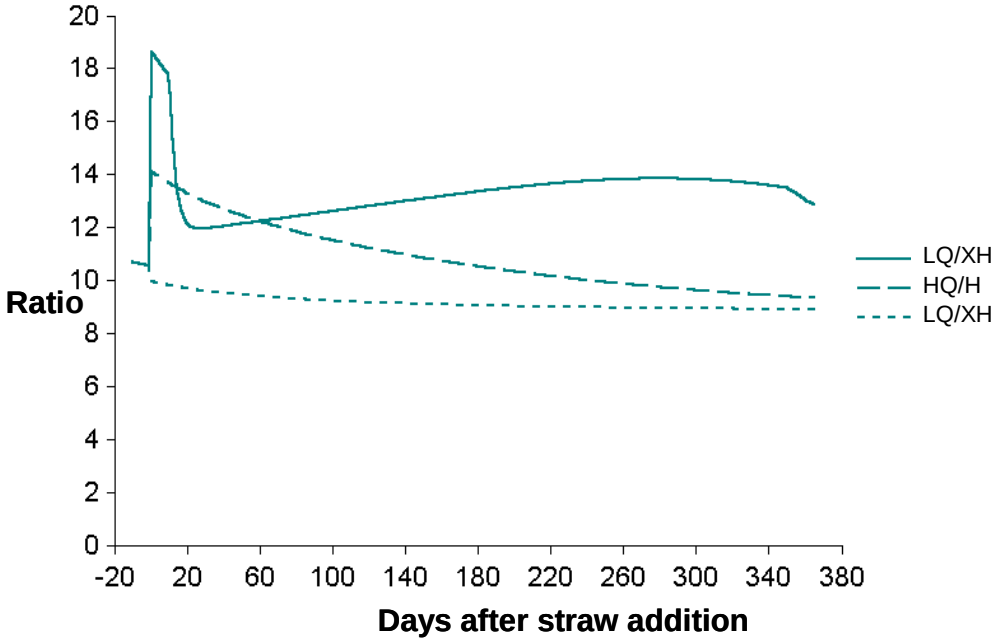

changes in the status of the system (or specific fractions) result in an instantaneous response, a characteristic feature of substrate-orientated models in general. Also, a minimum criterion for the utilisation of substrates (in this case, as is typical, the C-to-N ratio of the substrate) may be simplistic.

4.3.5. Sensitivity of the model to parameter values

The outcome of the sensitivity test with respect to flow limitation in the LQ/XH scenario is shown in Table 4.7. In view of the extreme scenario, N limitation was quite sensitive to ρBug. Also, reducing *kLF1* by 60 % prevented flow limitation. Although only a four-fold increase mitigated the effect through in $SolN_0$ (the overall demand from C incorporation being sufficient to exhaust a considerably greater N supply), field variation in mineral N is high.

The effect of altering parameter values on the C and N balance within specific compartments was examined using the HQ/H scenario. The predicted 35 % decrease in ***LF2C*** in this scenario could be mitigated by increasing the value of $\phi LF2$ from 0·20 to 0·50, effectively increasing the ***LF2C*** component of the relocation flow. The result was a decrease in the proportion of the relocation flow transferred to ***SolC*** ($1-\phi LF2-\phi HF$), except where the source was ***HFC***, with ***SolC*** the sole recipient. However, due to the low value of ρBug, the impact of this change on the recipient compartments of the ***Bug*** relocation flow (also governed by $\phi LF2$ and ϕHF) was significant.

It was not possible to maintain $LF2C_0$ by altering the proportion of flows from ***LF1C*** assigned to relocation flows (i.e. by altering the values of η and α within an

Table 4.7. Threshold parameter values for preventing limitation of C incorporation in the otherwise N-limited scenario of an atypical addition of low quality straw (LQ/XH scenario)

Parameter	Description	Value used for LQ/XH	Non-limiting value
Partitioners			
α	Respration coefficient	0.55	n/e
η	Microbial incorporation coefficient	0.30	0.23
$\phi LF2$	Universal flow partitioner	0.20	n/e
ϕiHF	Universal flow partitioner	0.50	0.25
ρbug	Microbial C-to-N ratio	6.00	8.00
theta	Assimilable ***Sol*** fraction	0.30	n/e
Reactivity constants			
kLF1	Reactivity constant	0.01	0.04
ksol	Reactivity constant	0.03	n/e
kmort	Mortality constant	0.0150	0.0450
Initial values			
$light1C_0$ +	FREE organic matter	0.30	n/e
C input +	Straw input	2.70	1.20
$SolN_0$	Soluble N	0.0100	0.0410
$BugC_0$ +	Microbial biomass	0.40	0.50

\+ with corresponding change in N

n/e = no effect within the constraint range

acceptable range), without also changing $\phi LF2$ and ϕHF. In general terms, an increase in the proportion of C in relocation flows might be required to maintain system C at a specific level with a given level of organic matter input. However, altering these parameters has concomitant impacts on the increase in ***Bug**** (through smaller C incorporation flows), or requires a decrease in the respiration constant (α) to be justified. These changes have a more fundamental (general) impact on the behaviour of the N model, and on gross processes. The sensitivity of the model to C input was tested implicitly through the contrasting incorporation rates encompassed by the scenarios, the XH rate being three times that of H.

4.4. Conclusion

The simulation of flow limitation was important in determining the outcome of the scenarios, and its representation raised a number of issues. In order to establish its true importance and the its mechanistic basis, a detailed *in situ* study of microbial C transformations and associated N flows will be required. Since the interaction of plants will have a major influence on determining N limitation though competition for mineral N and the supply of C substrates as exudates, a parameterised SOM model will need to be integrated into a robust soil–plant system model.

If the initial values used for the model compartments were realistic the reactivity assigned to the input compartment ($kLF1$=0.01 d^{-1}) was too great: ***LF1C*** declined – despite the magnitude of the simulated straw addition – to below the pre-addition level after 55 to 120 days of incorporation. However, in a planted system, continuing inputs below ground would partially offset the decomposition of crop residues and maintain a

minimum quantity of material in the dynamic fraction (such as that reflected in its initial magnitude, in the scenario). Also, climatic effects were excluded from the scenarios (the modifiers were set to 1·0) which, depending on their pattern of their variation relative to the timing of inputs, could significantly alter the outcome.

CHAPTER 5: A PARAMETERISATION DATASET

5.1. Introduction

In a mathematical model describing flows between measurable SOM fractions, the reactivity of the different components can be inferred from data, and then the model used to verifiably predict mineralisation from their measured magnitude and contrasting dynamics. The primary criteria required of modelled SOM fractions were defined in Chapter 2 together with a compatible method for their isolation. On the basis of measured differences in composition (Chapter 3), concepts for the interaction of the fractions were developed, and these translated into a mathematical model in Chapter 4.

The parameters invoked in the model – including the reactivity of the compartments – will be evaluated by optimising against experimental data i.e. matching model output to the measured status of the SOM fractions over time (Chapter 6). The sets of parameter values that provide a given level of agreement are fewer where the number of measurements made on each fraction is greater. The number of apparent solutions is also reduced where the dataset encompasses a larger number of time points, and the simulation period is appropriate to the application. A lower number of solutions will increase the probability of a particular set of values being applicable to other soils or situations, and result in a more robust model. For the three standard fractions, determination of isotope ratio as well as C and N content increases the number of measurements at each time point to 12. The objective of this chapter is to derive experimental data that enables a robust parameterisation of the mathematical model described in Chapter 4.

5.1.1. Obtaining a minimum dataset for model parameterisation

To properly evaluate the reactivity of each fraction and other model parameters, parameterisation data must be obtained from a soil in which all fractions are present and thus all flows extant. Situations in which mineralisation is induced by adding fresh plant debris (e.g. crop residues) are particularly useful since they will, by definition, include flows between active as well as more stable components of SOM. The addition of plant material also facilitates the introduction of isotopic tracers into SOM. As well as increasing the number of measurements that can be obtained from each SOM fraction, tracers provide data that is more challenging to reconcile with model outputs: isotope ratios may be dynamic even when C and N measurements suggest steady-state (Section 1.5.).

Given the value of simultaneous measurements of ^{13}C and ^{15}N as well as C and N, a minimum dataset for model parameterisation may be obtained by adding C_4 plant material enriched in ^{15}N to soil containing only C_3-derived organic matter (using ^{13}C as a tracer at levels of natural abundance). Since the main purpose of the model proposed in Chapter 4 is to predict mineralisation over the short to medium term, accurate determination of the reactivity of more active SOM fractions is particularly important. The intervals at which C, N and their tracers are measured in each fraction should reflect their likely decay kinetics. Since plant roots are likely to have direct and indirect effects on SOM turnover, it is desirable to use unplanted soil in the first instance (further parameterisation with a linked plant model can be undertaken at a later stage). Established relationships linking soil temperature and moisture to microbial activity (and hence SOM turnover) may be incorporated into the model in order to use

parameterisation data generated under field (rather than controlled) conditions. Although a minimum dataset has been proposed, additional experimental measurements offer the possibility of verifying simulation of processes (as the sum of several model flows). Such measurements would include gross N mineralisation (using isotope dilution techniques), and the production of CO_2. The simulated magnitude of the microbial C and N and (potentially) the corresponding tracer compartments can be measured using the fumigation–extraction method.

5.2. Materials and methods

The model variables measured in this experiment are listed in Table 5.1. These provide the minimum dataset identified above and additional independent measurements for verifying process simulation. Isotope tracers for C and N were introduced to pots of unplanted C_3 soil as ^{15}N-labelled maize straw. Four pots were destructively sampled on seven occasions during a 448-day incubation for isolation and analysis of the standard SOM fractions. The duration of the experiment was relevant to crop nutrient supply, and exceeded that required for complete decomposition of fresh plant debris. The dynamics of native SOM and maize residues were compared by simultaneously incubating additional soil pots without added maize as a control.

Equivalent unlabelled maize residues were also incubated to measure gross N mineralisation by isotope dilution (and thus assess process simulation). These estimates are derived from short-term change in isotopic composition of the NH_4^+ pool that results from mineralisation of unlabelled substrate after injection of $^{15}NH_3$. The same

Table 5.1. Variables measured during soil incubation for the purpose of model parameterisation

Model variable	Description	Relevant compartments or flows			
		C	N	^{13}C	^{15}N
Initial values					
light1$_0$*	initial magnitude of FREE organic matter compartments	✓	✓	✓	✓
light2$_0$*	initial magnitude of INTRA-AGGREGATE compartments	✓	✓	✓	✓
heavy$_0$*	initial magnitude of ORGANOMINERAL compartments	✓	✓	✓	✓
Sol$_0$*	initial magnitude of soluble compartments	(✓)*(✓)*		est	est
Bug$_0$*	initial magnitude of microbial biomass compartments	(✓) (✓)		est	est
Gas$_0$*	initial magnitude of gaseous compartments	nom	nom	est	est
Model constants					
ρ bug			✓	-	-
Measurable compartments (dynamic measures)					
*light1**	magnitude of FREE organicatter compartments	✓	✓	✓	✓
*light2**	magnitude of INTRA-AGGREGATE compartments	✓	✓	✓	✓
*heavy**	magnitude of ORGANOMINERAL compartments	✓	✓	✓	✓
*retained**	sum of measured compartments	*	*	*	*
***Sol** **	magnitude of soluble compartments	(✓)*(✓)*		-	-
***Bug** **	magnitude oficrobial biomass compartments	(✓) (✓)		-	-
***Gas** **	magnitude of gaseous compartments	(✓) (✓)		-	-
Measureable processes					
GNM	rate of gross N mineralisation (sum of model flows)	n/a	✓	n/a	n/a
CO2	rate of C mineralisation / CO_2 production (sum of flows)	✓	n/a	n/a	n/a

nom = nominal value assigned
est = estimated / established value used
n/a = not applicable

measurements were also made in the non-amended soil in the model. Other measurements made independently of fractionation included soluble fractions, microbial biomass, and CO_2 production. These measurements do not necessarily equate directly to the modelled variables (Table 5.1.) – soil mineral N for example was measured using a conventional salt extraction procedure whilst ***SolN*** represents N released into NaI during density fractionation.

Due to the number and size of the pots used in the experiment, the soil and added residues (where applicable) were incubated under field conditions. In simulating the measurements the model can account for variations in soil temperature and moisture through their respective rate modifiers (Section 4.2.6.).

5.2.1. Decomposition experiment

5.2.1.1. Preparation of maize residues

Maize plants were grown in the field in two adjacent blocks, separated by a margin, during summer 1996. The first block received a single application of double-labelled ammonium nitrate (11·8 atom% ^{15}N) five days after sowing (equivalent to 200 kgN ha^{-1}). The second received an equivalent rate of non-enriched N. Maize was harvested from both blocks 21 weeks after sowing, with the bulk of the plants cut 20 cm from the base and dried at 80 ºC. However, six plants from the first block were selected at random, pulled by the roots, and divided into various physical components to assess variation in ^{15}N enrichment (Figure 5.1.). The upper and lower stems did not differ significantly in their enrichment, and thus a mixture of the two was chosen for the

incubation. For each block, these components were separated from the harvested plants, and mixed together after chopping into sections 20 to 30 mm long. The chemical composition of the incorporated maize straw is shown in Table 5.2.

5.2.1.2. Soil collection

The soil taken for the incubation was from the same location as the sandy loam used in defining the fractionation procedure in Chapter 2 (see Table 2.1 for soil properties). The sampling was made in the 0 to 23-cm horizon (the plough layer) using spades, and homogenised in the field. The sampling was made in March 1997, and the soil had lain bare since the harvest of winter wheat in September 1996. The bulk density of the sampled horizon was 1·35 g cm^{-3}. The collected soil was immediately sieved to remove stones and coarse organic debris > 6·25 mm diam. The amount of the latter was negligible and not recorded. The incubations were started within five days and without adjustment of soil moisture content.

5.2.1.3. Incorporation and incubation of maize straw

The pot incubation allowed the incorporation of maize straw to be controlled, and variations in its spatial distribution minimised. To provide a physically continuous environment, the pots were sunk into a sand bed. Four replicate pots for each sampling were distributed randomly across the four blocks. The pots had a nominal volume of 7 L (depth 17 cm, max. diam. 26 cm) but were only sunk (and subsequently filled) to a depth of 13 cm, giving a soil volume of 4·86 L. At the measured field density of 1·35 g cm^{-3}, this equated to an oven-dry soil weight of 6·569 kg. Holes in the base of

Table 5.2. Chemical and isotopic composition of the ^{15}N labelled maize straw incorporated into soil for the incubation experiment

Fraction	Content
Isotopic	
C (mg g^{-1})	419.2
N (mg g^{-1})	5.24
C-to-N	80.0
$\delta^{13}C$ (‰)	-12.49
^{15}N (atom%)	5.323
Chemical (mg g^{-1})	
Lignin	41
Cellulose	270
Hemicellulose	290
Water soluble carbohydrate	220
Total ash	50

Figure 5.1. Differential ^{15}N enrichment in components of the maize plants grown for incorporation during the incubation study (upper and lower stems were incorporated)

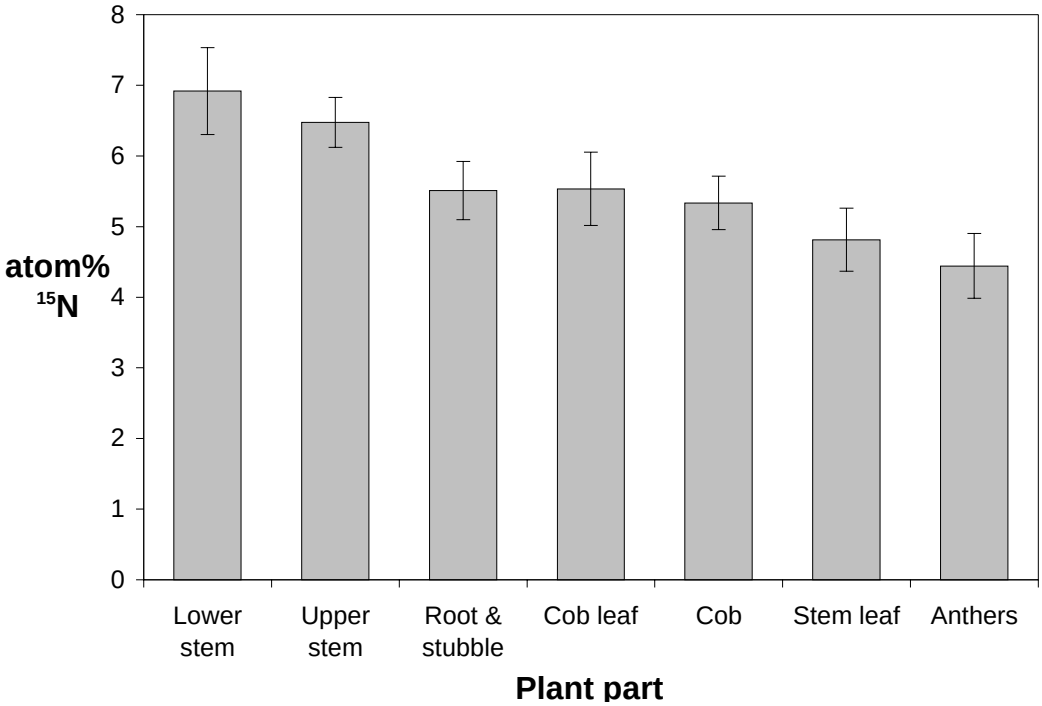

each pot (2·6-cm diam.) allowed free drainage to the sand bed, and a nylon mesh contained the soil.

The rate of maize straw incorporation was equivalent to 3·5 t ha^{-1} dry matter. Pre-weighed samples of soil were mixed thoroughly (where applicable) with maize straw (mixed upper and lower stems, ^{15}N-labelled or unlabelled), and packed into their designated pots. Separate samples of maize straw were taken to establish the precise amount of C, N, ^{13}C and ^{15}N added to the soils (Table 5.3.). There was minimal weed growth during the incubation, and where seedlings appeared they were immediately removed. Temperature in the soil was monitored intermittently so that a correlation could be made with continuous monitoring at the automatic weather station 200 m away.

5.2.2. Measurement of modelled SOM fractions

Eight designated pots were destructively sampled 4, 10, 24, 55, 108, 228 and 448 days after packing, four containing soil with ^{15}N-labelled maize added, and four only soil. Macro-organic matter was removed from the soil in each straw amended pots by sieving at 6·25 mm. The retained material, which comprised lightly decomposed maize, was washed, dried at 80 ºC, and weighed. These samples were subsequently milled to a fine powder and analysed by mass spectrometry (see Section 5.2.2.2.). Sub-samples of the sieved soil were taken for a comparison with summed data from various SOM fractions, and for the determination of microbial biomass and soluble components.

Table 5.3. The calculated effect of maize straw incorporation on the C and N content and isotopic composition of the pre-incubation soil

	Composition of fractions (mg g^{-1})		Change with addition of straw	
	Maize (added)	Soil	Total (mg g^{-1})	Change (%)
C	0.464	7.197	7.661	6.1
N	0.00580	0.57323	0.57903	1.0
^{13}C	0.00515	0.07866	0.08381	6.1
^{15}N	0.000309	0.002104	0.002412	12.8
$\delta^{13}C$ (‰)	-12.49	-27.38	-26.48	3.3
C-to-N	80.1	12.6	13.2	5.4

Additional soil was taken to determine the moisture content of the soil in each pot, by drying overnight at 105 ºC. The remainder was quartered twice to reduce sample bulk, and stored frozen prior to fractionation.

5.2.2.1. Physical fractionation

The stored soils were thawed at 4 ºC for 24 h immediately before physical fractionation using a procedure based on that proposed in Chapter 2 (see Figure 2.4.). However, in this experiment the corresponding fractions from three 15-g sub-samples were combined during isolation. The intention was to minimise variability in the data, the reported mean values and associated errors reflecting the variation in the measurements between replicate pots. The density of the NaI solution used to separate light fractions was set to 1·81 g cm^{-3}, and the recovered solution checked to confirm separation occurred at 1·80 ± 0.005 cm^{-3}. The solution was also cleaned prior to re-use. Finally, an ultrasonic energy input of 750 J g^{-1} was used to disperse aggregates (identical to that described in Chapter 3). The ORGANOMINERAL fraction was divided into size sub-fractions on the basis of particle-size, using a combination of sieving and sedimentation.

Density fractionation

Briefly, 90 ml of NaI solution (of density 1·81 g cm^{-3}, assessed by hydrometer) was added to each of three 250-mL centrifuge bottles, each containing 15-g sub-samples of the thawed soil sample. The contents of the bottles were swirled by hand for 30 s to allow particulate SOM released by the disintegration of macro-aggregates to surface.

Sedimentation of heavy particles was accelerated by centrifuging the bottles for 30 min at 8000 × *g*. The floating FREE fraction was removed from the three bottles (together with NaI solution), and isolated on a single pre-weighed (oven dry) glass fibre filter (Whatman type GF/A, 47 mm diam., 1.6 μm retention). The NaI filtrate was redistributed amongst the three centrifuge bottles, and the filter and retained material thoroughly rinsed with deionised water and dried at 40 ºC before re-weighing. The centrifuge bottles were briefly shaken to disperse the residual pellet, and then the suspensions sonicated for 200 s in an ice bath using a Misonix 2020 ultrasound generator (Misonix Inc., Farmingdale, USA) fitted with a dual horn and twin 19-mm diam. probes. The bottles were centrifuged as before, and the released INTRA-AGGREGATE fractions isolated as for the FREE fraction.

To avoid transfer of soluble C and N (and their tracers) between samples, NaI solution was cleaned before re-use. Approximately 10 g of activated charcoal powder was added to the residual solution (approx. volume 250 mL). The suspension was stirred for 60 min before coarse filtration though 30-cm diam. Whatman No. 2 filter, and repeated vacuum filtration using Whatman type GF/A glass fibre filters (1·6 μm retention) (Whatman International Ltd., Kent).

Particle size separation

The residual ORGANOMINERAL fractions for each sample were combined and sub-divided by particle size. A Fritsch Analysette 3E electromagnetic wet sieving machine (Fritsch GMBH, Idar-Oberstein, Germany) was used to separate stones (2 to 6 mm) and coarse sand (2 mm to 212 μm), fine sand (212 to 53 μm), coarse silt (53

to 25 μm) fractions. ORGANOMINERAL clay in the residual suspension (0 to 2 μm) was progressively separated from ORGANOMINERAL silt (25 to 2 μm) by repeated gravity sedimentation. The suspensions were added to plastic cylinders 35 cm high and 6 cm diam., and their volume made up to 1200 mL. After settling for 17·25 h at 25 ºC, the top 25 cm of each suspension contained only clay size particles.. Thus ORGANOMINERAL clay fractions were accumulated in 1 L centrifuge bottles by repeated sedimentation–centrifugation cycles (2500 × g after flocculation of fine clay with 2·5 mL of 1 M $CaCl_2$). ORGANOMINERAL silt comprised the residual material in the cylinders after complete removal of clay size particles. All ORGANOMINERAL sub-fractions were isolated in pre-weighed plastic Petri dishes by evaporation of excess water at 50 ºC. Stones were discarded after weighing.

5.2.2.2. Mass spectrometry

In preparation for analysis, FREE and INTRA-AGGREGATE fractions and glass fibre filters were cut coarsely into the chamber of a disc mill, and ground for three minutes at 960 rpm. Macro-organic matter, the ORGANOMINERAL sub-fractions, and whole soil sub-samples were also prepared for analysis by disc milling for three minutes.

For the FREE, INTRA-AGGREGATE and macro-organic matter fractions, 15-mg of each sample was analysed. To maintain a close match between the C content of the sample and that of the standard, different amounts of the ORGANOMINERAL sub-fractions were analysed: 15 mg for ORGANOMINERAL clay and ORGANOMINERAL silt, 25 mg for ORGANOMINERAL sand and samples of whole soil. All samples were weighed into pre-cleaned tin capsules and analysed in triplicate using a Tracermass automated nitrogen

and carbon analyser mass spectrometer (ANCA-MS; Europa Scientific Ltd., Cheshire). The % C and % N content of the samples was determined against 5-mg samples of a soil standard (2·38 g C kg^{-1}) and atom% ^{15}N against 5·0 ± 0·5-mg glycericic acid (1·53 % N, 0·3657 atom% ^{15}N, i.e. –0·0005 % excess air). Delta-^{13}C was determined against a wheat-flour standard, calibrated against V-PDB (IAEA, Vienna, Austria). In a minority of cases the coefficient of variation (CV) between triplicates exceeded 3 %. An outlier was excluded where applicable, or the sample re-analysed if the residual CV exceeded 10 %.

5.2.2.3. Calculations

The C and N contents and isotope ratios for FREE and INTRA-AGGREGATE organic matter, macro-organic matter, and ORGANOMINERAL sub-fractions were calculated from the analytical data and recorded sample weights (expressed in mg g^{-1} on a dry soil weight basis, excluding stones). Data for the four replicate pots removed at each sampling time were averaged and standard errors calculated for use in the model.

For ORGANOMINERAL sub-fractions, the gross recovery of C could be simply calculated from the determined C concentration of the sample ($\%C_{samp}$), and its recorded dry weight (W_{samp}). Dividing by the dry weight of fractionated soil ($W_{soil(dry)}$) gave the amount of fraction C in the standard units required by the model i.e. mg g^{-1} (dry soil weight was calculated using the measurements of moisture content, and subtraction of stone weights):

$$C_{frac}\ (\text{mg g}^{-1}) = (\ W_{samp}\ .\ \%C_{samp}\ )\ /\ (100\ .\ W_{soil(dry)}\ )$$

The FREE and INTRA-AGGREGATE fractions contained milled filter material as well as organic matter. To estimate C_{frac} the C content of the glass fibre filters (C_{filt}) was subtracted. The calculation of C_{filt} used the recorded filter weights (W_{filt}) and a mean value for their C content ($\%C_{filt}$). The value of C_{filt} was established as 0·31 %:

$$C_{frac}\ (\text{mg g}^{-1}) = [\ (\ W_{samp}\ .\ \%C_{samp} - W_{filt}\ .\ \%C_{filt}\ )\ ]\ /\ (\ 100\ .\ W_{soil(dry)}\ )$$

The contribution of C in the filters to the isotope ratio measured in these samples ($\delta^{13}C_{samp}$) was also accounted for: the $\delta^{13}C$ value of each fraction ($\delta^{13}C_{frac}$) was calculated using a mean value established for the filters ($\delta^{13}C_{filt}$ = –30·65 ‰):

$$\delta^{13}C_{frac}\ (‰) = (\ \delta^{13}C_{samp}\ .\ C_{samp}\ -\ \delta^{13}C_{filt}\ .\ C_{filt}\ )\ /\ C_{frac}$$

Measurements of $\delta^{13}C$ indicate C isotope ratios relative to a standard. However, the model described in Chapter 4 calculates isotope ratios internally (as γ variables) from the absolute magnitude of corresponding C and ^{13}C variables (Section 4.2.2.). The following equation was thus used to $^{13}C_{frac}$ from C_{frac} and $\delta^{13}C_{frac}$:

$$^{13}C_{frac}\ (\text{mg g}^{-1}) = [\ (\delta^{13}C_{frac}\ .\ 0{\cdot}0112372)\ /\ 1000 + 0{\cdot}0112372\ ]\ .\ C_{frac}$$

The $\delta^{13}C$ data indicate the proportion of C derived from added maize in each analysed fraction:

$$C_{maize}\ (\%\ of\ C) = [\ (\delta^{13}C_{frac} - \delta^{13}C_{control}) / (\delta^{13}C_{maize} - \delta^{13}C_{control})\ ] \cdot 100$$

This calculation can be combined with total C measurements to quantify the amount of maize derived C residing in the different fractions at each sampling time:

$$C_{maize} = [\ C_{maize}\ (\%\ of\ C) \cdot C_{frac}\ ] / 100$$

The N content of the glass fibre filters was negligible, so the N content of FREE and INTRA-AGGREGATE fractions was calculated simply as.

$$N_{frac}\ (mg\ g^{-1}) = (W_{samp} \cdot \%N_{samp} - W_{filt} \cdot \%N_{filt}) / (100 \cdot W_{soil\ (dry)})$$

The absolute ^{15}N content of the fractions was calculated from the concentrations of ^{15}N (atom%) and the N data:

$$^{15}N_{frac}\ (mg\ g^{-1}) = [^{15}N\ (atom\ \%)\ ] \cdot N_{frac} / 100$$

Macro-organic matter

The standardised yield of C, N, ^{13}C and ^{15}N in macro-organic matter (mg g^{-1}) was based on the yield from the whole pot. The mean stone content (0·0198 mg g^{-1}) measured in the fractionated sub-samples (during size separation) was used to correct the dry soil weight for the whole pots.

Consolidation of sub-fraction data

Although its dimension required prior separation, macro-organic matter is compatible with the defining characteristics of FREE organic matter using the standard method (i.e. density < 1·80 cm^{-3}). Thus the standardised C, N, ^{13}C and ^{15}N contents of these fractions was consolidated with the FREE organic matter data (before calculation of mean values and standard errors).

The model features a single compartment to represent all ORGANOMINERAL sub-fractions. Thus although means (and standard errors) are reported for the sub-fractions, equivalent statistics were also calculated for the composite fraction. Certain sub-fractions (specifically ORGANOMINERAL coarse sand and fine sand) contained insufficient C for determination of $\delta^{13}C$, even though the concentration of total C was quantifiable. For these samples the ^{13}C content was summed only for the coarse silt-, fine silt- and clay-size fractions, and $\delta^{13}C$ determined on the basis of their corresponding C contents.

Whole soil analysis

Samples of whole soils were analysed for comparison with summed data for the fractions. The mean stone content used in calculation of the macro organic matter yield (above) was used.

Estimation of NaI-soluble fraction

To estimate the magnitude of the SOM fraction soluble in NaI solution (which was not directly measured in this experiment), the C and N content of the sum of fractions was subtracted from the mean value for the corresponding whole soil sample.

5.2.3. Independent measurement of other pools and processes

5.2.3.1. Gross N mineralisation

Independent measurements of gross N mineralisation were made on Day 3, 9, 23, 52, 107, 227 (i.e. immediately prior to the first six samplings for SOM fractionation). On each sampling occasion two steel sleeves (60-mm diam.) were driven to the bottom of four designated pots containing unlabelled maize straw, and four of the pots containing non-amended soil. The NH_4^+ pool within each sleeve was homogeneously labelled by introducing an air–$^{15}NH_3$ mixture using a custom built injector (Murphy *et al.* 1999). Enriching the $^{15}NH_4^+$ pool using gas avoids artificial stimulation of mineralisation that results from addition of solution (Murphy *et al.* 1997). Gross N mineralisation was calculated from the difference in magnitude and enrichment of NH_4^+ in the two sleeves 18 and 90 h after injection. Extraction was performed immediately after removal of the cores using 0.5 *M* K_2SO_4, and NH_4^+ determined by continuous colourimetric flow analysis using a Skalar SAN^{PLUS} System (Skalar Analytical BV, Breda, The Netherlands). The ^{15}N enrichment of extracted NH_4 was measured using the diffusion method described by Brooks *et al*. (1989) and a Europa Integra mass spectrometer (Europa Scientific Ltd., Cheshire).

5.2.3.2. CO_2 production

The rate of CO_2 production in maize- and non-amended soil was estimated on 18 occasions during the experiment. Sub-samples from the relevant pots (cores 50 mm diam., 40 mm deep) were incubated in Kilner jars planted in the sand bed over three day periods. Vials containing 10 mL 0·5 *M* NaOH were placed in the jars to trap CO_2. The trapped C was estimated by autotitration with 0·5 *M* HCl (Tinsley *et al.* 1951).

5.2.3.3. Soluble C and mineral N

Total mineral N (NH_4^+ and NO_3^-) was determined in the K_2SO_4 extracts taken for calculation of gross N mineralisation using the Skalar SAN ^{PLUS} System (Skalar Analytical BV, Breda, The Netherlands) (see Section 5.2.3.1.). Soluble organic C was measured using separate extracts (required for estimation of microbial biomass, see below). An additional extraction was made at Day 0, immediately after packing the soil pots. The isotope ratios in the extracts were not determined.

5.2.3.4. Microbial C and N

Microbial C and N was measured using the fumigation–extraction procedure (Brookes *et al.* 1985; Wu *et al.* 1990). Briefly, microbial C and N was taken to be 2·22 times the difference in total organic C or N before and after chloroform fumigation. Separate extractions of 60-g soil sub-samples were made before and after 24-h fumigation. Soluble organic N was measured as NO_3^- after persulphate oxidation of the

extracts (Cabrera and Beare 1993). Total organic C was measured by UV-persulphate oxidation (Wu *et al.* 1990). As for soluble C and mineral N, an initial measurement was made at Day 0.

5.2.4. Statistical analysis

The measurements of C, N, and ^{15}N in FREE, INTRA-AGGREGATE and ORGANOMINERAL organic matter (i.e. standard fractions), as well as C-to-N ratio, $\delta^{13}C$ and ^{15}N atom%, were analysed using Genstat 5 Version 4.1 (NAG Ltd., Oxford) and the ANOVA procedure (Payne *et al.* 1993). Each fraction was treated as separate analysis, and differences considered significant where $P < 0{\cdot}001$.

5.3. Results and discussion

The main purpose of the maize addition was to stimulate mineralisation activity, and a response in the SOM fractions, the measurement of which would provide sufficient constraint to parameterise the model (and provide independent measurements to assess its process simulation). Measurements made in the non-amended (control) soil are discussed in detail, however, due to the contrasting behaviour of native and added organic matter. The dynamics of the fractions are discussed in the context of process and other independent measurements, which showed similar rates of gross N mineralisation in maize- and non-amended soil, and only short-term differences in CO_2 production (see Figures 5.9. and 5.11.).

5.3.1. Recovery of mass

FREE and INTRA-AGGREGATE fractions comprise mineral particles, material derived from the filters and residual NaI, as well as organic particles. The fraction weight was therefore not well correlated with C content (Figure 5.2.). It seemed likely that the weight of recovered light fraction was determined largely by variable co-recovery of dense mineral particles. There was a greater concentration of organic matter in the INTRA-AGGREGATE fraction than the FREE. The net recovery of mass in fractionation (sum fraction weight) was 99·1 ± 1·2 %. The ORGANOMINERAL sub-fractions comprised mainly sand-size particles. The distribution between fine- and coarse-sand sub-fractions was irregular up to Day 56 in both control and maize-amended soils (Tables 5.5.a and 5.5.b), fine sand increasing at the expense of coarse sand. The reason for this effect is not clear, but may reflect the perturbation of physical conditions in the soil with impacts on soil structure and stable aggregation (there were analogous impacts on the INTRA-AGGREGATE fraction).

5.3.2. Dynamics of C and N

At the beginning of the incubation FREE and INTRA-AGGREGATE organic matter in non-amended soil accounted for 2.14 and 7.62 % of total soil C respectively (Table 5.4.b; see also Figure 5.3.). That INTRA-AGGREGATE accounted for more C than the FREE was not surprising, since the soil had been bare for six months at the time of sampling.

The addition of maize straw had a significant impact on the subsequent dynamics of FREE organic matter C ($P < 0.001$). However, the amount of maize-derived

Figure 5.2. The weak correspondence between the mass and C content of light fractions recovered from soil during a 64-week incubation with and without straw

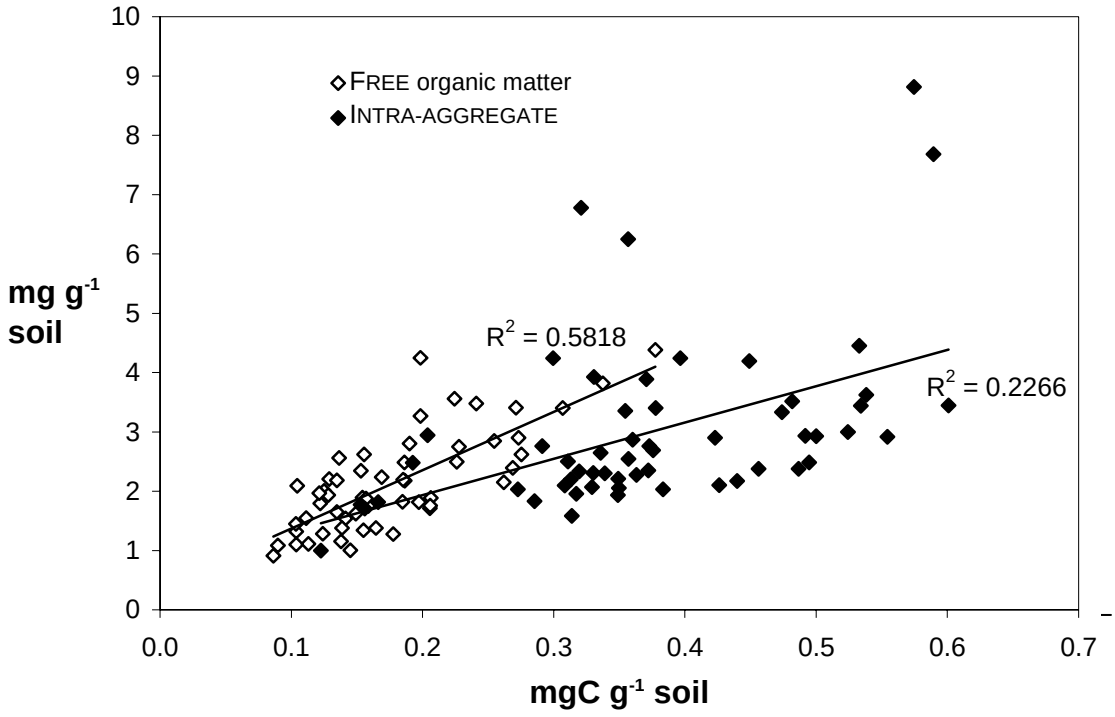

Table 5.4.a Analysis of the standard SOM fractions and organomineral sub-fractions isolated from maize-amended soils during incubation: (i) C content (ii) mass and (iii) C enrichment factor

(i)

Day	4		10		24		55		108		228		448	
n=4	mean	s.e.	mean	s.e.	mean	s.e.	mean	s.e.	mean	s.e.	mean	s.e.	mean	s.e.
	mgC g^{-1}													
FREE organic matter	0.597	0.012	0.570	0.050	0.562	0.011	0.456	0.048	0.274	0.038	0.214	0.019	0.144	0.028
INTRA-AGGREGATE	0.510	0.015	0.474	0.037	0.368	0.005	0.505	0.037	0.370	0.044	0.324	0.006	0.249	0.052
Coarse sand (2mm-212μm)	0.318	0.040	0.327	0.014	0.309	0.032	0.291	0.017	0.314	0.024	0.255	0.024	0.212	0.037
Fine sand (212-53μm)	0.407	0.031	0.390	0.015	0.486	0.019	0.452	0.015	0.484	0.012	0.450	0.011	0.385	0.048
Coarse silt (53-25μm)	0.340	0.008	0.373	0.009	0.376	0.058	0.338	0.006	0.374	0.008	0.344	0.004	0.335	0.006
Fine silt (25-2μm)	1.666	0.046	1.487	0.126	1.813	0.155	1.779	0.016	1.708	0.014	1.529	0.027	1.704	0.104
Clay (2-0μm)	2.622	0.087	2.648	0.191	2.577	0.179	2.902	0.022	2.671	0.054	2.767	0.038	2.700	0.032
ORGANOMINERAL	5.352	0.088	5.225	0.277	5.560	0.342	5.761	0.031	5.551	0.095	5.345	0.031	5.282	0.221
Sum of fractions	6.460	0.063	6.268	0.279	6.491	0.344	6.722	0.073	6.195	0.132	5.883	0.049	5.676	0.144
Whole soil	7.826	0.166	7.698	0.149	7.719	0.118	7.551	0.152	7.179	0.172	7.057	0.281	5.457	0.371

(ii)

Day	4		10		24		55		108		228		448	
n=4	mean	s.e.	mean	s.e.	mean	s.e.	mean	s.e.	mean	s.e.	mean	s.e.	mean	s.e.
	mg g^{-1}													
ORGANOMINERAL sub-fractions														
Coarse sand (2mm-212μm)	395	17.2	391	4.7	350	13.2	348	13.5	332	7.9	337	5.1	340	6.5
Fine sand (212-53μm)	278	15.4	289	7.7	324	13.0	343	8.1	352	8.5	346	4.3	348	5.0
Coarse silt (53-25μm)	64	0.3	64	0.6	61	8.9	62	0.6	64	1.2	64	1.2	60	2.6
Fine silt (25-2μm)	149	0.2	143	1.6	155	2.5	154	1.4	152	1.4	142	3.5	151	4.8
Clay (2-0μm)	95	0.9	93	1.0	89	1.2	94	0.7	90	1.2	91	1.1	88	0.9

(iii)

Day	4	10	24	55	108	228	448
	mean C enrichment factor						
ORGANOMINERAL sub-fractions							
Coarse sand (2mm-212μm)	0.13	0.13	0.18	0.17	0.20	0.19	0.21
Fine sand (212-53μm)	0.16	0.17	0.15	0.13	0.15	0.14	0.18
Coarse silt (53-25μm)	3.31	3.00	3.83	3.80	3.72	3.40	5.22
Fine silt (25-2μm)	2.25	2.40	2.16	2.50	2.45	2.75	3.27
Clay (2-0μm)	7.19	7.29	8.11	8.13	8.62	8.31	10.98

Table 5.4.b Analysis of the standard SOM fractions and organomineral sub-fractions isolated from non-amended soils during incubation: (i) C content (ii) mass and (iii) C enrichment factor

(i)

Day	4		10		24		55		108		228		448	
n=4	mean	s.e.	mean	s.e.	mean	s.e.	mean	s.e.	mean	s.e.	mean	s.e.	mean	s.e.
	mgC g^{-1}													
FREE organic matter	0.154	0.009	0.155	0.035	0.203	0.032	0.189	0.029	0.150	0.014	0.157	0.020	0.116	0.017
INTRA-AGGREGATE	0.549	0.014	0.356	0.026	0.352	0.032	0.387	0.032	0.312	0.008	0.342	0.014	0.169	0.019
Coarse sand (2mm-72mm)	0.370	0.052	0.464	0.072	0.411	0.070	0.337	0.049	0.259	0.014	0.249	0.013	0.253	0.020
Fine sand (72-53mm)	0.505	0.029	0.479	0.014	0.457	0.046	0.485	0.026	0.477	0.032	0.381	0.005	0.448	0.037
Coarse silt (53-11mm)	0.351	0.014	0.347	0.016	0.352	0.006	0.367	0.002	0.348	0.004	0.336	0.005	0.361	0.017
Fine silt (11-2mm)	1.872	0.204	1.758	0.031	1.755	0.040	1.557	0.026	1.604	0.023	1.584	0.038	1.572	0.048
Clay (2-0μm)	3.025	0.045	2.873	0.088	2.807	0.099	2.910	0.042	2.935	0.017	2.683	0.022	2.453	0.007
Organomineral	6.123	0.233	5.921	0.091	5.783	0.060	5.654	0.116	5.623	0.049	5.233	0.057	5.086	0.043
Sum of fractions	6.826	0.220	6.432	0.055	6.338	0.080	6.230	0.094	6.086	0.040	5.733	0.075	5.372	0.044
Whole soil	7.197	0.161	7.029	0.379	6.914	0.379	6.805	0.229	7.019	0.244	7.105	0.181	5.860	0.684

(ii)

	4		10		24		55		108		228		448	
n=4	mean	s.e.	mean	s.e.	mean	s.e.	mean	s.e.	mean	s.e.	mean	s.e.	mean	s.e.
	mg g^{-1}													
ORGANOMINERAL sub-fractions														
Coarse sand (2mm-212μm)	364	2.4	395	7.7	404	18.4	336	9.4	340	14.1	345	17.9	336	7.1
Fine sand (212-53μm)	314	5.8	293	7.2	292	17.9	346	8.4	344	12.0	341	13.7	347	10.6
Coarse silt (53-25μm)	63	1.3	64	0.8	61	1.1	66	0.6	65	0.6	65	1.1	64	0.9
Fine silt (25-2μm)	147	10.2	149	1.1	149	1.1	147	7.6	149	0.5	150	1.2	146	1.8
Clay (2-0μm)	92	1.6	90	1.4	87	2.5	91	0.5	92	0.5	91	0.5	88	0.8

(iii)

	4	10	24	55	108	228	448
	mean C enrichment factor						
ORGANOMINERAL sub-fractions							
Coarse sand (2mm-212μm)	0.19	0.17	0.16	0.21	0.20	0.16	0.23
Fine sand (212-53μm)	0.16	0.17	0.17	0.16	0.14	0.14	0.18
Coarse silt (53-25μm)	4.16	3.93	4.13	3.48	3.54	3.43	4.20
Fine silt (25-2μm)	2.85	2.75	2.73	2.91	2.80	2.51	2.87
Clay (2-0μm)	9.23	9.39	9.57	9.11	8.70	8.08	9.82

C in FREE organic matter at Day 4 (the first sampling) was only 70 % of that added (from Tables 5.4.a and 5.4.b; see also Figure 5.3.). The rapid disappearance of maize-derived C could be attributed to a limitation of the fractionation method i.e. incomplete recovery. However, the same four-day period also showed a large peak in CO_2 production (Figure 5.11.) and a sharp increase in microbial C (Figure 5.12.). These observations are consistent with the rapid utilisation of soluble C and rapid fungal growth, although the mean microbial C-to-N remained within the bacterial range. The high water soluble carbohydrate content of the maize straw (22 %, see Table 5.2.) would support this interpretation. Possibly due to the efficiency of utilisation, the peak in soluble soil C (Figure 5.13.) was small. These general patterns of decomposition will be difficult to reconcile, however, with the proposed model framework (Chapter 4) which assumes organic inputs occur solely to a FREE organic matter compartment of fixed reactivity.

There was a corresponding significant difference ($P < 0.001$) in the dynamics of N in FREE organic matter during the incubation, irrespective of whether maize straw was added. Contrary to the trend in FREE organic matter C, the maize amended soil displayed an initial decrease in FREE organic matter N, rapidly followed by a small increase (Figure 5.5.). It is possible that this reflected the balance between mineralisation and immobilisation activity associated with the maize substrate, the maize providing a good source of C deficient in N (supported by the tracer data, see below). There was only a small increase in the total microbial N content of the maize amended soil, however, and no significant difference when compared to the control soil.

It would be expected that the rapid drying of the soil in the weeks immediately following maize incorporation would have had a major impact on decomposition dynamics (see Figure 6.4.). The effect was indeed apparent in both declining CO_2 production and the size of the microbial C pool during the second week of incubation (Figures 5.11. and 5.12.). However, the decline in the amount of maize-derived C in FREE organic mater (Figure 5.3.) continued (to 40 % of that added by Day 55; Table 5.4a and Table 5.4.b), whilst net and gross rates of N mineralisation increased (Figures 5.9. and 5.14.). The mean rates of gross N mineralisation were equal in the maize amended and control soil, and probably resulted from increasing temperature (Figure 5.10.). Alternatively, there may have been some residual response to the effects of soil disturbance associated with sieving and packing of the soil pots for incubation. The apparently greater increase in soil mineral N in non-amended soil suggested continuing N immobilisation, although this was not apparent in the microbial N data.

Subsequent peaks in CO_2 production were attributable largely to drying and wetting cycles, and affected maize and non-amended soils similarly. With the initial re-wetting, microbial C-to-N increased concomitant with an increase in CO_2 production. Maize C continued to decline exponentially for the remainder of the incubation. That this appeared to occur largely irrespective of the external conditions (in contrast to rates of CO_2 production), suggested some physical transfer of organic matter occurred i.e. involving aggregation.

In the experiment as a whole, the most striking observations was the apparent stability of the native FREE organic matter: the C content of FREE organic matter in non-amended soil decreased by only 25 % during the incubation whilst almost all that added

as maize appeared was mineralised or transferred. There was a corresponding constancy in the native FREE organic matter N (C-to-N ≈ 20) A similar distinction between the behaviour of native and added SOM was seen by Magid *et al.* (1997) in their field study of light fractions following incorporation of oilseed rape straw. It is likely to prove problematic in fitting this data to the proposed model, which assumes fixed reactivity within fractions.

The C and N content of the INTRA-AGGREGATE fraction declined significantly during the incubation (Figures 5.3. and 5.5.). Importantly, this decline occurred irrespective of whether maize was added to the soil. This was consistent with the finding in Chapter 3 that the composition of the INTRA-AGGREGATE fraction is more homogeneous than that of the FREE. The decline in INTRA-AGGREGATE organic matter also suggests that the reactivity of this fraction is less than that of new FREE organic matter. The addition of maize did have, however, a significant effect on the C-to-N ratio of this fraction (Figure 5.8.). This may reflect the gradual transfer of recently added organic matter to the physical location that distinguishes the FREE and INTRA-AGGREGATE fractions. The general trend toward a higher C-to-N at the beginning of the incubation is consistent with this view. Initial variations in the magnitude of INTRA-AGGREGATE fraction may have been influenced by the disturbance of soil structure in establishing the experiment (the same influences affecting the yield of ORGANOMINERAL fine- and coarse-sand sub-fractions; Table 5.4.a and 5.4.b). Overall, the INTRA-AGGREGATE fraction was appreciably more dynamic than anticipated, but did not display the dichotomy in reactivity apparent in the FREE. Also, since the dynamics of this fraction were not significantly affected by the addition of maize straw, it may be assumed that it is influenced more by past additions of organic matter than new.

The ANOVA analysis showed no significant effect of time or maize addition on C, N or C-to-N ratio in the ORGANOMINERAL fraction. There were differences apparent in the yields of C and N between the ORGANOMINERAL sub-fractions. However these related more to variations in the yield of the different size classes rather than their composition (Table 5.4.a and 5.4.b). The C enrichment factors for ORGANOMINERAL sub-fractions (their C content relative to those of whole soil) showed the trend established for particle-size fractions (Christensen 1996a). ORGANOMINERAL clay displayed an enrichment factor of 5·3, whilst the sand (> 53 μm) fractions) (account for 69·1 % of soil weight) were relatively depleted in C (Tables 5.4.a and 5.4.b).

The standard fractions accounted for 80.7 to 104.0 % of the C measured in the sub-samples of whole soil. Estimation of NaI-soluble C and N by difference produced generally negative values in the latter stages of the incubation, and was not a reliable method for its estimation.

5.3.3. Dynamics of isotope tracers

Isotope tracers can produce discernible activity in SOM fractions that are at or close to steady state or turning over slowly, with relatively minor inputs of organic matter. This is potentially useful in model parameterisation. However, the major assumption in calculations based on isotope ratios (and SOM models simulating tracers) is that the recipient fractions are not only homogeneous in reactivity, but that the reactivity of incoming (i.e. labelled) material is comparable. It is also assumed that the labelled substrate is homogeneously enriched in the tracer and that isotopic

discrimination is not significant. An inability to reconcile the dynamics of C and N and their respective tracers will question these assumptions.

The decline of $\delta^{13}C$ in FREE organic matter after addition of maize straw (in the absence of any further input of substrates) confirmed preferential utilisation of the maize derived component (Figure 5.4.). Providing the background enrichment of SOM is known, estimating the proportion of maize-derived C from $\delta^{13}C$ data is straightforward. Calculated in this way, the turnover of the maize component was somewhat slower than suggested by the C data (a near-linear decrease from 70 % of total FREE organic matter C at Day 4 to 6 % after 448 days). This difference may indicate that certain chemical fractions within maize straw are more degradable, and / or that the isotopic composition of C in these fractions differs from the mean for the incorporated maize straw ($\delta^{13}C = -12.49$ ‰) (Schweizer *et al.* 1999). This aspect further complicates quantitative interpretation of the tracer data. Neither the INTRA-AGGREGATE or ORGANOMINERAL fractions showed a significant difference in $\delta^{13}C$ (($P < 0.001$), although the mean value for the INTRA-AGGREGATE increased linearly by 1·3 ‰ over the duration of the incubation ($P = 0.003$). This suggested that organic matter was incorporated into stable aggregates on a seasonal time scale and, if the figure is accurate, that 9 % of the C added in maize straw was incorporated over 448 days.

The mean addition of ^{15}N in maize residue was approx. 13 % of that present in the pre-incubation soil at natural abundance, and 13·4 times that present in native FREE organic matter (Table 5.3.). At Day 4 approx. 80 % of the ^{15}N added was recovered in FREE organic matter. The subsequent decline in enrichment was exponential (Figure 5.6.), which is not compatible with the assumption of constant reactivity. The

Figure 5.3. Dynamics of C in the standard SOM fractions after addition of maize straw (solid lines) compared to those in non-amended soil (dashed lines). Data for the ORGANOMINERAL fraction are plotted on the secondary axis

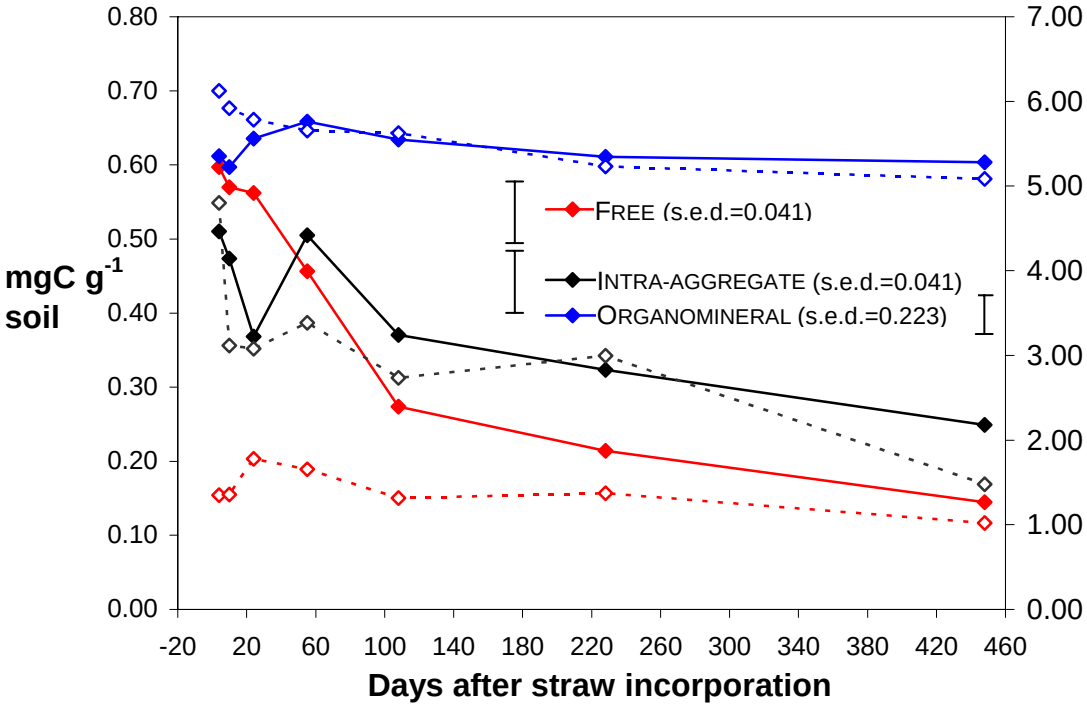

Figure 5.4. Dynamics of $\delta^{13}C$ in the standard SOM fractions after addition of maize straw (solid lines) compared to those in non-amended soil (dashed lines). Data for the ORGANOMINERAL fraction are plotted on the secondary axis

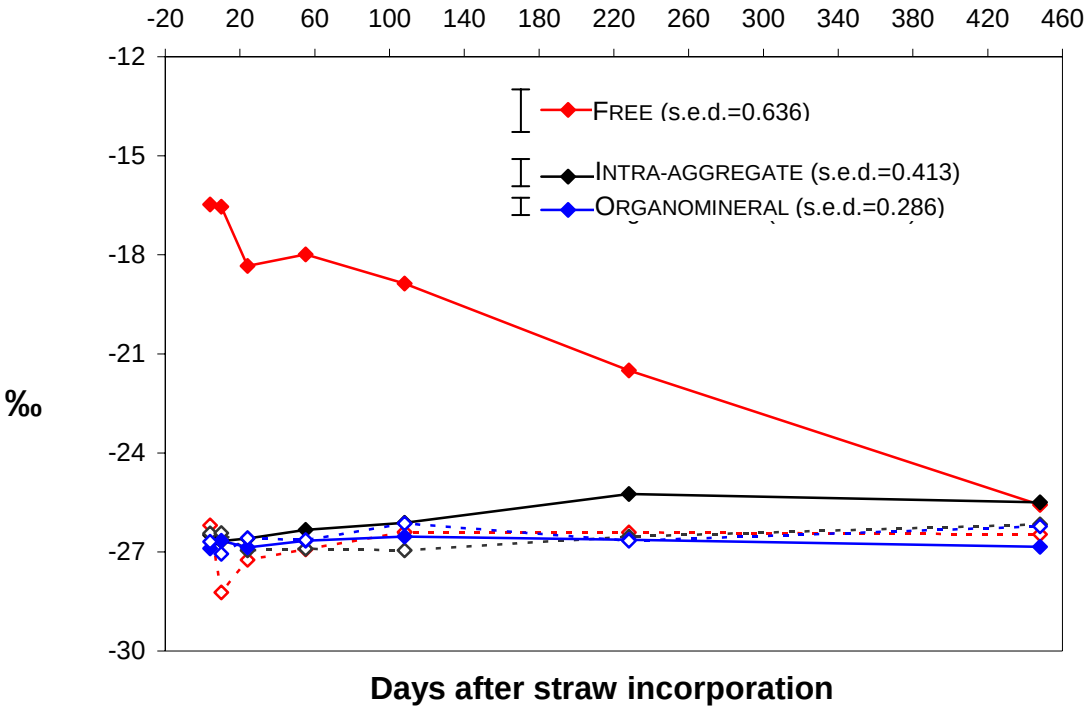

Figure 5.5. Dynamics of N in the standard SOM fractions after addition of maize straw (solid lines) compared to that in non-amended soil (dashed lines). Data for the ORGANOMINERAL fraction are plotted on the secondary axis

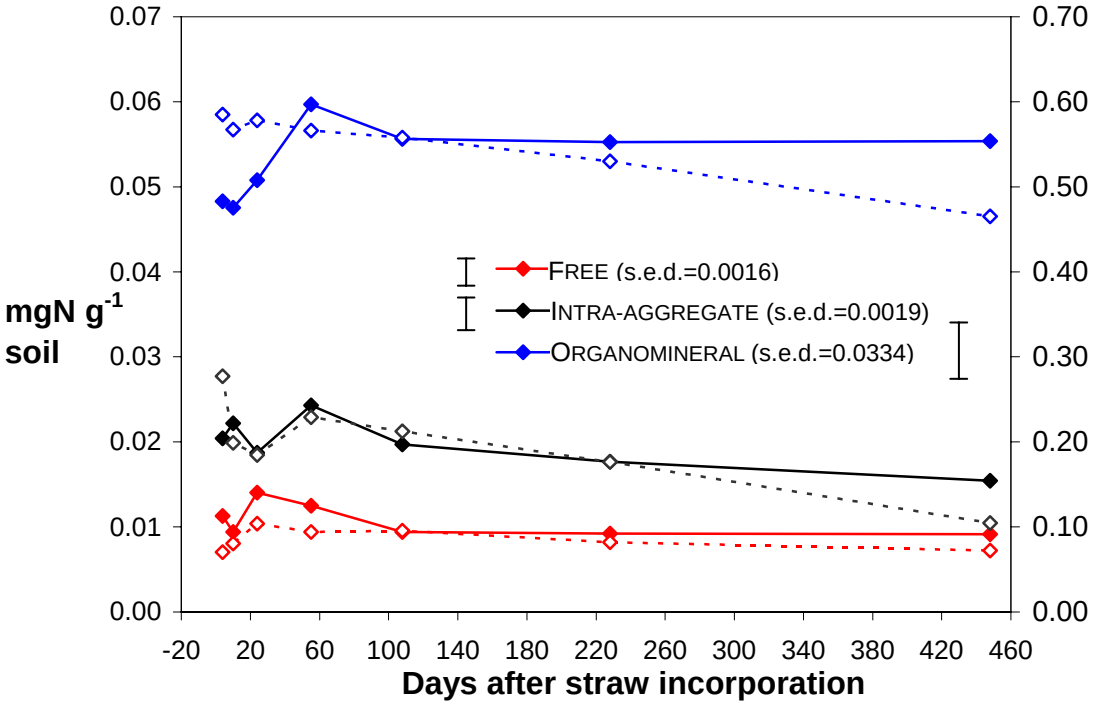

Figure 5.6. Dynamics of the ^{15}N content of the standard SOM fractions after addition of ^{15}N-labelled maize straw (solid lines) compared to those in non-amended soil (dashed lines). The ORGANOMINERAL data are plotted on the secondary axis

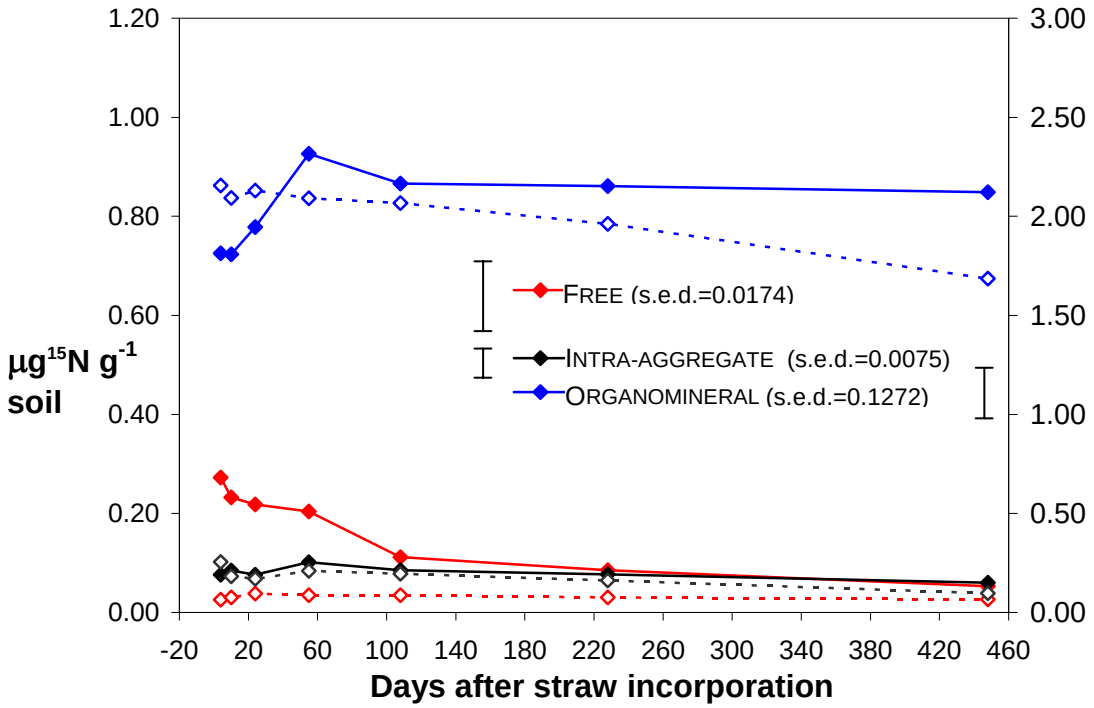

Figure 5.7. Dynamics of ^{15}N enrichment in standard fractions after addition of maize straw (solid lines) compared to those in non-amended soil (dashed lines)

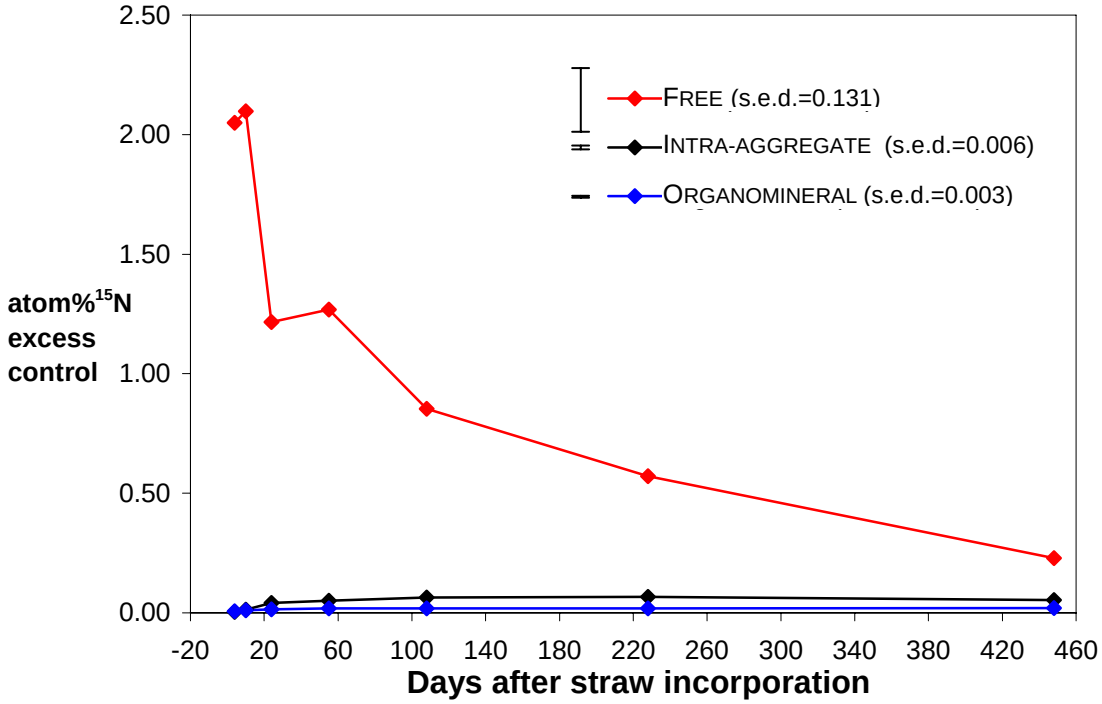

Figure 5.8. Dynamics of C-to-N ratio in standard SOM fractions after addition of maize straw (solid lines) and relative to those in non-amended soil (dashed lines)

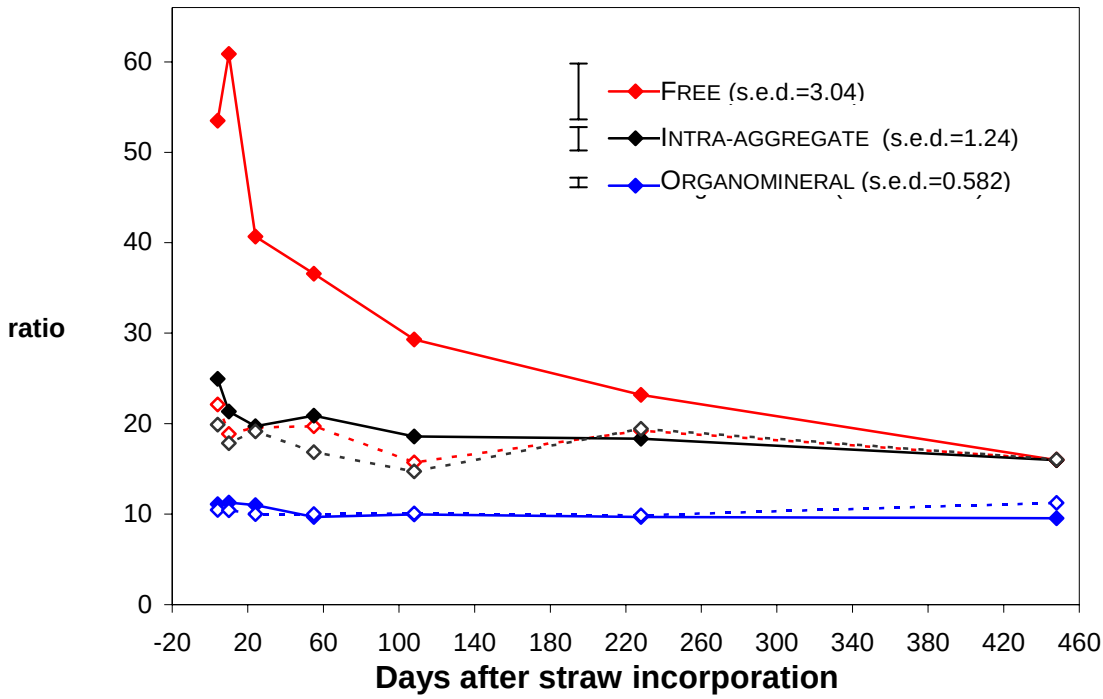

Figure 5.9. Rates of gross N mineralisation measured during incubation of soil with and without maize straw by ^{15}N isotope dilution (+/- s.e.; n = 4)

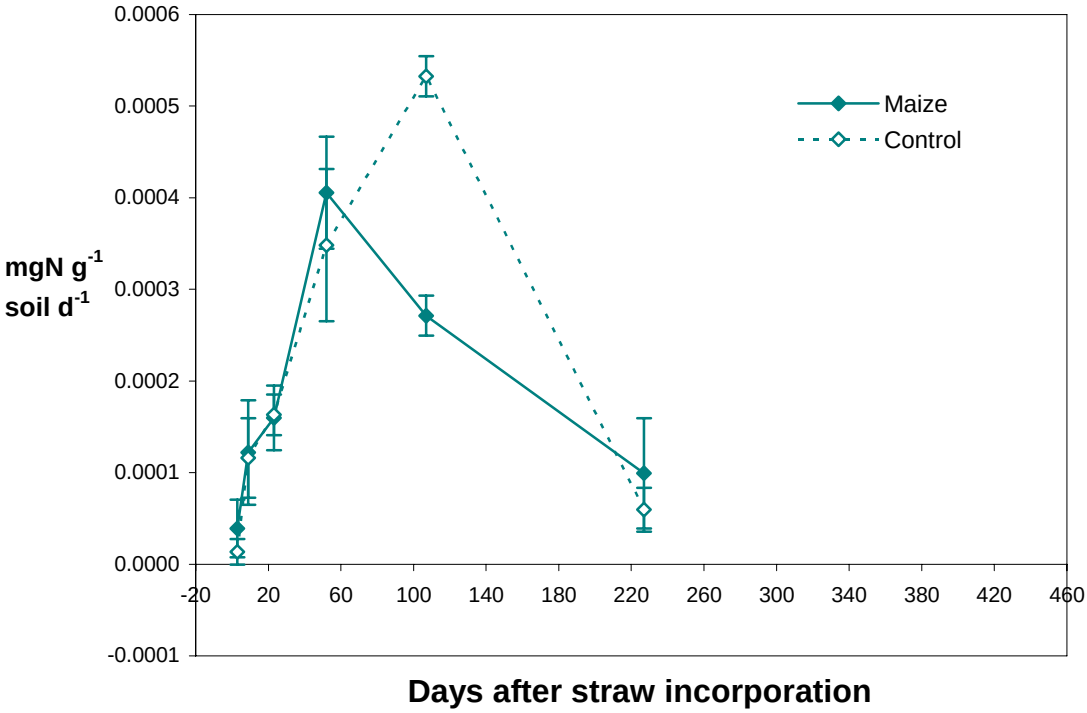

Figure 5.10. Spot measurements of the temperature in the sand-bed during incubation of soil with and without maize straw

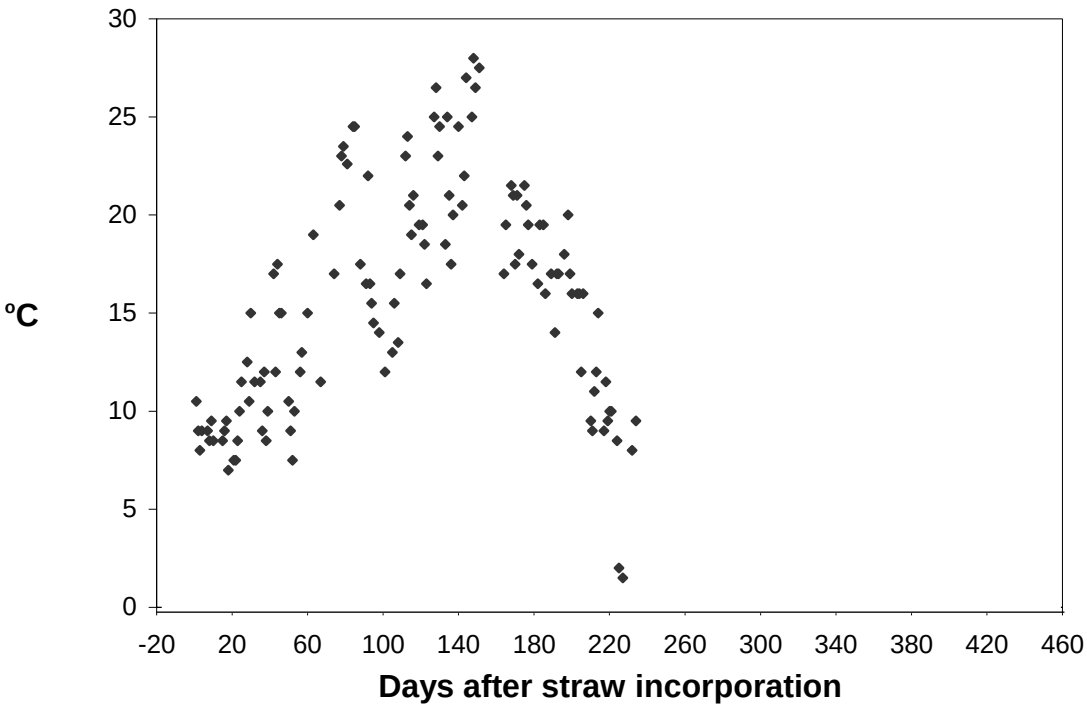

Figure 5.11. CO_2 production during incubation of soil with and without (control) maize straw measured by trapping in NaOH (+/- s.e.; n = 4)

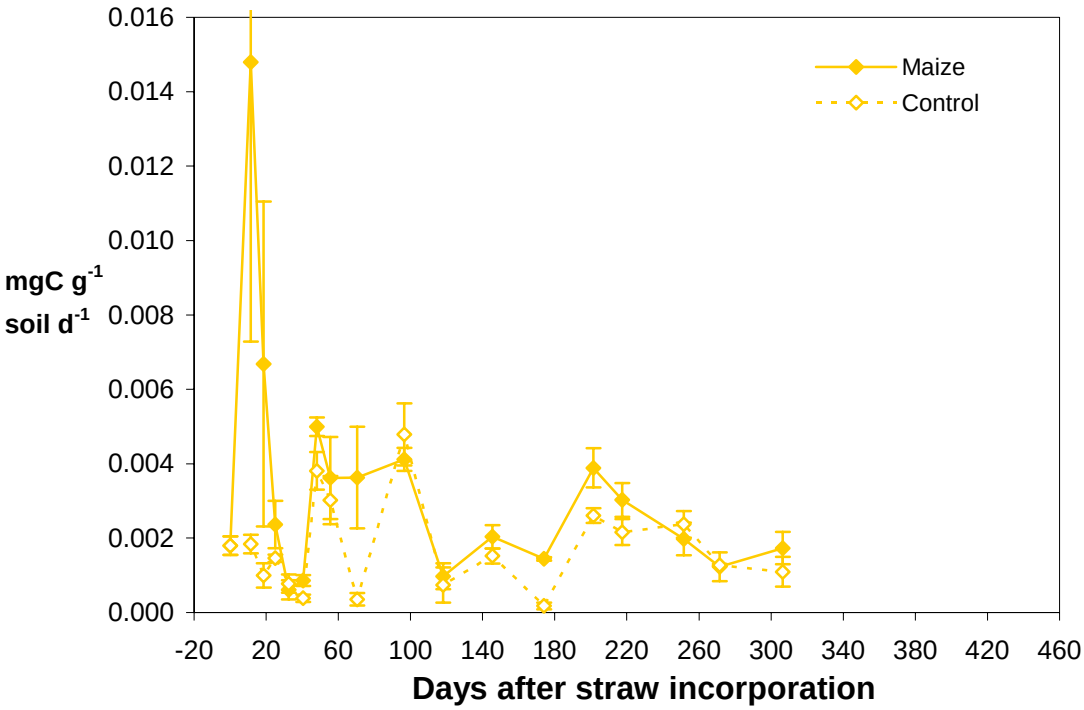

Figure 5.12. Dynamics of microbial C and N during incubation of soil with and without maize straw, measured by the fumigation–extraction method (+/- s.e.; n = 4)

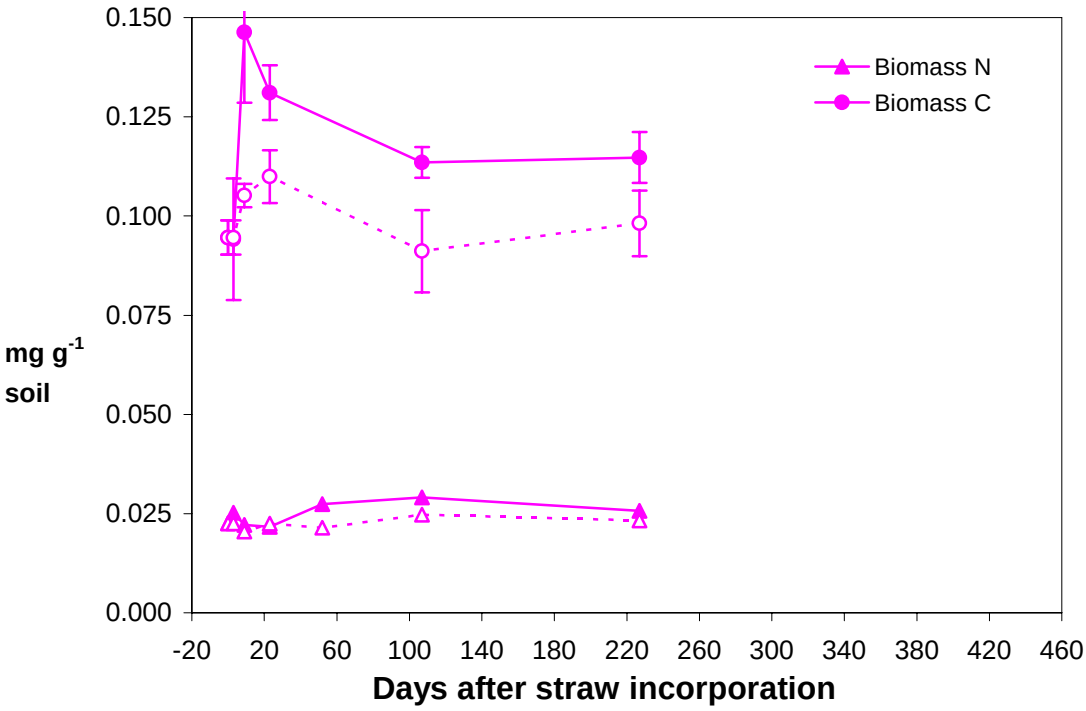

Figure 5.13. Dynamics of total soluble C during incubation of soil with and without maize straw (+/- s.e.; n = 4)

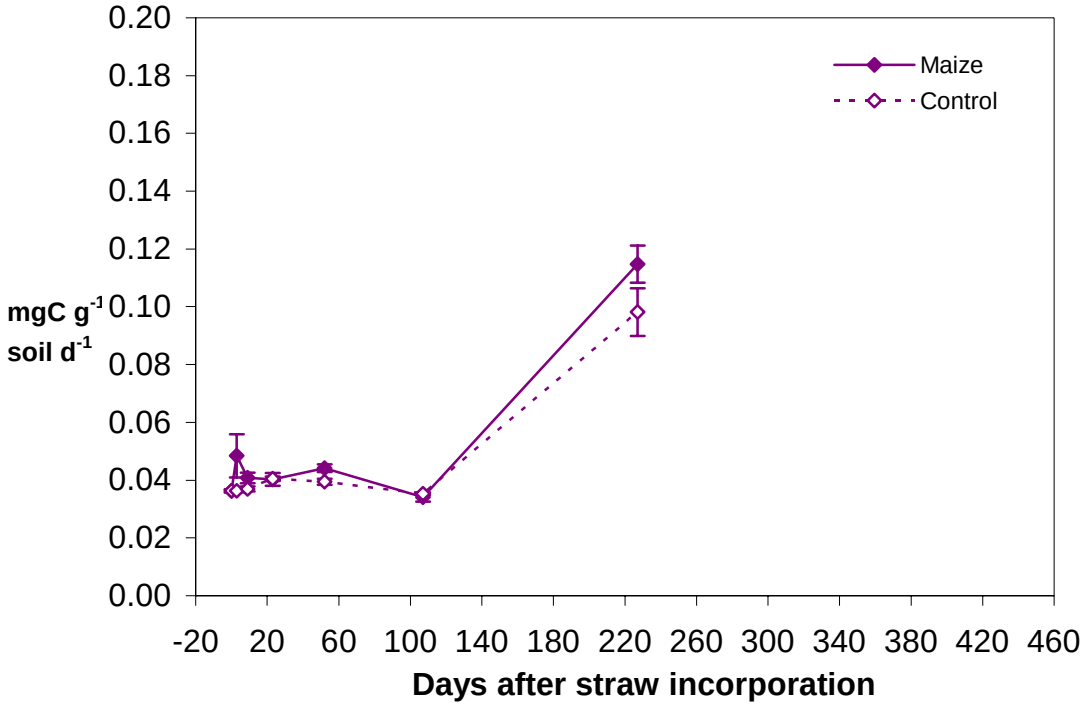

Figure 5.14. Dynamics of mineral N as a surrogate for NaI-soluble N during incubation of soil with and without maize straw (+/- s.e.; n = 4)

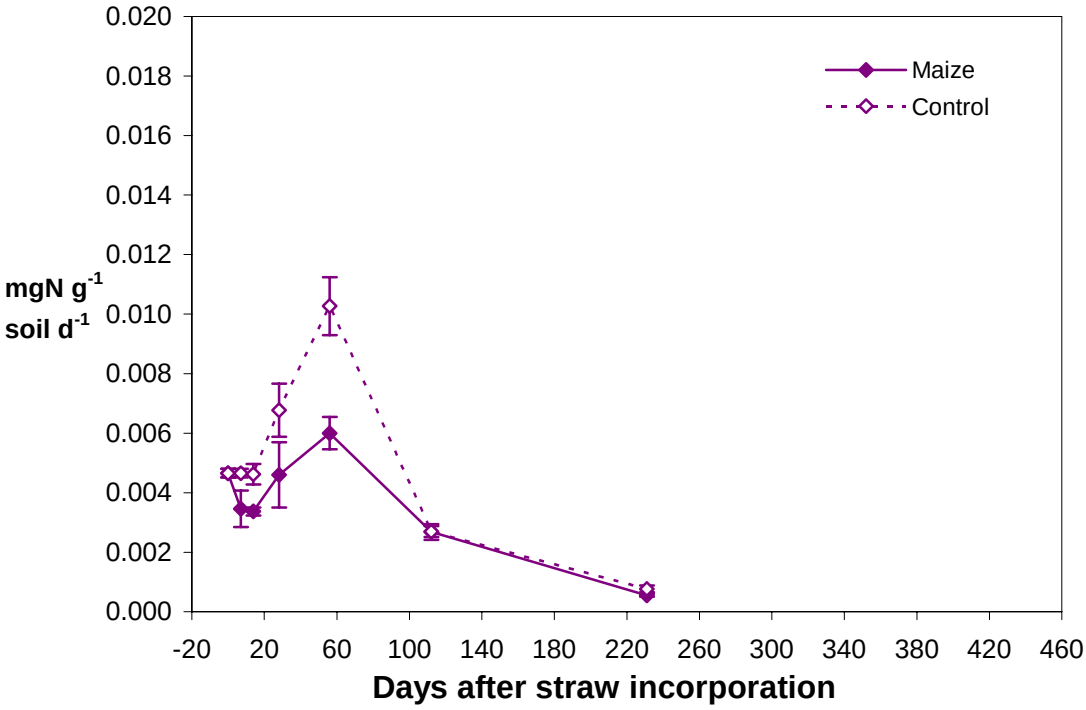

Table 5.5. The comparative ^{15}N enrichments of ORGANOMINERAL sub-fractions during the incubation with ^{15}N labelled maize straw relative to the corresponding fractions from non-amended soil

Day	4	10	24	55	108	228	448
	---------- atom% ^{15}N (excess control) ----------						
ORGANOMINERAL sub-fractions							
Coarse sand (2mm-212mm)	-0.0011	-0.0021	-0.0027	-0.0009	0.0065	0.0085	n/a
s.e.	0.0021	0.0009	0.0008	0.0014	0.0036	0.0029	0.0000
Fine sand (212-53mm)	-0.0017	0.0009	0.0046	0.0039	0.0137	0.0187	n/a
s.e.	0.0007	0.0010	0.0006	0.0007	0.0022	0.0019	0.0000
Coarse silt (53-25mm)	-0.0005	0.0036	0.0091	0.0083	0.0131	0.0272	0.0400
s.e.	0.0005	0.0005	0.0005	0.0010	0.0015	0.0034	0.0024
Fine silt (25-2mm)	0.0014	0.0047	0.0111	0.0204	0.0228	0.0282	0.0166
s.e.	0.0012	0.0005	0.0004	0.0029	0.0015	0.0050	0.0020
Clay (2-0mm)	0.0111	0.0171	0.0191	0.0206	0.0199	0.0169	0.0133
s.e.	0.0011	0.0008	0.0007	0.0017	0.0010	0.0075	0.0019
ORGANOMINERAL standard fraction	0.0069	0.0111	0.0146	0.0184	0.0188	0.0192	0.0206
s.e.	0.0009	0.0006	0.0005	0.0016	0.0009	0.0052	0.0027

N-isotope composition of both INTRA-AGGREGATE and ORGANOMINERAL fractions was significantly altered with the addition of labelled maize straw to soil ($P < 0.001$). There was also significant change in the ^{15}N enrichment of the INTRA-AGGREGATE fraction although, with the decline in the enrichment of the source fraction, this occurred in the relatively early stages of the incubation (Figures 5.6 and 5.7.). The ^{15}N enrichment of all three fractions is plotted relative to that of the corresponding fractions in non-amended soil in Figure 5.7. (^{15}N atom% excess control). On the basis of this data, the INTRA-AGGREGATE fraction accounted for a maximum of only 6 to 7 % of the N added in maize straw. The small (but statistically significant) enrichment of the large ORGANOMINERAL fraction is quantitatively more important, and presumably provided the major sink for ^{15}N. Comparatively large changes in the enrichment of ORGANOMINERAL clay were apparent after two weeks incubation (Table 5.5.).

5.4. Conclusion

Combining the incubation of ^{15}N-labelled maize straw with fractionation and independent measurements of other processes and pools enhanced the understanding of the dynamics and interactions between the standard SOM fractions. In particular, the experiment provided direct evidence that the INTRA-AGGREGATE fraction is active on a seasonal time scale, and thus likely to be relevant to crop nutrient supply. Contrary to the findings in Chapter 3, at least one of the model compartments (corresponding to FREE organic matter) is heterogeneous materials and includes a quite stable fraction. This may fundamentally limit the ability to fit a model that assumes constant reactivity within compartments.

CHAPTER 6: MODEL PARAMETERISATION

6.1. Introduction

The objective of this chapter is to use the fractionation data from the maize-straw decomposition experiment (Chapter 5) to evaluate the parameters invoked in the mathematical model (Chapter 4). This will be achieved by optimisation i.e. matching of model output to the measured dynamics of C, N, ^{15}N and $\delta^{13}C$ in FREE, INTRA-AGGREGATE and ORGANOMINERAL fractions. The simulation of independently measured variables, including measurements of gross N mineralisation will enable the simulation of processes to be assessed. Parameterised using data from soil receiving maize straw, the model will then be tested against corresponding data for soil containing only native SOM.

6.2. Method

Two datasets from the soil incubation experiment described in Chapter 5 were consolidated with the mathematical model using *ModelMaker 3.0* (Adept Scientific, Oxford). Each dataset comprised measurements of C, N and their respective tracers in the standard SOM fractions, independent measurements corresponding to other model variables, and model variables calculated from the above (Table 6.1.). The first dataset related to the soil incubated with ^{15}N-labelled maize straw, the second the non-amended soil. Both mean values and standard errors were included for each variable. The variables measured independently of fractionation, and calculated variables (identified

Table 6.1. List of primary variables available for model parameterisation, with decription. The variables used in optimisation of model parameters are emboldened and calculated variables identified in red

Fraction / process	Status	Model variable
CO_2 production	Independent meaurable	*CO2*
Cumulative CO_2	Calculated	***GasC***
Gross N mineralisation	Independent meaurable	*GNM*
Biomass C	Independent meaurable	***BugC***
Biomass N	Independent meaurable	***BugN***
Biomass C:N ratio	Calculated	ρbug
K_2SO_4 extractable C	Independent meaurable	***SolC***
K_2SO_4 extractable mineral N	Independent meaurable	***SolN***
FREE organic matter C	Meaurable	*light1C*
INTRA-AGGREGATE C	Meaurable	*light2C*
ORGANOMINERAL C	Meaurable	***HeavyC***
Current total C - total initial C	Calculated	*lostC*
Current total C	Calculated	*retainedC*
FREE organic matter N	Meaurable	*light1N*
INTRA-AGGREGATE N	Meaurable	*light2N*
ORGANOMINERAL N	Meaurable	***HeavyN***
Current total N - total initial N	Calculated	*lostN*
Current total N	Calculated	*retainedN*
FREE organic matter ^{13}C	Meaurable	***Light1^{13}C***
INTRA-AGGREGATE ^{13}C	Meaurable	***Light2^{13}C***
ORGANOMINERAL ^{13}C	Meaurable	***Heavy^{13}C***
Current total ^{13}C - total initial ^{13}C	Calculated	*lost^{13}C*
Current total ^{13}C	Calculated	*retained^{13}C*
FREE organic matter ^{15}N	Meaurable	***Light1^{15}N***
INTRA-AGGREGATE ^{15}N	Meaurable	***Light2^{15}N***
ORGANOMINERAL ^{15}N	Meaurable	*heavy^{15}N*
Current total ^{15}N - total initial ^{15}N	Calculated	*lost^{15}N*
Current total ^{15}N	Calculated	*retained^{15}N*
FREE organic matter δ^{13}C	Calculated	$\delta light1$
INTRA-AGGREGATE δ^{13}C	Calculated	$\delta light2$
ORGANOMINERAL δ^{13}C	Calculated	$\delta heavy$
^{15}N isotope ratio in FREE organic matter	Calculated	$\alpha light1$
^{15}N Isotope ratio in INTRA-AGGREGATE	Calculated	$\alpha light2$
^{15}N Isotope ratio in ORGANOMINERAL fraction	Calculated	$\alpha heavy$
C:N in FREE organic matter	Calculated	$\rho light1$
C:N in INTRA-AGGREGATE	Calculated	$\rho light2$
C:N in ORGANOMINERAL	Calculated	$\rho heavy$

in Table 6.1.) were not used in optimisation. Daily values for driving (climatic) variables were calculated from meteorological data.

6.2.1. Temperature rate modifier

The measurements of soil temperature (Figure 5.10.) were not sufficient for the simulations since a daily timestep is used in the model. A linear regression was performed to establish the relationship between the occasional measurements in the sand bed and the daily mean temperature 10 cm under soil at the nearby automatic weather recording station ($r^2 = 0.91$) (Figure 6.1.). The latter averages hourly temperature measurements to provide a daily mean. The regression equation was applied to provide daily values for the sand bed from the weather station data (Figure 6.2.). These values were used to calculate the temperature modifier (*temp*) for each timestep using the equation in Section 4.2.7. (Figure 6.3.).

6.2.2. Soil moisture rate modifier

Soil moisture was directly determined only with destructive sampling of the pots for fractionation i.e. on seven occasions. Again, to calculate the rate modifier on a timestep compatible with the model, rainfall and open pan evaporation data from the automatic weather recording station were used (see above). A running balance of volumetric soil moisture for the pots was calculated from rainfall and soil-surface evaporation (the latter estimated from open pan evaporation measurements, multiplying by a factor of 0·75; see Coleman and Jenkinson 1996). The lower and upper limits for soil moisture were taken as the established water holding capacity and wilting points

Figure 6.1. The relationship between spot temperature measurements in the sand-bed and the 24-hour mean temperature recorded at the meteorological station

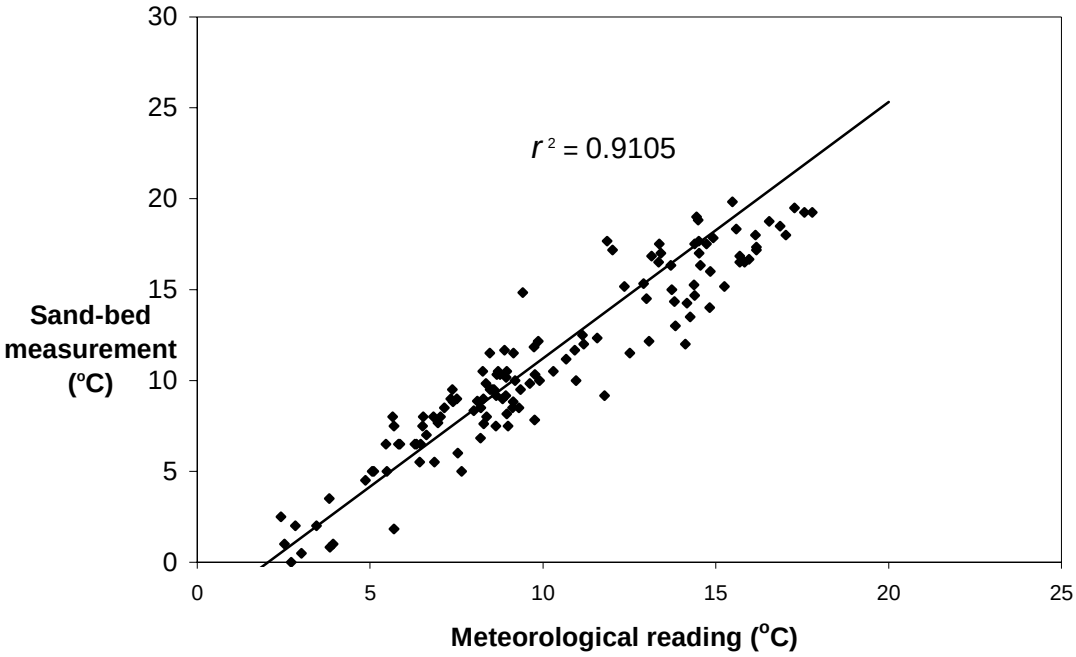

Figure 6.2. The daily mean temperature in the sand bed estimated using data from the meteorological station

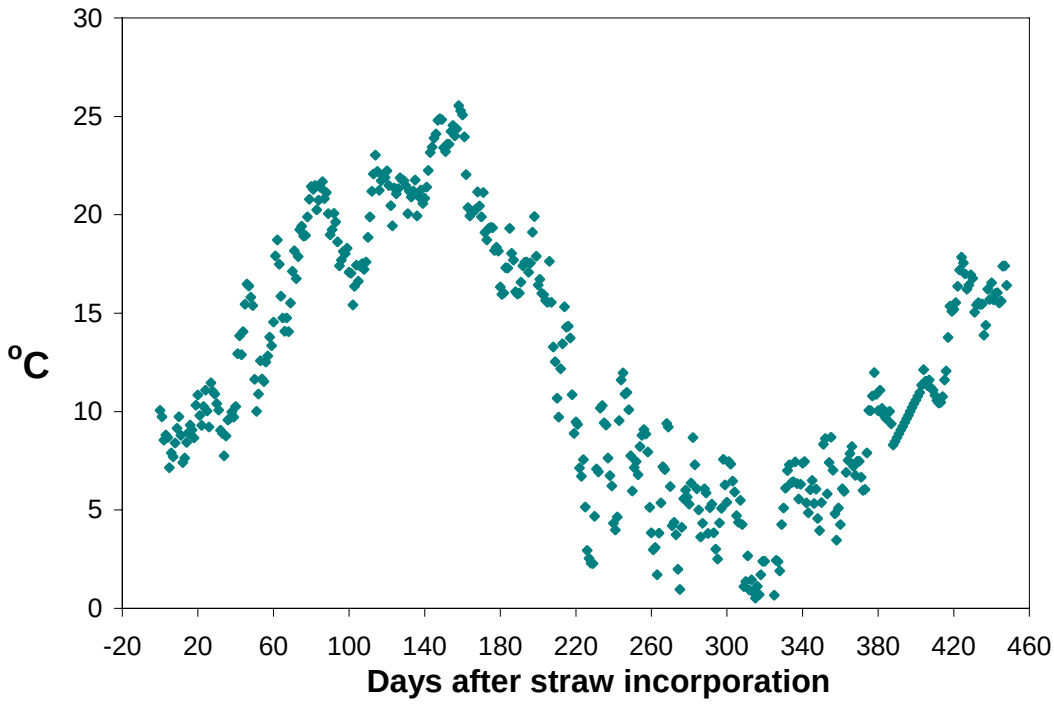

respectively. Volumetric (mm) and gravimetric (g g^{-1}) soil moisture (M_v and M_g respectively) were related using the following equations:

$$M_v = M_g \times \text{bulk density (g cm}^{-3}) \times \text{profile depth (mm)}$$

$$M_g = M_v \ / \ [\text{bulk density (g cm}^{-3}) \times \text{profile depth (mm)}]$$

The daily estimates of M_g were compared with the measurements made at the seven sampling times (Figure 6.4.), and daily values for the moisture modifier calculated according to the equation in Section 4.2.6. (Figure 6.5.). The combined influence of the temperature and soil moisture modifiers applied to C utilisation flows (Section 4.2.3) is illustrated in Figure 6.6.

6.2.3. Initial values

Parameters representing the initial magnitude of key model variables are listed in Table 4.1. Values for these parameters are necessary to run the model. Initial values for *light1**, *light2** and *heavy** define the magnitude of model compartments at the beginning of the simulation i.e. Day –10. In the first instance these were taken from the measurements of FREE, INTRA-AGGREGATE and ORGANOMINERAL fractions in non-amended soil at Day 4 (see Figures 5.3. to 5.6.).

As noted in Section 5.2.2.3., although C was determined in all standard and sub-fractions, the concentration in some ORGANOMINERAL sub-fractions was insufficient to determine $\delta^{13}C$. To provide simulation of $\delta^{13}C$ in the ORGANOMINERAL fraction, the

Figure 6.3. The status of the temperature rate modifier during the incubation

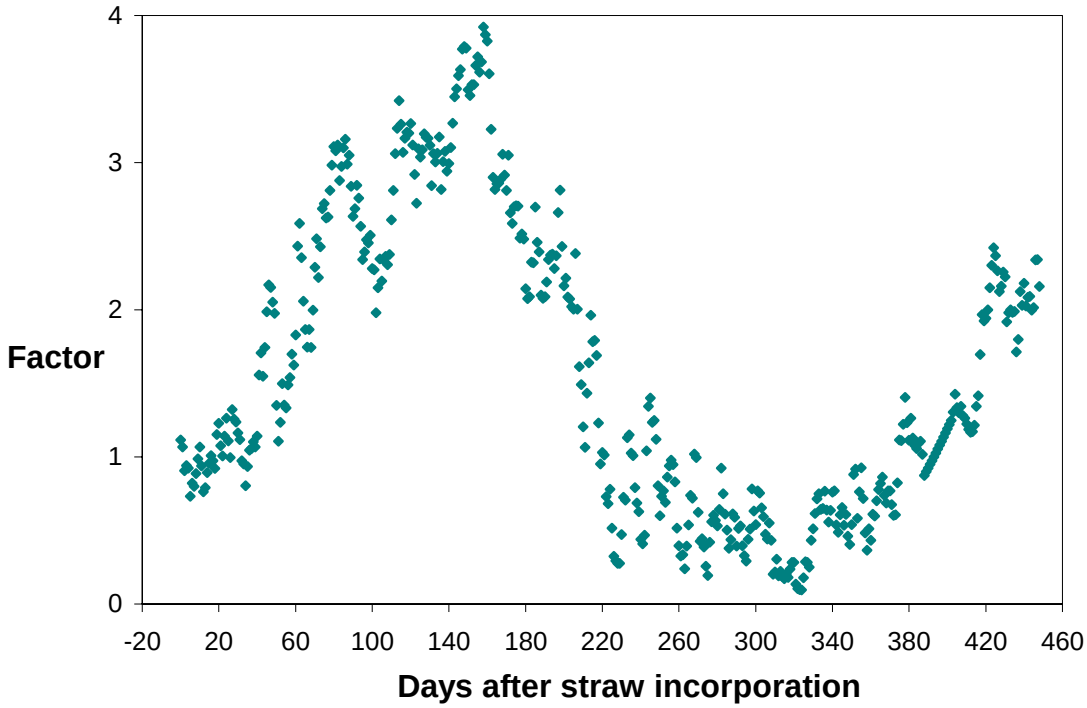

Figure 6.4. Comparison of estimated and occasionally measured gravimetric soil moisture content during the incubation

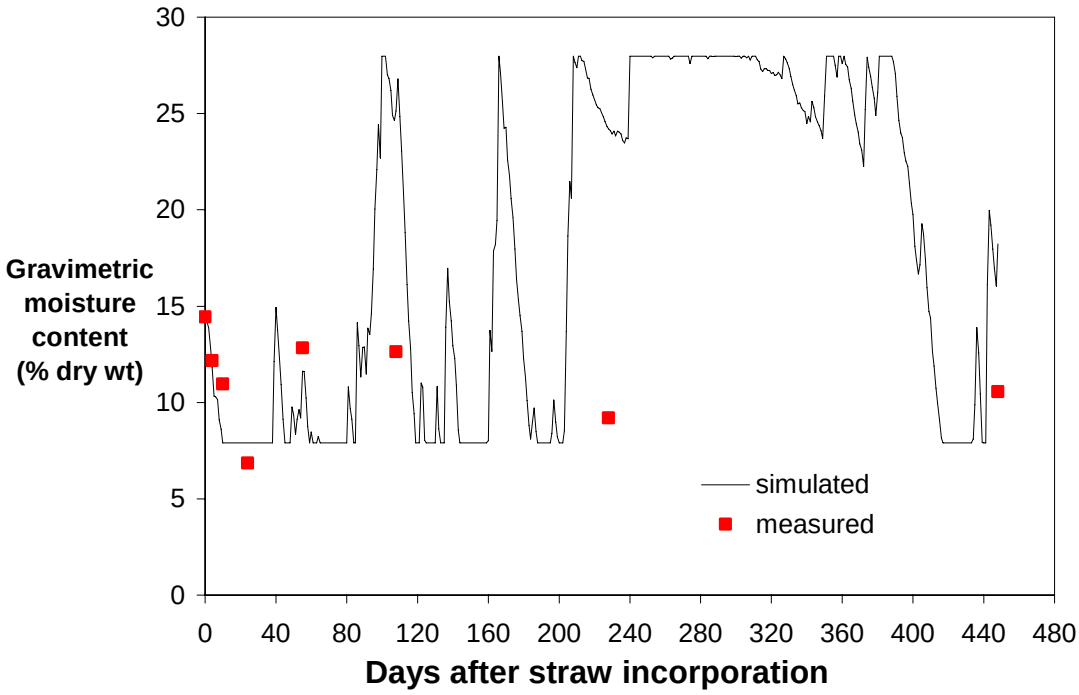

Figure 6.5. Status of the soil moisture rate modifier during the incubation

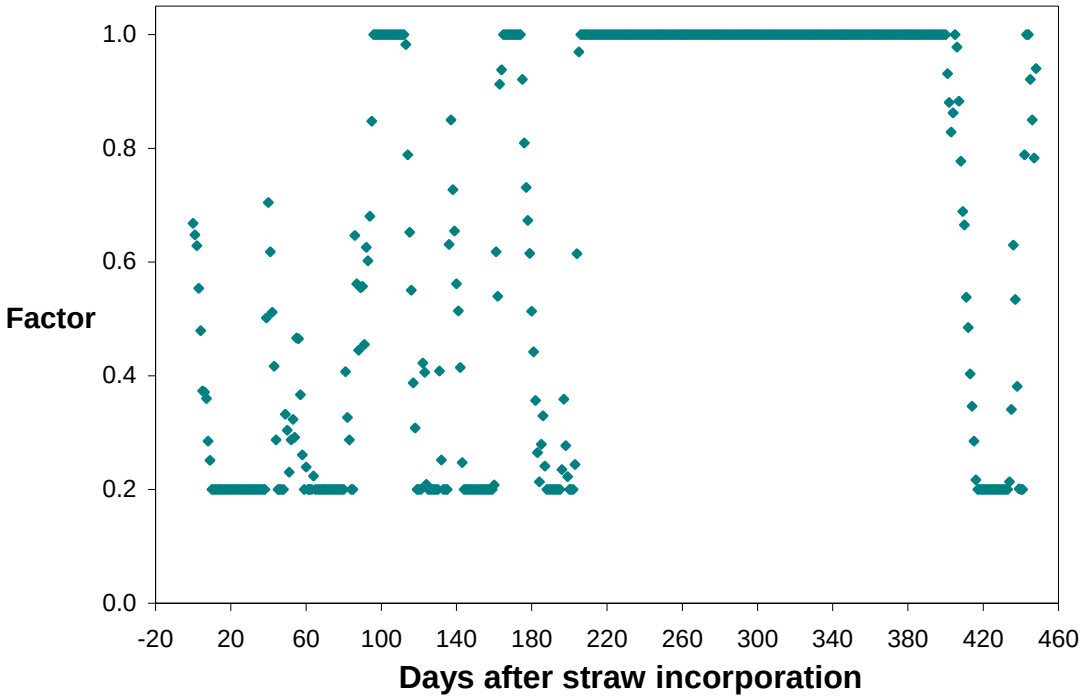

Figure 6.6. The combined effect of temperature and soil moisture modifiers on substrate utilisation rates

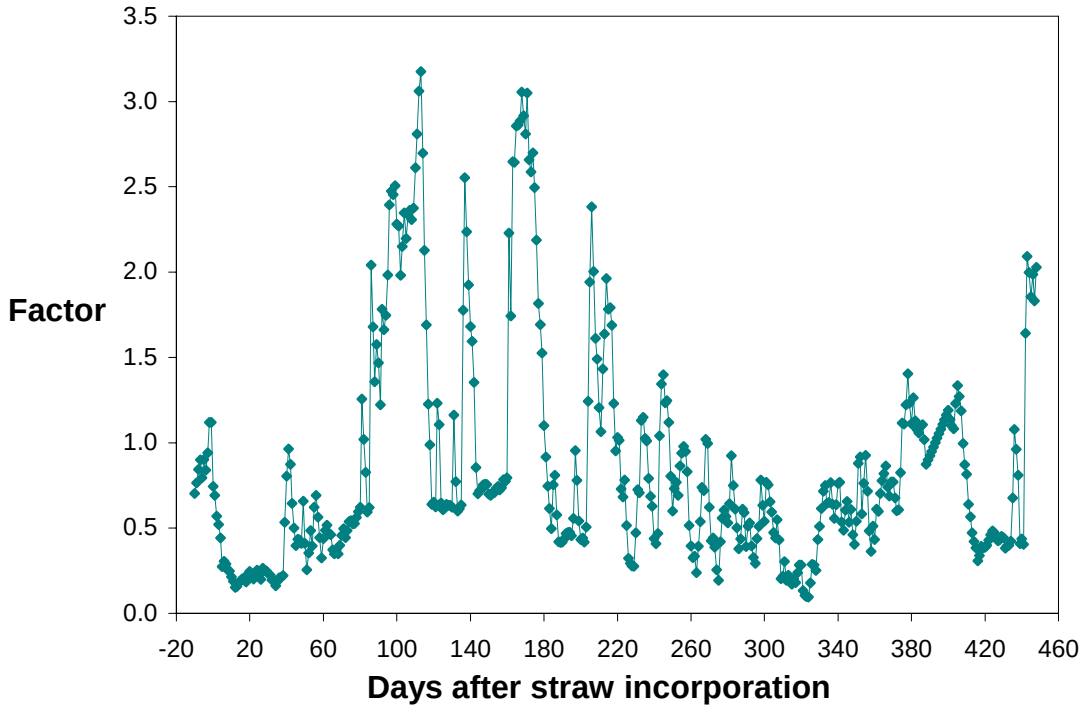

amount of ^{13}C in the ORGANOMINERAL fraction was estimated from the measurements of total C in all sub-fractions, and the available sub-fraction measurements of $\delta^{13}C$.

The value for $BugC_0$ (required to calculate the initial magnitude of ***LF1****, ***LF2**** and ***HF**** from the measured variables $light1*_0$, $light2*_0$, $heavy*_0$) was taken as the measured status of microbial biomass at Day 0 (see Figure 5.12.). Since the relationship between mineral N and NaI-soluble organic matter could not be established, $SolN_0$ was taken as soil mineral N measured at Day 0. Similarly, total soluble organic C at Day 0 was used as a measured of $SolC_0$. Initial tracer values for ***Sol**** and ***Bug**** were calculated from $SolC_0$ and $SolN_0$, and estimates of their isotope ratio (see Section 4.2.8.).

6.2.4. Organic inputs

The input of C and N and their tracers at Day 0 were calculated for the maize-amended soils from the mass of added maize straw and its isotopic composition (outlined in Table 5.3.). The input to the model was through ***LF1**** (see Section 4.2.1.).

6.2.5. Parameter optimisation of model constants

The model was optimised against 18 variables, namely $*C$, $*N$, $*^{13}C$, $*15N$, $\delta*$and $*CN$ (from measurements of C, N, ^{15}N and $\delta^{13}C$ in FREE, INTRA-AGGREGATE and ORGANOMINERAL fractions; Table 6.1). The choice of optimisation variables was subjective in that $\delta*$ and $*CN$ are not truly independent. Although the model contains a relatively large number of measurable variables compared to established SOM models

(Table 5.1.) the number of optimisable parameters exceeded the number that could be evaluated by non-linear (Marquadt) algorithms within *ModelMaker* alone. Instead, an initial optimisation was conducted by trial and error, using a knowledge of the sensitivity of each parameter gained in Chapter 4 (particularly the interaction between C and N dynamics through ***Bug****). Agreement between model output and measured data was judged visually, and on the basis of r^2 values calculated by *ModelMaker*. The Marquadt optimisation routines within *ModelMaker* were then used to refine the preliminarily (starting) values, and maximise the proportion of variation explained by the model. Marquadt optimisation was found most effective when applied to single or paired parameters at a time, and selecting the least-squares method in the first instance. The outcome of the optimisation was sensitive to the starting values, so the initial trial and error optimisation was important to the final outcome.

6.2.6. Sensitivity analysis

The sensitivity of the optimised model to optimised parameter values was established by systematically varying their value and observing the effect on the simulation of the fractionation data, and simulated processes.

6.3. Results and discussion

6.3.1. Optimisation of initial values and model parameters

It was immediately apparent that taking the initial value of *light1**, *light2** and *heavy** as their measured magnitude in the control soil at Day 4 (the first sampling)

would not – given the known additions to ***LF1**** in maize straw – provide adequate simulation of the measurements at later samplings. Thus the *light1*$*_0$, *light2*$*_0$ and *heavy*$*_0$ parameters were optimised alongside those listed in Table 6.3., to obtain the best overall fit (legitimate within the range of the measurement error). The optimised initial values for $*C$ and $*N$ (i.e. $*C_0$ and $*N_0$) are compared with their measured values and standard errors in Table 6.2. The preliminarily optimised values (obtained by trial and error) are also shown, together with calculated values for $*^{13}C_0$ and $*^{15}N_0$,. The latter cannot be optimised, but calculated from the optimised values for $*C_0$ and $*N_0$ and the relevant isotope ratio.

The necessary adjustment to the initial values exceeded the S.D. of the measurements (indicated in the last column of Table 6.2.). It seems likely that the rapid decline in *light1** between Day 0 and Day 4 (i.e. prior to the first sampling) can be explained by the high concentration of water-soluble carbohydrate in the added maize straw (22 % of dry weight; Table 5.2.). Since a substantial proportion of the straw dissipated from *light1** very rapidly, it may effectively have been added to a fraction or compartment other than ***LF1**** (specifically, ***Sol***). Treating maize straw as an addition only to ***LF1**** probably explains the need for optimisation of the *light1*$*_0$ variables. The problem that this presented was particularly great for ^{15}N, where the calculated addition was 13.4 times greater than the measured value of *light1*$^{15}N_0$ (the native FREE organic matter reflecting the low natural abundance of ^{15}N; see also Section 5.3.3.). Since the measured value of *light*$^{N}15_0$ was small relative to the addition of ^{15}N, the magnitude of the ^{15}N input was adjusted to provide sufficient latitude for the optimisation. The magnitude of the ^{15}N input was thus decreased to allow optimisation to provide the best overall fit.

Table 6.2. Optimisation of initial value parameters in the model using Marquadt algorithms, with the starting values obtained by prior trial and error optimisation against the experimental data

Variable	Measured value + Mean	S.D.	*Marquadt* start value	Optimised value	Model value	Diff %
light1C $_0$	0.154	0.0173	0.179	0.179	0.179	16 *
light2C $_0$	0.549	0.0274	0.496	0.496	0.496	-10 *
HeavyC $_0$	6.123	0.1044	5.528	5.520	5.520	-10 *
Input C	0.464	-	-	0.464	0.464	
Total C	**7.290**			**6.660**	**6.660**	**-9**
light1N $_0$	0.007	0.0008	0.010	0.009	0.009	26 *
light2N $_0$	0.028	0.0029	0.023	0.021	0.021	-24 *
HeavyN $_0$	0.585	0.0026	0.533	0.533	0.533	-9 *
Input N	0.006	-	-	0.006	0.006	
Total N	**0.626**			**0.569**	**0.569**	**-9**
light1 $^{13}C_0$	0.0017	0.00019	-	-	0.0020	16 *
light2 $^{13}C_0$	0.0060	0.00030	-	-	0.0054	-10 *
heavy $^{13}C_0$	0.0672	0.00000	-	-	0.0604	-10 *
Input ^{13}C	0.0052	-	-	-	0.0052	0
Total ^{13}C	**0.0801**				**0.0729**	**-9**
light1 $^{15}N_0$	0.00003	0.000003	-	-	0.00003	26 *
light2 $^{15}N_0$	0.00010	0.000011	-	-	0.00008	-24 *
heavy $^{15}N_0$	0.00216	0.000009	-	-	0.00196	-9 *
Input ^{15}N	0.00031	-	-	-	0.00013	-59
Total ^{15}N	**0.00259**				**0.00220**	**-15**
r^2					**0.4002**	

* $^{13}C_0$ are calculated from corresponding C value according to measured values for $\delta^{13}C$

* $^{15}N_0$ are calculated from corresponding N value and measured isotope ratio (not for input)

+ Measured values are from the control (non-amended) soil at Day 4

* Indicates that the optimised value differs from the measured by more than 1 S.D.

For *light2** (representing INTRA-AGGREGATE organic matter), an initial rapid decline may have resulted from the disturbance of soil structure during preparation and packing of the soil pots for incubation. This required the adjustment of $light2^*_0$ beyond the S.D. of the measurement during optimisation

With optimisation of initial values, 9 % of the C and N that should have been present in the soil at the beginning of the incubation (from measurements at Day 4 in the control soil, and the known magnitude of the maize inputs), was not accounted for in the optimised model. For C and N this could be partly a consequence of experimental error, although the magnitude of the optimisation exceeded the S.D. of the measurements (Table 6.2). However, 59 % of the ^{15}N input had to be discounted (leaving 15 % of total soil ^{15}N unaccounted for). The apparently large dissipation of ^{15}N from FREE organic matter at the beginning of the incubation is further discussed in Chapter 7.

The final values for the key optimisable parameters are listed in Table 6.3., alongside their starting values (taken from those used in the scenarios in Chapter 4; see Section 4.2.9.), and values obtained through the preliminary trial and error optimisation. Assessed against the 18 measured variables used in optimisation and seven time points, the preliminary optimisation resulted in $r^2 = 0.368$ (or $r^2=0.106$ without optimisation of initial values). After Marquadt optimisation, the level of fit was increased to $r^2 = 0.401$.

Table 6.3. The optimised values for the key model parameters evaluated against experimental data using Marquadt algorithms and starting values obtained from trial and error optimisation of the values used for the scenarios run in Chapter 4

	Scenario value	*Marquadt* start value	Optimised value
η	0.3	0.25	0.258
α	0.55	0.5	0.324
kLF1	0.01	0.004	0.0040
kLF2	0.002	0.002	0.0023
kHF	0.00005	0.00005	0.00005
kmort	0.015	0.01	n/c
ksol	0.03	0.1	n/c
θ	0.3	0.3	n/c
ρbug	6	6.5	5.32
$\beta LF1$	0.1	0.3	0.30
$\beta LF2$	0.1	0.1	0.15
$\phi LF2$	0.2	0.1	n/c
ϕHF	0.5	0.5	n/c
kfix	0.0005	0.001	n/c
kgas	0.001	0.001	n/c

The sensitivity of model output to the value of the various parameters, particularly the initial magnitude of the model compartments, is examined in a later section with specific reference to the effect on N limitation. The optimised values of the model parameters are discussed after a description and explanation for the simulation of C and N, their respective tracers, and independent measurements of other fractions and rate processes (and in their context).

6.3.2. Considerations in interpretation of optimised model

Temperature- and soil-moisture modifiers were the major influence on the overall dynamics of the system (see Figures 6.3. and 6.5., and for their combined effect Figure 6.6.). In the substrate utilisation flows, large day-to-day variation occurred in the flow rates due mainly to the influence of the moisture modifier, the effect of temperature being more seasonal. It is questionable that the effect of the modifiers should have been so large, particularly in view of the comparison of model output with measured rates of gross N mineralisation and CO_2 production (Section 6.3.5.).

The other major influence on the pattern of decomposition was N limitation, the general effects of which were established in Section 4.2.4. For this incubation, intermittent N limitation was simulated between Days 84 and 220 (Figure 6.7.). The combined effect of temperature, moisture and N limitation on units of C respired per unit of N mineralised is apparent in Figure 6.8.

Figure 6.7. The status of the C flow limiter λ during the incubation of soil and straw as simulated by the parameterised model

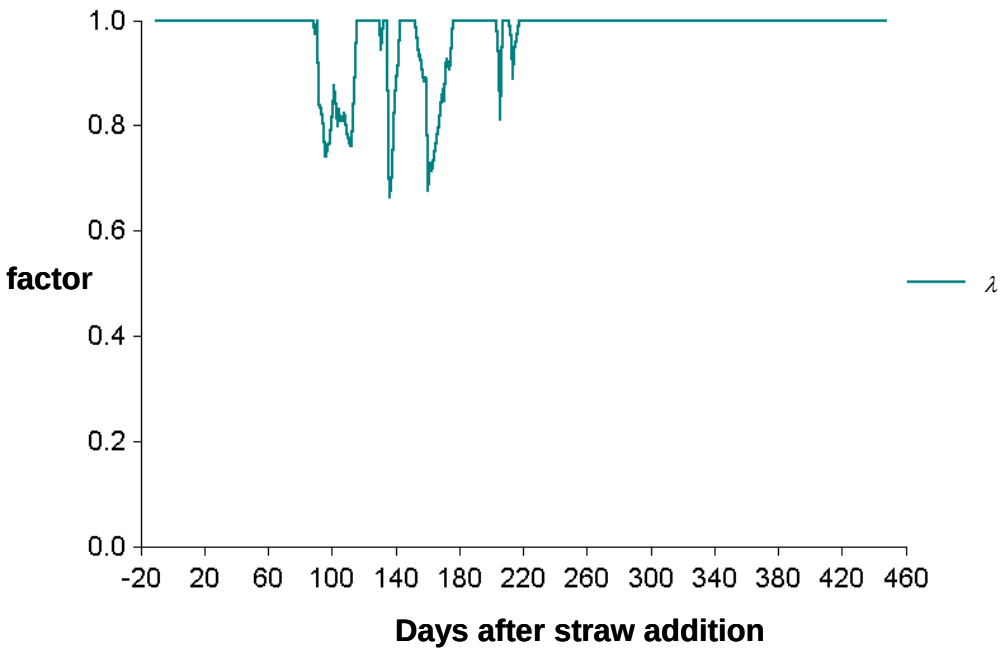

Figure 6.8. The variation in the ratio of C utilised to N mineralised during the incubation of soil and straw as simulated by the parameterised model

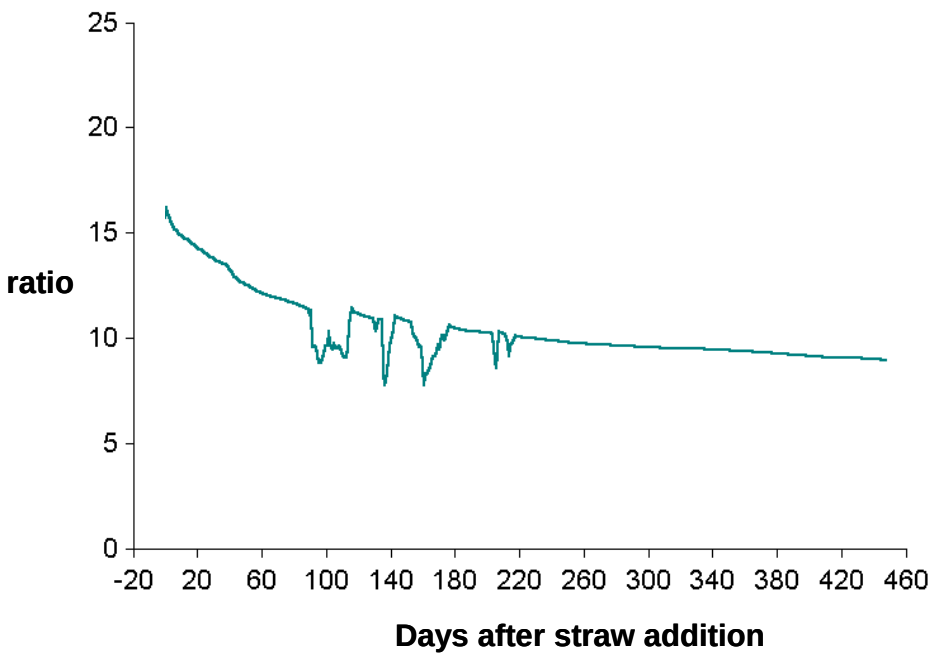

6.3.3. Simulation of C, N and tracer dynamics in measured fractions

Following optimisation, the predicted and measured status of light fraction C (both as FREE and INTRA-AGGREGATE organic matter, as *light1C* and *light2C* respectively) were well matched at the beginning and end of the incubation (Figure 6.9.a). Agreement in the intervening period was not entirely satisfactory for *light1C*, lying beyond the error of the measurements. This stemmed mainly from a rather slow rate of decomposition in the initial stages (approx. Day 0 to Day 80 in the simulation). This in part reflected the unfavourable status of rate modifiers (which conversely may have contributed to a more rapid than measured decline between Day 120 and Day 220). Although the soil was measurably dry in the early stages of the incubation (Day 0 to Day 25), at least one subsequent measurement suggested daily estimates of soil moisture based on the running balance of evaporation and rainfall were not necessarily in good agreement (see Figure 6.4.). Also, the algorithm used to calculate the modifier itself may be deficient, overestimating the impact on decomposition rate, at least in *light1**, when applied on a daily timestep.

However, it is clear – particularly with evidence from the tracer data (see below) – that a changing level of reactivity within FREE organic matter was the major limitation to fitting the model. This view was supported by the fact that the data for INTRA-AGGREGATE organic matter – which appeared more likely to be homogeneous in its reactivity from its chemical characterisation (Chapter 3) – could be fitted to measurements of *light2** over the duration (excluding the outlier at Day 24).

Figure 6.9. The status of measurable (a) C and (b) N variables during incubation of soil and straw (points) and their simulation by the parameterised model (lines)

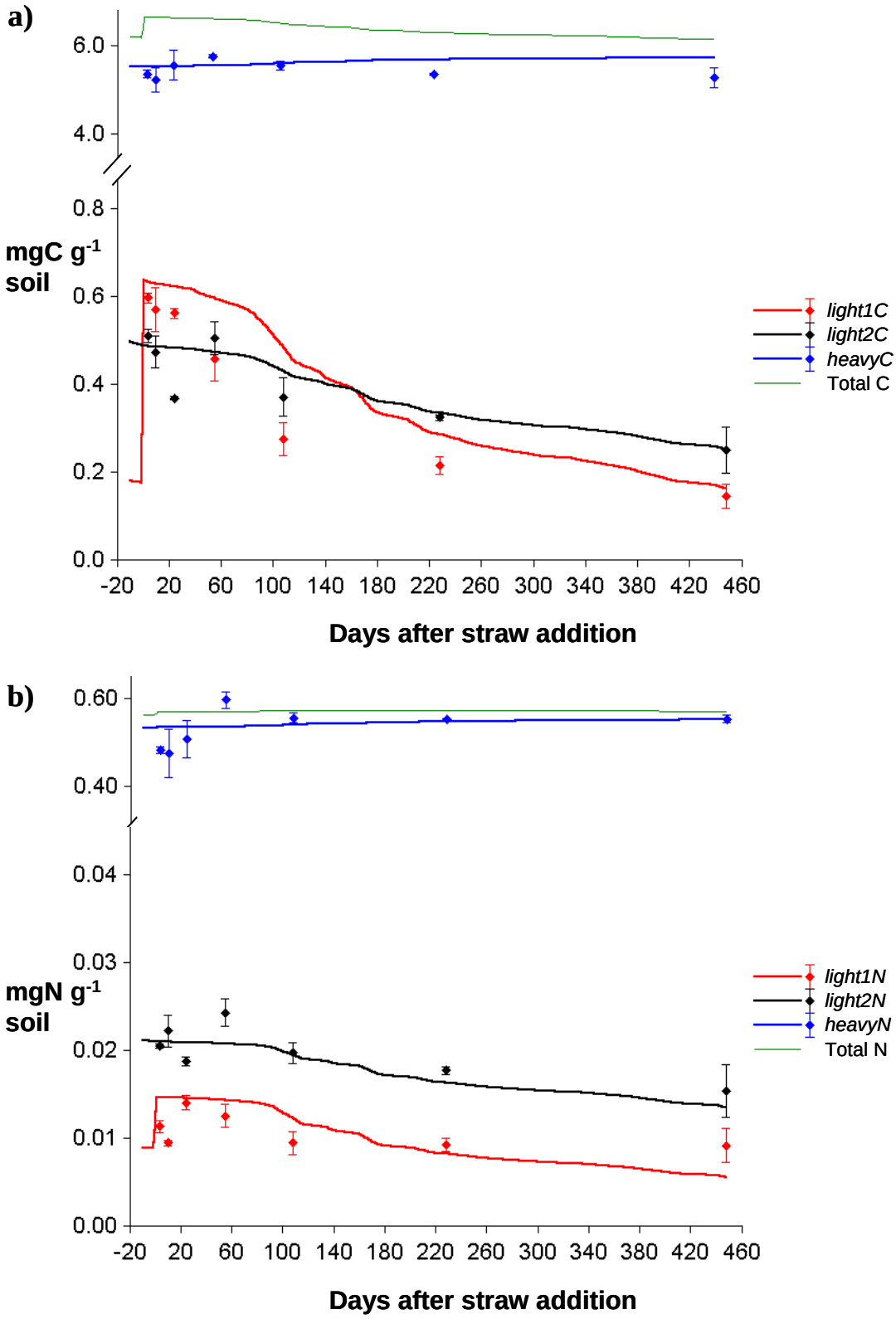

The model largely succeeded in reconciling the contrasting dynamics of C and N in *light1** and *light2** (Figure 6.9.b) (the decline in *light1N* for example was approx. 30 %, against approx. 45 % for C; Figure 5.5. and 5.3.). In the absence of further organic inputs (and N fixation flows set to zero), the simulated influences on the C-to-N ratio of FREE organic matter (*ρlight1*) were the associated microbial biomass, and N limitation (which results in relative depletion of substrate N). ***Bug*** was important in governing the dynamics of C-to-N within fractions since – reflecting its low, fixed C-to-N ratio – it was a proportionally greater component of *light1N* than *light1C* (see Figure 6.10.). The dynamics of *light1N* are therefore more sensitive to the dynamics of ***Bug***. With a lower absolute decline in ***BugC*** than *light1C*, the C-to-N ratio may increase (the dynamics of ***Bug*** are discussed in a later section). The C-to-N of other fractions (such as INTRA-AGGREGATE organic matter) may be further influenced by C-dominated relocation flows, and N-enriched mortality flows from ***Bug*** (see Section 4.2.3.). In addition, relocation-N flows from substrates with low C-to-N increase with N-limitation (see Section 4.2.5.). The measured differences in the dynamics of C and N are compared, through simulation of their C-to-N ratios, in Figure 6.11. The simulated accumulation of C in the ORGANOMINERAL fraction was not reflected in experimental measurements (Figure 6.9.a), and could not be overcome whilst maintaining correct simulation of total soil N (Figure 6.9.b).

Dynamics of tracer C and N

If ***LF1*** was homogeneous in it reactivity, there would be only minor change in its isotopic composition in the absence of further inputs. It was therefore fundamentally problematic to fit the current model to the $\delta^{13}C$ and ^{15}N data for FREE organic matter

Figure 6.10. The relative magnitude of measurable (a) C and (b) N variables (solid lines) and the model compartments to which they approximate (dashed lines), simulated by the parameterised model

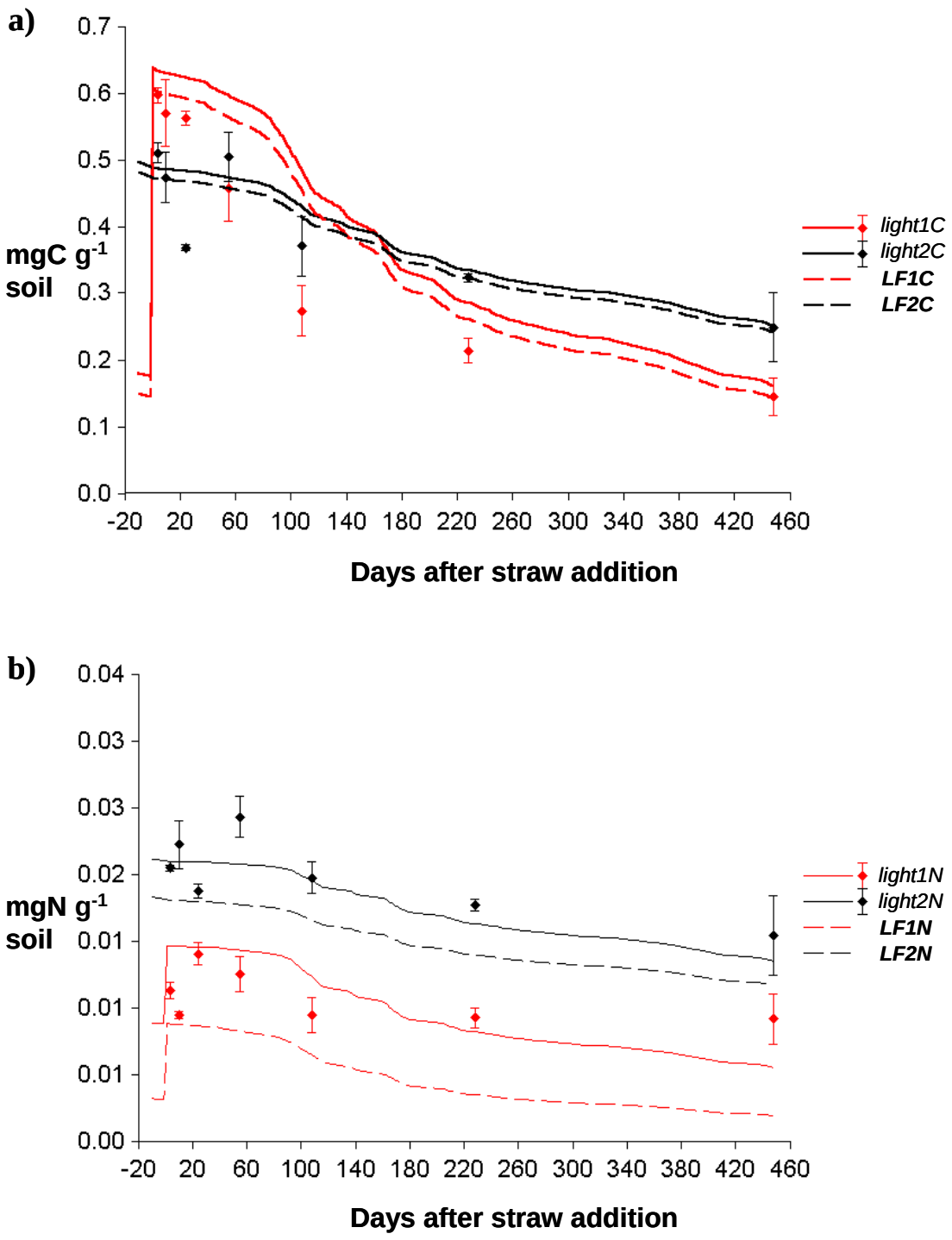

Figure 6.11. The simulated status of variables reflecting the ratio in the C and N content of the standard SOM fractions during incubation of soil and straw

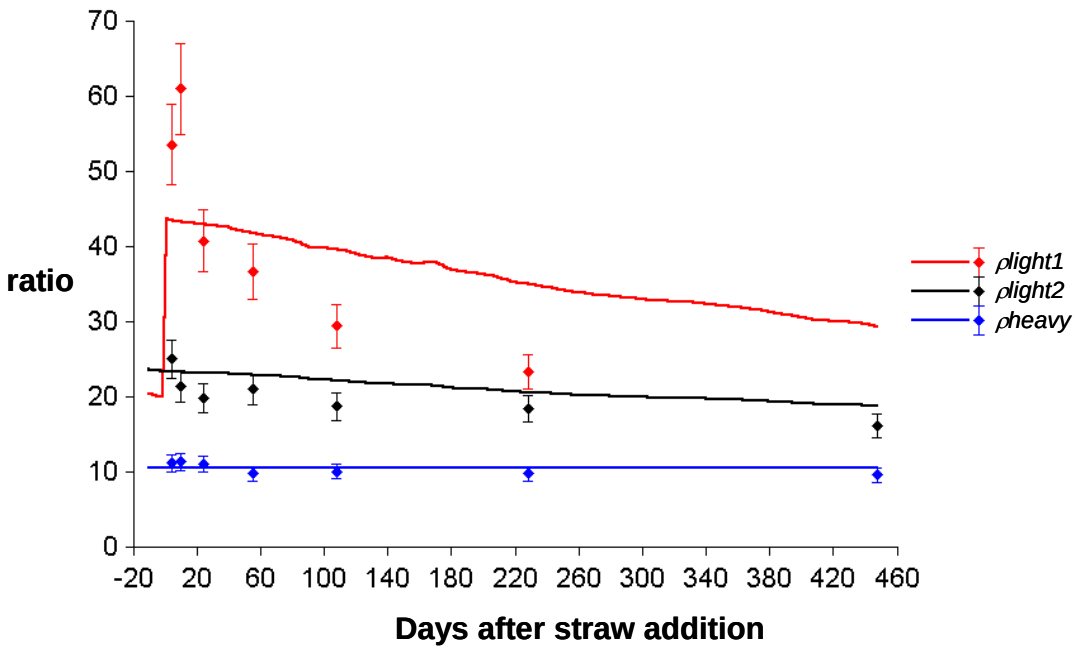

Figure 6.12. The simulated status of variables reflecting the C isotope ratio ($\delta^{13}C$) of the standard SOM fractions during incubation of soil and straw

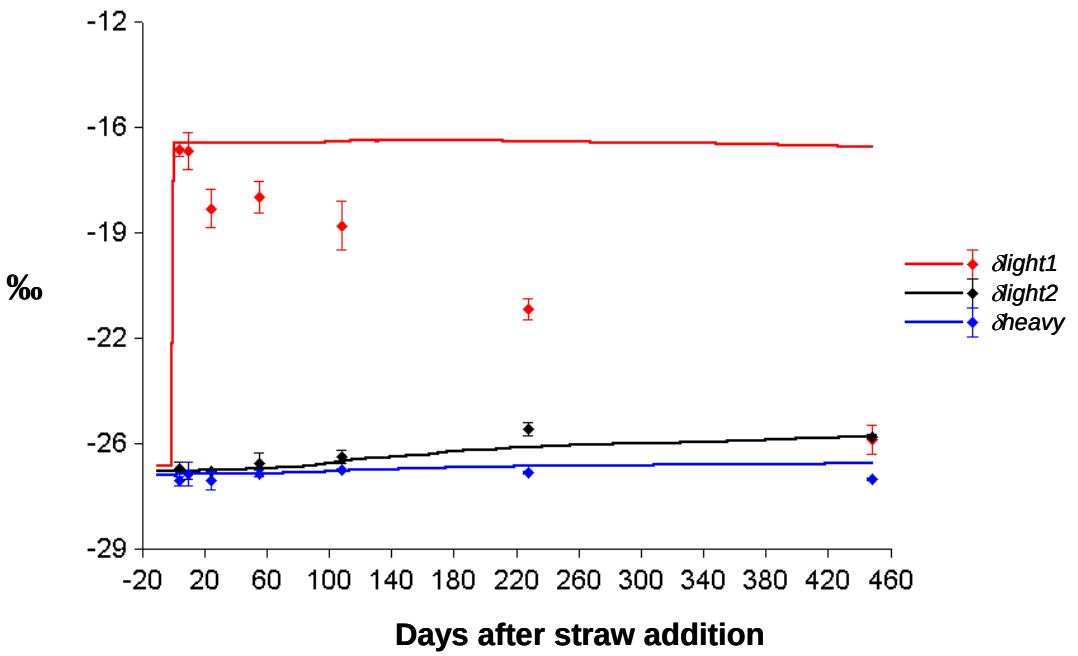

(*light1**), highlighting the contrasting behaviour of native C and N added in maize straw (Figures 6.12. and 6.13; see also figures and discussion in Chapter 5). This was accentuated by the fact that only 8 % of *light1*^{15}N was native, and none of the C_4 influence (see Figures 5.6. and 5.4.). With a rapid decline in the enrichment of input fraction, the continuing transfer of enrichment simulated by the model did not occur in the incubation experiment. The effect less apparent for the C and N data since approx. 45 % of C and approx. 75 % of N in *light1* was native. The magnitude and enrichment of ***Bug*** associated with ***LF1*** – as the only external influence on the composition of *light1* – differed slightly from that of ***LF1***. The inability to reconcile the high reactivity of the labelled maize component was probably compounded by the stability of native *light1*. In Section 6.3.7 the optimised model is applied to the data from the non-amended soil i.e. soil containing only native *light1*, to establish whether this component has greater homogeneity and thus compatible with a model assuming constant average reactivity (*k*) within compartments. The possibilities for overcoming the limitation of variable reactivity within *light1* are discussed in Chapter 7.

6.3.4. Simulation of *Sol* and *Bug*

The independent measurements of mineral N, total soluble organic C, and microbial C and N are plotted against their model equivalents or analogues in Figure 6.15. (the relationship between ***BugC*** and ***BugN*** is fixed, according to the value of ρbug). The simulated dynamics of ***SolN*** were of particular significance since they determined the onset of N-limitation by exhaustion of supplementary N supply, and hence govern the scaling down of C flows to ***Bug***. The simulation of ***SolN*** (representing the N soluble in NaI) did not tie precisely with measured mineral N, although both were

Figure 6.13. The status of measurable (a) ^{13}C and (b) ^{15}N variables during incubation of soil and straw and their simulation by the parameterised model

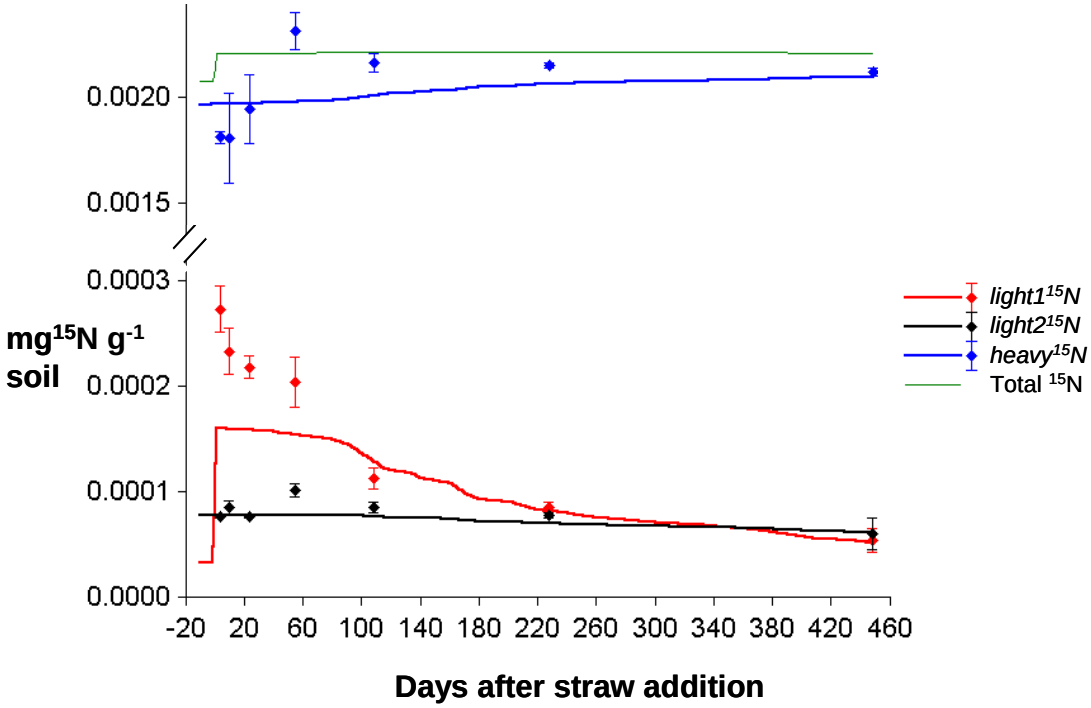

Figure 6.14. The simulated status of variables reflecting the measured N isotope ratio of the standard SOM fractions during incubation of soil and straw

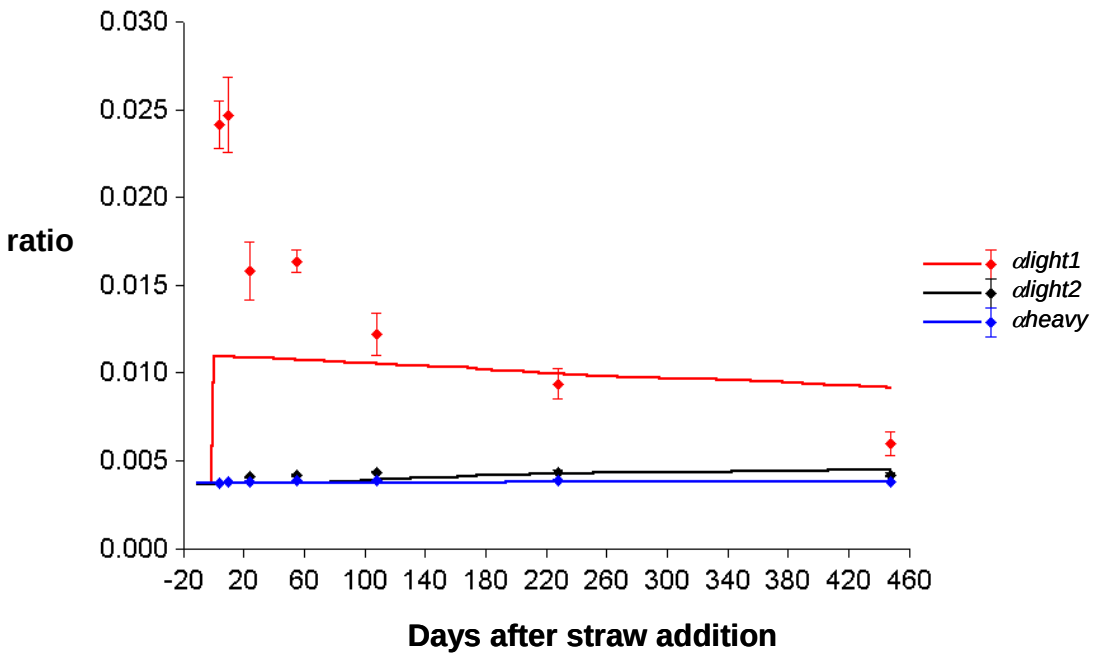

negligible mid-incubation. The simulated dynamics showed ***SolN*** depleted by Day 95 whilst for mineral N this appeared to occur between Day 107 and Day 224 (following a rapid decrease between Day 52 and Day 107). The precise timing of the depletion was difficult to ascertain due to the period between measurements. Due to the importance of ***SolN*** in controlling N limitation, surrogate measurements (such as mineral N) are not ideal for verification of this mechanism. The simulation of ***BugC*** agreed quite well with measurements of microbial biomass, which is a direct model equivalent. However, ***BugN*** was not well simulated due to the assumption of fixed microbial C-to-N ratio.

6.3.5. Simulation of measured processes

Gross N mineralisation

The simulated rates of gross N mineralisation during the incubation (Section 4.2.5.) are compared with occasional measurements using the isotope dilution technique (Section 5.2.3.1.) in Figure 6.16. The effect of the changing balance between SOM fractions was masked by large day to day variation in the status of the soil temperature and moisture modifiers. The match between simulated and measured rates was heavily dependent on the estimate of environmental conditions for the relevant 3-day measurement period. On this basis it was difficult to conclude whether measured rates of gross N mineralisation were in basic agreement with model prediction. The most obvious deficiency in the model simulation was the absence of the initial measured peak, which could be partly due to the status of the modifiers in the relevant period.

Figure 6.15. Simulation of variables approximating to independently measured microbial and soluble C and N during incubation of soil and straw

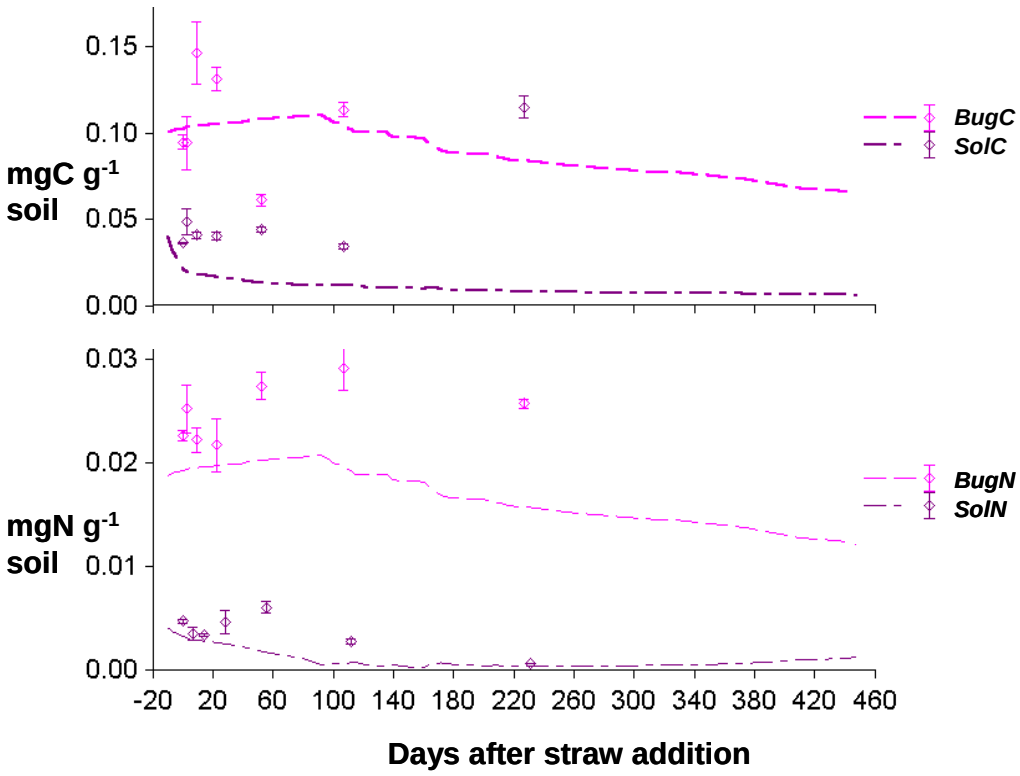

Figure 6.16. The simulated status of gross N mineralisation rate (*GNM*) during incubation of soil and straw, plotted against experimental measurements

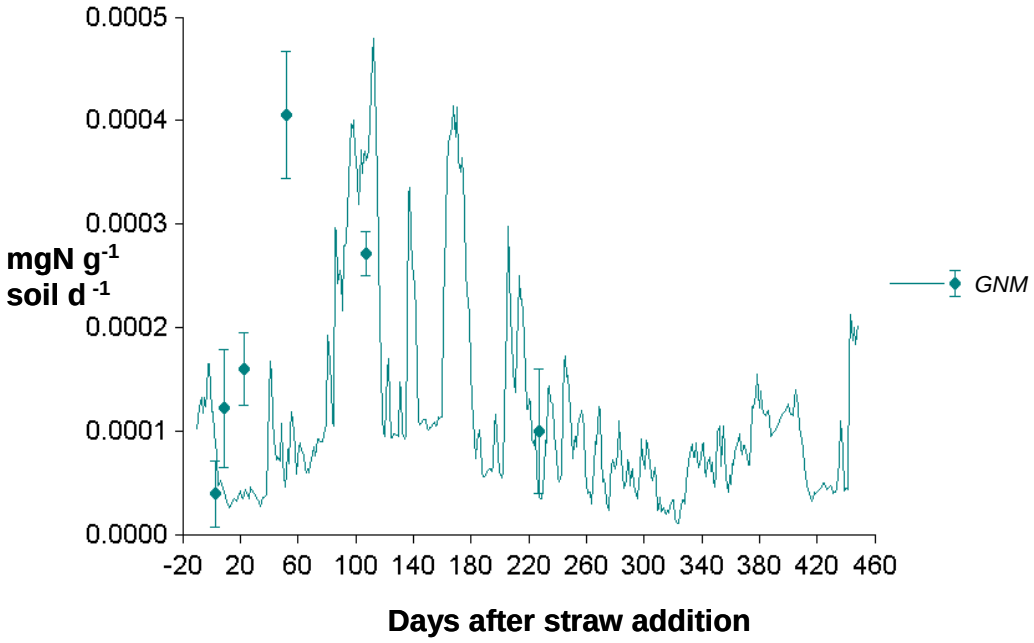

To compare the relative, simulated contribution of each SOM fractions to gross N mineralisation, the sum flow from compartments other than ***Bug*** were divided (Figure 6.17.). The ***LF1*** compartment was a declining source of mineralising N, its contribution to the non-mortality flows declining from 38 % immediately after the incorporation of maize straw, to 15 % at Day 448. The other sources – of which ***LF2*** was the largest – increased in relative terms. A perturbation to these trends occurred mid-simulation through N limitation: the contribution from substrates with high C-to-N ratio (ρ*), and relocation flows from compartments of low ρ*, being enhanced.

CO_2 production

The model did not well reflect measured rates of CO_2 production, and failed to simulate an apparent peak in activity during the first few days of the incubation (Figure 6.14.). If the initial peak resulted from rapid utilisation of soluble C (Section 6.3.1), simulation could be improved relatively by introducing a split-input compartment similar to that proposed by Christensen (1996). Initial underestimation of CO_2 production is also apparent when the cumulative data is plotted (Figure 6.19.), and may be attributable to the status of the combined rate modifier during this period (Figure 6.6.). A divergence in cumulative CO_2 production is also apparent in the latter stages of the incubation when the status of the temperature modifier increased.

6.3.6. Sensitivity analysis of model parameters

The optimised parameter values were listed in Table 6.3. Due to the sensitivity of r^2 to the specific combination of values for the key parameters, the sensitivity of the

Figure 6.17. The simulated contributions of flows other than microbial mortality to gross N mineralisation during incubation of soil and straw

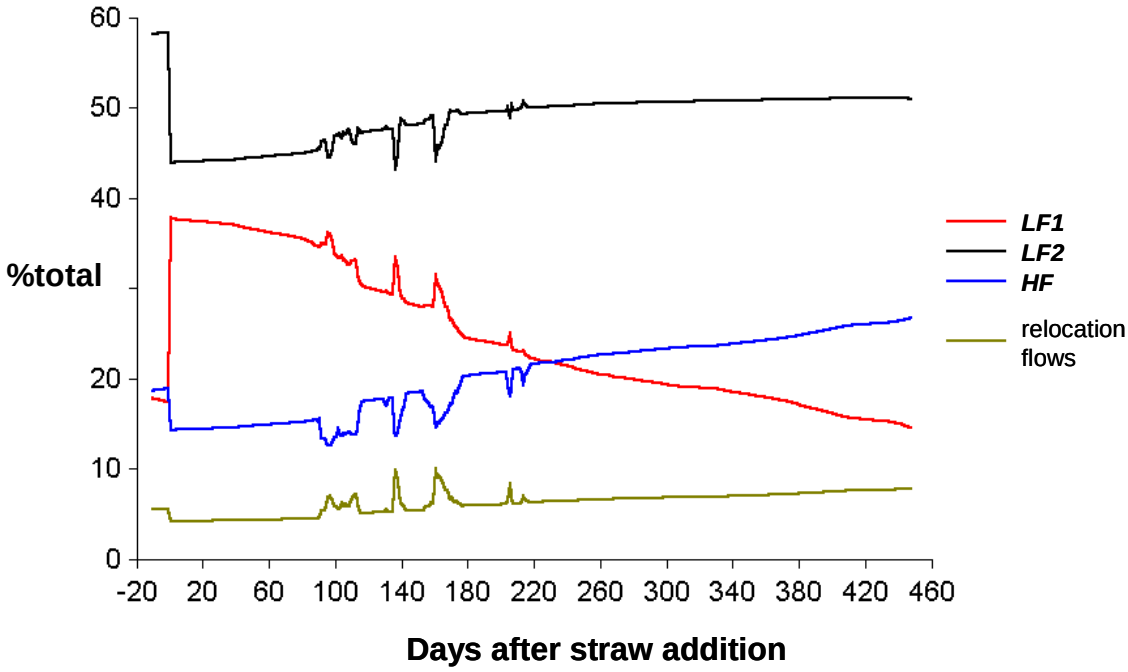

Figure 6.18. Simulated rates of CO_2 production during incubation of soil and straw, plotted against experimental measurements by NaOH trapping

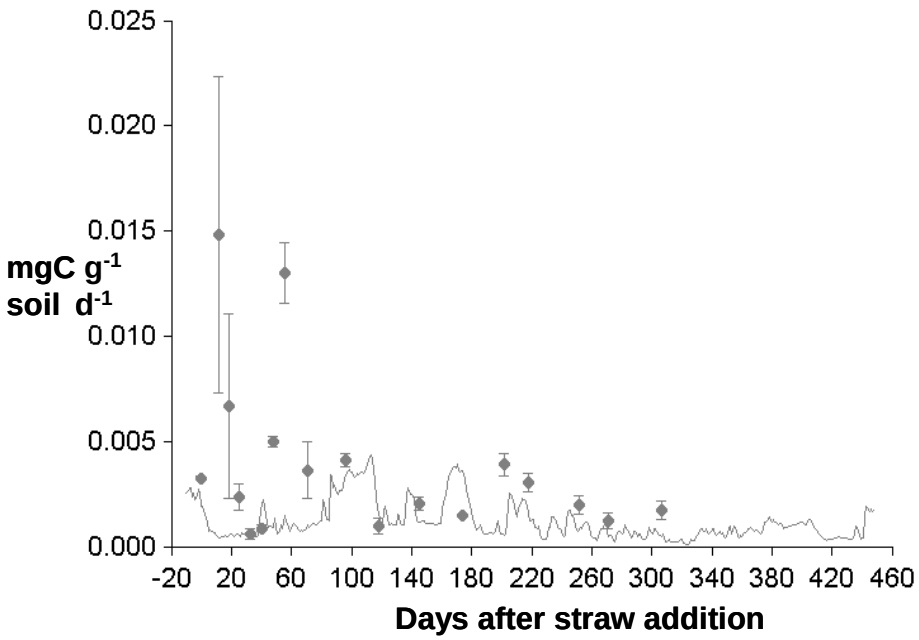

Figure 6.19. Cumulative CO_2 production simulated by the parameterised model, plotted against that calculated from periodic rate measurements

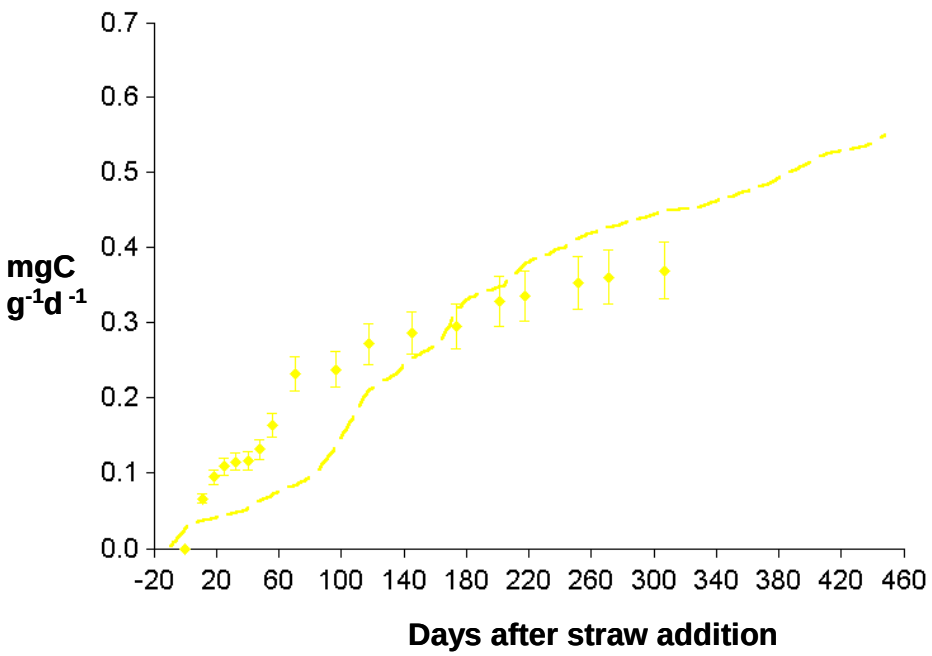

model output was assessed visually using *light1C* and *light2C* as dynamic test variables. The results of the tests are shown in Figures 6.20. to 6.24. The parameters of major influence were η, representing microbial incorporation (Figure 6.20.), and to a lesser extent *kmort* (microbial mortality rate) and ρ*bug* (microbial C-to-N ratio) (Figures 6.23. and 6.24. respectively). The model did not appear particularly sensitive to the initial value of ***Bug*** or ***Sol***, or to α (the respiration coefficient) which has a large influence on the C respired per unit of N mineralised (with implications for CO_2 production).

Compartment size and gross N mineralisation

To examine the effect of compartment size (and hence measurements of SOM fractions) on N mineralisation, the optimised model was run with the temperature and moisture rate modifiers set to 1·0. This excluded the noise in the data resulting from day to day variation in the climatic conditions (see Figures 6.6. and 6.16). The Day 0 magnitude of *light1** (native FREE organic matter that added as maize) or *light2** were independently changed to assess the effect on gross and net N mineralisation. Doubling *light1** increased cumulative gross N mineralisation by 35 % and halving it decreased mineralisation by 18 % (integrated over the duration of the simulation from Figure 6.25.a). The effect of altering *light2* was less, resulting in a corresponding 28 % increase and 20 % decrease respectively (from Figure 6.25.b).

Simulation of non-amended soil fractions

To further examine the contrasting reactivity of the native and added components of *light1** the model, optimised using the data from the maize straw

Figure 6.20. Sensitivity of optimised model simulation (solid lines) to the microbial incorporation constant η (with respect to key measurable variables)

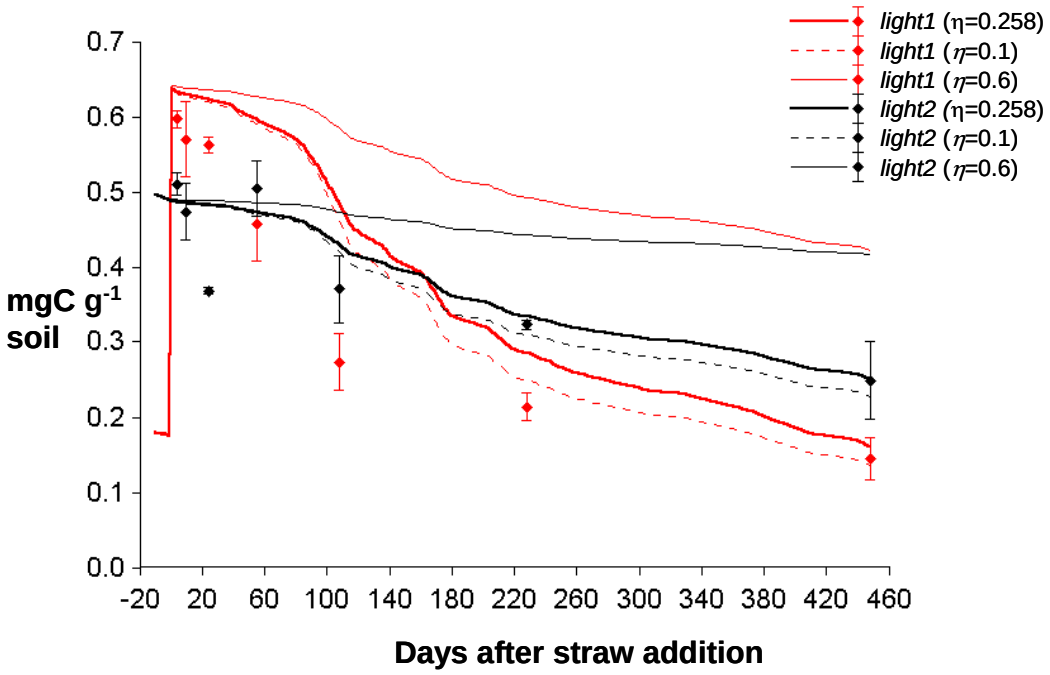

Figure 6.21. Sensitivity of optimised model simulation (solid lines) to the microbial incorporation constant α (with respect to key measurable variables)

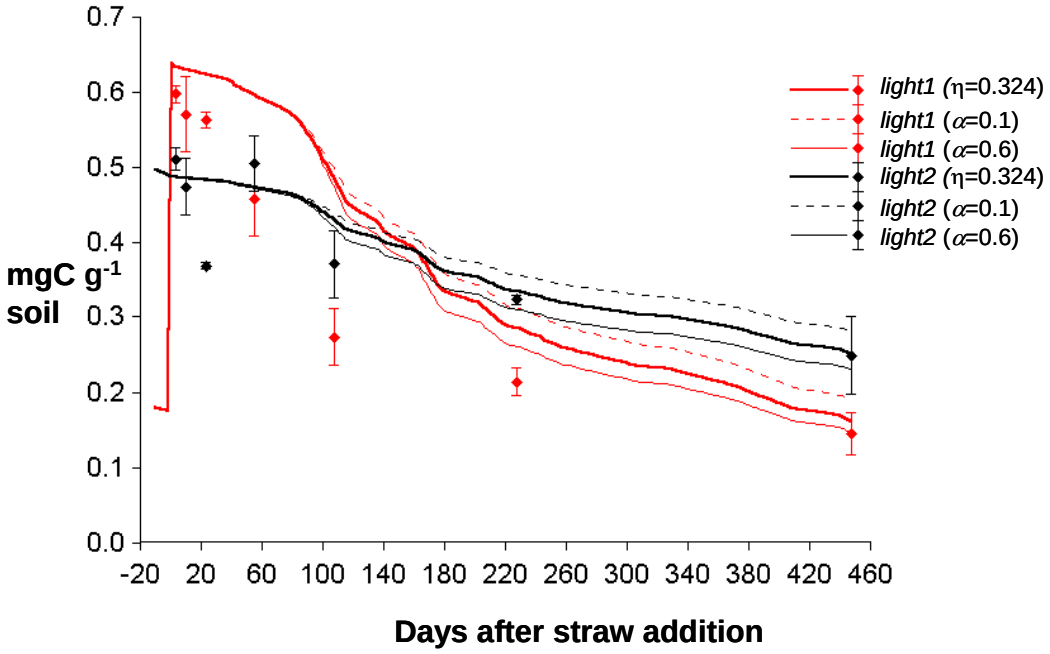

Figure 6.22. Sensitivity of optimised model simulation (solid lines) to the initial magnitude of the soluble N fraction (with respect to key measurables)

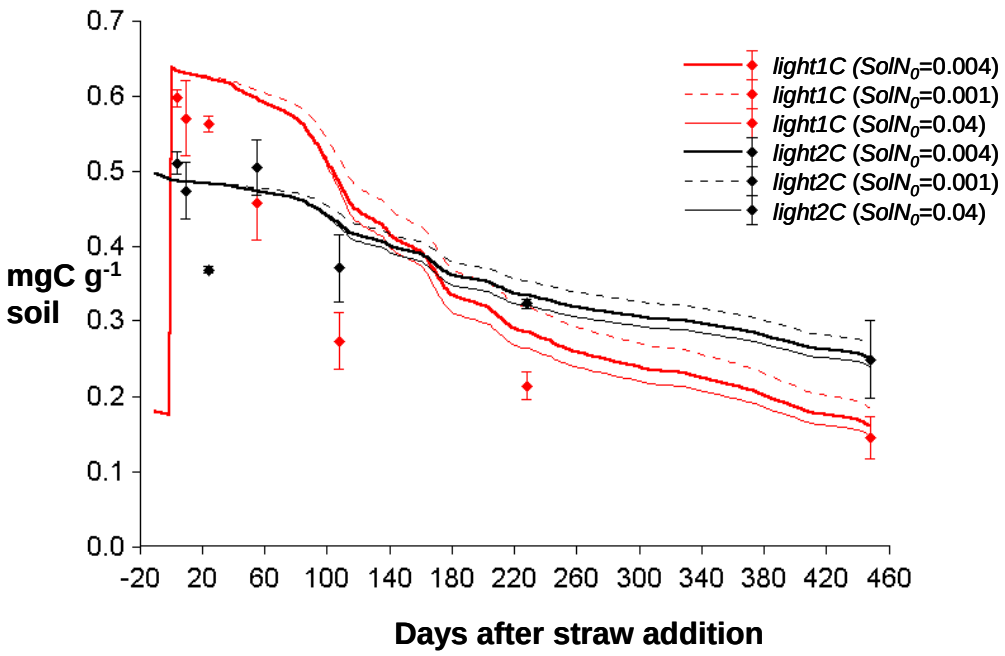

Figure 6.23. Sensitivity of optimised model simulation (solid lines) to the intrinsic mortality rate of microbial biomass (with respect to key measurables)

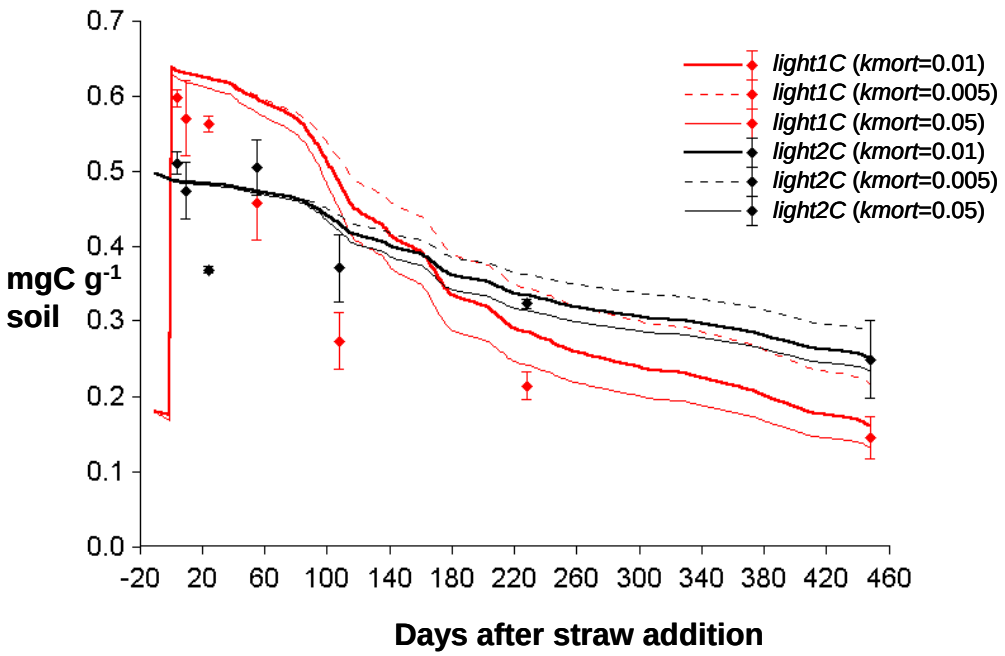

Figure 6.24. Sensitivity of optimised model simulation (solid lines) to microbial C-to-N ratio (with respect to key measurable variables)

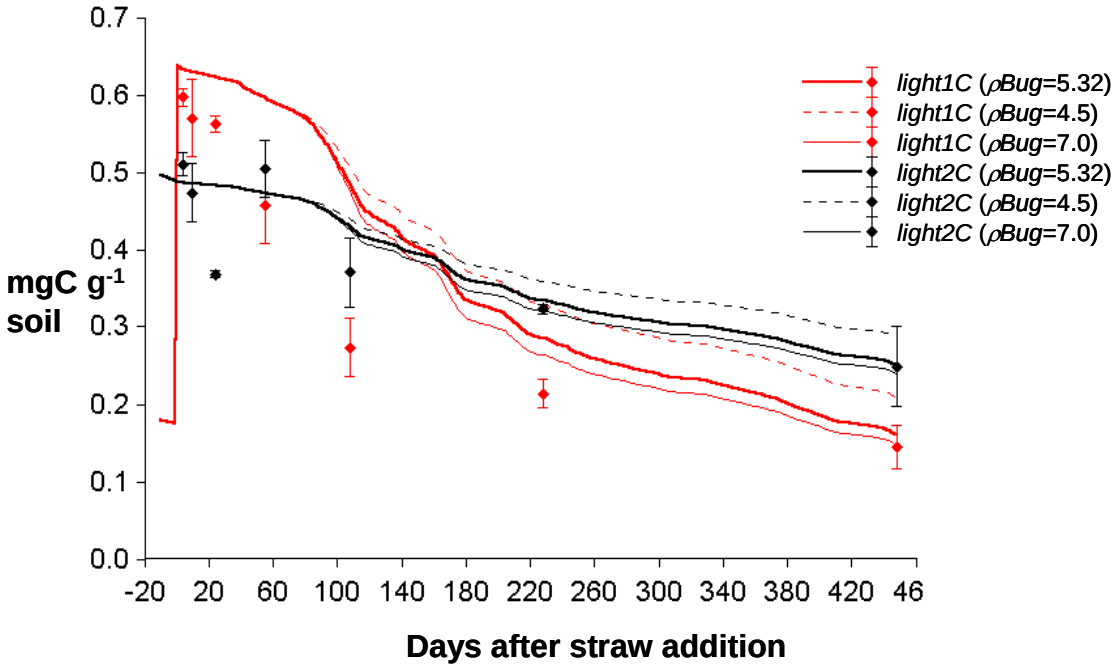

Figure 6.25. Sensitivity of gross and net N mineralisation simulated by the parameterised model (under standardised conditions) to variables representing the initial magnitude of (a) FREE and (b) INTRA-AGGREGATE fractions

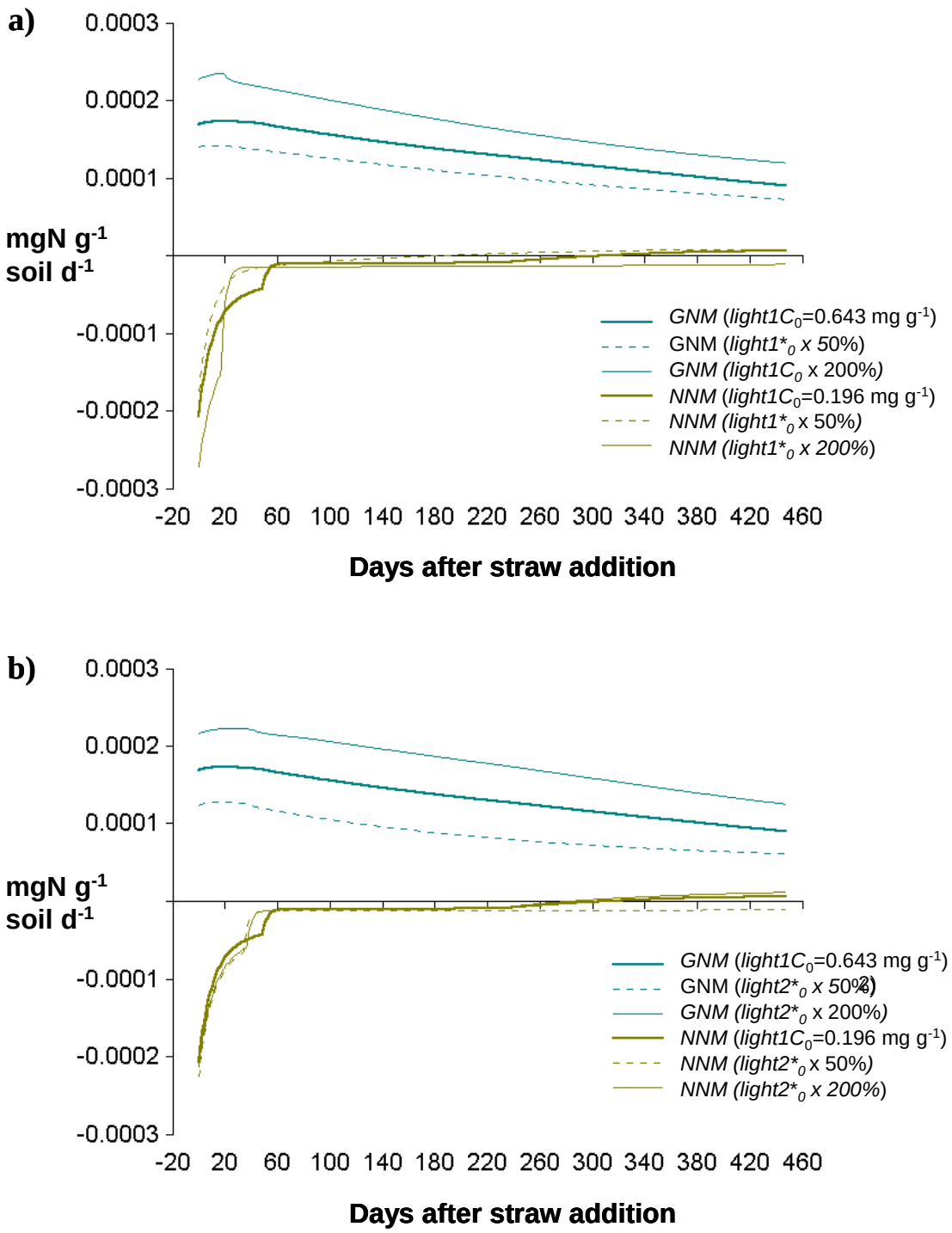

Figure 6.26. The status of measurable (a) C and (b) N variables during soil incubation without straw and their simulation by the parameterised model

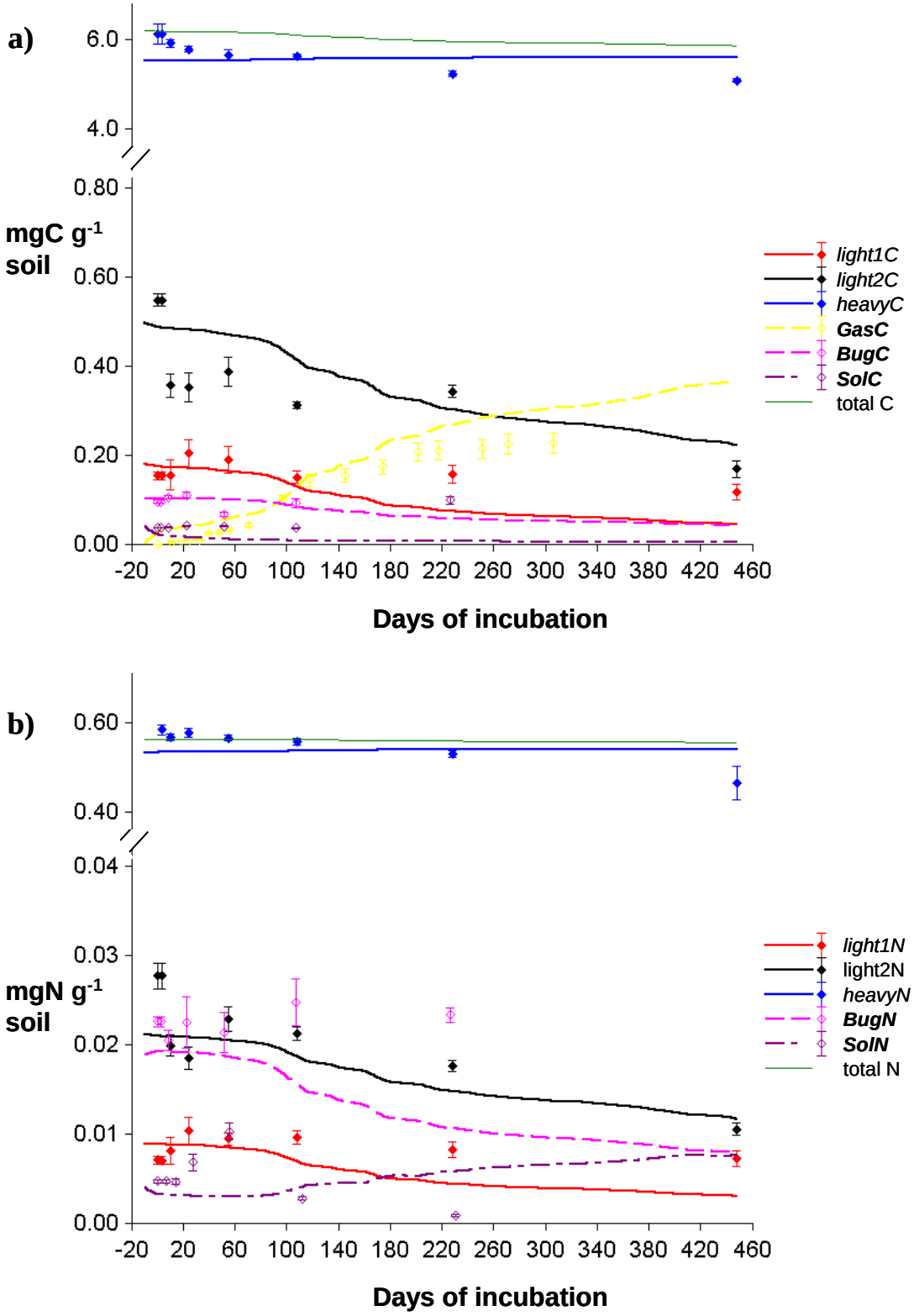

treatment, was applied to the equivalent dataset for the non-amended soil, which contained only native SOM (Figure 6.26). The same climate data was used, but there was no input of new organic matter to the soil. For this data, the model simulated rather well the dynamics of C, and especially N, in *light1** and *light2**. However, it failed to simulate the measured decline in *heavy**. Rates of CO_2 production was better simulated than for the maize treatment, according with the better fit with the fractionation data.

6.4. Conclusions

The parameters invoked in the mathematical model (Chapter 4) were optimised against the data from the maize straw decomposition experiment from Chapter 5. Although the parameterised model was able to simulate the dynamics of certain compartments and seemingly N limitation, the simulation of *light1** (corresponding to FREE organic matter) proved problematic. This resulted from the contrasting reactivity of native and maize-derived components, a difficulty magnified in attempting to simulate the tracer data. There is good potential however, for the parameterisation to be improved with relatively straightforward amendments to its structure, notably the division of inputs between several compartments (of contrasting reactivity). The suitability of the rate modifiers used to account for variation in soil temperature and moisture should also be examined: their short-term variation appeared to mask the ability of the model to simulate soil processes.

CHAPTER 7: GENERAL DISCUSSION AND FUTURE WORK

The objective of this research was to parameterise a model based on measurable SOM fractions. This has previously been identified as the most promising means to overcome the limitations of existing C–N models (Molina *et al.* 1994; Christensen 1996b; Elliott *et al.* 1996; Smith *et al.* Submitted). Measurable fractions permit direct initialisation of the model at any location (by experimental measurement), and potentially a more mechanistic simulation of decomposition processes (Molina *et al.* 1994; McGill 1996). Suitable fractions should be small in number (to confer robustness), sequentially isolated (and thus mutually exclusive), and collectively account for all C and N in the system (to aid parameterisation). Each should display differences in chemical composition that are consistent across soils (to justify the assumption of fixed reactivity, *k*, within compartments), at least two should be dynamic on a relevant timescale (to provide relevant output),

The physical fractionation method proposed in Chapter 2 uses a sequential two-stage density separation to divide SOM into three components by its associations with aggregates or mineral particles. FREE organic matter is obtained by flotation at a separation density of 1·80 g cm^{-3} after minimal soil dispersion, INTRA-AGGREGATE organic matter by flotation at the same density after disruption of aggregates, and ORGANOMINERAL fraction as the residual heavy material. The only unmeasured fraction is that organic matter which is soluble in the NaI separation medium, although methods to measure this are also under development.

Being separated by a physical rather than chemical procedure, measured differences in the composition of the fractions should reflect their *in situ* reactivity. In an analysis of 26 soils from eight long-term sites, the FREE and INTRA-AGGREGATE fractions were not only found to significantly differ in five of the eight categories of C measured using the ^{13}C NMR, but that the differences were much greater than those within fractions resulting from contrasting management. This finding suggested that FREE and INTRA-AGGREGATE fractions display distinct and relatively consistent levels of reactivity, and lie between theoretical gaps in the decomposability continuum (Balesdent *et al.* 1987; Molina *et al.* 1994). Thus, the mechanistic model based on the measured fractions (Chapter 4) retained the conventional assumption of fixed reactivity within compartments. Unreported monitoring of the fractions in the field, as well as in the incubation experiment (Chapter 5) showed that both light fractions are dynamic on a seasonal time scale, and thus relevant to crop nutrient supply. Similar dynamics have also been reported for particulate organic matter fractions e.g. Magid *et al.* 1997; Cadisch *et al.* 1996.

In the incubation experiment ^{15}N-labelled maize was introduced to the soil to precipitate an observable episode of mineralisation activity. FREE organic matter was found to comprise components of contrasting decomposition kinetics, effectively an active maize-derived component and a stable native one. The decline in the reactivity of this fraction over time proved a fundamental problem in parameterising the model (in view of its the assumption of fixed k). The tracer data did not enhance the optimisation by providing additional constraint as anticipated, but instead weakened the general agreement obtained with the model.

Heterogeneity of FREE organic matter

The incubation of soil without added plant material showed that a component of FREE organic matter turns over very slowly. It has been postulated that light fractions (including FREE organic matter) may contain charcoal, and this has been observed in soils with a history of forest burning (Cadisch *et al.* 1996; Golchin *et al.* 1997; Skjemstad *et al.* 1999). However more limited quantities of charcoal may result from stubble burning. Indeed, the measurable-compartments model proposed by Christensen (1996) featured a light sub-fraction to represent "inert SOM…charcoal etc, not firmly associated with soil minerals". The soil incubated in this study was also from a site that might – on the basis of direct observation as well as circumstantial evidence such as slightly elevated C-to-N ratio – contain rather large amounts of charcoal. Unfortunately, the well defined ^{12}C NMR peak assignment for charcoal is overlapped by other aromatic peaks in solid-state spectra so this could not be confirmed (the NMR spectra in Figure 2.6.a are for fractions taken from an adjacent plot.

Although Elliott *et al.* (1996) have suggested recovery of charcoal may limit the applicability of density methods to modelling, measurement methods have been proposed, most recently a method based on UV oxidation. This has already been used to examine the influence of charcoal on the ^{13}C NMR spectra of physical SOM fractions by spectrum subtraction (Skjemstad *et al.* 1999; Smernik *et al.* 2000). If charcoal is found to be a major constituent of the stable FREE sub-fraction, these methods could enable a modified model containing a biologically inert compartment (similar to the inert organic matter compartment in the RothC model; Coleman and Jenkinson 1996) to be parameterised and run.

However, data from the incubation experiment did not support the charcoal explanation. The C-to-N ratio of the stable sub-fraction (≈ 20) was similar to that of typical crop inputs, and also the INTRA-AGGREGATE fraction (C-to-N ≈ 18) which was both active and homogeneous (in composition and reactivity). The C-to-N ratio of the stable fraction also changed over time (Figure 5.8.), suggesting some limited mineralisation activity. Thus an alternative explanation is that biological competition for N leads to certain, more recalcitrant C substrates become excluded from decomposition, a theory which can be tested by conducting incubations with soil supplied with supplementary N (Trinsoutrot *et al.* 2000). In the absence of continuing inputs above or below ground, the stable component of FREE organic matter would become more apparent. The zero N plot on Broadbalk continually receives minimal organic matter inputs and should therefore contain proportionally more stable FREE material. This was demonstrated through ^{13}C NMR analysis, which showed a greater proportion of recalcitrant C groups.

Nevertheless, even disregarding the most stable component of FREE organic matter, the isotope tracer data suggested the reactivity of the fraction may change substantially following a fresh input of organic matter. Simulation of the parameterisation data would be improved by incorporating a separate input compartment, from which organic matter is partitioned into a number of others, including the soluble fraction. Such division is standard in existing models (McGill 1996; Molina and Smith 1997), for example metabolic versus structural in CENTURY (Parton *et al.* 1987) and decomposable versus resistant in RothC (Coleman and Jenkinson 1996). However, this increases the number of optimisable parameters, and a

more robust approach would be to change the mathematical description of decomposition kinetics for the compartment representing FREE organic matter. This could involve time-dependent change in *k* (see below) or the use of second-order equations (Whitmore 1996). It has already been shown that a second-order equation can considerably improve the prediction of short-term CO_2 release from substrate decomposition (Alvarez and Alvarez 2000).

The use of the tracer data in model parameterisation

A combination of isotope tracers and measurable compartments should provide maximum constraint for model optimisation. However, the ^{15}N enrichment of FREE organic matter decreased much more rapidly than total N after the addition of labelled maize straw. Although some differential ^{15}N enrichment of the maize may have resulted from its pulse labelling (after sowing), the assumptions of homogeneous labelling and zero isotopic fractionation were probably not a significant explanation. Rather, heterogeneity of the FREE organic matter was the cause. The model assumes that the mean reactivity of corresponding N and ^{15}N compartments is equal, whilst 92 % of the added ^{15}N was maize-derived (see Section 5.3.3.) and the majority of N in native, apparently recalcitrant, SOM. The relative dynamics of N and ^{15}N highlighted a disparity between the two components, and fundamentally limited the ability to fit the tracer data. It was the significant factor compromising the r^2 for the optimised model against parameterisation data ($r^2 = 0.40$). For C the trace was at levels of natural abundance ($\delta^{13}C$) and pulse labelling was not a factor. However, a similar disparity between the dynamics of native and added C and ^{13}C in the FREE organic matter.

Comparison of compartment reactivity

The optimised *k* values are provisional pending possible amendments to model structure as outlined above, but are comparable to those of functionally analogous compartments of existing models. Unusually, however, the *k* values for three of the model compartments (***LF1***, ***LF2*** and ***Bug***) fall within a single order of magnitude, albeit in the range encompassed by those of other models i.e. $0.05 > k > 0.005$ d^{-1} (Molina *et al.* 1994). Interestingly the optimised values for *kLF1* (0.0040 d^{-1}) and *kLF2* (0.0023 d^{-1}) correspond to those inferred for similar fractions in a field study (also in sandy loam soil; Gregorich *et al.* 1997). Conceptual compartments in existing models of similar reactivity to ***LF1*** or ***LF2*** include active SOM in CENTURY (Parton *et al.* 1987), added organic matter (AOM1) in DAISY (Mueller *et al.* 1996), resistant active C–N materials (van Veen *et al.* 1984), active fraction (Paul and Juma 1981) and Pool II (resistant) in NCSOIL (Molina *et al.* 1983). The ***LF1*** compartment had a lower reactivity than decomposable non-protected SOM (Paul and van Veen 1978), and the easily decomposable fraction (van der Linden *et al.* 1987). Their reactivity also overlapped with those of microbial compartments in other models.

Many models feature microbial biomass compartments with a similar reactivity to that determined for ***Bug*** ($k = 0.01$): microbial biomass (Paul and van Veen 1978; van der Linden *et al.* 1987; Paul and Juma 1981), unprotected microbial biomass (van Veen *et al.* 1985), biomass developed on available substrate (van Veen *et al.* 1985), and non-protected microbial biomass (Gunnewick 1996). However, three of these models possess additional microbial compartments with contrasting reactivity. The biomass

compartment of the RothC model has a considerably slower turnover (Coleman and Jenkinson 1996), presumably due to the lack of an alternative intermediate-turnover compartment.

On the basis of model output, both ***LF1*** and ***LF2*** were significant, contrasting contributors to mineralisation flows (see Figure 6.17.) suggesting that compartments with rather small differences in *k* can be useful in simulation of medium term C–N dynamics. That the sub-division of relatively active compartments is necessary to achieve this using existing models tied to experimental measurements is consistent with this view (Sitompul *et al.* 2000). In fact it may be more important to establish whether the model has sufficient compartments to predict longer term changes in SOM, the lowest *k* value in the model (assigned to ***HF***, and approximating to the ORGANOMINERAL fraction) equates to a mean residence time of approx. 55 y. However, this reactivity is actually close to that of the humus compartments in RothC (Coleman and Jenkinson 1996), and compares with old organic matter (van Veen *et al.* 1985) or recalcitrant organic matter (van der Linden *et al.* 1987). Indeed C–N models designed for annual simulations and fertiliser recommendations e.g. SUNDIAL (Smith *et al.* 1996), feature lower-reactivity compartments, with mean residence times of between 44 days and approx. 5 y. The ^{15}N tracer data from the soil–straw incubation suggested that silt- and clay-size ORGANOMINERAL sub-fractions display contrasting dynamics. For longer-term simulations it may prove useful to model them separately. If this further modification is made, the model structure will closely resemble that originally proposed by Christensen (1996).

A few models have used conceptual compartments in which reactivity *k* changes as a function of time e.g. Russel (1975). This is a mathematical device to deal with varying reactivity that, taken to extremes, leads to the cohort approach of Bosatta and Agren (1996). However, in a model where key variables are measurable, there is potential for establishing a pre-defined change in reactivity experimentally. An analytical approach for defining time-dependent relationships for *k* from fractionation data has been proposed by Arah (2000). This data must comprise C, N and tracer measurements in mutually exclusive model compartments that account for all soil C and N. This is highly compatible with the fractionation method implemented in this thesis, providing a method for measuring the soluble fraction can be established.

Parameters and control mechanisms in the optimised model

A few models treat microbial biomass as a catalyst for SOM decomposition, and do not feature a discrete microbial biomass compartment e.g. SOMM (Chertov and Komarov 1996). Although the model described here required additional optimisable parameters to define the physical distribution of biomass between measured fractions ($\beta LF1$ and $\beta LF2$), microbial activity enabled mechanisms for modelling the C-to-N ratio of SOM fractions, the effect of limiting N, and the physical relocation of substrate residues. In the current model, the location of substrate is assumed to change with their partial utilisation, and hence without incorporation into microbial cells. Flows of "residual, partly processed material" were part of the model structure proposed by Christensen (1996), and will be important for the modelling of SOM protection and aggregate formation and turnover (Gregorich and Janzen 1996; Tisdall 1996). This type of flow is unconventional, but may be considered analogous to the direct flows between

surface structural and slow compartments in CENTURY (Parton 1996). The proportion of substrate C that is not directly transferred to another SOM compartment (in relocation) or respired, but incorporated into microbial biomass should be reflected in the optimised value of η (0·26) (the respired fraction, α, was evaluated as 0·34). If microbial efficiency is viewed as the incorporated portion of non-relocation flows, its value has been inferred – by parameterisation – to be 43 %. This is closer to existing estimates than that value reflected in η itself.

To minimise the number of invoked parameters, the partitioners for substrate flows ($\phi LF1$ and $\phi LF2$) were also applied to the relocation of microbial products (i.e. flows resulting from mortality). Implicitly, the relocation of microbial products is assumed independent of the initial, physical location. Although the distribution of biomass between locations was fixed (by $\beta LF1$ and $\beta LF2$), it was prevented from becoming too large a proportion of any measured SOM fraction by its own decline in the absence of sufficient substrate. The ^{13}C NMR spectra for INTRA-AGGREGATE fractions tended to show prominent peaks in the alkyl region indicative of lipids, and hence the presence of intact microbial cells (as well as microbial products). Methods for measuring the distribution of microbial biomass have already been tested (Monrozier *et al.* 1991; Alvarez *et al.* 1998), and could allow $\beta LF1$ and $\beta LF2$ to determined directly.

In contrast to that of C, complete acquisition efficiency was assumed for N, and was N-relocation only occurred where it is present in excess of the fixed requirement of the microbial biomass (reflected in the ρbug parameter). The mechanism for limiting C flow results in the acquisition efficiency of N in relative terms, in the absence of supplementary N (when demand exceeds supply in the system as a whole). This change

applies to all physical locations, even where a specific fraction contains N in excess of the microbial requirement. The mechanism also influences the ratio of corresponding C and N compartments, and hence the ability for the model to simulate measured changes in fraction C-to-N over time (it is more difficult to envisage fractions being isolated which define compartments of fixed C to-N ratio e.g. DAISY (Mueller *et al.* 1996), Verberne (Gunnewick 1996) and DNDC (Li 1996). The availability of supplementary N (as a portion of the soluble fraction) was – as is conventional in models without explicit consideration of soil structure – assumed universally accessible.

Simulation of processes

The nature and dynamics of individual model flows (including relocation) reflect important concepts, but cannot be quantified. Instead, robust parameterisation confers certainty to the simulation of modelled processes. Also, the sum of certain generic flows can be equated to measurable rate processes such as C respiration and gross N mineralisation. If good simulation of these processes is found, then the model can be used with greater confidence to interpret the relative contribution of different source compartments e.g. Figure 6.17. The rate modifiers for temperature and moisture strongly masked general trends attributable to the dynamics of substrate compartments, and their corresponding measured SOM fractions. Quantitative comparison of measurements and simulations was difficult, being sensitive to the precise status of the modifiers over the short measurement periods. The modifiers used in this study are based on empirical relationships developed for models that operate on a lengthier timestep (months rather than days). They may be ill suited to providing daily estimates not only because instantaneous response of microbial biomass is unrealistic, but because

monthly balances between evaporation and rainfall are less erratic than daily measurements which reflect individual rainfall events. The sensitivity of interpretation to the reliability of the rate modifiers provides a case for conducting future incubations under controlled conditions.

An important test of SOM models predicting soil N supply is the ability to simulate the dynamics of mineral N. In the current model, this is limited by uncertainty in the relationship between the soluble N compartment and the measured fraction (extracted by NaI during density fractionation). The model simulated the measured depletion of assimilable soluble N (invoking limitation to C flows), but the timing did not coincide with the measured exhaustion of mineral N measured by conventional K_2SO_4 extraction.

Future work

If modifications to the model the structure of the model and the kinetics of ***LF1*** lead to the expected improvement in description of the experimental data, there will be good reason to believe the model simulates processes and flows with a basis in reality. To be used in a predictive sense, robust relationships relating model parameters to soil type, tillage and crop and other site-specific variables will be required. Texture modifiers in existing models, usually defined as a function of clay content, implicitly recognise the importance of soil structural effects (Paustian 1994; McGill 1996) and the major or dominant influence of physical location on decomposition of SOM (Balesdent and Mariotti 1990). The fractions represented in the current model are defined by physical location, and thus directly sensitive to soil texture. The magnitude of the

fractions may differ between soils (e.g. Figure 2.2), suggesting (by definition) an influence of soil texture on flow partitioning (Christensen 1996b). Whether texture should modify compartment *k* is less clear: the minimum accessibility (and hence reactivity) of a particular fraction should be constant across soils, providing the amount of energy used in its release is fixed (the mean accessibility may vary). If the anticipated, relatively robust relationships between model parameters and indices of soil texture can be established, the model may be applicable at any location (Christensen 1992, 1995). To establish these relationships, incubations using soils of contrasting texture will be required. These incubations may be conducted under controlled conditions to eliminate the uncertainty associated with rate modifiers for temperature and soil moisture content. Methods for directly measuring and characterising NaI-soluble SOM will be important to improve parameterisation by accounting for all C and N.

Field applications will require the influence of plant–soil interactions to be captured in the model. Whilst FREE organic matter is conceptually compatible with above ground inputs such as straw, it is likely that inputs from roots interact strongly with other fractions e.g. INTRA-AGGREGATE and soluble, the roots exuding substrates but also providing centres for aggregate formation during senescence (Gale *et al.* 2000). It may be possible to explore the nature of these interactions using ^{13}C natural abundance (Balesdent and Balabane 1992; Qian and Doran 1996) or ^{14}C pulse labelling (Jensen 1993). The improvement to system level prediction achieved using the modified SOM model would be assessed by substitution into a system framework such as SUNDIAL (Smith *et al.* 1996).

CONCLUSION

It is well established that SOM models containing measurable variables are required for improved short- to medium-term simulation of SOM dynamics and nutrient supply. Although a number of attempts have been made to correlate individual compartments in existing models with physically or chemically defined SOM fractions, this research has – for the first time – tested a model based only on measurable, mutually exclusive SOM fractions defined by physical location. The limitations of the current model provide the basis for future progress. Within the same conceptual framework, a range of robust models should be possible, suitable for diverse applications in a range of environments.

REFERENCES

Alvarez, C.R., R. Alvarez, M.S. Grigera and R.S. Lavado (1998). Associations between organic matter fractions and the active soil microbial biomass. Soil Biology and Biochemistry **30**: 767–773.

Alvarez, R. and C.R. Alvarez (2000). Soil organic matter pools and their associations with carbon mineralization dynamics. Soil Science Society of America Journal **64**: 184–189.

Amato, M. and J.N. Ladd (1992). Decomposition of ^{14}C–labelled glucose and legume material in soils: Properties influencing the accumulation of organic residue C and microbial biomass C. Soil Biology and Biochemistry **24**: 455–464.

Amelung, W., R. Bol and C. Friedrich (1999). Natural ^{13}C abundance: a tool to trace the incorporation of dung-derived C into soil particle-size fractions. Rapid Communications in Mass Spectroscopy **13**: 1291-1294.

Angers, D.A., A. N'dayegamiye and D. Cote (1993). Tillage induced differences in organic matter of particle-size fractions and microbial biomass. Soil Science Society of America Journal **57**: 512–516.

Appel, T. and K. Mengel (1998). Prediction of mineralization nitrogen in soils on the basis of an analysis of extractable organic N. Journal of Plant Nutrition and Soil Science **161**: 433–452.

Arah, J.R.M. (2000). Modeling SOM cycling in rice-based production systems. In: G.J.D. Kirk and D.S. Olk (ed.) Carbon and Nitrogen Dynamics in Flooded Soils. International Rice Research Institute, Los Banos.

Arrouays, D., J. Balesdent, A. Mariotti and C. Girardin (1995). Modelling organic carbon turnover in cleared temperate forest soils converted to maize cropping by using ^{13}C natural abundance measurements. Plant and Soil **173**: 191–196.

Arshad, M.A., J.A. Ripmeester and M. Schnitzer (1988). Attempts to improve solid state ^{13}C NMR spectra of whole mineral soils. Canadian Journal of Soil Research **68**: 593–602.

Baes, A.U. and P.R. Bloom (1989). Diffuse reflectance and transmission Fourier transform infrared (DRIFT) spectroscopy of humic and fulvic acids. Soil Science Society of America Journal **53**: 695–700.

Baldock, J., J. Oades, A. Waters, X. Peng, A. Vasallo and M. Wilson (1992). Aspects of the chemical structure of soil organic materials as revealed by solid-state ^{13}C NMR spectroscopy. Biogeochemistry **16**: 1–42.

Balesdent, J. (1996). The significance of organic separates to carbon dynamics and its modelling in some cultivated soils. European Journal of Soil Science **47**: 485–493.

Balesdent, J. and M. Balabane (1992). Maize root-derived soil organic carbon estimated by natural ^{13}C abundance. Soil Biology and Biochemistry **24**: 97–101.

Balesdent, J. and A. Mariotti (1990). The turnover of soil organic carbon and of soil organic matter fractions estimated from ^{13}C natural abundance in corn fields. Transactions of the 14th International Congress Soil Science Volume II. pp 411–412.

Balesdent, J., A. Marotti and B. Guillet (1987). Natural ^{13}C abundance as a tracer for studies of soil organic matter. Soil Biology and Biochemistry **19**: 25–30.

Barraclough, D. (1995). ^{15}N isotope dilution techniques to study soil nitrogen transformations and plant uptake. Fertilizer Research **42**: 185–192.

Barraclough, D. (1997). The direct or MIT route for nitrogen immobilization: a ^{15}N mirror image study with leucine and glycine. Soil Biology and Biochemistry **29**: 101–108.

Beare, M.H., M.L. Cabrera, P.F. Hendrix and D.C. Coleman (1994). Aggregate-protected and unprotected organic matter pools in conventional- and no-tillage soils. Soil Science Society of America Journal **58**: 787–795.

Benner, R., M. Fogel, E. Sprague and R. Hodson (1987). Depletion of ^{13}C in lignin and its implications for stable isotope studies. Nature **329**: 708–710.

Bloom, P.R. and J.A. Leenheer (1989). Vibrational, electronic, and high-energy spectroscopic methods for characterizing humic substances. In: M.H.B. Hayes, P. MacCarthy, R.L. Malcolm and R.S. Swift (ed.) Humic substances II. In search of structure. John Wiley & Sons, Chichester. pp 409–446.

Bonde, T.A., B.T. Christensen and C.A. Cerri (1992). Dynamics of soil organic matter as reflected by natural ^{13}C abundance in particle size fractions of forested and cultivated oxisols. Soil Biology and Biochemistry **24**: 275–277.

Bosatta, E. and G.I. Ågren (1985). Theoretical analysis of decomposition of heterogeneous substrates. Soil Biology and Biochemistry **16**: 63–67.

Bosatta, E. and G.I. Ågren (1996). Theoretical analyses of carbon and nutrient dynamics in soil profiles. Soil Biology and Biochemistry **28**: 1523–1531.

Boutton, T.W. (1996). Stable carbon isotope ratios of soil organic matter and their use as indicators of vegetation and climate change. In: T.W. Boutton and S. Yamasaki (ed.) Mass spectrometry of soils. Marcel Dekker, New York. pp 47–82.

Bremer, E., H.H. Janzen and A.M. Johnston (1994). Sensitivity of total, light fraction, and mineralizable organic matter to management practices in a Lethbridge soil. Canadian Journal of Soil Science **74**: 131–138.

Brookes, P.C., A. Landman, G. Pruden and D.S. Jenkinson (1985). Chloroform fumigation and the release of soil nitrogen: a rapid direct extraction method for measuring microbial biomass nitrogen in soil. Soil Biology and Biochemistry **17**: 837–842.

Brooks, P.D., J.M. Stark, B.B. McInteer and T. Preston (1989). Diffusion method to prepare soil extracts for automated nitrogen-15 analysis. Soil Science Society of America Journal **53**: 1707–1711.

Burns, I.G. and D.J. Greenwood (1982). Estimation of the year-to-year variations in nitrate leaching in different soils and regions of England and Wales. Agriculture and Environment **7**: 35–45.

Cabrera, M.L. and M.H. Beare (1993). Alkaline persulfate oxidation for determining total nitrogen in microbial biomass extracts. Soil Science Society of America Journal **57**: 1007–1012.

Cadisch, G. and K.E. Giller (1996). Estimating the contribution of legumes to soil organic matter build up in mixed communities of C3/C4 plants. Soil Biology and Biochemistry **28**: 823–825.

Cadisch, G., H. Imhof, S. Urquiaga, B. Boddey and K.E. Giller (1996). Carbon turnover ($\delta^{13}C$) and nitrogen mineralisation potential of particulate light soil organic matter after rainforest clearing. Soil Biology and Biochemistry **28**: 1555–1567.

Cadisch, G., K. Hairiah and K.E. Giller (2000). Applicability of the natural ^{15}N abundance technique to measure N_2 fixation in *Arachis hypogaea* grown on an Ultisol. Netherlands Journal of Agricultural Science **48**: 31–45.

Cambardella, C.A. (1997). Experimental verification of simulated soil organic matter pools. In: R. Lal, J.M. Kimble, R.F. Follett and B.A. Stewart (ed.) Soil Processes and the Carbon Cycle. CRC Press, Boca Raton. pp 519–526.

Cambardella, C.A. and E.T. Elliott (1992). Particulate soil organic-matter changes across a grassland cultivation sequence. Soil Science Society of America Journal **56**: 777–783.

CEC (1991). Council Directive of 12 December 1991 concerning the protection of waters against polluition caused by nitrates from agricultural sources (91/676/EEC). Official Journal of the European Communities L 135/40–52.

Chertov, O.G. and A.S. Komarov (1996). SOMM – a model of soil organic matter and nitrogen dynamics in terrestrial ecosystems. In: D.S. Powlson, P. Smith and J.U. Smith (ed.) Evaluation of soil organic matter models. Springer-Verlag, Berlin Heidelberg. pp 231–236

Cheshire, M.V., C.N. Bedrock, B.L. Williams, S.J. Chapman, I. Solntseva and I. Thomsen (1999). The immobilisation of nitrogen by straw decomposing in soil. European Journal of Soil Science **50**: 329–341.

Cheshire, M.V. and C.M. Mundie (1990). Organic matter contributed to soil by plant roots during the growth and decomposition of maize. Plant and Soil **121**: 107–114.

Chotte, J.L., J.N. Ladd and M. Amato (1998). Sites of microbial assimilation, and turnover of soluble and particulate ^{14}C-labelled substrates decomposing in a clay soil. Soil Biology and Biochemistry **30**: 205–218.

Christensen, B.T. (1992). Physical fractionation of soil and organic matter in primary particle size and density separates. Advances in Soil Science **20**: 1–90.

Christensen, B.T. (1996a). Carbon in primary and secondary organomineral complexes. In: M.R. Carter and B.A. stewart (ed.) Structure and organic matter storage in agricultural soils. CRC Press, Boca Raton. pp 97–165.

Christensen, B.T. (1996b). Matching measurable soil organic matter fractions with conceptual pools in simulation models of carbon turnover: revision of model structure. Evaluation of soil organic matter models. D.S. Powlson, P. Smith and J.U. Smith. Berlin Heidelberg, Springer-Verlag. pp 143–159.

Christensen, B.T. and A.E. Johnston (1997). Soil organic matter and soil quality-lessons learned from long-term experiments at Askov and Rothamsted. In: E.G. Gregorich and M.R. Carter (ed.) Soil Quality for Crop Production and Ecosystem Health. Elsevier Science Publishers, Amsterdam.

Coleman, K. and D.S. Jenkinson (1996). RothC-26.3 – a model for the turnover of carbon in soil. In: D.S. Powlson, P. Smith and J.U. Smith (ed.) Evaluation of soil organic matter models. Springer-Verlag, Berlin Heidelberg. pp 237–246.

de Ruiter, P.C. and H.G. van Faassen (1994.). A comparison between an organic matter dynamics model and a food web model simulating nitrogen mineralisation in agro-ecosystems. European Journal of Agronomy **3**: 347–354.

de Willigen, P. (1991). Nitrogen turnover in the soil crop system; comparison of fourteen simulation models. Fertiliser Research **27**: 141–149.

Dixon, W.T. (1982). Spinning-sideband-free and spinning-sideband-only NMR spectra in spinning samples. Journal of Chemical Physics **77**: 1800–1809.

Dyke, G.V., B.J. George, A.E. Johnston, P.R. Poulton and A.D. Todd (1983). The Broadbalk wheat experiment 1968–1978: yields and plant nutrition in crops grown continuously and in rotation. Rothamsted Report for 1982 Part II. pp 5-40

Elliott, E.T., K. Paustian and S.D. Frey (1996). Modelling the measurable or measuring the modelable: a hierarchical approach to isolating meaningful soil organic matter fractions. In: D.S. Powlson, P. Smith and J.U. Smith (ed.) Evaluation of soil organic matter models. Springer-Verlag, Berlin Heidelberg. pp 161–179.

Figgis, B.N. and R.S. Nyholm. 1958. A convenient solid for calibration of the Gouy susceptibility apparatus. The Journal of the Chemical Society. pp 4190–4191.

FMA (1999). British Survey of Fertiliser Practice: fertiliser use on farm crops for crop year 1998, Fertilizer Manufacturers Association, Peterborough.

Fog, K. (1988). The effect of added nitrogen on the rate of decomposition of organic matter. Biological Reviews **63**: 433–462.

Gale, W.J., C.A. Cambardella and T.B. Bailey (2000). Surface residue- and root-derived carbon in stable and unstable aggregates. Soil Science Society of America Journal **64**: 196–201.

Gaunt, J.L., D.V. Murphy and K.W.T. Goulding (1998). Use of ^{15}N isotopic dilution to separate the processes of mineralisation and immobilisation. 16th World Soils Congress, Montpellier, August 1998.

Gee, G.W. and J.W. Bauder (1986). Particle-size analysis. Agronomy Monographs **9**: 383–411.

Golchin, A., J.M. Oades, J.O. Skjemstad and P. Clarke (1994a). Soil structure and carbon cycling. Australian Journal of Soil Research **32**: 1043–1068.

Golchin, A., J.M. Oades, J.O. Skjemstad and P. Clarke (1994b). Study of free and occluded particulate organic matter in soils by solid sate ^{13}C CP/MAS NMR spectroscopy and scanning electron microscopy. Australian Journal of Soil Research **32**: 285–309.

Golchin, A., P. Clarke, J.A. Baldock, T. Higashi, J.O. Skjemtad and J.M. Oades (1997). The effects of vegetation burning on the chemical composition of soil organic matter in a volcanic ash soil as shown by 13C NMR spectroscopy. I. Whole soil and humic acid fractions. Australian Journal of Soil Research **76**: 155–174.

Gregorich, E. and H. Janzen (1996). Storage of soil carbon in the light fraction and macroorganic matter. In: M.R. Carter and B.A. Stewart (ed.) Structure and organic matter storage in agricultural soils. CRC Press, Boca Raton. pp 167–192.

Gregorich, E.G., R.P. Voroney and R.G. Kachanoski (1991). Turnover of carbon through the microbial biomass in soils with different textures. Soil Biology and Biochemistry **23**: 799–805.

Gregorich, E.G., B.H. Ellert and C.M. Monreal (1995). Turnover of soil organic matter and storage of corn residue carbon estimated from natural ^{13}C abundance. Canadian Journal of Soil Science **75**: 161–167.

Gregorich, E.G., B.H. Ellert, C.F. Drury and B.C. Liang (1996). Fertilization effects on soil organic matter turnover and corn residue C storage. Soil Science Society of America Journal **60**: 472–476.

Gregorich, E.G., C.F. Drury, B.H. Ellert and B.C. Liang (1997). Fertilization effects on physically protected light fraction organic matter. Soil Science Society of America Journal **61**: 482–484.

Gregorich, E.G., B.C. Liang, C.F. Drury, A.F. Mackenzie and W.B. McGill (2000). Elucidation of the source and turnover of water soluble and microbial biomass carbon in agricultural soils. Soil Biology and Biochemistry **32**: 581–587.

Guggenberger, G., W. Zech and R.J. Thomas (1995). Lignin and carbohydrate alteration in particle-size separates of an oxisol under tropical pastures following native savanna. Soil Biology and Biochemistry **27**: 1629–1638.

Gunnewick, H.K. (1996). Organic matter dynamics simulated with the 'Verberne' model. In: D.S. Powlson, P. Smith and J.U. Smith (ed.) Evaluation of soil organic matter models. Springer-Verlag, Berlin Heidelberg. pp 255–261.

Handayanto, E., G. Cadisch and K.E. Giller (1995). Manipulation of quality and mineralization of tropical legume tree prunings by varying nitrogen supply. Plant Soil **176**: 149–160.

Harrison, R. (1996). Nitrogen uptake by cover crops and its subsequent fate in arable systems. In: J.H. Clark, D.H.K. Davies, P.M.R. Dampney, R.J. Froud-Williams, P.J. Griffith, A. Lane, L. Sim and D.B. Stevens (ed.) Rotations and cropping systems. pp 51–58.

Hassink, J. and J.W. Dalenberg (1996). Decomposition and transfer of plant residue ^{14}C between size and density fractions in soil. Plant and Soil **179**: 159–169.

Hinds, A.A. and L.E. Lowe (1980). Use of an ultrasonic probe in soil dispersion in the bulk isolation of organo-mineral complexes. Canadian Journal of Soil Science **60**: 389–392.

Hopkins, D.W., J.A. Chudek, E.A. Webster and D. Barraclough (1997). Following the decomposition of ryegrass labelled with ^{13}C and ^{15}N in soil by solid-state nuclear magnetic resonance spectroscopy. European Journal of Soil Science **48**: 623–631.

Hopkins, D.W., R.E. Wheatley and D. Robinson (1998). Stable isotope studies of nitrogen transformations in soil. In: H. Griffiths (ed) Stable Isotopes and the Integration of Biological, Ecological and Geochemical Processes. Bios Scientific Publishers, Oxford. pp 75–88.

Li, C. (1996). The DNDC model. In: D.S. Powlson, P. Smith and J.U. Smith (ed.) Evaluation of soil organic matter models. Springer-Verlag, Berlin Heidelberg. pp 263–267.

Jansson, S.L. and J. Persson (1982). Mineralization and immobilization of soil nitrogen. In: F.J. Stevenson (ed) Nitrogen in agricultural soils. ASA, Madison. pp 229–252.

Jenkinson, D.S. (1988). Determination of microbial biomass carbon and nitrogen in soil. In: J.R. Wilson (ed) Advances in nitrogen cycling in agricultural ecosystems. CAB International, Wallingford. pp 368–386.

Jenkinson, D.S. (1990). The turnover of organic carbon and nitrogen in soil. Philosophical Transactions of the Royal Society London Series B **329**: 361–368.

Jenkinson, D.D. and J.H. Rayner (1977). The turnover of soil organic matter in some of the Rothamsted classical experiments. Soil Science **123**: 298–305.

Jenkinson, D.S. and K. Coleman (1994). Calculating the annual input of organic matter to soil from measurements of total carbon and radiocarbon. European Journal of Soil Science **45**: 167–174.

Jensen, B. (1993). Rhizodeposition by $^{14}CO_2$-pulse-labelled spring barley grown in small field plots on sandy loam. Soil Biology and Biochemistry **25**: 1553–1559.

Kinchesh, P., D.S. Powlson and E.W. Randall (1995). ^{13}C NMR studies of organic matter in whole soils: I. Quantitation possibilities. European Journal of Soil Science **46**: 125–138.

Kogel-Knabner, I. (1998). ^{13}C and ^{15}N NMR spectroscopy as a tool in soil organic matter studies. Geoderma **80**: 243–270.

Ladd, J.N., M. Amato, P.R. Grace and J.A. van Veen (1995). Simulation of ^{14}C turnover through the microbial biomass in soils incubated with ^{14}C-labelled plant residues. Soil Biology and Biochemistry. **27**: 777–783.

Ladd, J.N., M. van Gestel, L.J. Monrozier and M. Amato (1996). Distribution of organic ^{14}C and ^{15}N in particle-size fractions of soils incubated with ^{14}C, ^{15}N-labelled glucose/NH_4, and legume and wheat straw residues. Soil Biology and Biochemistry **28**: 893–905.

Larney, F.J., E. Bremer, H.H. Janzen, A.M. Johnson and C.W. Lindwall (1997). Changes in total, mineralizable and light fraction soil organic matter with cropping and tillage intensities in semi-arid southern Alberta, Canada. Soil and Tillage Research **42**: 229–240.

Leifield, J. and I. Kogel-Knabner (2000). Free and occluded particulate organic matter in agricultural soils under different management as characterised by CPMAS ^{13}C NMR spectroscopy. Proceedings of the 2nd European Symposium NMR in Soil Science, February-March 2000, Freising, Germany.

Leinweber, O., H.-R. Schulten and M. Korschens (1994). Seasonal variations of soil organic matter in a long-term agricultural experiment. Plant and Soil **160**: 225–235.

Madari, B., S.P. Sohi, N. Mahieu, J.L. Gaunt, T. Nemeth and E. Micheli (Submitted). The effect of inorganic and organic fertilisation on the molecular composition of

soil organic matter pools examined by ^{13}C NMR, DRIFT spectroscopy and size-exclusion chromatography. European Journal of Soil Science.

MAFF. (1999). Tackling nitrate from agriculture: strategy from science. MAFF Publications, London.

Magid, J., A. Gorissen and K.E. Giller (1996a). In search of the elusive "active" fraction of soil organic matter: three size–density fractionation methods for tracing the fate of homogeneously ^{14}C-labelled plant materials. Soil Biology and Biochemistry **28**: 89–99.

Magid, J., T. Mueller, L.S. Jensen and N.E. Nielsen (1996b). Modelling the measurable: interpretation of field scale CO2 and N-mineralisation, soil microbial biomass and light fractions as indicators of oilseed rape, maize and barley straw decomposition. In: G. Cadisch and K.E. Giller (ed.) Driven by nature: plant litter quality and decomposition. CAB International, Wallingford. pp 349-362.

Magid, J., L.S. Jensen, T. Mueller and N.E. Nielsen (1997). Size–density fractionation for in-situ measurements of rape straw incorporation – an alternative to the litterbag approach? Soil Biology and Biochemistry **29**: 1125–1133.

Mahieu, N., D.S. Powlson and E.W. Randall (1998). A review of soil organic matter as seen by ^{13}C nuclear magnetic resonance. Proceedings of the 16th World Soils Congress, Montpellier, August 1998.

Mariotti, A. (1983). Atmospheric nitrogen is a reliabke standard for natural ^{15}N abundance measurements. Nature **303**: 685–687.

McGill, W.B. (1996). Review and classification of ten soil organic matter (SOM) models. In: D.S. Powlson, P. Smith and J.U. Smith (ed.) Evaluation of soil organic matter models. Springer-Verlag, Berlin Heidelberg. pp 111–132.

Molina, J.A.E. (1996). Description of the model NCSOIL. In: D.S. Powlson, P. Smith and J.U. Smith (ed.) Evaluation of soil organic matter models. Springer-Verlag, Berlin Heidelberg. pp 269–274.

Molina, J.-A. and P. Smith (1997). Modeling carbon and nitrogen processes in the soil. Advances in Agronomy **62**: 253–298.

Molina, J.A.E., C.E. Clapp, M.J. Shaffer, F.W. Chichester and W.E. Larson (1983). NCSOIL, a model of nitrogen and carbon transformation in soil: description, calibration, and behaviour. Soil Science Society of America Journal **47**: 85–91.

Molina, J.A.E., H.H. Cheng, B. Nicolardot, R. Chaussod and S. Houot (1994). Biologically active soil organics: a case of double identity. In: J.W. Doran, D.C. Coleman, D.F. Bezdicek and B.A. Stewart (ed.) Defining soil quality for a sustainable environment. SSSA Special Publication Number 35. SSSA/ASA, Madison. pp 169–177.

Monrozier, L.J., J.N. Ladd, R.W. Fitzpatrick, R.C. Foster and M. Raupach (1991). Components and microbial biomass content of size fractions in soils of contrasting aggregation. Geoderma **49**: 37–62.

Morra, M.J., R.R. Blank, L.L. Freeborn and B. Shafii (1991). Size fractionation of soil organo-material complexes using ultrasonic dispersion. Soil Science **152**: 294–303.

Mueller, T., L.S. Jensen, S. Hansen and N.E. Nielsen (1996). Simulating soil carbon and nitrogen dynamics with the soil–plant–atmosphere system model DAISY. In:: D.S. Powlson, P. Smith and J.U. Smith (ed.) Evaluation of soil organic matter models. Springer-Verlag, Berlin Heidelberg. pp 275–281.

Murphy, D.V., I.R.P. Fillery and G.P. Sparling (1997). Method to lable soil cores with $^{15}NH_3$ gas as a prerequisite for ^{15}N isotopic dilution and measurement of gross N mineralization. Soil Biology & Biochemistry **29**: 1731–1741.

Murphy, D.V., A. Bhogal, M.A. Shepherd, K.W.T. Goulding, S.C. Jarvis, D. Barraclough and J.L. Gaunt (1999). Comparison of ^{15}N labelling methods to measure gross nitrogen mineralisation. Soil Biology and Biochemistry **31**: 2015–2024.

Myers, R.E. (1996). Synchrony of nutrient release and plant demand: plant litter quality, soil environment and farmer management options. In: G. Cadisch and

K.E. Giller (ed.) Driven by nature: plant litter quality and decomposition. CAB International, Wallingford. pp 215–229.

J. Niemeyer, Y. Chen and J.-M. Bollag (1992). Characterisation of humic acids, composts and peat by DRIFT. Soil Science Society America Journal **56**: 135–140.

North, P. (1976). Towards an absolute measurement of soil structural stability using ultrasound. Soil Science **27**: 441–459.

Oades, J.M. (1995). Organic matter: chemical and physical fractions. In: R.D.B. Lefroy, G.J. Blair and E.T. Craswell (ed.) Soil organic matter for sustainable agriculture. Australian Centre for International Agricultural Research, Canberra. pp 135–139.

Oades, J.M. and A.G. Waters (1991). Aggregate hierarchy in soils. Australian Journal of Soil Research **29**: 815–828.

Oades, J.M., A.M. Vassallo, A.G. Waters and M.A. Wilson (1987). Characterization of organic matter in particle size and density fractions from a Red-brown Earth by solid state ^{13}C NMR. Australian Journal of Soil Research **25**: 71–82.

Pain, B. and K. Smith (1994). Organic manures and nitrate leaching. Solving the nitrate problem. MAFF Publications, London.

Parton, W.J. (1996). The CENTURY model. In: D.S. Powlson, P. Smith and J.U. Smith (ed.) Evaluation of soil organic matter models. Springer-Verlag, Berlin Heidelberg. pp 284–291.

Parton, W.J., D.S. Schimel, C.V. Cole and D.S. Ojima (1987). Analysis of factors controlling soil organic matter levels in Great Plains Grasslands. Soil Science Society of America Journal **51**: 1173–1179.

Paul, E.A. and N.G. Juma (1981). Mineralization and immobilization of soil nitrogen by micro-organisms. In: F.E. Clark and T. Rosswall (ed.) Terrestrial nitrogen cycles, processes, ecosystems, strategies and management inputs. Swedish Natural Science Research Council, Stockholm. pp 179–204.

Paul, E.A. and J.A. van Veen (1978). The use of tracers to determine the dynamic nature of organic matter. Transactions 11th International Congress Soil Science. Bucharest, Romania Volume III. pp 179-204.

Paul, E.A., R.F. Follett, S.W. Leavitt, A.D. Halvorson, G.A. Peterson and D. Lyon (1997). Radiocarbon dating for determination of soil organic matter pool sizes and dynamics. Soil Science Society of America Journal **61**: 1058–1067.

Paustian, K. (1994). Modelling soil biology and biochemical processes for sustainable agriculture research. In: Z.E. Pankhurst, B.M. Doube, V.V.S.R. Gupta and P.R. Grace (ed.) Soil biota management in sustainable farming systems. Melbourne, CSIRO Information Services.

Paustian, K., H.P. Collins and E.A. Paul (1996). Management controls on soil carbon. Soil organic matter in temperate agroecosystems: long term experiments in North America. E.A. Paul, K. Paustian, E.T. Elliott and C.V. Cole. Boca Raton, Florida, CRC Press, pp 15–49.

Payne, R.W., P.W. Lane, P.G.N. Digby, S.A. Harding, P.K. Leech, G.W. Morgan, A.D. Todd, R. Thompson, G.T. Wilson, S.J. Welham and R.P. White (1993). Genstat 5 Release 3 reference manual. Clarendeon Press, Oxford.

Powlson, D.S., G. Pruden, A.E. Johnston and D.S. Jenkinson (1986). The nitrogen cycle in the Broadbalk wheat experiment: recovery and losses of ^{15}N-labelled fertilizer applied in spring and inputs of nitrogen from the atmosphere. Journal of Agricultural Science **107**: 591–609.

Preston, C.M. (1996). Applications of NMR to soil organic matter analysis: history and prospects. Soil Science **161**: 144–166.

Preston, C.M., R.H. Newman and P. Rother (1994). Using ^{13}C CPMAS NMR to assess effects of cultivation on the organic matter of particle size fractions in a grassland soil. Soil Science **157**: 26–35.

Qian, J.H. and J.W. Doran (1996). Available carbon released from crop roots during growth as determined by carbon-13 natural abundance. Soil Science Society of America Journal **60**: 828–831.

Randall, E.W., N. Mahieu, D.S. Powlson and B.T. Christensen (1995). Fertilization effects on organic matter in physically fractionated soils as studied by ^{13}C NMR: Results from two long-term field experiments. European Journal of Soil Science **46**: 557–565.

Richter, D.D., D. Markewitz, S.E. Trumbore and C.G. Wells (1999). Rapid accumulation and turnover of soil carbon in a re-establishing forest. Nature **400**: 56–58.

Rijetma, P.E. and J.G. Kroes (1991). Some results of nitrogen simulations with the model ANIMO. Fertilizer Research **27**: 189–198.

Royal Society (1983). Nitrogen cycle of the United Kingdom: report of a Royal Society Study Group. Royal Society, London.

Russel, J.S. (1975). A mathematical treatment of the effect of cropping system on soil organic nitrogen in two long-term sequential experiments. Soil Science **120**: 37–44.

Russell, J.D. and A.R. Fraser (1988). Rumen digestion of untreated and alkali-treated cereal straw: A study by multiple internal reflectance infrared spectroscopy. Journal of Science of Food and Agriculture **45**: 95–107.

Ryan, M.C., R. Aravena and R.W. Gillham (1995). The use of ^{13}C natural abundance to investigate the turnover of the microbial biomass and active fractions of soil organic matter under two tillage treatments. In: R. Lal, J. Kimble, E. Levine and B.A. Stewart (ed.) Soils and Global Change. CRC Press, Boca Raton. pp 351–360.

Schweizer, M., J. Fear and G. Cadisch (1999). Isotopic ^{13}C fractionation during plant residue decomposition and its implications for soil organic matter studies. Rapid Communications in Mass Spectroscopy **13**: 1284-1290.

Shepherd, M.A., Stockdale, E.A., Powlson, D.S. and S.C. Jarvis. (1996). The influence of organic N mineralisation on the management of agricultural systems in the UK. Soil Use and Management **12**: 76–85.

Sitompul, S.M., K. Hairiah, G. Cadisch and M.V. Nordwijk (2000). Dynamics of density fractions of macro-organic matter after forest conversion to sugarcane and woodlots, accounted for in a modified Century model. Netherlands Journal of Agricultural Science **48**: 61–73.

Skjemstad, J.O., P. Clarke, J.A. Taylor, J.M. Oades and S.G. McClure (1996). The chemistry and nature of protected carbon in soils. Australian Journal of Soil Research **34**: 251–271.

Skjemstad, J.O., L.J. Janik and J.A. Taylor (1998). Non-living organic matter: what do we know about it? Australian Journal of Experimental Agriculture **38**: 667–680.

Skjemstad, J.O., J.A. Taylor, L.J. Janik and S.P. Marvanek (1999a). Soil organic carbon dynamics under long-term sugarcane monoculture. Australian Journal of Soil Research **37**: 151–164.

Skjemstad, J.O., J.A. Taylor and R.J. Smernik (1999b). Estimation of charcoal (char) in soils. Communications of Soil Science and Plant Analysis **30**: 2283–2298.

Smernik, R.J., J.O. Skjemstad and J.M. Oades (2000). Virtual fractionation of charcoal from soil organic matter using solid-state ^{13}C NMR spectral editing. Australian Journal of Soil Research **38**: 665–83.

Smith, B.N. and S. Epstein (1971). Two categories of $^{13}C/^{12}C$ ratios for higher plants. Plant Physiology **47**: 380–384.

Smith, J.U. and M.J. Glendining (1996). A decision support system for optimising the use of nitrogen in crop rotations. Aspects of Applied Biology **47**: 103–110.

Smith, J.U., N. Bradbury and T.M. Addiscott (1996a). SUNDIAL: a PC-based system for simulating nitrogen dynamics in arable land. Agronomy Journal **88**: 38–43.

Smith, J.U., P. Smith and T.M. Addiscott (1996b). Quantitative methods to evaluate and compare soil organic matter (SOM) models. In: D.S. Powlson, P. Smith and J.U. Smith (ed.) Evaluation of soil organic matter models. Springer-Verlag, Berlin Heidelberg. pp 181–199.

Smith, J.U., P. Smith, R. Monaghan and A.J. Macdonald (Submitted). When is a measured soil organic matter fraction equivalent to a model pool? European Journal of Soil Science.

Spycher, G., P. Sollins and S. Rose (1983). Carbon and nitrogen in the light fraction of a forest soil: Vertical distribution and seasonal patterns. Soil Science **135**: 79–87.

Steele, K.W., B.M. Bonish, R.M. Daniel and G.W. O'Hara (1983). Effects of strain and host plant on nitrogen isotopic fractionation in legumes. Plant Physiology **72**: 1001–1004.

Stevenson, F.J. (1994). Humus chemistry: genesis, composition, reactions. John Wiley and Sons, New York. 496 pp.

Stockdale, E.A., J.L. Gaunt and J.Vos (1997). Soil–plant nitrogen dynamics: what concepts are required? European Journal of Agronomy **7**: 145–159.

Sutton, M.A., C.E.R. Pitcairn and D. Fowler (1993). The exchange of ammonia between the atmosphere and plant communities. Advances in Ecological Research **24**: 301–393.

Tanner, C.B. and M.L. Jackson (1947). Nomographs of sedimentation times for soil particles under gravity or centrifugal acceleration. Soil Science Society Proceedings pp 60–65.

Theng, B.K.G., K.R. Tate, P. Sollins, N. Moris, N. Nadkerni and R.L. Tate (1989). Constituents of organic matter in temperate and tropical soils. In: D.C. Coleman, J.M. Oades and G. Uehara (ed.) Dynamics of soil organic matter in tropical ecosystems. NifTAL Project. University of Hawaii.

Tiessen, H. and J.W.B. Stewart (1983). Particle-size fractions and their use in studies of soil organic matter: II. Cultivation effects on organic matter composition of size fractions. Soil Science Society of America Journal **47**: 509–514.

Tinsley, J., T.J. Taylor and J.H. Moore (1951). The determination of carbon dioxide derived from carbonates in agricultural and biological materials. Analyst **76**: 300–310.

Tisdall, J.M. (1996). Formation of soil aggregates and accumulation of soil organic matter. Advances in Soil Science. In: M.R. Carter and B.A. Stewart (ed.) Structure and organic matter storage in agricultural soils. CRC Press, Boca Raton. pp 57-96.

Tisdall, J.M. and J.M. Oades (1982). Organic matter and water-stable aggregates in soil. Journal of Soil Science **33**: 141–163.

Townsend, A.R., P.M. Vitousek and S.E. Trumbore (1995). Soil organic matter dynamics along gradients in temperature and land use on the island of Hawaii. Ecology **76**: 721–733.

Trinsoutrot, I., S. Recous, B. Bentz, M. Lineres, D. Cheneby and B. Nicolardot (2000). Biochemical quality of crop residues and carbon and nitrogen mineralization kinetics under nonlimiting nitrogen conditions. Soil Science Society of America Journal **64:** 918–926.

van der Linden, A.M.A., J.A. van Veen and M.J. Frissel (1987). Modelling soil organic matter levels after long-term applications of crop residues, and farmyard and green manures. Plant and Soil **101**: 21–28.

van Veen, J.A., J.N. Ladd and M.J. Frissel (1984). Modelling C and N turnover through the microbial biomass in soil. Plant and Soil **76**: 257–274.

van Veen, J.A., J.N. Ladd and M. Amato (1985). Turnover of carbon and nitrogen through the microbial biomass in a sandy loam and a clay soil incubated with (^{14}C(U)Glucose and [^{15}N]$(NH_4)_2SO_4$ under different moisture regimes. Soil Biology and Biochemistry **17**: 747–756.

Verberne, E.L.J., J. Hassink, P. de Willigen, J.J.R. Groot and J.A. van Veen (1990). Modelling soil organic matter dynamics in different soils. Netherlands Journal of Agricultural Science **38**: 221–238.

Watson, J.R. (1971). Ultrasonic vibration as a method of soil dispersion. Soil Fertility **34**: 127–134.

Whitmore, A.P. (1996a). Alternative kinetic laws to describe the turnover of the microbial biomass. Plant and Soil **181**: 169–171.

Whitmore, A.P. (1996b). Describing the mineralization of carbon added to soil in crop residues using second-order kinetics. Soil Biology and Biochemistry **28**: 1435–1442

Wolf, D.C., J.O. Legg and T.W. Boutton (1994). Isotopic methods for the study of soil organic matter dynamics. Methods of Soil Analysis: Part 2 – Microbiological and Biochemical Properties. SSSA Book Series Number 5. SSSA, Madison pp 865–906.

Wu, J., R.G. Joergensen, B. Pommerening, R. Chaussod and P.C. Brookes (1990). Measurement of soil microbial biomass C by fumigation–extraction – an automated procedure. Soil Biology and Biochemistry **22**: 1167–1169.

View publication stats